الجمهورية الجزائرية الديمقراطية الشعبية
République Algérienne Démocratique et Populaire
وزارة التعليم العالي والبحث العلمي
Ministère de l'Enseignement Supérieur et de la Recherche Scientifique

جامعة زيان عاشور بالجلفة
Université Ziane Achour de Djelfa

كلية العلوم والتكنولوجيا
Faculté des Sciences et de la Technologie

Département : Génie Electrique

N° d'Ordre :. …. / 2023

Autorisation de Soutenance N° ……/2023

THESE DE DOCTORAT

Doctorat 3ème Cycle (D-LMD)

Présentée par

Khaled Omer Mokhtar TOUATI

En vue de l'obtention du diplôme de Docteur en 3ème Cycle D-LMD

Filière : Génie Electrique

Spécialité : Instrumentation

Thème

Contribution à la surveillance et au diagnostic des défaillances des réseaux électriques

Soutenue publiquement, le 22 / 07 /2023, devant le jury composé de :

Nom et Prénom	Grade	Etablissement de rattachement	Désignation
Mr Lakhmissi CHERROUN	MCA	Université de Djelfa	Président
Mr Mohamed BOUDIAF	MCA	Université de Djelfa	Directeur de thèse
Mr Lakhdar MAZOUZ	MCA	Université de Djelfa	Co Directeur de thèse
Mr Karim NEGADI	Professeur	Université de Tiaret	Examinateur
Mr Youcef BOT	MCA	Université de Khmis Miliana	Examinateur

Université de Djelfa, FST, 2023

الجمهورية الجزائرية الديمقراطية الشعبية
People's Democratic Republic of Algeria
وزارة التعليم العالي والبحث العلمي
Ministry of Higher Education and Scientific Research

جامعة زيان عاشور بالجلفة
Ziane Achour University of Djelfa

كلية العلوم والتكنولوجيا
Faculty of Science and Technology

Department: Electrical Engineering

Order N° : . …. / 2023

Defense authorization N° ……/2023

DOCTORAL THESIS

3rd Cycle Doctoral (D-LMD)

Presented by

Khaled Omer Mokhtar TOUATI

With a view to obtaining the doctoral diploma in 3rd Cycle Doctoral (D-LMD)

Branch: Electrical Engineering

Specialty: Instrumentation

Topic

Contribution to the monitoring and diagnosis of electrical power system faults

Supported, on 22 /07 / 2023, before the jury composed of:

Last and first name	Grade	Institution of affiliation	Designation
Mr Lakhmissi CHERROUN	MCA	Djelfa University	President
Mr Mohamed BOUDIAF	MCA	Djelfa University	Thesis director
Mr Lakhdar MAZOUZ	MCA	Djelfa University	Thesis co-director
Mr Karim NEGADI	Professor	Tiaret University	Examiner
Mr Youcef BOT	MCA	Khmis Miliana University	Examiner

Djelfa University, FST – 2023

Acknowledgement

First I thank Allah, the Almighty, for the mercy and the strength he gave me to finally complete the thesis.

I'd want to thank my supervisors. Mr. Mohamed Boudiaf and Mr. Lakhdar Mazouz for their thoughtful direction, inspiration, and counsel throughout this dissertation.

I want to express my sincere appreciation. to Mr. Cherroun Lakhmissi, Mr. Negadi Karim, and Mr. Bot Youcef of the examination committee for allowing me to defend my thesis.

Finally, I'd want to thank all of my colleagues and the staff of the department of electrical engineering. and every member in the Applied Automation and Industrial Diagnostics Laboratory.

.

Touati Khaled Omer Mokhtar

Dedication

I dedicate this modest work as a sign of gratitude to all those I adore in particular:

To my mother,

To my father,

To my sisters,

And to all my family and friends.

List of Contents

Acknowledgements

Figures list

Tables list

General Introduction

Chapter 1: State of the Art: Faults Diagnosis in Industrial Systems 5

1.1 Introduction 6

1.2 Notions and concepts of system diagnostics 6

1.3 Notion of redundancy (hardware and analytical) 7

1.3.1 Hardware redundancy 7

1.3.2 Analytical redundancy 8

1.4 Diagnosis principle (FDI system) 8

1.5 The different diagnostic methods 10

1.5.1 Diagnosis based on signal processing 10

1.5.2 Diagnosis based on artificial Intelligence 14

1.5.3 Model-based diagnosis 17

1.6 The incidence matrix (fault signature matrix) 25

1.7 Residual Generation 27

1.8 Diagnostic performance 27

1.9 Conclusion 28

Chapter 2: Transmission Line Fault Diagnosis using Signal-based Methods 29

2.1 Introduction 30

2.2 Diagnostic by Park's Method 30

2.2.1 Park's Method implementation in test power system 30

2.2.2 The modeling of the transmission line 31

2.2.3 Park's Method 33
2.2.4 Simulation results of Park's vectors 36
2.2.5 Park's vectors performance evaluation 43
2.3 Diagnostic by the Wavelet transform 44
2.3.1 Proposed scheme 46
2.3.2 Simulation results and discussion 47
2.4 Conclusion 53
Chapter 3: Transmission Line Fault Diagnosis using Artificial Neural Network 54
3.1 Introduction 55
3.2 Principle of diagnosis by neural network 55
3.3 Artificial neural networks 55
3.4 Neural networks principle 55
3.5 Natural neuron 56
3.6 Formal neuron 57
3.7 Architectures of neural networks 59
3.7.1 Learning neural networks 62
3.7.2 Supervised and unsupervised learning 63
3.7.3 Learning methods 64
3.8 Faults diagnosis of power transmission line by artificial neural networks (Application and simulation) 66
3.8.1 Implementation of ANN in test power system 66
3.8.2 Faults types 66
3.8.3 Diagnosis system output 67
3.8.4 Diagnostic by the artificial neural network ANN 68
3.8.5 Neural network structure 69
3.8.6 Training algorithms (Levenberg-Marquardt method) 70

3.8.7 Training base 72
3.9 Simulation results 76
3.10 Diagnostic performances 76
3.10.1 Faults detection in zone 1. 76
3.10.2 Short circuit fault in Ph_a-GND 76
3.10.3 Short circuit fault in Pha-GND – Side 1 79
3.10.4 Short circuit fault in Pha-GND – Side 2 82
3.10.5 Open circuit fault in Pha 84
3.10.6 Faults detection in zone 2 87
3.10.7 Faults detection in zone 3 92
3.10.8 Robustness test 95
3.11 Conclusion 100
Chapter 4: Transmission Line Fault Diagnosis using Fuzzy Logic 102
4.1 Introduction 103
4.2 Fuzzy Logic 103
4.3 Fuzzy set theory 104
4.4 Linguistic variable 105
4.5 Principle of fuzzy logic 106
4.5.1 Membership functions 106
4.5.2 Operations on fuzzy sets 108
4.6 Structure of a fuzzy process 110
4.6.1 Fuzzification 110
4.6.2 Base of knowledge 111
4.6.3 Mechanisms of inference 111
4.6.4 Defuzzification 112

4.7 Implementation of Fuzzy Logic in power system test 114
4.7.1 Fuzzification and Rule base 115
4.7.2 Inference 120
4.7.3 Defuzzification 120
4.8 Simulation results 120
4.8.1 Diagnostic performances 120
4.8.2 Robustness test 139
4.9 Conclusion 144
General Conclusion 145
Bibliography 147

List of figures

Figure 1.1 Analytical and hardware redundancy architecture 8
Figure 1.2 Faults types occur in a system 9
Figure 1.3 Different diagnostic methods 10
Figure 1.4 Healthy system graphic representation of Park vectors 12
Figure 1.5 Graphical representation of Park vectors for different faults 12
Figure 1.6 Temporal to frequency representations 13
Figure 1.7 ANN structure 16
Figure 1.8 Representation of a neuro-fuzzy system 17
Figure 1.9 Model-based diagnosis method representation 18
Figure 1.10 Observer-based fault diagnostics block diagram 19
Figure 1.11 Structure of dedicated back observers 20
Figure 1.12 Generalized observer structure 21
Figure 1.13 Luenberger observer structure 22
Figure 1.14 Sliding mode observer structure 24
Figure 1.15 Principle of the parameter estimation approach 25
Figure 2.1 Implementation of a diagnosis system in the transmission line. 30
Figure 2.2 The schematic of the transmission line. 31
Figure 2.3 The mathematical model of the transmission line 32
Figure 2.4 The corresponding reactance (Xeq) of a fault-free transmission line 32
Figure 2.5 The corresponding reactance (Xeq') of the under fault transmission line 32
Figure 2.6 Healthy system behavior (a) Three phase currents 35
Figure 2.7 System behavior with a fault of phA in zone 1, (a) Three phase currents ,(b) Park circle without fault 36
Figure 2.8 Short-circuit (Ph_a-Gnd) fault 37
Figure 2.9 Short-circuit (Ph_b-Gnd) fault 37
Figure 2.10 Short-circuit (Ph_c-Gnd) fault 38
Figure 2.11 Ph_a–Gnd short circuit in all zones 39
Figure 2.12 Short circuit fault Ph_a-ph_b-Gnd 40
Figure 2.13 Ph_b-phc-Gnd Short circuit 41

Figure 2.14 Ph_a-ph_c-Gnd Short circuit 41
Figure 2.15 Short circuit on both lines (2L) 42
Figure 2.16 Short circuit fault of three phases Ph_{abc} 43
Figure 2.17 Discrete wavelet transform for Signal decomposition. 45
Figure 2.18 Flowchart of proposed algorithm 46
Figure 2.19 Current signals during normal operation 47
Figure 2.20 Current signals of PhA-g fault 48
Figure 2.21 Current signals of PhBC fault without the ground 48
Figure 2.22 Current signals of PhBC-g fault 48
Figure 2.23(a) Current signal (phA) (d1 to d6) detail coefficient from level 1 to level 6 during LG fault 49
Figure 2.24 Variation of detail Coefficient of AG ,BG,CG fault at 50% of the Transmission line 50
Figure 2.25 Variations in the ABCG Fault's three phase current fault indexes 50
Figure 3.1 Simplified diagram of a human brain neuron. 56
Figure 3.2 Diagram of the functioning of a formal neuron 58
Figure 3.3 The different architects of neural networks 60
Figure 3.4 PMC neural network. 61
Figure 3.5 Radial basis function neural network. 61
Figure 3.6 Recurrent neural network. 62
Figure 3.7 Supervised learning 63
Figure 3.8 Non supervised learning 64
Figure 3.9 Diagram of the diagnostic system 66
Figure 3.10 Faults types 67
Figure 3.11 Two Surveillance systems 67
Figure 3.12 Diagnosis system output 68
Figure 3.13 ANN Diagnosis system output 68
Figure 3.14 Artificial neurons network structure 70
Figure 3.15 Voltages V_{abc1} and currents I_{abc1} of Ph_a-Gnd short-circuit 77
Figure 3.16 Voltages V_{abc2} and currents I_{abc2} of Ph_a-Gnd short-circuit 77
Figure 3.17 Pha-Gnd SC zone detection of the fault 78
Figure 3.18 Identification of the fault type (SC-Side1 and SC-Side2) 78

Figure 3.19 Faulty phase classification (Ph_a-GND)....79
Figure 3.20 Voltages V_{abc1} and currents I_{abc1} of Ph_a-Gnd sc-side1 80
Figure 3.21 Voltages V_{abc2} and currents I_{abc2} of Ph_a-Gnd sc-side1 80
Figure 3.22 SC Ph_a-Gnd-Side1 fault zone detection....81
Figure 3.23 Identification of the fault type (SC-Side1 and OC-Side2) 81
Figure 3.24 Identification of the fault phase (Ph_a-GND-Side1) 82
Figure 3.25 Voltages V_{abc1} and currents I_{abc1} of Ph_a-Gnd-Side2 during SC....82
Figure 3.26 V_{abc2} and I_{abc2} of SC fault of Ph_a-Gnd-Side2....83
Figure 3.27 SC ph_a-Gnd-Side2 fault zone detection.....83
Figure 3.28 Identification of the fault type (OC to Side1 & SC to Side2). 84
Figure 3.29 Identification of the fault phase (Ph_a-GND-Side2) 84
Figure 3.30 Voltages V_{abc1} and currents I_{abc1} of Pha during OC fault....85
Figure 3.31 Voltages V_{abc1} and currents I_{abc1} of OC fault of Pha....85
Figure 3.32 OC Pha fault zone detection....86
Figure 3.33 Identification of the fault type (OC-Side1 and OC-Side2)....86
Figure 3.34 Identification of the fault phase (Pha) 87
Figure 3.35 V_{abc1} and I_{abc1} of SC fault of Pha-Phb-Gnd....87
Figure 3.36 V_{abc2} and I_{abc2} with SC fault of Pha-Phb-Gnd....88
Figure 3.37 SC Pha-Phb-Gnd fault zone detection....88
Figure 3.38 Identification of the fault type (SC-Side1 and SC-Side2)....89
Figure 3.39 Identification of the fault phase (Pha-Phb-GND)....89
Figure 3.40 Voltages V_{abc1} and currents I_{abc1} of SC fault of Pha-Phb-Gnd (Fault at 15 km)....90
Figure 3.41 Voltages V_{abc2} and currents I_{abc2} of SC fault of Pha-Phb-GND (at 15 km). 90
Figure 3.42 SC Pha-Phb-GND(Fault by15 km) fault zone detection. 91
Figure 3.43 Faulty phase classification (SC-Side1 and SC-Side2): displacement by 15 km 91
Figure 3.44 Identification of the fault phase (Pha-Phb-GND): displacement by 15 km. 92
Figure 3.45 V_{abc1} and I_{abc1} of Pha-Phb during short-circuit....92
Figure 3.46 V_{abc2} and I_{abc2} of Pha-Phb during short-circuit....93
Figure 3.47 SC Pha-Phb fault zone detection 93
Figure 3.48 Identification of the fault type (SC-Side1 and SC-Side2)....94
Figure 3.49 Identification of the fault phase (Pha-Phb)....94

Figure 3.50 V_{abc1} and I_{abc1} of SC fault (at 15 Ω) of Ph_a-Gnd-Side1 95
Figure 3.51 Voltages V_{abc2} and currents I_{abc2} of SC fault (at 15 Ω) of Pha-Gnd-Side1 96
Figure 3.52 SC Pha-Gnd-Side1 (15 Ω) fault zone detection 96
Figure 3.53 Fault type identification (SC-Side1 and OC-Side2): resistance variation by 15 Ω 97
Figure 3.54 Faulty phase classification (Pha-GND-Side1): resistance variation by 15 Ω 97
Figure 3.55 V_{abc1} and I_{abc1} of Pha during of short-circuit with load variation (side 1) 98
Figure 3.56 V_{abc1} and I_{abc1} of Pha during of short-circuit with load variation (side 2) 98
Figure 3.57 SC Ph_a-Gnd-Side1 (load variation) fault zone detection 99
Figure 3.58 Identification of the fault type (SC-Side1 and OC-Side2) with load variation 99
Figure 3.59 Identification of the fault phase (Pha-GND-Side1) with load variation 100
Figure 4.1 The characteristics of a fuzzy set 105
Figure 4.2 Example of the characteristics of a fuzzy set 106
Figure 4.3 Form of function Triangular 107
Figure 4.4 Form of trapezoidal function 107
Figure 4.5 Form of Gaussian function 108
Figure 4.6 Two fuzzy subsets union 109
Figure 4.7 Two fuzzy subsets intersection 109
Figure 4.8 Fuzzy complement figure 110
Figure 4.9 Fuzzy logic structure 110
Figure 4.10 Defuzzification by center of gravity 113
Figure 4.11 Defuzzification by the average of the maxima 114
Figure 4.12 Fuzzy logic implantation 114
Figure 4.13 Implantation of Fuzzy logic in the transmission line ends. 115
Figure 4.14 Membership function 115
Figure 4.15 Current (I_a, I_b, and I_c) Fuzzification 116
Figure 4.16 Fuzzification of the Voltage (V_a, V_b, and V_c) 116
Figure 4.17 Fuzzification Outputs 117
Figure 4.18 Voltages V_{abc1} & currents I_{abc1} of Pha during short-circuit 121
Figure 4.19 Voltages V_{abc2} & currents I_{abc2} of Pha during short-circuit 121
Figure 4.20 SC ph_a-GND fault zone detection 122
Figure 4.21 Identification of the fault type (SC-Side1 and SC-Side2) 122

Figure 4.22 Identification of the fault phase (Ph_a-GND) 123
Figure 4.23 Voltages V_{abc1} and currents I_{abc1} of Pha during short-circuit to side1 124
Figure 4.24 V_{abc2} & I_{abc2} of Pha during short-circuit to side2 124
Figure 4.25 SC pha-GND-Side1 fault zone detection 125
Figure 4.26 Identification of the fault type (SC-Side1 & OC-Side2) 125
Figure 4.27 Identification of the fault phase (Ph_a-GND-Side1) 126
Figure 4.28 Voltages V_{abc1} and currents I_{abc1} of Pha during short-circuit side 1 126
Figure 4.29 V_{abc2} & I_{abc2} of Pha during short-circuit side 2 127
Figure 4.30 SC ph_a-GND-Side2 fault zone detection 127
Figure 4.31 Identification of the fault type (OC-Side1 and SC-Side2) 128
Figure 4.32 Identification of the fault phase (Ph_a-GND-Side2) 128
Figure 4.33 V_{abc1} and I_{abc1} of Ph_a during open circuit side1 129
Figure 4.34 Voltages V_{abc2} and currents I_{abc2} of Ph_a during open circuit side 2 129
Figure 4.35 OC ph_a fault zone detection 130
Figure 4.36 Identification of the fault type (OC to both sides) 130
Figure 4.37 Identification of the fault phase (Ph_a) 131
Figure 4.38 V_{abc1} and I_{abc1} of Pha-Phb-Gnd during short-circuit 131
Figure 4.39 Voltages V_{abc2} and currents I_{abc2} of Pha-Phb-Gnd during short-circuit 132
Figure 4.40 SC Pha-Phb-Gnd fault zone detection 132
Figure 4.41 Identification of the fault type (SC to sides) 133
Figure 4.42 Identification of faulty phase (Pha-Phb-GND) 133
Figure 4.43 V_{abc1} and I_{abc1} of Phag-Phbg during short-circuit (by 15 km) 134
Figure 4.44 V_{abc2} and I_{abc2} of Phag-Phbg during short-circuit (by 15 km) 134
Figure 4.45 Zone detection of Phag-Phbg SC (by 15 km) 135
Figure 4.46 Identification of the fault type short-circuit to both sides (by 15 km) 135
Figure 4.47 Identification of the faulty phase Phag-Phbg short-circuit (by 15 km). 136
Figure 4.48 Voltages V_{abc1} and currents I_{abc1} of Pha-Phb during short-circuit 136
Figure 4.49 V_{abc2} and I_{abc2} of Pha-Phb during short-circuit 137
Figure 4.50 SC Ph_a-Ph_b fault zone detection 137
Figure 4.51 Identification of the fault type (short-circuit to both Sides) 138
Figure 4.52 Identification of the fault phase (Ph_a-Ph_b) 138

Figure 4.53 V_{abc1} and I_{abc1} of SC fault (at 15 Ω). 139
Figure 4.54 Voltages V_{abc1} and currents I_{abc1} of SC fault (at 15 Ω) of Pha-GND-Side1 139
Figure 4.55 Zone detection of short-circuit to side1 (at 15 Ω) 140
Figure 4.56 Identification of the fault type (SC to Side1 and OC to Side2): at 15 Ω 140
Figure 4.57 Identification of faulty phase (Ph_{ag}): of 15 Ω resistance 141
Figure 4.58 Voltages V_{abc1} and currents I_{abc1} of Phag short-circuit to side1(load variation) 142
Figure 4.59 Voltages V_{abc2} and currents I_{abc2} of Phag short-circuit to side2(load variation) 142
Figure 4.60 SC Ph_a-GND-Side1 fault zone detection (For load variation) 143
Figure 4.61 Identification of the fault type (SC-Side1 and OC-Side2): For load variation 143
Figure 4.62 Identification of the fault phase (Pha-GND-Side1): For load variation 144

List of tables

Table 1-1 Non-locating signature 26
Table 1-2 Weakly localizing signature 26
Table 1-3 Strongly localizing signature 27
Table 2-1 Shunt reactance of different fault types 33
Table 2-2 Detail coefficients values variations of pha-phb fault 51
Table 2-3 Detail coefficients values variations of PhB-PhC fault 52
Table 2-4 Detail coefficients values variations of PhA-PhC fault 52
Table 3-1 Most used activation functions 59
Table 3-2 Sides point of view of the faults 68
Table 3-3 Variation intervals as ANN inputs 73
Table 3-4 Training data for ANN 76
Table 4-1 Inferences Rules 119

General Introduction

General Introduction

Transmission lines are used to transfer power between generating plants and load centers, however they suffer from different types of faults that occur randomly and damage the equipment or harm humans. to reduce the damage to the power system, it is vital to establish a well-coordinated protection system that can immediately identify and isolate faults.

These faults can be classified in to series faults (open conductor fault) and shunt faults (short circuit fault) [1] , which have several types: single line to ground L-G (Pha-gnd ,Phb-gnd, Phc-gnd), double line to ground 2L-G (Phab-gnd, Phbc-gnd, Phac-gnd), double line in contact without the ground L-L (Pha-b,Phb-c,Pha-c) and three phase fault 3L-G (Pha-b-c) [2, 3]. Similar to short circuits, open circuit faults can affect one, two, or three phases.

To diagnose transmission lines, a variety of techniques have been used. These techniques can be categorized into many groups such as impedance measurement [4, 5], the time domain methods based on current & voltage measurements [6], artificial intelligence techniques [7, 8] and traveling wave techniques [9].

Impedance-based techniques can be broadly categorized as two ends techniques [10, 11] and one end techniques [12, 13], both are regarded as precise and comprehensive, yet, they raise the cost of calculation and increase complexity. because some asynchronous methods may produce contradictory results, which requires the use of a satellite as well as a precise representation of the faulty transmission line. Additionally, the accuracy may be impacted by the fault resistance.

Using high-frequency forward and backward fault signals propagating to both ends of the transmission line and knowing the wave propagation velocity, when these signals reach the ends they utilized to locate the fault using traveling wave techniques [14, 15]. These techniques are often divided into two ends techniques [16, 17], one end techniques [18, 19] or both, in [20] ,the algorithm is effective and beneficial for locating simultaneous faults, but the accuracy attained is dependent on exact synchronization between the transmission line's ends, and it is not economical. By eliminating the synchronization problem, the authors of [21], developed a traveling-wave technique to increase the accuracy of fault location.. Nevertheless, many measurement equipment and satellites are needed in order to implement this method. In [22], TW and machine learning were combined. In general, these methods have a lot of benefits, they are not impacted by changes in load or high ground resistance., and have exceptional precision, speed, and reliability. however, there are some drawbacks to this approach.

The accuracy decreases when the fault gets further away, and they require a significant number of samples and data. They also require high sampling frequencies and expensive. To synchronize the signals at the two ends, some two-end techniques also utilize a Global Positioning System (GPS) [21, 23].

Time domain techniques rely on measurements of currents and voltages. [24, 25]. Utilizing these measures vary, For high impedance faults, the authors in [26] provide a method based on instantaneous phase angles ,it is resilient to harmonics but needs a large sampling rate. [27] provides a novel, dependable, and precise method solution based on an auto-reclosing positive sequence superimposed network. But its execution duration is 3 minutes. While Kalman Filter, an efficient and simple method, is presented in [28] , Other techniques for extracting features from signals like S-transform [29] ,FFT [19] , Wavelet transform [30, 31], DFT [32, 33] depend on converting signals to the frequency domain. These techniques considered insufficient and need additional algorithms. But even if they produce satisfactory outcomes, these techniques need in-depth expertise regarding the system configuration. These methods are insufficient and need an additional algorithm. and in-depth understanding of the system configuration.

Due to the advantages of using intelligent algorithms, a lot of researchers have become interested in this field recently These methods rely on collecting data under various faults conditions and utilize them to build databases and train the algorithms, determining the location and fault type by evaluating the test results comparing with the database. The convolutional neural network (CNN)-based method described in [34] merits more study because of the huge amount of data needed and the system's usage of image processing to provide only fault classifications. Also CNN was used in [8, 35, 36]. Extreme learning machine is widely used such in [37, 38], and an artificial neural network method was used in [39]. In [40] an "end-to-end long short-term memory model" is suggested and utilized by an algorithm for machine learning. In [41] a multi-stage approach based on convolutional sparse auto encoder and unsupervised feature learning was presented. Combinations of artificial neural network ANN, FIR filter, and SVMs [42].methods based on Fuzzy logic analyzed in [43, 44], S-transform and fuzzy logic [3],K-Nearest Neighbor method [45]. These methods need a lot of data, and some are only effective in fault classification.

None of the previous solutions took open-circuit faults into account and instead concentrated on short-circuit faults., utilizing fuzzy logic and artificial neural networks, two intelligent transmission line fault diagnosis methods were suggested in this work., both short–circuit faults & open-circuit faults

were considered, a new technique is proposed to distinguish between them as some of these faults could be a short–circuit and an open-circuit at the same time.

This thesis also contributes by examining how fuzzy logic and artificial neural networks are implemented. then comparing their performances with the classical methods (Park's vectors method and Wavelet Transform method), the effectiveness of. Both approaches are tested against various load angle variations, various fault types, as well as varied fault resistances. The results indicate that both of these modern techniques present a robust performance and reliable to implement in smart grids.in addition both are fast and economical as they do not require a complex computational costs.

There are four chapters in this thesis:

The first chapter introduces the state of the art on faults diagnosis in the industrial systems starting with some terminologies and concepts then presenting the most used diagnosis methods in general. Chapter two presents the short-circuit detection of the transmission line by signal-based methods, the first method is Park' vectors and the other method is the Wavelet transformation. Transmission line fault diagnosis by artificial neural network is covered in Chapter three. Another artificial intelligence method is presented in chapter four where the fuzzy logic implementation in power system transmission line protection is introduced and analyzed.

Chapter 1: State of the Art: Faults Diagnosis in Industrial Systems

1.1 Introduction

The diagnosis of industrial system faults consists on detection, identification and location of faults or any abnormal operating mode [46], allowing the introduction of command to clarify any faults or failures and to return to an operating mode more suited to the mission for which this system was designed. It is therefore an essential element of an industrial system or any system to remain in operating mode. Therefore, this Chapter is structured as follows: at first, in Section1.2 a few important definitions and concepts about fault diagnosis of industrial systems, then is section 1.3 the redundancy (hardware and analytic) is presented, after that the diagnosis principle (FDI system) in section 1.4, section 1.5 introduce the different diagnostic methods (model-based and signal-based) finally this chapter ends with the residual generation, diagnostic performance and the conclusion.

1.2 Notions and concepts of system diagnostics

First, a recall of the main terms used in the diagnosis of industrial systems. A non-exhaustive number of definitions are proposed in order to clarify the concepts used in this work. These used terminologies in this thesis intends to be as much as possible consistent with that proposed by the IFAC "Technical Committee on Fault Detection, Supervision and Safety of Technical Processes (SAFEPROCESS)". As a result of the suggestions made by the SAFEPROCESS Technical Committee, the terminologies used in FDI have become reasonably standardized [47].

The following set of definitions was firstly suggested by the authors in [47] based on the discussion within the Committee during the period 1991 - 1995. Many other works in the literature, agree with this nomenclature.

- **"*Fault Detection*:** Determination of the faults present in a system and the time of detection".
- **"*Fault Isolation*:** Determination of the kind, location and time of detection of a fault". Follows fault detection
- **"*Fault Identification*:** Determination of the size and time-variant behavior of a fault". Follows fault isolation.
- **"*Fault diagnosis*:** Determination of the kind, size, location and time of detection of a fault. Includes fault detection, isolation and identification".
- **"*Fault*:** An unpermitted deviation of at least one characteristic property or parameter of the system from the acceptable/usual/standard condition".

• **"Failure:** A permanent interruption of a system's ability to perform a required function under specified operating conditions".

• **"Malfunction:** An intermittent irregularity in the fulfilment of a system's desired function".

• **"Error:** A deviation between a measured or computed value (of an output variable) and the true, specified or theoretically correct value".

• "**Disturbance**: An unknown (and uncontrolled) input acting on a system".

• "**Perturbation**: An input acting on a system, which results in a temporary departure from the current state".

• "**Residual**: A fault indicator, based on a deviation between measurements and model equation-based computations".

• "**Symptom**: A change of an observable quantity from normal behavior".

1.3 Notion of redundancy (hardware and analytical)

The basic concept of diagnostic systems is the verification of the consistency of the various information available on the system. This is only possible if there is a certain degree of redundancy between this information. This redundancy can be obtained by the multiplication of actuators and sensors (hardware redundancy) and the use of process models by techniques such as analytical redundancy.

1.3.1 Hardware redundancy

Hardware redundancy consists of installing a series of sensors measuring the same physical quantity on the same component of the system. The comparisons by difference of the measurements of the sensors two by two then form the residuals. If one of the sensors is faulty, it is then easily detected and isolated, because it affects all the residues where it occurs. Many industrial applications apply this diagnostic method. This method is mainly dedicated to systems presenting high risks, such as nuclear power plants, aeronautics, etc. these are systems on which safety takes priority over the cost and maintenance of the sensors [48].

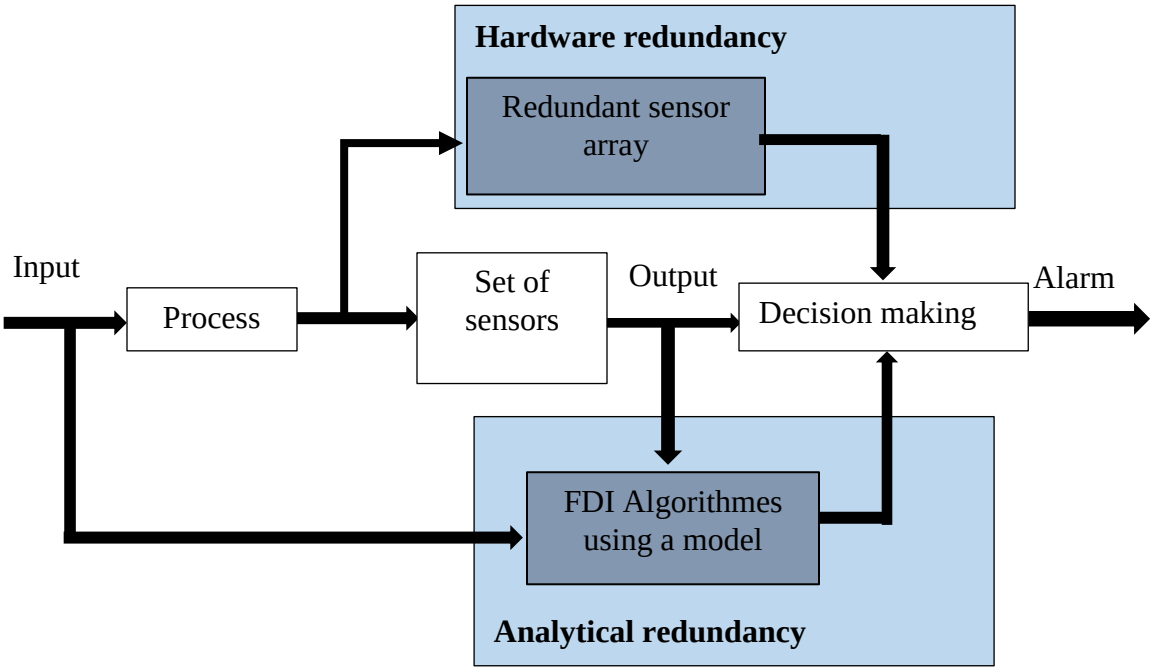

Figure 1.1 Analytical and hardware redundancy architecture

1.3.2 Analytical redundancy

From the physical system model equations, expressing relations of connection between the internal variables, it is possible to highlight an analytical redundancy. the knowledge of the values of certain variables (the measurements carried out on the process), can give rise to an informational redundancy and the checking of the coherence of this redundancy makes it possible to generate the residues which will be used to detect an abnormal operation of the process [49].

1.4 Diagnosis principle (FDI system)

In general, an industrial system is composed of three parts where the faults can occur on any of these three them:

– the actuators,

– the sensors,

– the process.

The fault detection and fault isolation (location) are the two fundamental processes in fault diagnosis. To accomplish the detection, a signal indicating the presence of a fault is created. This signal, called residue, once generated it is then used to find the fault after being detected. These two operations are done with the help of algorithms known as FDI (Fault Detection and Isolation). Then the fault is located in order to carry out the appropriate kind of maintenance.

It is possible to implement fault diagnosis algorithms on the system either in operation or offline, depending on the type of maintenance implemented, corrective or preventive. The identification will also allow the implementation of fault-tolerant procedures such as the reconfiguration of the control [50].

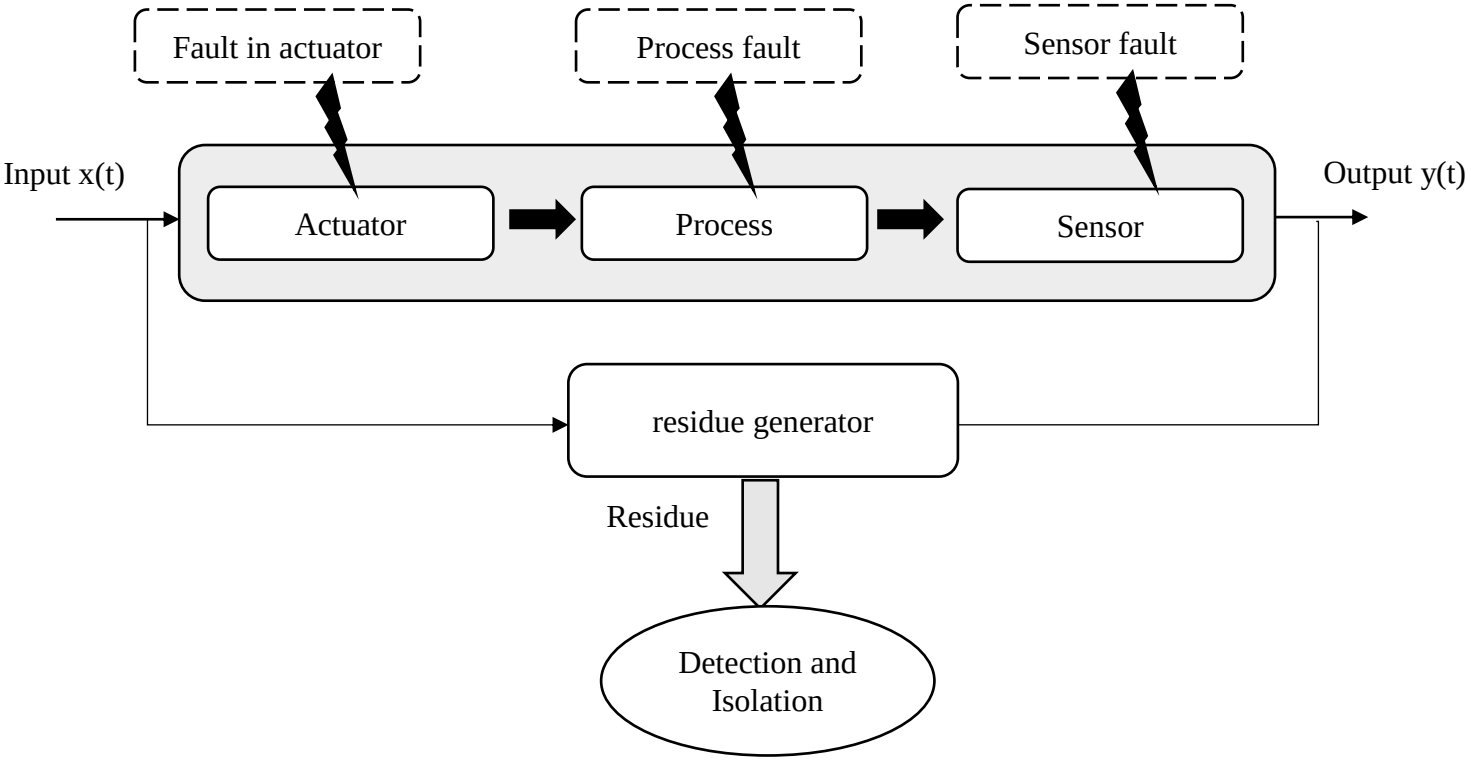

Figure 1.2 Faults types occur in a system

The diagnostic logic (Figure 1.2) consists of making decisions resulting directly from the evaluation of the residuals r(t). Zero residuals signify that the system is in excellent condition. thus continuing monitoring the system in continuous time. Non-zero residuals indicate a malfunction

of the system. Thus understanding the reasons through the detection and isolation steps that make up r(t)=0 or r(t)=/0.

1.5 The different diagnostic methods

Two large families can be taken into consideration: models-based methods and methods without models also called the methods based on signal as shown in figure 1.3. The first family is based on an in-depth knowledge of the system including the causal relationships between the different elements while the second on knowledge obtained from past experiences.

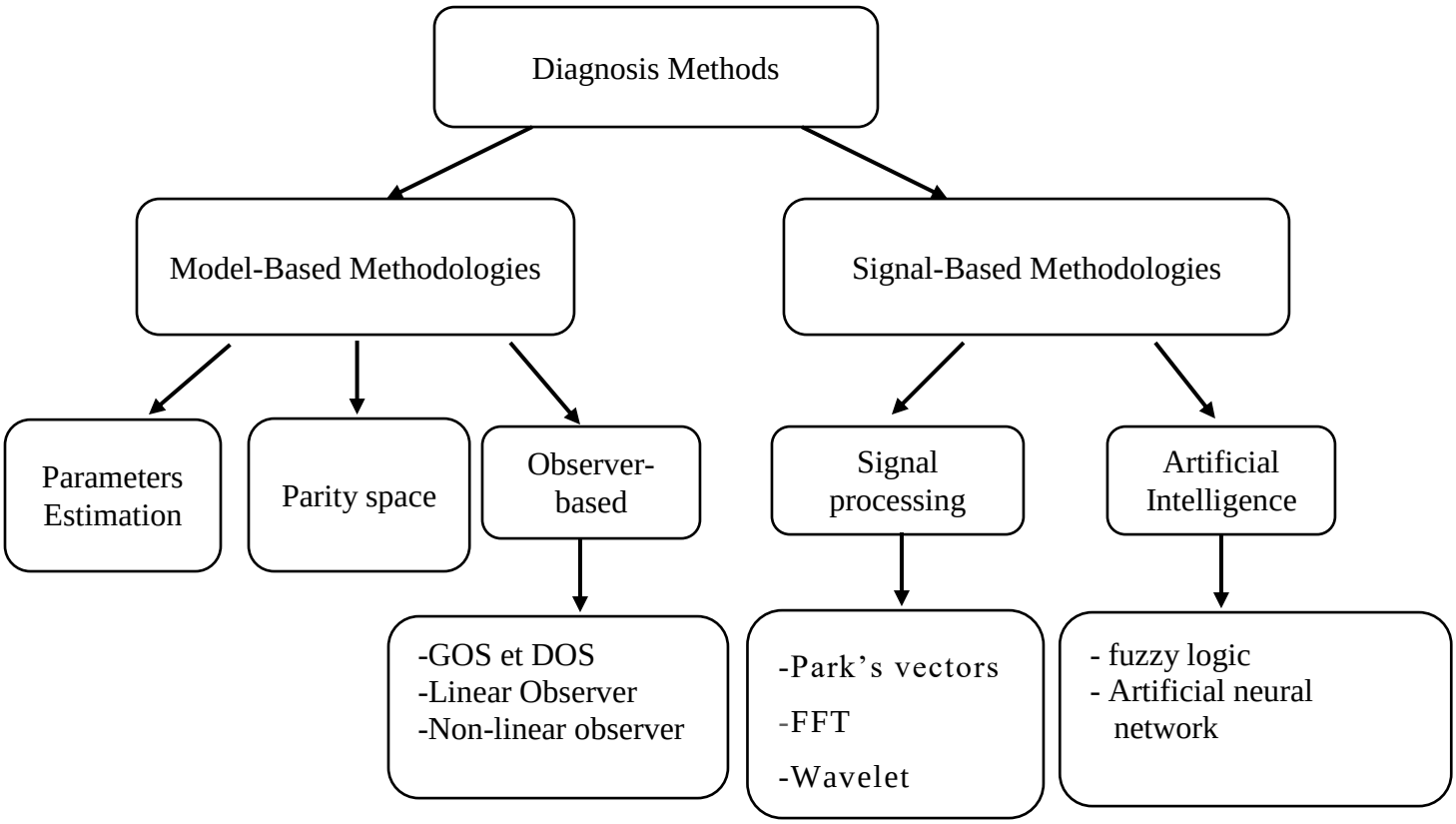

Figure 1.3 Different diagnostic methods

1.5.1 Diagnosis based on signal processing

In some industrial applications, obtaining a system model is difficult, if not impossible. This difficulty is explained by the complexity of the system. In fact, only diagnostic methods based on signal processing (model-free) are available for this type of application. these diagnostic methods

are relying on extracting features from the signals, then applying the fault diagnosis by checking difference between the known signal of the fault-free system (without fault) and the signal of the system under fault. These techniques classified into three families: frequency-domain, time-domain, or both time-frequency-domain signal processing techniques.

1.5.1.1 Diagnosis by Park's vectors

Fault diagnosis by the Park vector approach (time-domain method) was initially made public by Cardoso in 1986 [51]. This method, is simple to understand and use, it depends on the Park transformation of the three-phase currents into two equivalent current vectors. The two equations that allow a three-phase system to become a two-phase system are given by [52].

$$id = \sqrt{\frac{2}{3}ia} - \frac{1}{\sqrt{6}}ib - \frac{1}{\sqrt{6}}ic \qquad 1.1$$

$$iq = \frac{1}{\sqrt{2}}ib - \frac{1}{\sqrt{2}}ic \qquad 1.2$$

Where "a," "b," and "c" are the three phases' respective currents, and id and iq represent the transformation of these currents into Park currents (two-phase system).

In case of a supposedly perfect, i.e. symmetric, system, the representation of the Park currents (Park vectors) of the system is the equivalent of a perfect circle shown in Figure 1.4. This representation displays the vector values of Park id as a function of iq, or vice versa.

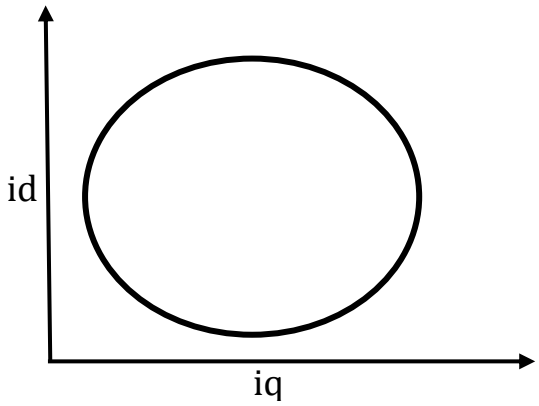

Figure 1.4 Healthy system graphic representation of Park vectors

During a fault, this graphic representation of the currents is no longer the same., the existence of imbalance in the three-phase currents of system leads to a deformation of the perfect circle that we had previously, as illustrated in Figure 1.5 The park circle offers the possibility of visualizing faults, its shape, thickness and inclination make it possible to detect faults.

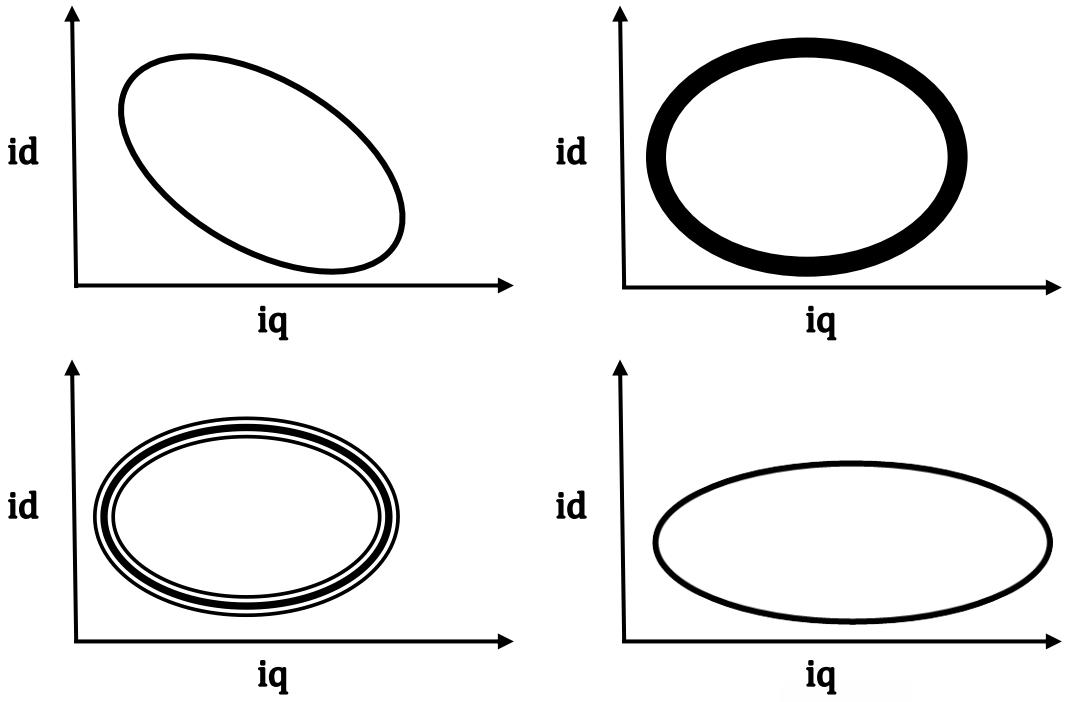

Figure 1.5 Graphical representation of Park vectors for different faults

1.5.1.2 Diagnosis by Fast Fourier Transform (FFT)

An alternative to the temporal representation of the signal consists in representing its frequency content. This is obtained by calculating its Fourier transform (FT) [53], defined for a signal x(t) of finite energy by:

$$X(f) = \int_{-\infty}^{+\infty} x(t) e^{-j2\pi f t} dt \qquad 1.3$$

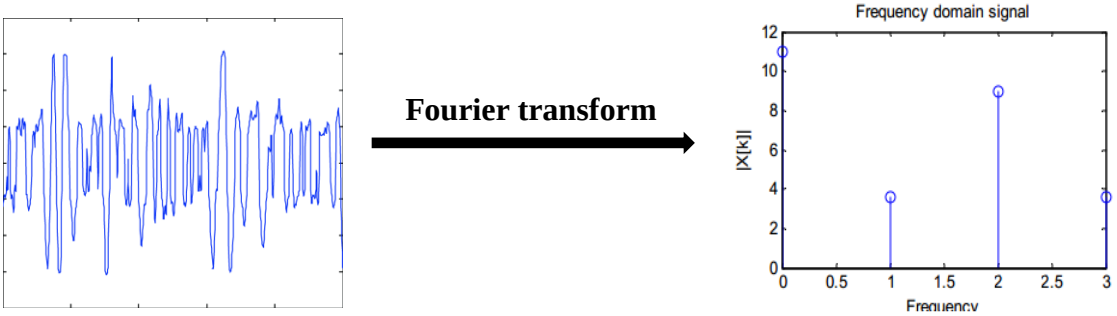

Figure 1.6 Temporal to frequency representations

Using a sample time of T, its discrete Fourier transform of N points is:

$$X(k) = \sum_{n=0}^{N-1} x(n) e^{-j2\pi \frac{nk}{N}} \qquad 1.4$$

The Fast Fourier Transform (FFT) is a valuable technique for reducing the discrete Fourier transform's time and operations number. This transform's fundamental algorithm makes use of a number of points. N^2which makes it possible to obtain a time saving of calculates, compared to a calculation with the discrete Fourier transform of $\frac{N}{log_2(N)}$.

1.5.1.3 Wavelet diagnostics

The wavelet transform (time-frequency-domain method) is a signal processing tool that decomposes signals into several frequency bands with different resolutions using a bank of high-pass and low-pass filters [54]. It is especially effective at analyzing non-stationary signals or to detect sudden variations in electrical parameters such as voltage, current, frequency. A signal's f(t) continuous wavelet transform can be written:

$$T(\tau, s) = \frac{1}{\sqrt{s}} \int_{-\infty}^{+\infty} f(t)\psi^*(\frac{t-\tau}{s})\, dt \qquad 1.5$$

ψ(.) is the base function of wavelet and ψ^* represents its complex conjugate;
s is the scale factor and τ is the offset factor.

1.5.2 Diagnosis based on artificial Intelligence

1.5.2.1 By fuzzy logic

The "if-then" relationship is the basis for this approach. In contrary to the concept of Boolean logic, fuzzy logic accepts values between [0, 1], where 0 denotes total untruth and 1 denotes absolute truth., to signify the degree of truth[55]. It is utilized for system failure classification, localization, and detection. This method requires less calculation [56].

Fuzzification, inference fuzzy system, rule fuzzy base, and defuzzification make up a fuzzy scheme's basic global organization [57], In the fuzzification stage, a fuzzy set is created by mapping the net numbers into it. After being fuzzified, Using the provided fuzzy rule basis, the

fuzzy inputs are passed to the fuzzy inference system. The output fuzzy set from the defuzzification stage is the last step.

1.5.2.2 By neural network

Artificial neural networks (ANN) are networks which process information using complicated mathematical equations [58]. They are founded on a model of how synapses and neurons function in the human brain. Single nodes, also known as neurons or units, are connected by neural networks [59], just like the human brain does. The term "neural network" refers to a network of nodes made up of a number of these nodes. These neurons take in information, combine it with their own activation function, and optionally add to it a threshold. It then generates the output using an output function. Each connection in the neural network sends an output from one neuron, which then serves as an input to another neuron in the network. Each connection in the neural network is given a weight that signifies its amount of importance. Many-to-many connections between inputs and outputs are possible between any two neurons.

The usage of ANN in diagnostics is similar to pattern recognition in that each fault is connected to its most likely source. One can obtain an output that represents the system status from an input vector that contains the system parameters to be diagnosed as well as the signals from the sensors [60, 61].

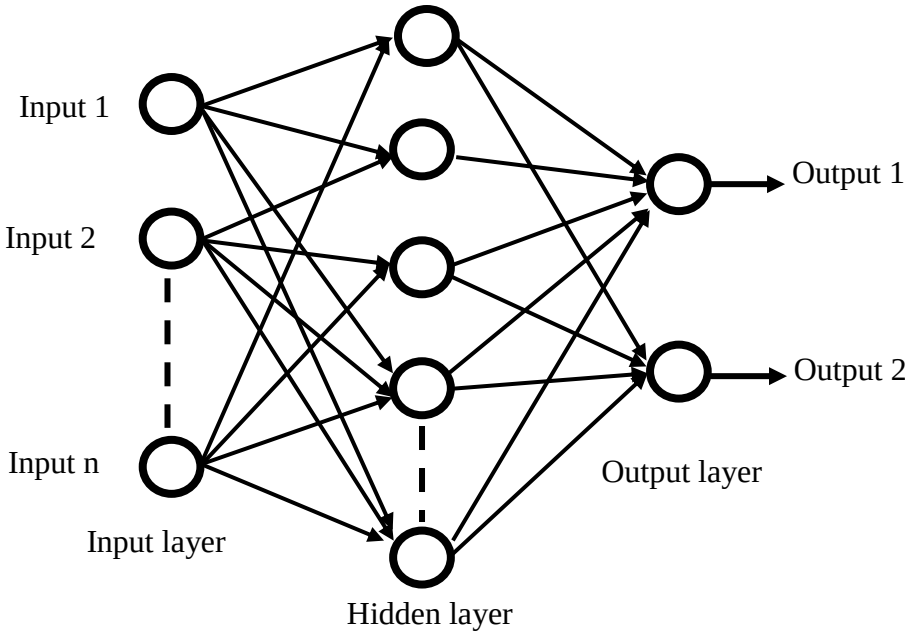

Figure 1.7 ANN structure

1.5.2.3 By neuro-fuzzy

Fuzzy logic and neural networks were merged to produce neuro-fuzzy networks in order to take advantage of each methodology's capabilities. Their primary characteristic is the capacity to combine symbolic and numerical knowledge of a system into a single tool. These are neural networks whose basic element is a fuzzy operator which is often called the fuzzy neuron. A fuzzy neuron (NF) is a mathematical system with the same architecture as its counterpart, the formal neuron. The difference is that either all of its parameters or part of them are explained by fuzzy logic [62].

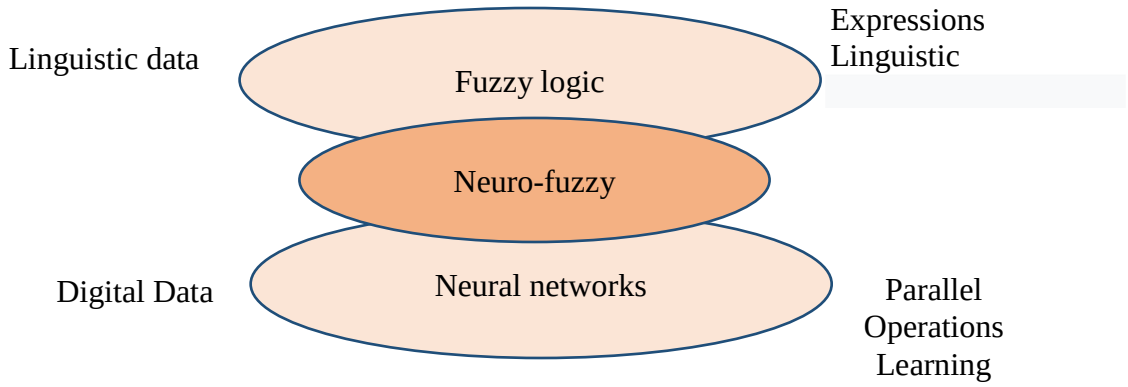

Figure 1.8 Representation of a neuro-fuzzy system

The three subcategories of neuro-fuzzy systems are cooperative neuro-fuzzy systems, concurrent neuro-fuzzy systems, and hybrid neuro-fuzzy systems.

Cooperative neuro-fuzzy systems only use one of the two systems fuzzy or neural to carry out a particular task. The second system injects and makes use of the first's findings. Contrarily, neuro-fuzzy systems continuously interfere to carry out a certain task.

A hybrid neuro-fuzzy system is created by combining a fuzzy inference system and neural network. It is possible to use a neural network with fuzzy parameters., known as a fuzzy neural network, or a fuzzy system, known as a neural fuzzy system, whose parameters are updated by learning thanks to the neural network.

1.5.3 Model-based diagnosis

These techniques compare the system's real behavior with that of the existing qualitative and/or quantitative model [63]. Any deviation is then synonymous with a fault, as shown in the diagram in Figure 1.9.

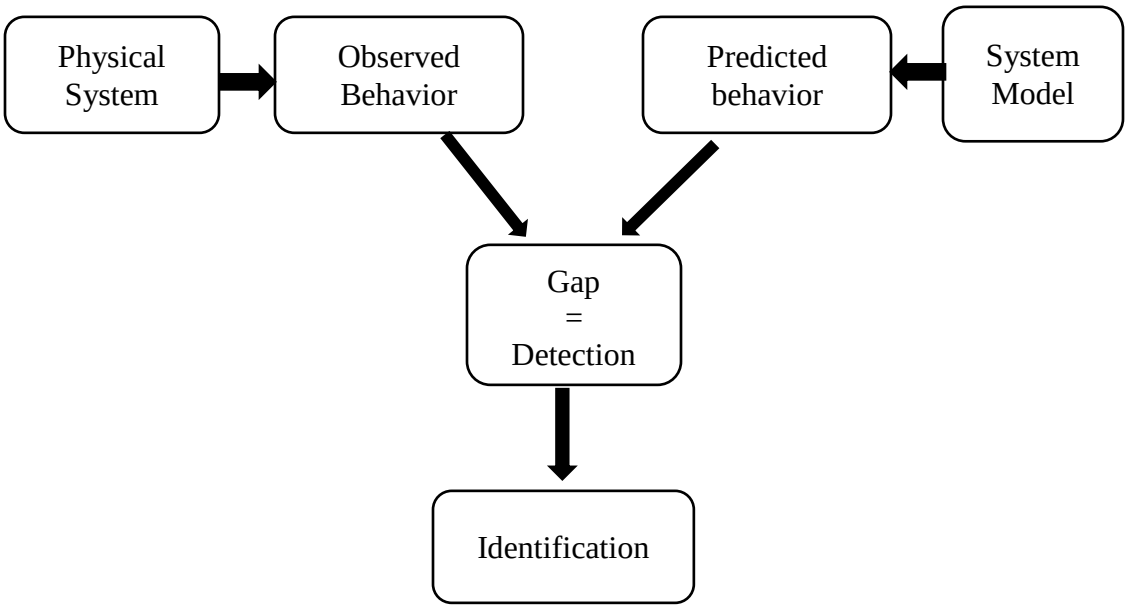

Figure 1.9 Model-based diagnosis method representation

Depending on the type of model (qualitative and/or quantitative), it can distinguish two branches of methods: quantitative methods from the FDI (Fault Detection and Identification) community and qualitative methods from the IA and SED communities. The dissociation between qualitative methods and quantitative methods does not imply that these two aspects are disjoint. In reality, these two types of approach can coexist within the same diagnostic method.

1.5.3.1 Non-linear systems

The assumed nonlinear dynamical system's state representation, defined under normal circumstances:

$$\begin{cases} \dot{x}(t) = g(x,u,t) \\ y(t) = h(x,u,t) \end{cases} \quad 1.6$$

Where t stands for time, x is the state vector, u is the control or input vector, y is the measurement or output vector, and g and h are the non-linear equations that correspond to the state's dynamic equation and the measurement equation, respectively.

1.5.3.2 Linear systems

Linear dynamical systems' state representation which are assumed to be defined under nominal conditions is:

$$\begin{cases} \dot{x}(t) = A(t)x(t) + B(t)u(t) \\ y(t) = C(t)x(t) + D(t)u(t) \end{cases} \quad 1.7$$

Where t, x, u, and y are defined for the system, and A(t), B(t), C(t), and D(t) stand for the state, command, measure, and order measurement matrices, respectively.

1.5.3.3 Observer-based quantitative diagnosis (GOS and DOS)

The concept that residuals are produced by comparing the quantities that are currently accessible in the real system with those that are estimated (by the observer) is the foundation of the observer-based fault diagnosis. Signals for faults indication are produced using the differences in real and predicted outputs. The differences tend to zero in case of absence of faults, but in case of fault, the differences are no longer zero. Any physical system is exposed to unavoidable disturbances, which are translated, just like the faults, by a change in the process model. These disturbances then lead to an inconsistency between the outputs of the physical system and that of the observer. Figure 8 represent Block diagram of fault diagnosis based on observers [64].

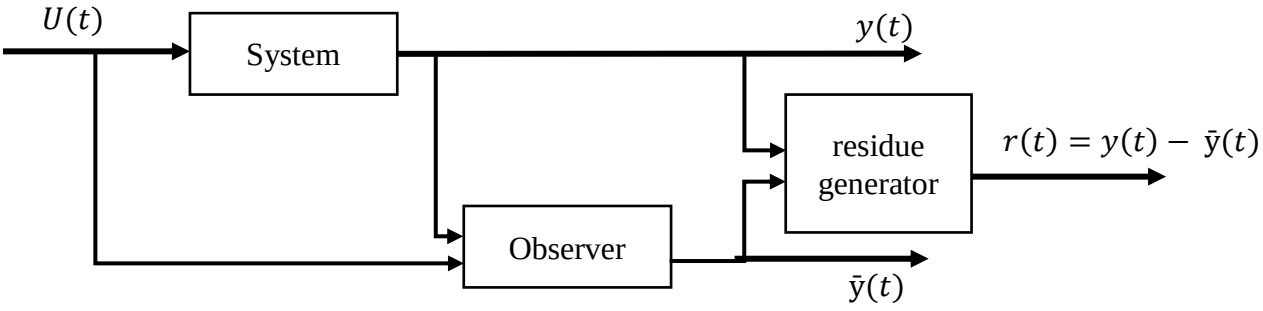

Figure 1.10 Observer-based fault diagnostics block diagram

The literature contains multiple schemes for creating structured residues, among them we can cite:

- Dedicated Observer Scheme (DOS),
- Generalized observer schemes (GOS).

In a dedicated observer scheme (DOS), it is possible to create observer sensitive to a particular fault and ignoring other faults and treating them as as unknown inputs. (i.e., disturbances).Each residual in this case is affected by a single fault. This structure sometimes gives good results but its design remains very limited because it does not allow to overcome unknown inputs and noises [65].

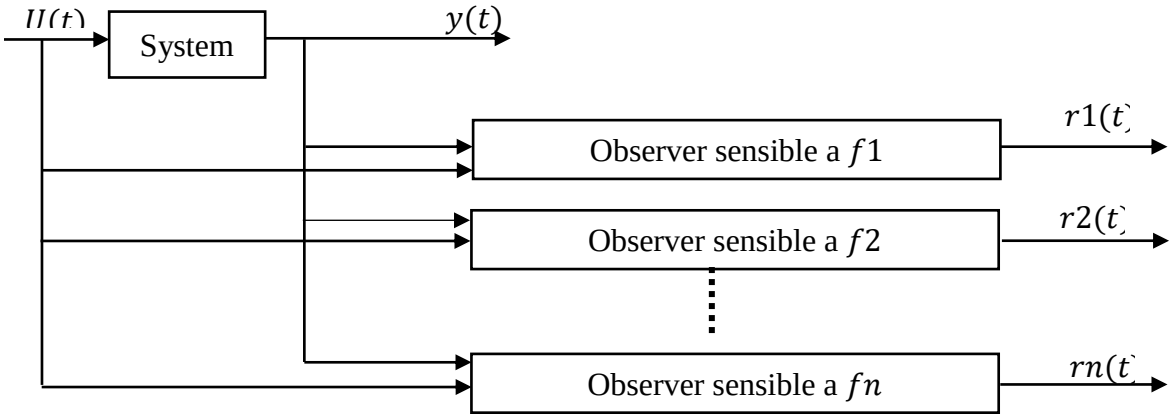

Figure 1.11 Structure of dedicated back observers

Figure 1.13 depicts a Generalized Observer Scheme (GOS). In this kind of structure, it is a question of synthesizing a certain number of observers where each of them being insensitive to a single fault. If a fault then appears, all the state estimates will be erroneous except those coming from the observer insensitive to this single fault. This scheme provides additional design flexibility for the observer designing. and allows to increase the robustness. However, in addition to not being generally able to solve fault location problems, the interactions between the subsystems are still the method's problem. Indeed, if these interactions are weak (even zero), a fault will only affect the estimation of the corresponding local observer [66].

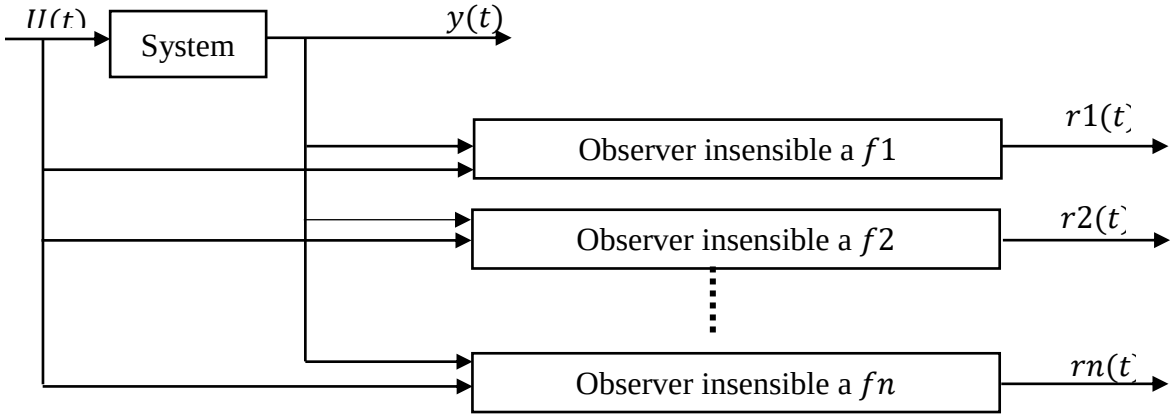

Figure 1.12 Generalized observer structure

1.5.3.4 Quantitative diagnosis based on a linear observer

The state estimation problem for linear processes was solved simply by Luenberger; in this particular case, we consider the linear system's dynamic model as specified by:

$$\begin{aligned} \dot{x}(t) &= Ax(t) + Bu(t) + Lw(t) \\ y(t) &= Cx(t) + V(t) \end{aligned} \qquad 1.8$$

where x(t) stands for the state vector, u(t) for the input vector, y(t) for the output vector, w(t) and V(t) for two Gaussian blanks with zero expectation, and x(0)=x_0 for the initial conditions.

.

1.5.3.5 Luenberger observer

In simple terms, pole placement techniques provide the foundation of Luenberger's theory of observation. Luenberger recommends the following observer for the system, presuming that the noises w and v are both zero.

$$\begin{cases} \dot{\hat{x}}(t) = A\hat{x}(t) + Bu(t) + L(y(t) - \hat{y}(t)) \\ \hat{y}(t) = C\hat{x}(t) \end{cases} \qquad 1.9$$

The Luenberger observer is an asymptotic state observer. The equation e(t)=x(t)-x(t) expresses the estimation error between the system's actual state and the reconstructed state. The dynamics of the estimating error are given by the formula: e(t)=(A-LC) e(t) Thus, choosing the observer's gain L is sufficient using a pole placement strategy so that the matrix (A - LC), demonstrates how the Luenberger observer is represented. Figure 1.14 [67].

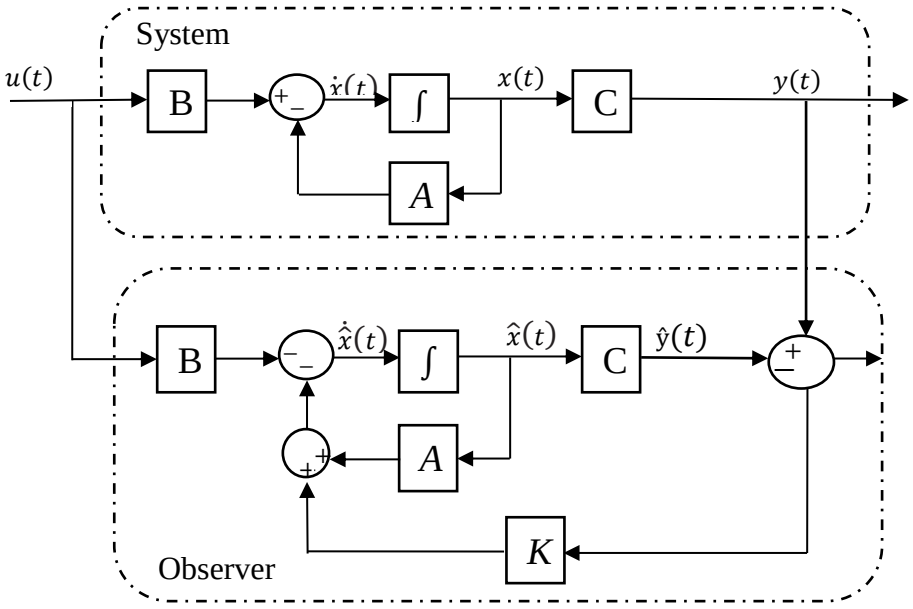

Figure 1.13 Luenberger observer structure

1.5.3.6 Quantitative diagnosis based on a non-linear observer

1.5.3.7 based on a high-gain observer

High-gain observers have outstanding global properties, account for the system's nonlinear nature, and guarantee convergence and stability with a variable convergence speed.

The system's structure is directly used to design the observer [68]. Lyapunov's stability theory can be used to, this strategy applies the strategies created for linear systems to the category of nonlinear systems that the model shows.

$$\begin{cases} x(t) = Ax(t) + f(u(t), x(t)) \\ \hat{y}(t) = C\hat{x}(t) \end{cases} \quad 1.10$$

An uncontrolled linear and a controlled nonlinear component make up the state's dynamics.

The high-gain observer is composed of the following:

$$\dot{\hat{x}}(t) = A\hat{x}(t) + f(\hat{x}(t), u(t)) + K(y(t) - C\hat{x}(t)) \quad 1.11$$

"high gain" refers to the observer's structure, which causes even a little difference between the actual states and estimated states to reflect and amplify when the nonlinear function's Lipschitz constant is big. In order to offset this error amplification, the observer gain K must be high. The estimating error's dynamics are.

$$\begin{aligned} e(t) &= x(t) - \hat{x}(t) \\ \dot{e}(t) &= (A - LC)e(t) + f(x(t), u(t)) - f(\hat{x}(t), u(t)) \end{aligned} \qquad 1.12$$

1.5.3.8 Sliding mode observer

Making an order n's system dynamics converge toward a manifold s of dimension (n-p), This is known as the sliding surface, where p is the measurement vector's dimension., is the basic principle behind sliding mode observers. conditions termed "slipping conditions" make this surface appealing. The system approaches the sliding surface and changes there. in accordance with an order (n-p) dynamic if these conditions are met [69].

When sliding mode observers are involved, observation errors, or e(t)=x(t)-x (t), govern the dynamics. These errors decrease from their initial values, e(t)=0, two stages to reach the equilibrium values. The trajectory of the observation errors first advances in the direction of a sliding surface where the measurements and the observer's output are identical. the name for this stage, which is often quite dynamic, is the reaching mode.

To eliminate all errors, the trajectory of the observation errors is forced to slide on the sliding surface during the second phase.

Consider a nonlinear order n state system:

$$\begin{cases} \dot{x}(t) = f(x, u) \\ y(t) = h(x) \end{cases} \qquad 1.13$$

where x stands for the state vector. The command or input vector is u, while the output vector is y.

The input u is measurable and locally bounded, and the vector fields on x are considered to be sufficiently continuously differentiable for the functions f. The following structure describes the sliding mode observer.

$$\begin{cases} \dot{\hat{x}}(t) = f(\hat{x}, u) - Ksign(\hat{y} - y) \\ \hat{y}(t) = h(\hat{x}) \end{cases} \quad 1.14$$

The (n-p) dimension gain matrix is called K. The obtained observer, as we can see, is a duplicate of the model for the system plus a corrective term. that proves x's convergence to the sliding surface in this situation is established by:

$$s(x) = \hat{y} - y \quad 1.15$$

The corrective term is proportional to the error of the output applied discontinuous function sign, where function sign(x) is defined by:

$$sign(x) = \begin{cases} 1 & if \quad x > 0 \\ 0 & if \quad x = 0 \\ -1 & if \quad x < 0 \end{cases} \quad 1.16$$

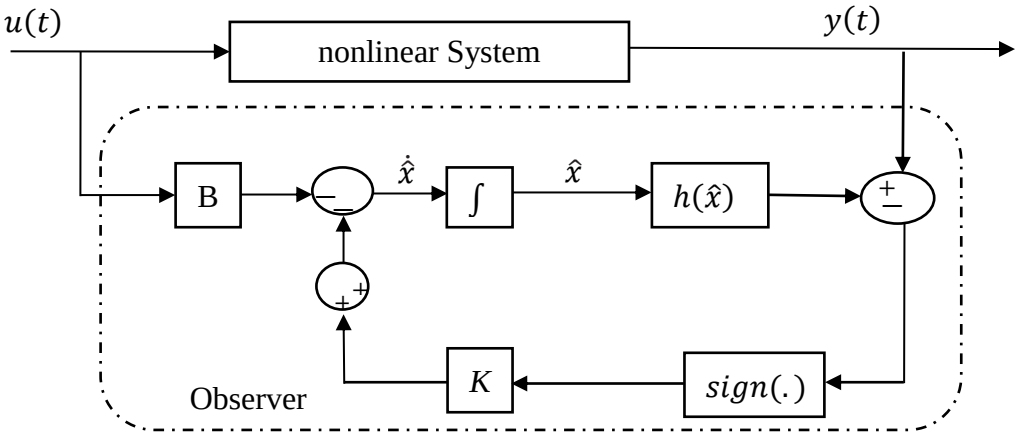

Figure 1.14 Sliding mode observer structure

1.5.3.9 Parameter Estimation based-diagnosis

The parametric estimation method considers the idea that the fault influence reflects the system's dynamic behavior's. The fundamental idea behind this approach is to continuously estimate process parameters using input/output measurements and estimate how far they are from the values of reference for the process's steady state. By parameter, we imply a collection of several physical parameters or specific system constants (such as mass, coefficient of viscosity, etc.) [70]

The benefit of parametric estimate is that it can tell you how important the variations are. However, one of the method's major drawbacks is the need for a physically excited system that is constantly active. poses practical issues as a result of being costly, risky, or functioning in a stationary manner. Additionally, the invertibility of relationships between mathematical parameters is not always guaranteed, which complicates the task of residue-based diagnosis.

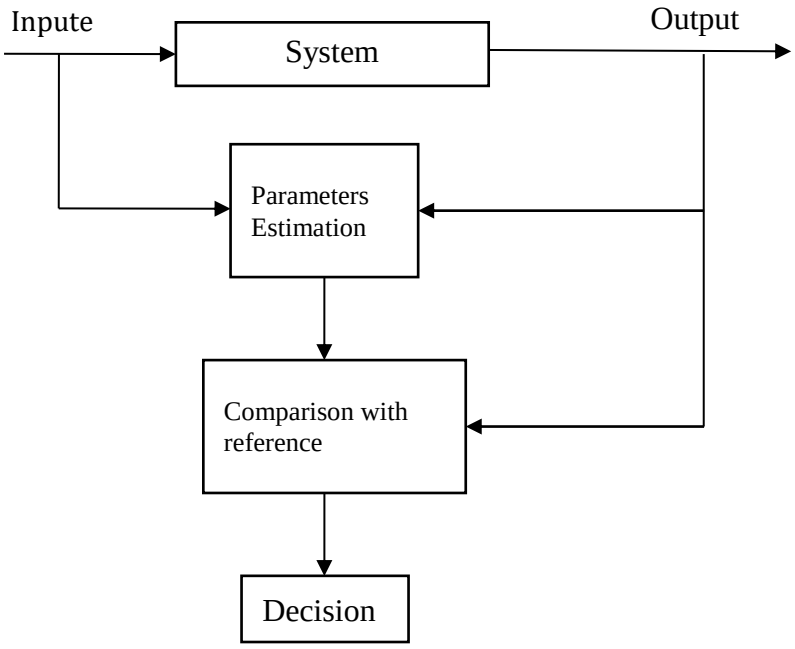

Figure 1.15 Principle of the parameter estimation approach

1.6 The incidence matrix (fault signature matrix)

The theoretical signature of a fault can be considered as the results of detection when all the tests sensitive to the fault react. Indeed, most of the time, the values of the residuals are compared to thresholds at each moment. Each decision made by the tests, produces a Boolean value (0: the residual value is below the threshold; 1: the residual value has beyond the predefined threshold).

A binary vector called Fault Signature is made up of all of these Boolean values [71]. An assessment of the system's condition—normal functioning, identified failure, and finally unidentified failure—is made as a result of this comparison. the set of signals r_{ij} defined by a table of theoretical signatures is then produced.

$$r_{ij}=\begin{cases} 1 \; if \; the \; residue \; sensitive \; to \; the \; fault fi \\ 0 \; if \; the \; residue \; unsensitive \; to \; the \; fault fi \end{cases} \quad 1.17$$

Localization following detection can be performed using the signature table. The columns of this table are representative of the different faults and the rows of the different residues. The diagnostic sets in the FDI approach are given in terms of faults present in the signature table. The generation of diagnostic sets is based on an interpretation of the columns of the signature table and consists of comparing the signature of the observations with that of the faults. For all faults to be detectable, no column of the theoretical fault signature matrix must be zero, and for all = faults to be located, all theoretical signatures must be distinct without the exoneration assumption [48] . distinguish three types of signature matrices.

– Not localizing (a column is null or at least two columns are identical).

– Weakly localizing (the columns are non-zero and distinct two by two).

– Strongly localizing (in addition to being weakly localizing, no column can be obtained from another by replacing a "1" with a "0").

	f_1	**f_2**	**f_3**
r_1	*1*	*1*	*1*
r_2	*1*	*1*	*1*
r_3	*1*	*0*	*0*

Table 1-1 Non-locating signature

	f_1	**f_2**	**f_3**
r_1	*1*	*1*	*1*
r_2	*1*	*0*	*1*
r_3	*1*	*1*	*0*

Table 1-2 Weakly localizing signature

	f_1	f_2	f_3
r_1	*1*	*1*	*0*
r_2	*1*	*0*	*1*
r_3	*0*	*1*	*0*

Table 1-3 Strongly localizing signature

A non-locating table does not allow certain faults to be distinguished from each other. A weakly localizing table makes it possible to locate single faults under the assumption of exemption. A strongly localizing table ensures that the various residual sensitivities with regard to faults do not result in an incorrect diagnosis.

1.7 Residual Generation

The generation of residues is a typical first step in a diagnosis system. This step involves building a vector of residues with dimensions more or equal to the number of faults, each of which must be insensitive to system disturbances while being sensitive to a single fault [72].

The main problem in residuals generation is the detectability of the fault and that of the fault-disturbance decoupling.

Only when a fault affects at least one of the system outputs is detectable. Using a transformation, faults and disturbances can be separated. The goal of this transformation is to divide a system with faults and disturbances into two subsystems, one of which is sensitive to faults and the other immune to disturbances. Various decoupling techniques have been created in accordance with the nonlinear system model under consideration.

1.8 Diagnostic performance

The system diagnostic process's detection step is crucial. Incorrect execution of this phase may result in poorly or incorrectly detected faults and false alarms. The robustness of detection in the face of model uncertainties plays a role in its efficacy. Therefore, the quality criteria for the diagnostic method are what determines how well a procedure for finding and isolating faults will perform., broken down into criteria to be minimized, such as the delay in detection and the rate of false alarms and poor detection and in criteria to be maximized such as sensitivity to low amplitude faults and insensitivity to noise and disturbances but also to uncertainties on the parameters of the model.

1.9 Conclusion

The state-of-the-art of the various diagnostic techniques is covered in this chapter., first giving some definitions and terminologies used in this domain. then presetting the two techniques (model-based and signal-based) that are most frequently used in literature for fault diagnosis, the three crucial steps of the diagnostic procedures discussed in the literature are detection, localization, and identification. The diagnostic technique applied for system monitoring depends on the type of presentation of the systems to be monitored (with or without model), as well as the type of faults (sensor, actuator or system).

The next chapter presents the diagnosis of the fault of power system transmission line using classical methods (signal-based) : By Park transformation and Wavelet transform.

Chapter 2: Transmission Line Fault Diagnosis using Signal-based Methods

2.1 Introduction

This chapter discusses two signal-based techniques to detect short-circuit fault, classify, and localize them in power transmission lines. Firstly, a description of the used system and the modeling of the transmission lines are provided. Then the Park's transformation method is discussed and its performance is evaluated under different conditions. After that the wavelet transform also discussed and analyzed during various fault types and locations. Finally, the simulations result of both methods are presented.

2.2 Diagnostic by Park's Method

2.2.1 Park's Method implementation in test power system

Figure 1 displays the schematic of the power system under examination. It composed of a 200km AC overhead transmission cable connecting two sources. Four zones are created based on 50 km for each one. The measurements block is positioned at the start of the transmission line, the three phases currents are used as inputs for Park's transformation, which produces results in the form of circles with various shapes for each individual fault.

transmission line parameters: S_b=500MVA, Ub=230kV, l=200km for 1km: R=0.103 Ω, L=0.0013 H, C=8.2e-9F.

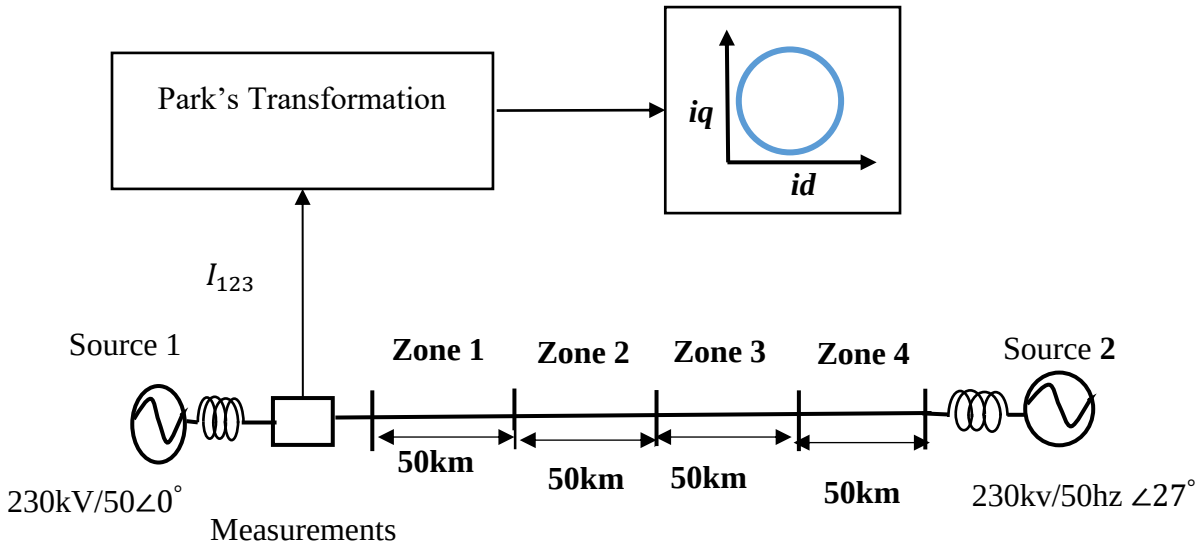

Figure 2.1 Implementation of a diagnosis system in the transmission line.

2.2.2 The modeling of the transmission line

Figure 2 shows the transmission line as a simple circuit with capacitors at both ends, an inductance, and a resistor connected in series.

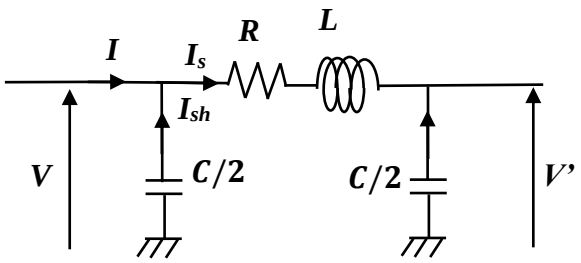

Figure 2.2 The schematic of the transmission line.

Obtaining from the modeling:

$$I = I_{\mathrm{sh}} + I_{\mathrm{s}} \qquad 2.1$$

$$V - V' = RI_{\mathrm{s}} + \mathrm{L}\frac{\mathrm{d}I_{\mathrm{s}}}{\mathrm{dt}} \qquad 2.2$$

applying Laplace Transformation, the equations (1) and (2) are as follows:

$$I_{\mathrm{s}} = \frac{V - V'}{\mathrm{R} + \mathrm{LS}} \qquad 2.3$$

$$I_{\mathrm{sh}} = \frac{\mathrm{c}}{2}.\frac{\mathrm{dV}}{\mathrm{dt}} \xrightarrow{LT} \qquad I_{\mathrm{sh}} = \frac{\mathrm{c}}{2}.S.V \qquad 2.4$$

From (3) and (4) we obtain:

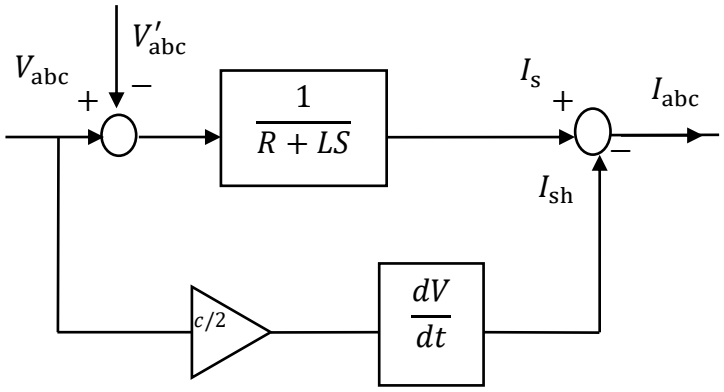

Figure 2.3 The mathematical model of the transmission line .

Figures (2.4) and (2.5) show the behavior of the transmission line during fault.

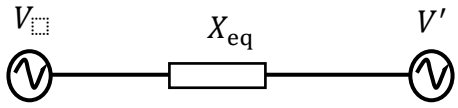

Figure 2.4 The corresponding reactance (X_{eq}) of a fault-free transmission line

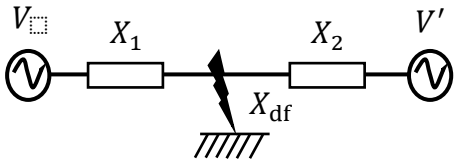

(a)

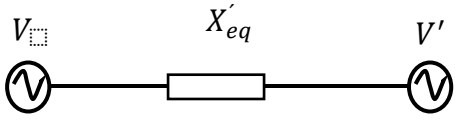

(b)

Figure 2.5 The corresponding reactance (X'_{eq}) of the under fault transmission line

The equivalent reactance during the fault can be calculated with the formula below:

$$X_{eq}^{'}=X_1+X_2+\frac{X_1X_2}{X_{df}} \quad 2.5$$

Where:

$$X_1+X_2=X_{eq} \quad 2.6$$

X_{df}: Fault reactance

Table 1 is used to calculate X_{df}

Fault type	3L	LL-G	LL	L-G
X_{df}	0	$\frac{X_iX_0}{X_i+X_0}$	X_i	X_i+X_0

Table 2-1 Shunt reactance of different fault types

The fault point's negative and zero sequence reactance are defined by the symbols X_i and X_0, respectively.

2.2.3 Park's Method

This technique is often used to analyze three-phase electrical systems ,it is based on Park's vectors [52] [73, 74]. The two-dimensional representation of the three phases of an electrical network allows us to determine the current Park's vectors. This function makes use of the id and iq components of the line current. based on the mains phase variable (ia, ib, ic) [75].

The Id and Iq vector components of the Park transformation are:

$$i_d=\sqrt{\frac{2}{3}}i_a-\frac{1}{\sqrt{6}}i_b-\frac{1}{\sqrt{6}}i_c \quad 2.7$$

$$i_q=\frac{1}{\sqrt{2}}i_b-\frac{1}{\sqrt{2}}i_c \quad 2.8$$

In perfect conditions, three-phase currents generate a Park's vector that includes the following elements:

$$i_d = \frac{\sqrt{6}}{2} I \sin(\omega t) \qquad 2.9$$

$$i_q = \frac{\sqrt{6}}{2} I \sin\left(\omega t - \frac{\pi}{2}\right) \qquad 2.10$$

I = maximum value of the phase current.

ω= frequency.

A circular pattern makes up its representation. This simple reference figure makes it possible to spot unusual conditions by identifying deviations from well-known patterns.

Transmission line faults can be diagnosed using Park's vector approach [76] . The Park's vectors can be exploited to simplify the analysis of the three phases. If it is a perfect circle, the system is said to be in excellent condition. The system is faulty if an elliptical pattern is seen in its representation. The ellipse's properties can be used to determine the fault type. With increasing fault severity, ellipticity increases.

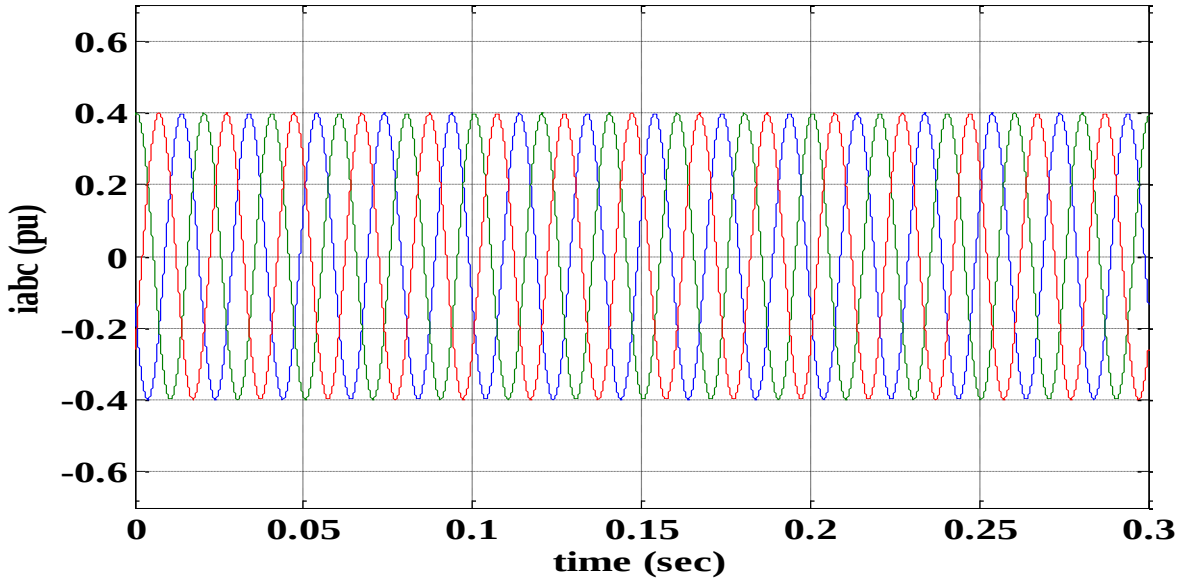

(a) Three phase currents

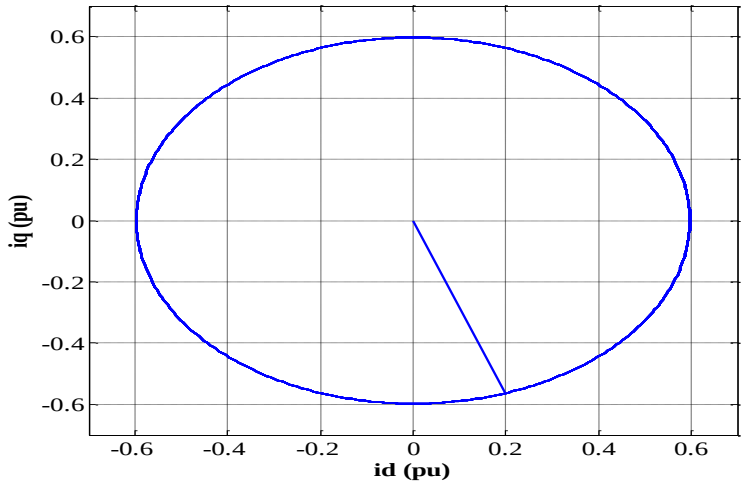

(b) Park circle healthy system

Figure 2.6 Healthy system behavior (a) Three phase currents
(b) Park circle of healthy system

In case of fault in the transmission line, the harmonics created by the fault cause the circular curve to fluctuate in shape and circumferential thickness. The two circular curves in the operating conditions of the healthy and the faulty transmission lines, as shown in Fig. 2.7.

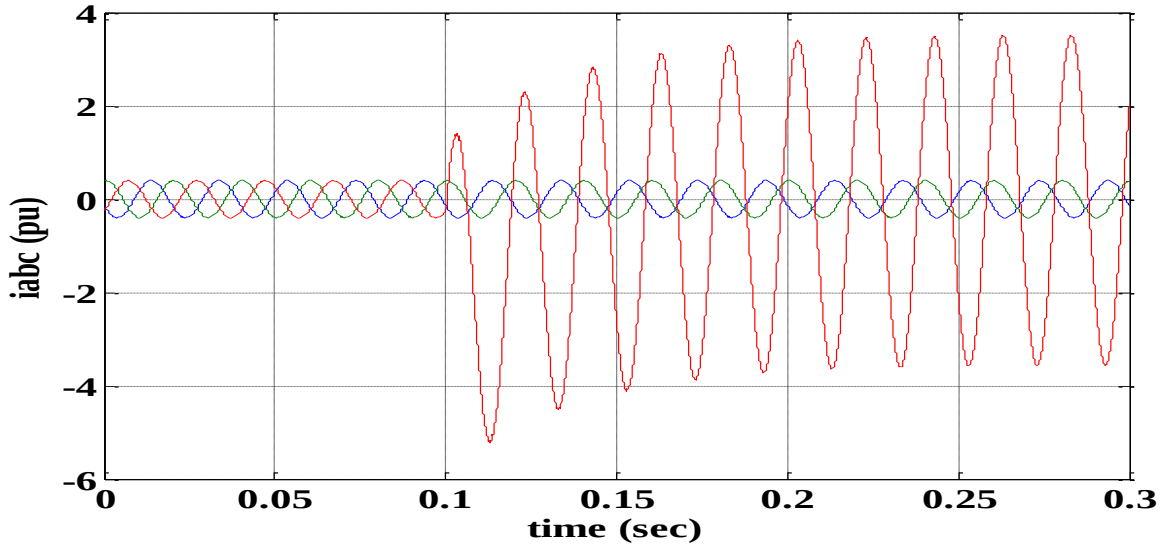

(a) The currents of the three phases

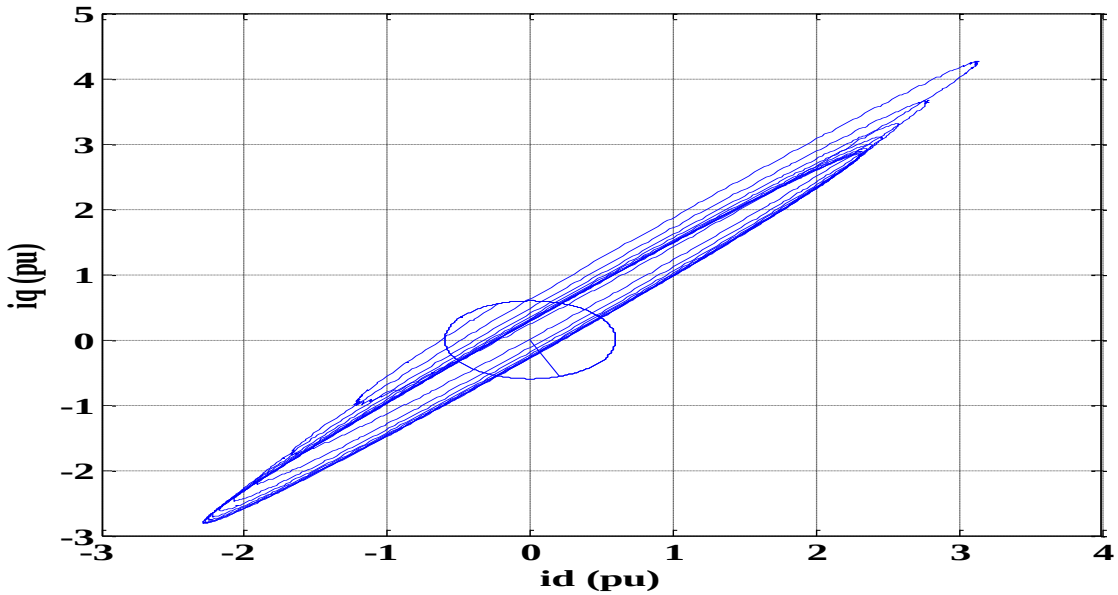

(b) Park's vectors representation

Figure 2.7 System behavior with a fault of phA in zone 1, (a) Three phase currents ,(b) Park circle without fault

2.2.4 Simulation results of Park's vectors

Ten short circuit faults, three of which were single-phase short circuit faults (Pha-Gnd, Phb-Gnd, and Phc-Gnd), were evaluated in each of the four zones to determine how well Park's method performed. Next, three double-phase short-circuit faults (2L-Gnd), then three double-phase short-circuit faults (2L), and finally three phases (3L). as a result, 40 faults in total. The random circles stand in for the fault-causing transition regime.

2.2.4.1 Single phase(Ph-Gnd) short-circuit fault

Figures 8, 9, and 10 depict the Park's circle's deformation when an unbalanced single-phase fault is applied in the transmission line's first zone. According to the classification of the short-circuit a fault in the three phases (a, b, and c), there are three distinct scenarios: In the event of a short-circuit in phase (a), we see a little tilt of the Park ellipse with a change in diameter. However, in the event of a SC on phases (b) and (c), there will be a significant elliptical inclination with a

significant fluctuation in diameter (inclination clockwise for phase c and counterclockwise for phase b).

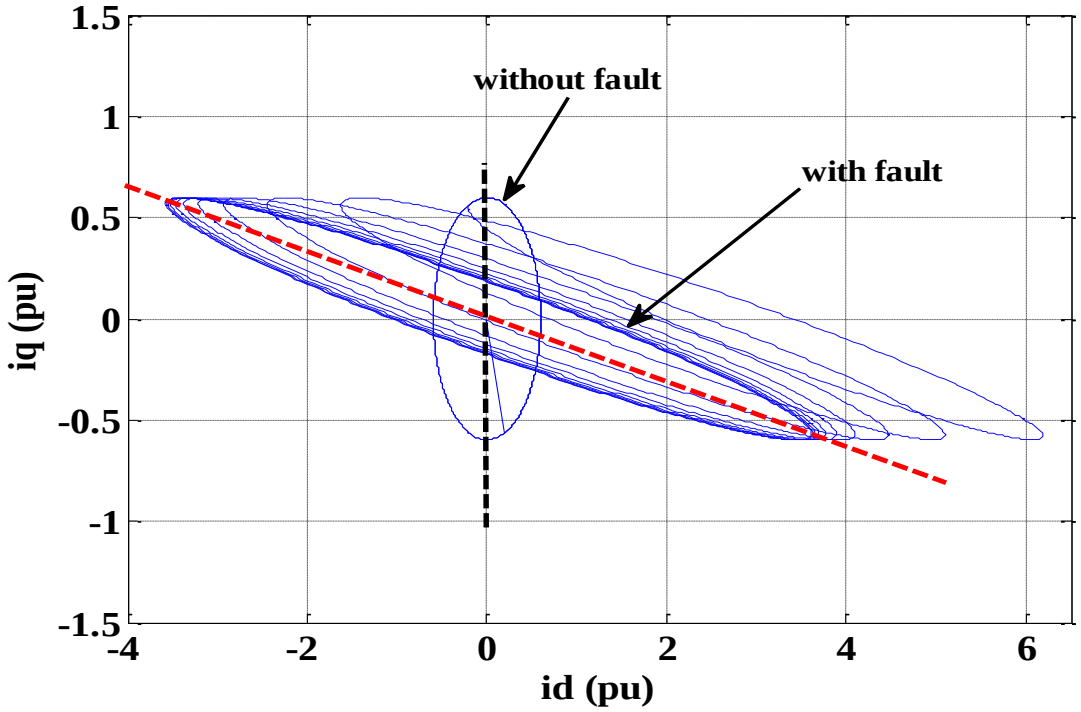

Figure 2.8 Short-circuit (Ph_a-Gnd) fault

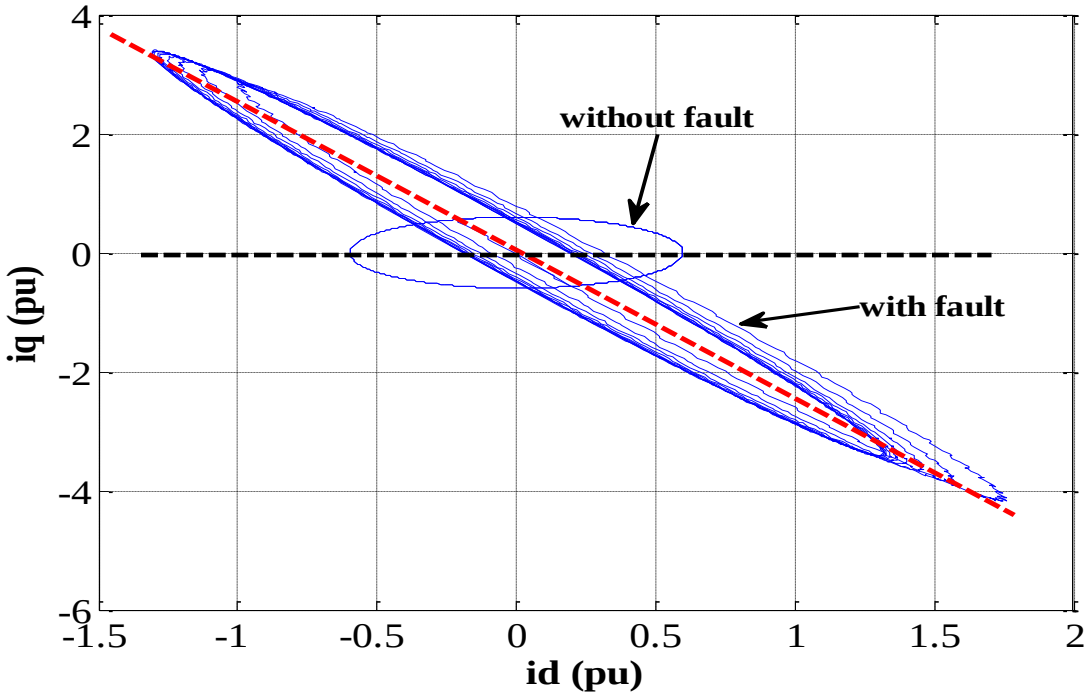

Figure 2.9 Short-circuit (Ph_b-Gnd) fault

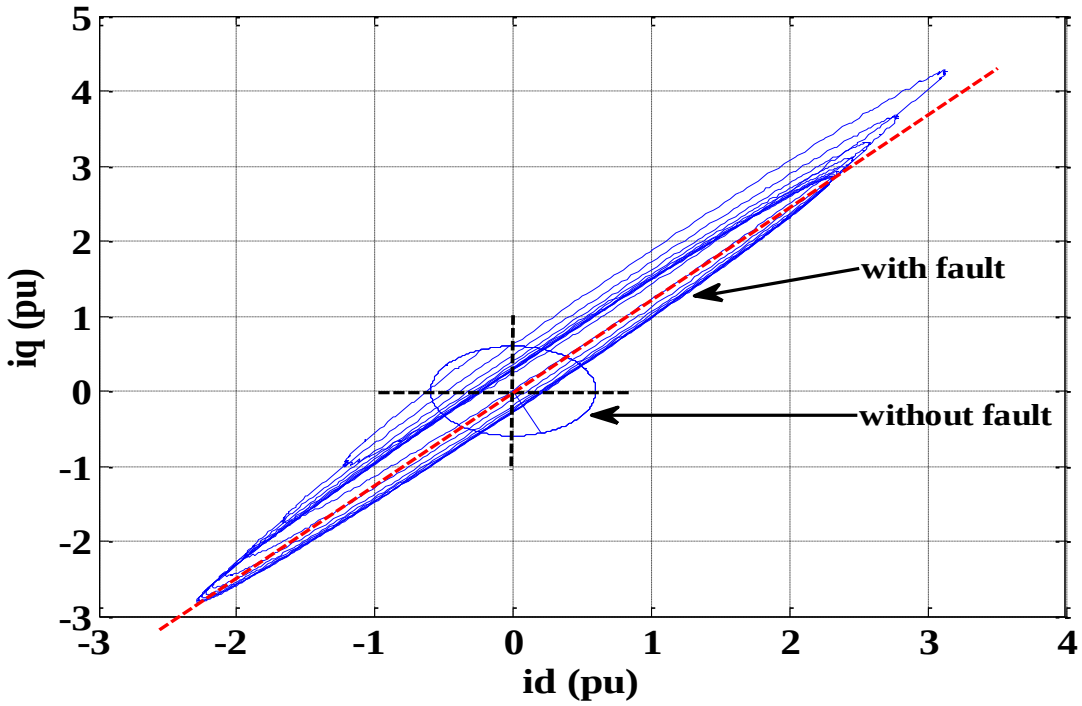

Figure 2.10 Short-circuit (Ph_c-Gnd) fault

In order to locate the fault, at each zone (1,2,3,4) we generated 4 single-line short circuit faults with the same fault type Pha-Gnd. Figures 11(a) and 11(b) demonstrate how the Park's ellipse's angle of inclination varies as a function of the transmission line's fault zone (inversely proportional): the angle of inclination decreases as the fault location increases in relation to the current measurement point.

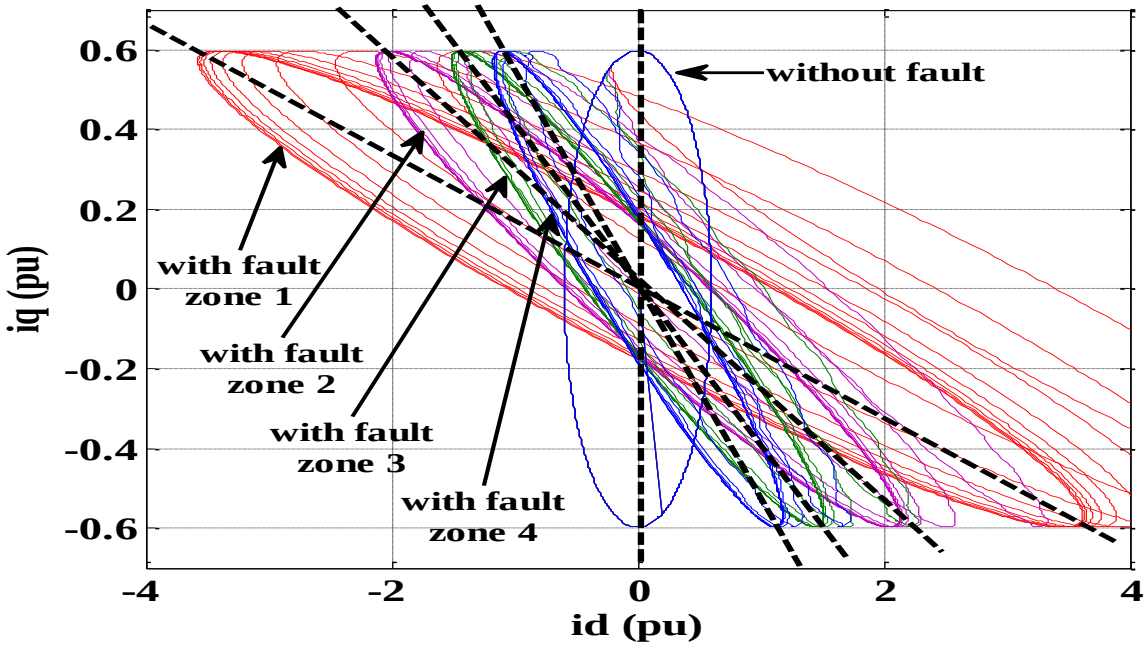

(a) Park ellipse

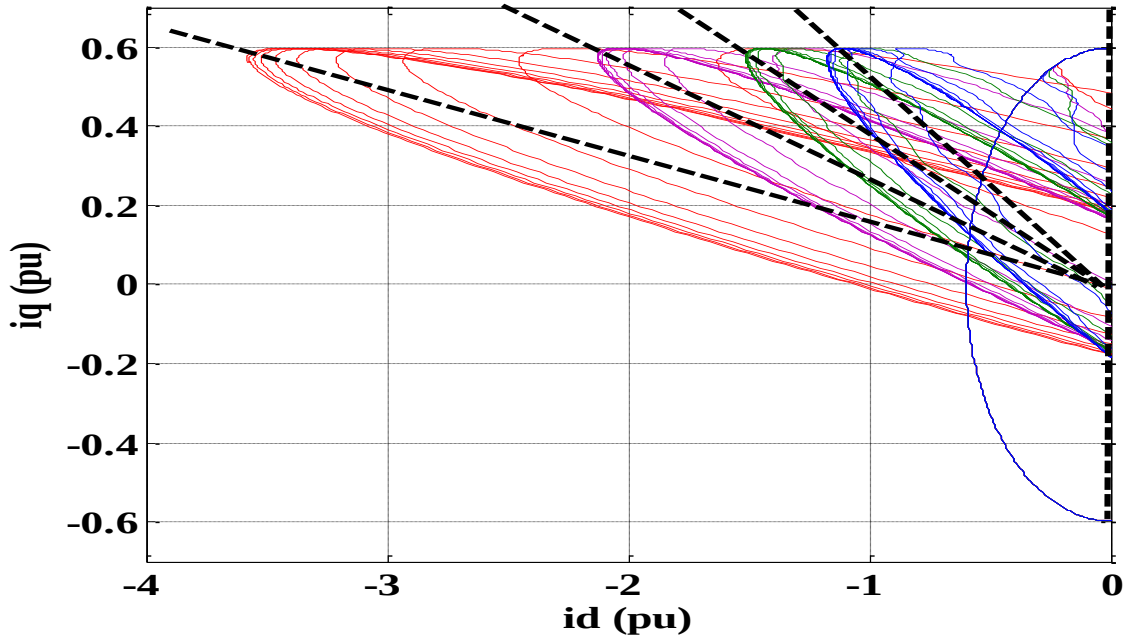

(b) Park ellipse zoomed

Figure 2.11 Ph_a–Gnd short circuit in all zones

2.2.4.2 2L- Gnd Short circuit faults

Twelve different faults were tested in all for these three (2L-G) faults, Pha-Phb-Gnd, Phb-Phc-Gnd, and Pha-Phc-Gnd. Figures (12), (13) and (14) illustrate the results of these tests, respectively; each figure shows the same fault in all zones. Each fault type in each zone displays the same ellipse form and thickness; the variation is in size, with zone 1 having the largest ellipse and zone 4 having the smallest., The size and form of the ellipse indicate the location and type of the fault, respectively. Where the Park ellipse's diameter decreases in relation to the increase of the fault location on the transmission line and a variation in the ellipse's angle of inclination with respect to the various fault phases: Phases ab to the ground have an inclination that is counterclockwise (Fig.2 12), phases ac to the ground have an inclination that is clockwise (Fig. 2.14), and phases bc to the ground have a low inclination (Fig.2.13).

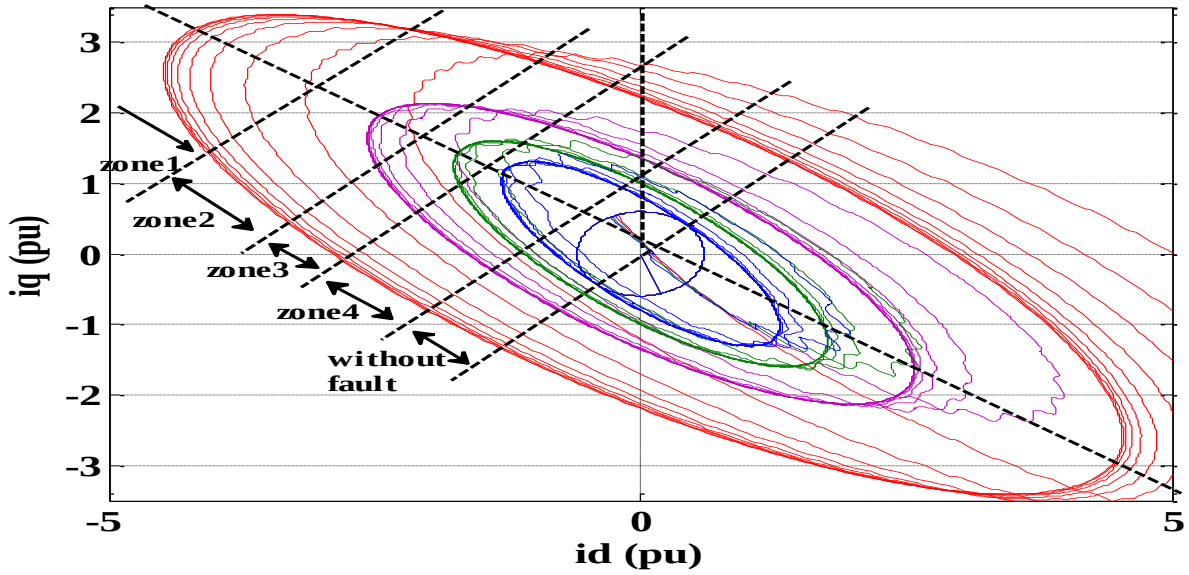

Figure 2.12 Short circuit fault Ph_a-ph_b-Gnd

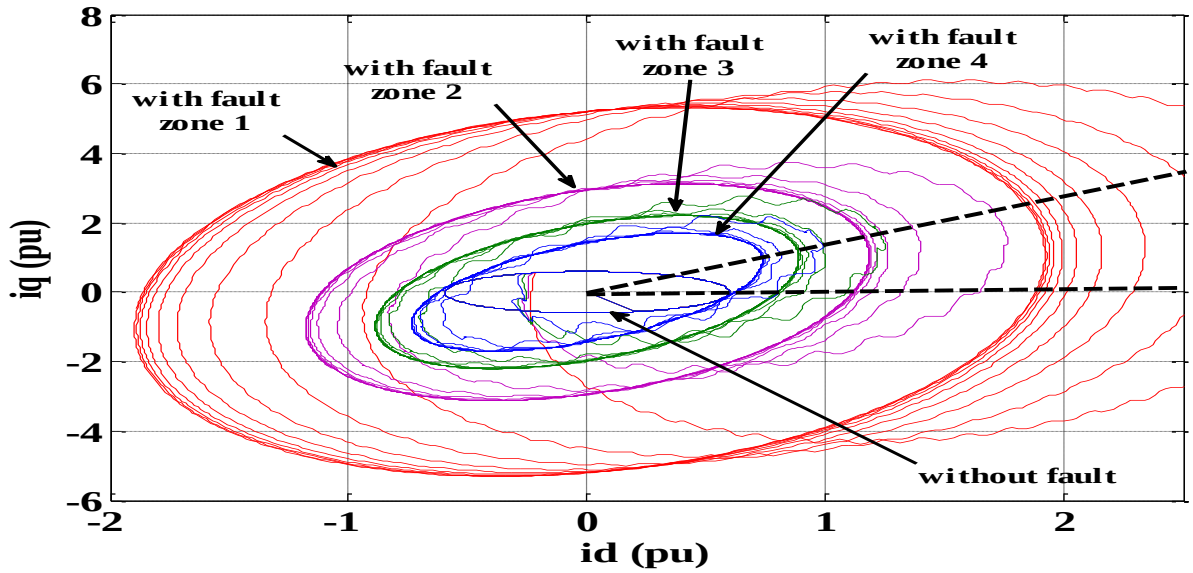

Figure 2.13 Ph_b-phc-Gnd Short circuit

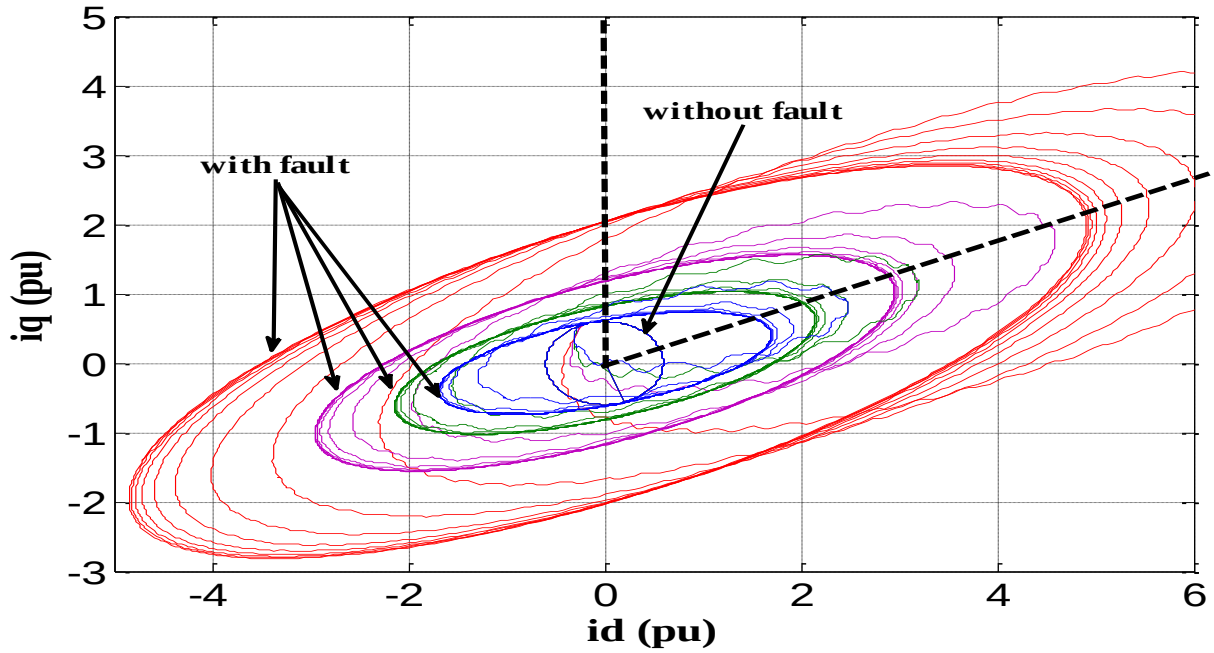

Figure 2.14 Ph_a-ph_c-Gnd Short circuit

2.2.4.3 Double lines (2L) short circuit without ground

In the event of a two-phase 2L short circuit fault (the contact of one phase with another), Figure 2.15 depicts the Park circle deformation., with regard to the various fault phases, we consistently notice variations in the ellipse's angle of inclination. The elliptical shape and angle of inclination make it simple to identify the fault classification.

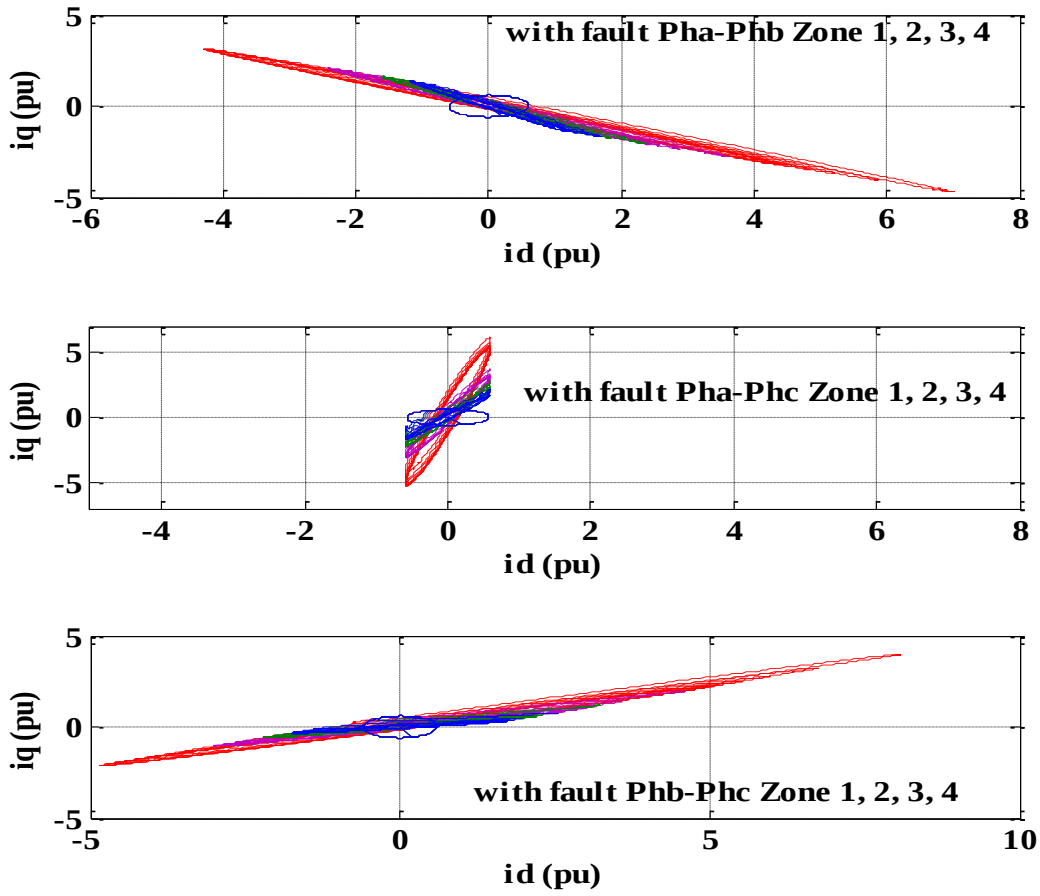

(a) Park ellipse

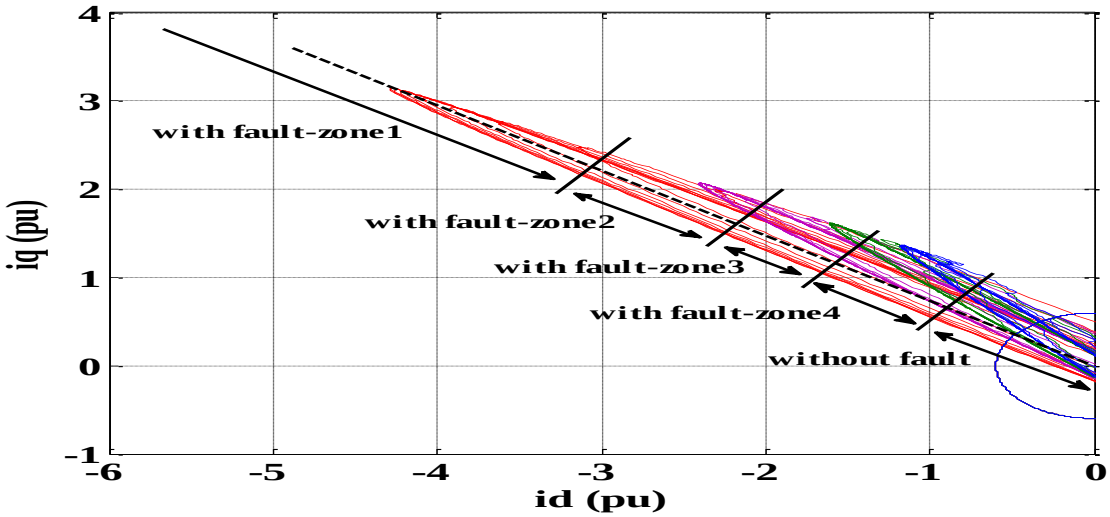

(b) Park ellipse zoomed

Figure 2.15 Short circuit on both lines (2L)

2.2.4.4 Three phases short circuit 3L (Ph_a-ph_b-ph_c)

Figure 2.16 illustrates the results of testing three phases 3L short circuit in all zones. As can be seen, Because the fault is symmetrical, the circle is perfectly shaped. As was previously stated, the size of the circle (the radius or the circumference) determines the fault location (zone). It is clear that variations in the diameter of Park's circle are inversely correlated with the location of the fault on the power line. Therefore, the circle's radius is greater the closer the fault location is to the measurement point since the circle's radius represents the fault's current.

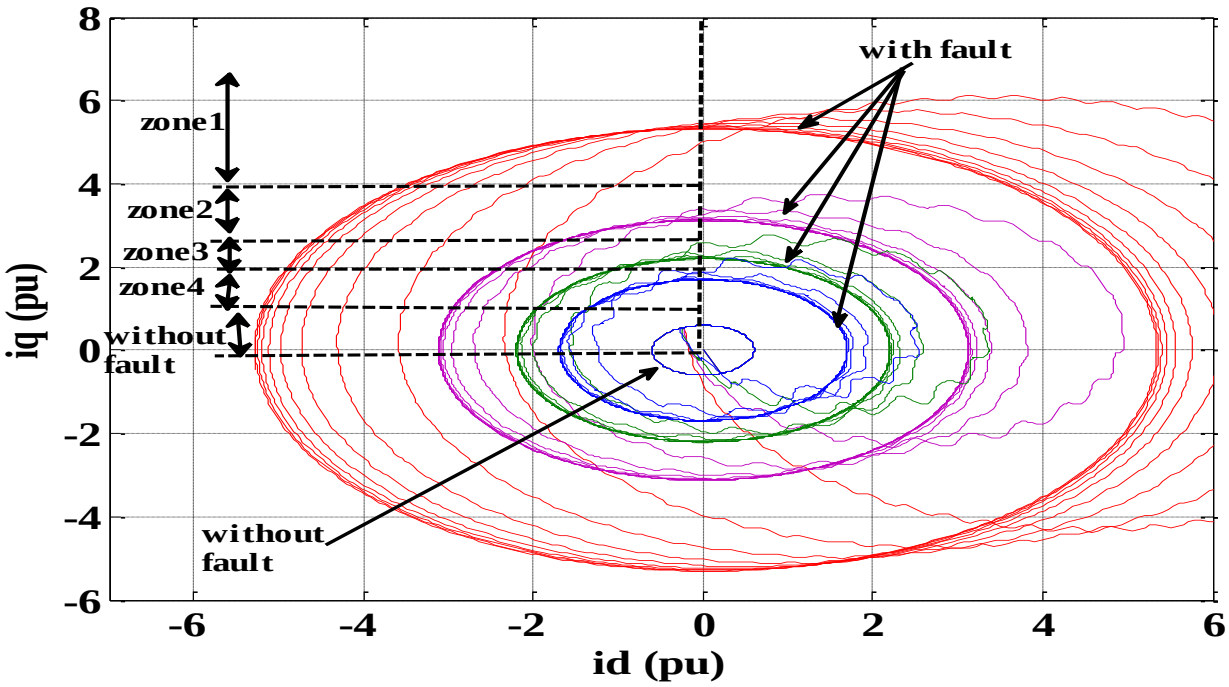

Figure 2.16 Short circuit fault of three phases Ph_{abc}

2.2.5 Park's vectors performance evaluation

This section describes the use of the Park's vectors approach for the detection, localization, and classification of short-circuit faults in the transmission line. Different transmission line conditions in both healthy and faulty cases have been researched and examined. Using this method, all potential short-circuit faults are tested and simulated. The simulation results demonstrate the efficiency of the employed diagnosing technique, as each type of fault has a certain Park circle form and a varied circumference thickness. Faults can be accurately identified and investigated in all transmission zones. Results from the employed approach for various faults are quite encouraging. effective, dependable, safe to use, and accurate.

2.2.5.1 Park's vectors disadvantages

- Detection by the Park's Vectors is based on the comparison of images with a database, which requires another decision support strategy
- It presents difficulties in distinguishing approximate cases.
- works in short-circuit faults only and doesn't work in open-circuit faults

The diagnosing of power systems can be improved by combining Park's method with intelligent tools like artificial neural networks. An interesting use for this technique is image classification using convolutional neural network CNN.

2.3 Diagnostic by the Wavelet transform

The signal can have a better time-frequency resolution with the Wavelet transform than with the Fourier transform [54]. Electrical transients in transmission lines can be precisely located and classified using the wavelet transform. The continuous wavelet transform (CWT) of a function f(t) can be computed by:

$$\mathrm{CWT(f,a,b)} = \frac{1}{\sqrt{a}}\int_{-\infty}^{+\infty} f(t)\,\psi^{*}\left(\frac{t-a}{b}\right)dt \qquad 2.11$$

a, b and ψ stand the scaling, time shift constants and the function of the mother wavelet respectively. Additionally, it is possible to compute the discrete wavelet transform (DWT) [77] by:

$$\mathrm{DWT(m,n)} = \frac{1}{\sqrt{a_0^m}}\sum_k f|k|\,\psi^{*}\left(\frac{n-ka_0^m}{a_0^m}\right)dt \qquad 2.12$$

f|k| is the sampled signal, a is the discretized parameters of scaling and b is parameter of time shift.

This section uses DWT to detect and classify the short-circuit faults in the same test power system transmission lines used in Figure 2.1's. The current signals taken from one end of the transmission line are analyzed in MATLAB using the wavelet transform. DWT is used to decompose the signal using a low-pass filter to provide the signal's approximation coefficients and a high-pass filter to deliver its detail coefficients, also using multi-stage filtering The filters

decompose the signal into 6 levels, by using these detail coefficients, faults in the transmission line are detected, classified and located.

Figure 2.17 show the DWT decomposition of the signal by multi-level filter bank each level has a high –pass filter filtering the signal to high frequencies and down sampling by 2 delivering the detail coefficients, similarly the low-pass filter delivers the approximation coefficients of level 1, the same process is repeated at each level up to level 6, finally taking the maximum of the detail coefficients as an indicator of fault which varies depending on the fault type and location, the whole process is applied to the three phase current signals collected at one end.

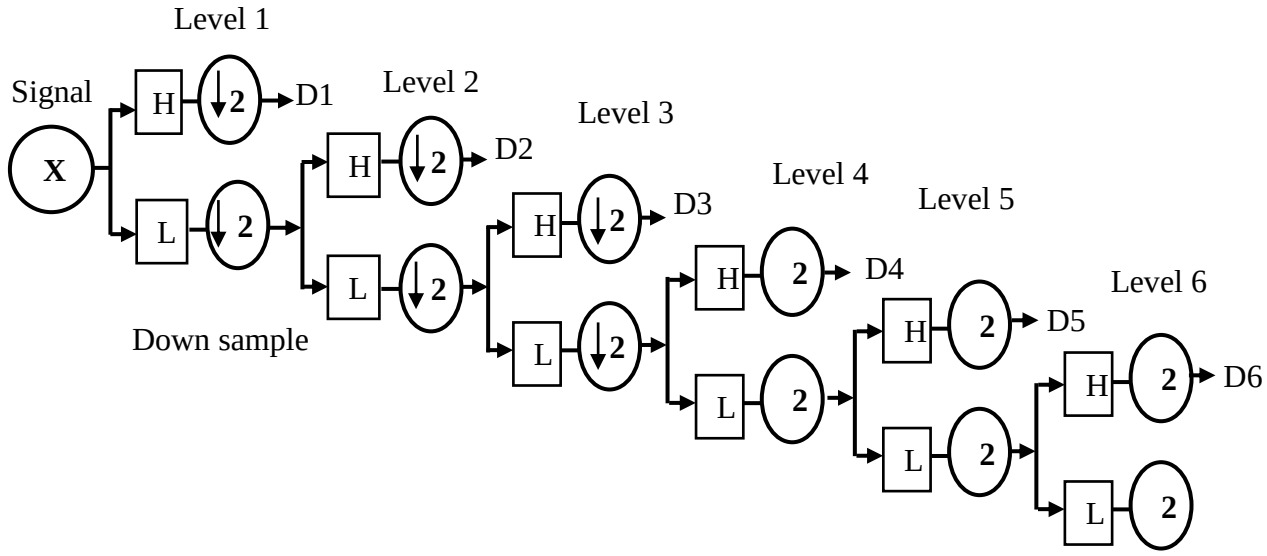

Figure 2.17 Discrete wavelet transform for Signal decomposition.

Comparing the current signals of each phase when a failure occurs, using the healthy system as a reference. Single-phase faults (L-G), double-phase faults (L-L), double-phase faults with ground (2L-G), and three-phase faults (3L or 3LG) are all included in fault simulation for power systems. By using the detail coefficients of the current waveform's sixth level decomposition, fault detection can be done using db4 wavelets. The threshold is set at the maximum discrete wavelet transform detail coefficient in the steady state, with the other values denoting various faults. If the discrete wavelet transform detail coefficient of the associated line current is below a certain threshold, the transmission line is considered to be in good condition. all of these detail coefficient values were calculated. Using the Daubechie's wavelet (db4) under various fault conditions with the fault starting at 0.1s till 0.3s.

2.3.1 Proposed scheme

The basic method consists of the following:

• Exploiting the current signal of (3 phases) at one end of bus 1

• process the obtained three phase current signals with DWT.

• Extracting the Approximate coefficients and Detail coefficients from the signals.

• compute the Detail coefficients to level 6.

• A fault is detected if the computed Detail coefficient above the threshold.

Figure 2.18 depicts the proposed method's flowchart.

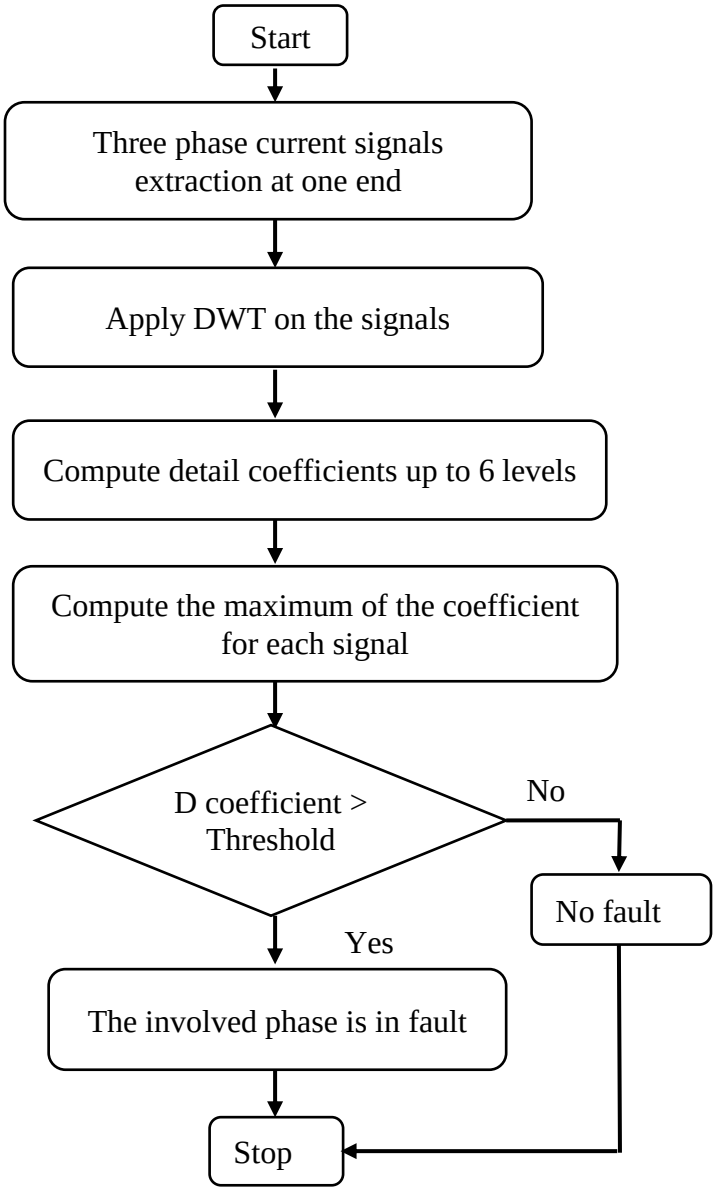

Figure 2.18 Flowchart of proposed algorithm

2.3.2 Simulation results and discussion

Short circuit faults in transmission lines have been detected using the discrete wavelet transform (DWT). This task has been completed using MATLAB/Simulink. Three phase fault with the ground (LLLG) faults, single-line to ground (LG), double line (LL), and double line to ground (LLG) faults are among the several fault types examined. The faults were generated 0.1 seconds after the simulation began, the simulation results have been plotted for 0.3 seconds. The wavelet-based decomposition uses bus 1 current signals. The detection, classification, and localization of faults have all been done using detail coefficients up to level 6. The following provides more information on the various case studies.

The current signals of three phases for healthy system (no fault) is represented in figure 2.19 , figures 2.20 ,2.21 and 2.22 respectively show the current signals of a L-G fault in phase A and during double phase PhBC (L-L) fault without the ground and with the ground PhBC-g (LL-G)., all the current signals are measured in per unit0 It can be notice from these figures that the current of the faulty phase highly increases to much higher values during the short-circuit fault meanwhile the current of the healthy line doesn't change.

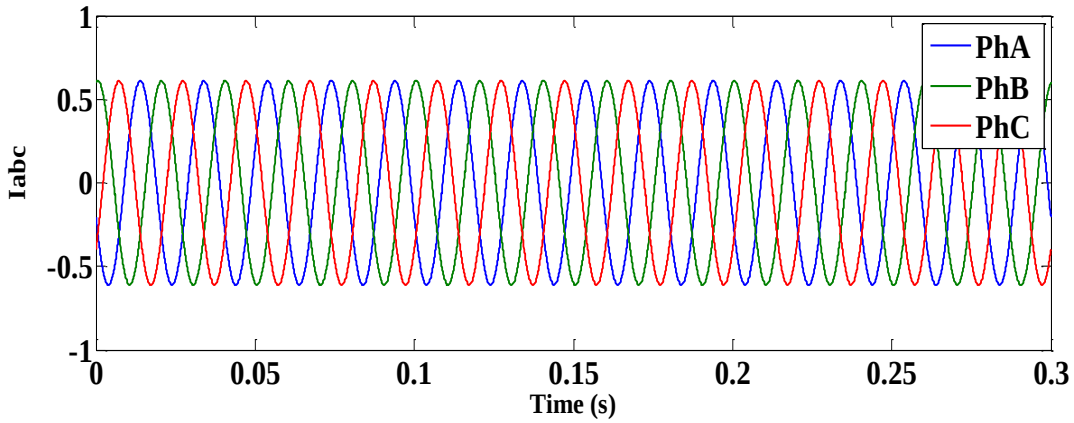

Figure 2.19 Current signals during normal operation

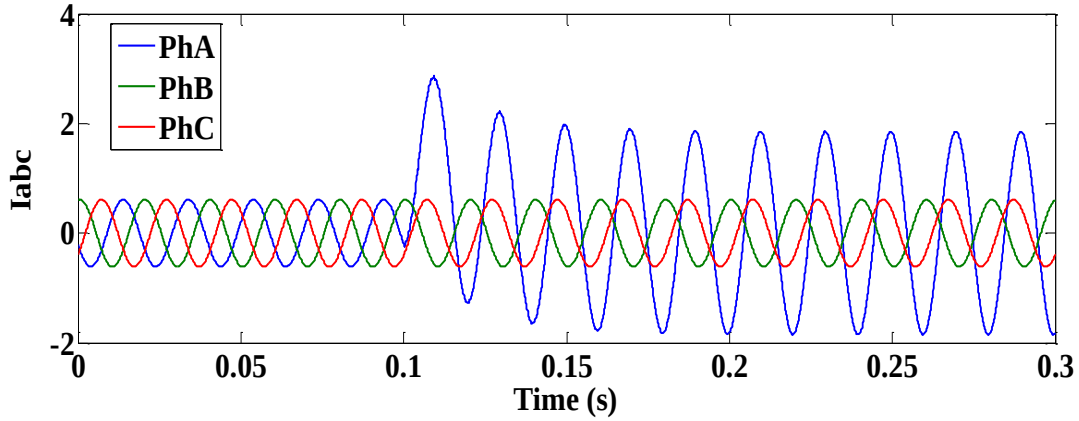

Figure 2.20 Current signals of PhA-g fault

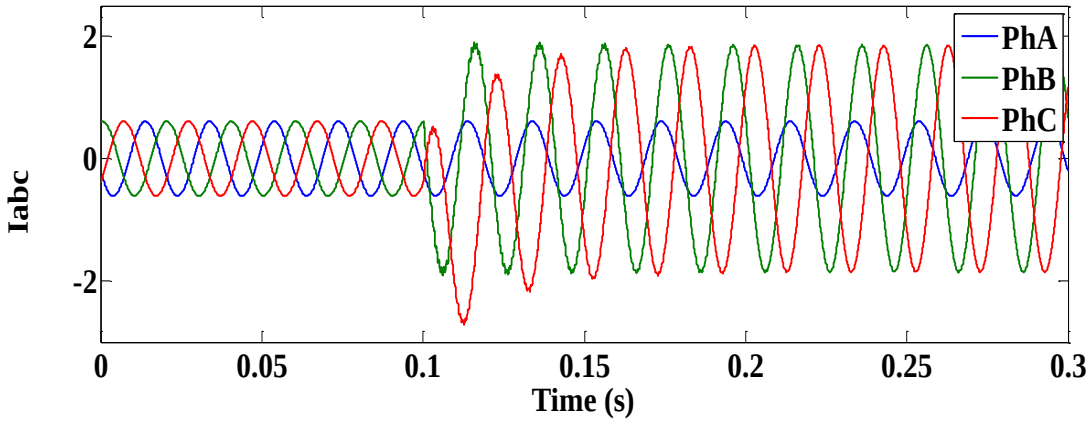

Figure 2.21 Current signals of PhBC fault without the ground

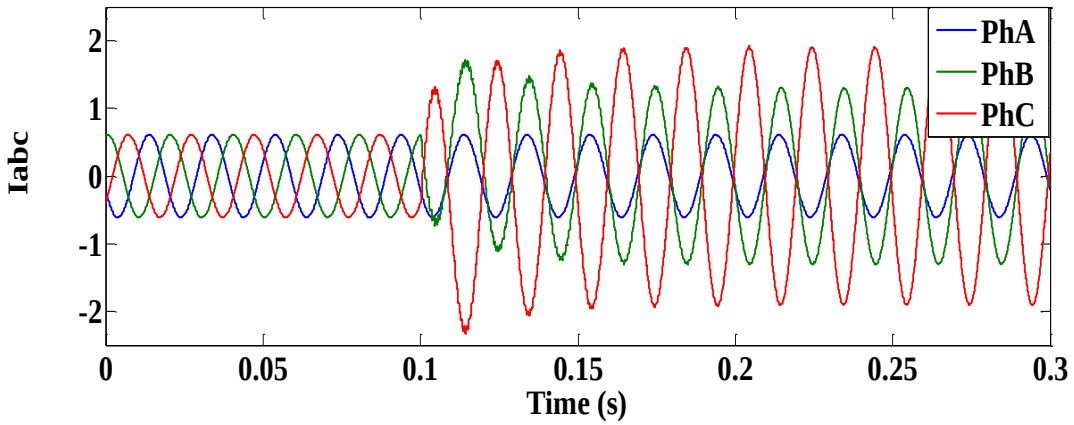

Figure 2.22 Current signals of PhBC-g fault

After showing the waveforms the current of the system in normal condition and during faults, a single Phase A-G to gnd fault is simulated to further present how to detect, classify and locate the fault, figure 2.23 represents the DWT decomposition of the obtained current with detail coefficients. The first subplot illustrates the signals of the phase A currents during the fault period starting from 0.1s, noticing the change in the waveform and increasing in current amplitude, subfigures d1, d2, d3, d4, d5, d6 show the variation of detail coefficients for each level from 1 to 6 respectively,

The d6 subplot of figure 8 shows the detail coefficients variation at level 6 which is well presented in figure 9, the detail coefficients variation at level 6 of phases PhA,PhB,PhC during PhA-G fault , PhB-G and for PhC-G fault are shown ,the maximum of these detail coefficients variation at level 6 is taken as an indicator of a fault at 50km of the transmission line , since this indicator varies depending on the location of the fault.

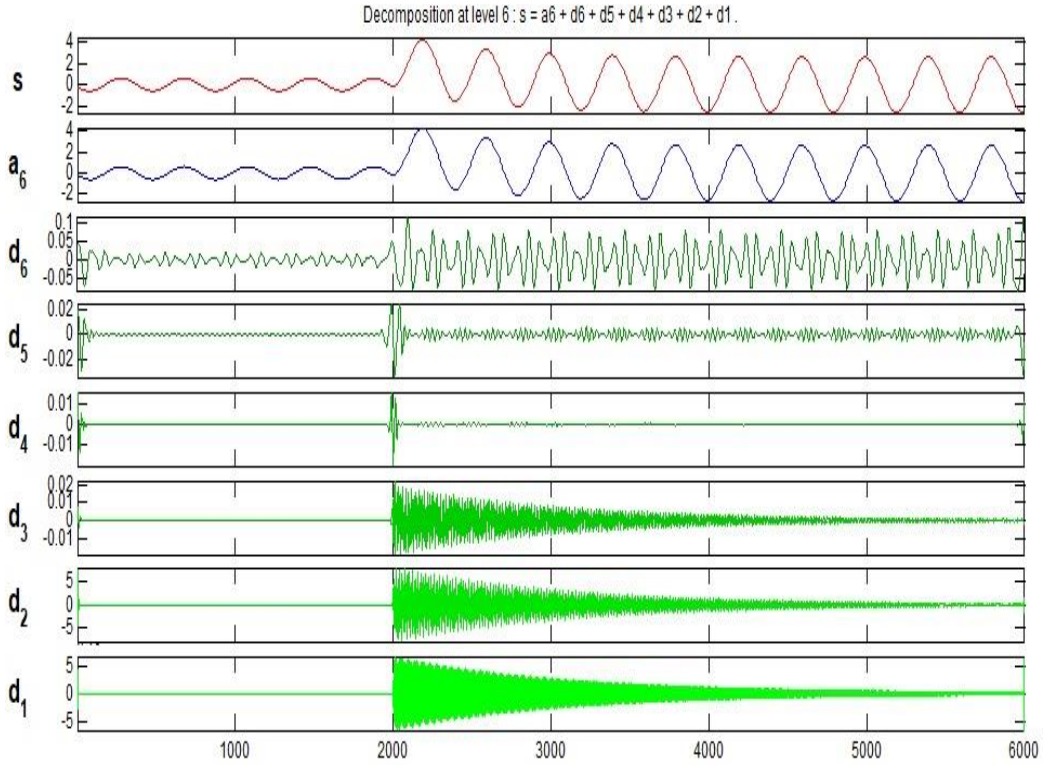

Figure 2.23(a) Current signal (phA) (d1 to d6) detail coefficient from level 1 to level 6 during LG fault

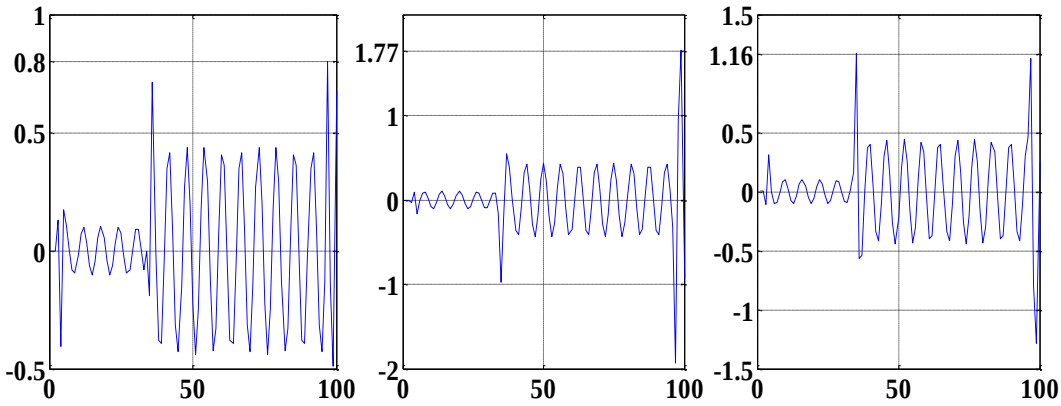

Figure 2.24 Variation of detail Coefficient of AG ,BG,CG fault at 50% of the Transmission line

2.3.2.1 Fault Location Variation

To demonstrate the performance of this method a variation in the fault location from the start of the power transmission line 1km to the end of the transmission lines 100km were tested, since faults can occur at different locations. figure 2.25 represents the variation of three-phase coefficients for different faults. During PhA-G fault, the maximum detail coefficients of PhA current signal varies from 3.5 to 1.5 according to the fault location meanwhile, the PhB and PhC detail coefficients have a value under the threshold indicating fault detection only in PhA , the same case as a PhB-G fault (varies 2.8 to 0.8) or fault in PhC-g (varies 1.5 to 0.7), also the double phase fault 2L-G faults and 3L-G can be determined by comparing the detail coefficients to the threshold as any value greater than 0.45 is considered a fault in the concerned line as for 3L-G fault, all the three phases' detail coefficients are greater than the threshold as shown in figure 2.25

.

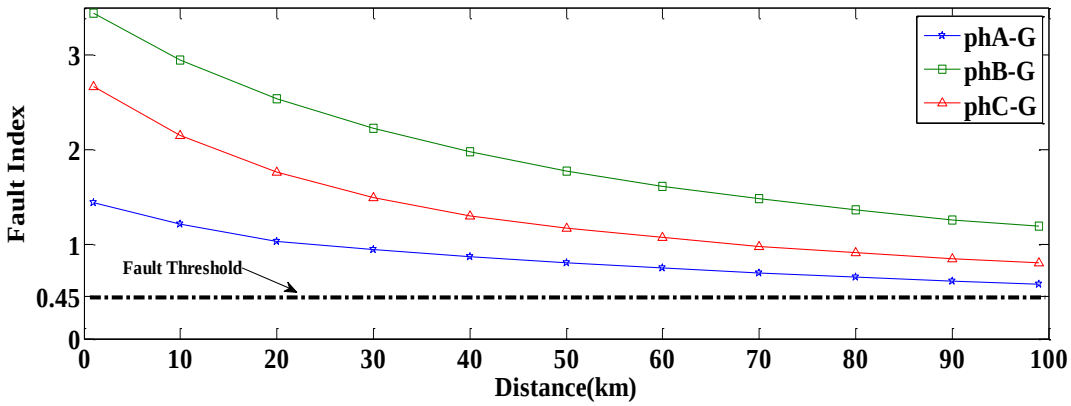

Figure 2.25 Variations in the ABCG Fault's three phase current fault indexes

Table 2-2, 2-3 and 2-4 respectively show the maximum detail coefficients values variations of PhA-PhB fault, of PhB-PhC fault and of PhB-PhC fault considering the fault location variations from 1km to 99 km along the transmission line for each 10 km. noticing in table 1 that the fault indicators for both PhA and PhB are greater than the threshold meanwhile the fault indicators of PhC is less than the threshold (0.45) indicating that it is PhAB fault and no fault in PhC thus determining the type classification, similarly table 2 for PhBC fault and table 3 for PhAC fault.

To distinguish the difference between 2L without the ground faults and 2L-G faults ,also the ground current signal at the source is taken in consideration to compute its detail coefficients and determines if the ground is affected by the fault as if it's greater than the threshold (1) then it's a 2L-G fault , if it's smaller than the threshold it's a 2L fault without the ground as shown in the tables 1,2 and 3 all the maximum detail coefficients values of the ground current are considerably small and less the threshold.

AB fault	***Phase A***	***Phase B***	***Phase C***	***Gnd***
1km	2.2795	2.1661	0.4145	0.1047
10km	1.9657	1.9378	0.4145	0.0828
20km	1.6929	1.7321	0.4145	0.0624
30km	1.4751	1.5632	0.4145	0.0523
40km	1.3002	1.4255	0.4145	0.0463
50km	1.1572	1.3116	0.4145	0.0398
60km	1.0403	1.2182	0.4145	0.0326
70km	0.9392	1.1362	0.4145	0.0272
80km	0.8536	1.0667	0.4145	0.018
90km	0.775	1.0016	0.4145	0.0217
99km	0.726	0.9635	0.4145	0.026

Table 2-2 Detail coefficients values variations of pha-phb fault

BC fault	*Phase A*	*Phase B*	*Phase C*	*Gnd*
1km	0.378	2.9866	3.4211	0.053
10km	0.3781	2.4734	2.8803	0.0442
20km	0.3781	2.0627	2.4521	0.0425
30km	0.3781	1.7583	2.1374	0.0403
40km	0.3781	1.5252	1.8981	0.0396
50km	0.3781	1.341	1.7099	0.0379
60km	0.3781	1.195	1.561	0.035
70km	0.3781	1.0706	1.4351	0.0304
80km	0.3781	0.9674	1.3306	0.0261
90km	0.3781	0.8739	1.2366	0.0263
99km	0.3781	0.817	1.1788	0.0296

Table 2-3 Detail coefficients values variations of PhB-PhC fault

AC fault	*Phase A*	*Phase B*	*Phase C*	*Gnd*
1km	1.215	0.1021	1.5119	0.0578
10km	1.0594	0.1021	1.2651	0.0798
20km	0.9293	0.1021	1.0679	0.0905
30km	0.8298	0.1021	0.9215	0.066
40km	0.7507	0.1021	0.8088	0.046
50km	0.6873	0.1021	0.7186	0.0376
60km	0.636	0.1021	0.6459	0.0376
70km	0.5925	0.1021	0.5838	0.0456
80km	0.5529	0.1021	0.5325	0.0606
90km	0.5207	0.1021	0.4887	0.0436
99km	0.4952	0.1022	0.4541	0.0449

Table 2-4 Detail coefficients values variations of PhA-PhC fault

This section demonstrates the use of discrete wavelet transforms for the detection, localization, and classification of faults in power system transmission lines. The detail coefficients are obtained by decomposition the current signals at one end, these coefficients are calculated to six level of DWT and they are used as a fault indicator when the detail coefficients are greater than a well determined threshold, since these coefficients have been shown to be efficient for the identification and classification of transmission line faults, the test was conducted on a transmission line with two buses. with a voltage of 230kV, a frequency of 50Hz, and a line length of 100km. Various short-circuit faults were tested, such as L-G, L-L, LL-G and LLL-G. For all types of defects, the results obtained are very satisfactory. And it has been tested for different locations and achieved fruitful results, so this method has a better application potential in transmission line protection systems that only use local-side data.

2.3.2.2 Discrete wavelet transform disadvantages

Despite the usefulness and the effectiveness of the discrete wavelet transform method however it requires a signal behavior analysis that allows direct fault signaling thus another decision support strategy is needed, also we found difficulties for the instantaneous and fast faults detection, another disadvantage it works in short-circuit faults only and doesn't work in open-circuit faults.

The diagnosing of power systems can be improved by combining the discrete wavelet transform method with intelligent tools like artificial neural networks or support vector machine.

2.4 Conclusion

This chapter has been dedicated to study and analyze two different signal-based methods in the detection, classification and the localization of faults in power system transmission lines starting with Park's transformation method and the second method is the Wavelet transform.

In both methods, we found difficulties for the instantaneous and fast signaling of faults, for this in the next chapters we are moving towards the algorithms of artificial intelligence as more effective and more efficient solutions. Where in chapter three we will discuss the exploitation of the artificial neural networks to diagnose the short-circuit and open-circuit faults in power transmission lines.

Chapter 3: Transmission Line Fault Diagnosis using Artificial Neural Network

Chapter 3: Transmission Line Fault Diagnosis using Artificial Neural Network

3.1 Introduction

Artificial intelligence (AI) is the perception, synthesis, and inference of information carried out by computers [78], compared to the intelligence displayed by humans or other animals. It can be used in Speech recognition, computer vision, diagnosis systems, translation across (natural) languages, and various mappings of inputs.

This chapter, contains an introduction of diagnosis by artificial neural network [79]. Firstly, presents the natural neuron and the formal neuron [80]. Then introduces the architectures of neural networks [81]. After that explains the learning of neural networks (supervised and unsupervised learning) and their methods (perceptron method, Hebb method, error gradient back-propagation method, Reinforcement learning and Levenberg-Marquardt method) [82]. Lastly we present the implementation of neural networks for the detection and signaling of faults in electrical transmission lines.

3.2 Principle of diagnosis by neural network

Techniques for diagnosing neural networks rely on learning databases, not models, as their basic operation is finding a correlation between input and output variables Input variables may be measurable (sensor outputs) or qualifyable (operator observations) [83].

The neural network must provide a response that tells the operating status of the equipment. It provides the detection function (normal operation or not), gives the classification and the types of faults on industrial systems.

3.3 Artificial neural networks

“Artificial neural networks are highly connected networks of elementary processors operating in parallel. Each elementary processor calculates a unique output based on the information it receives. Any hierarchical structure of networks is obviously a network” [84].

3.4 Neural networks principle

Artificial neural networks are built on an architecture similar, to that of the human brain. The network receives the information on a receiving layer of "neurons", processes this information with or without the help of one or more "hidden" layers containing one or more neurons and produces an output signal (or more). Each neuron, whether it belongs to the first layer, to the hidden layers or to the output layer, is linked to the other neurons by connections (similar to the synapses of the brain) to which weights are assigned. It exists two major types of network learning

depending on whether or not a dependent variable with known values is specified. In unsupervised learning, the network combines input information and analysis without reference to an output value. Such networks allow identification of specific characteristics, sorting, recognition of shapes, typologies, etc. Supervised learning, on the other hand, assumes a known "output". Each input information is coupled to an output value and the network seeks to approximate, by minimizing a distance, the implicit function contained in the input information and the output values. This type of learning corresponds to applications where one seeks to predict a dependent variable, whether in continuous or binary form (price, interest rate, probability of occurrence of an event, etc.) [85].

3.5 Natural neuron

The biological neuron is the basic functional element of the nervous system, there are around 10 billion neurons in the human brain each of them connected to about 100 other neurons which ensure the emission and reception of the signals generated by the neurons themselves.

In general, each biological neuron has an axon that can reach several tens of centimeters, a cell body where the neuron triggering mechanism is located, dendrites that receive information from other neurons and axon terminals that emit information to others. neurons (fig. 2.1). Neurons are interconnected by synapses, the number of which is about 10,000 billion. This means that a neuron receives on average excitations coming from 1000 neurons, and which also emits information to 1000 different neurons [86].

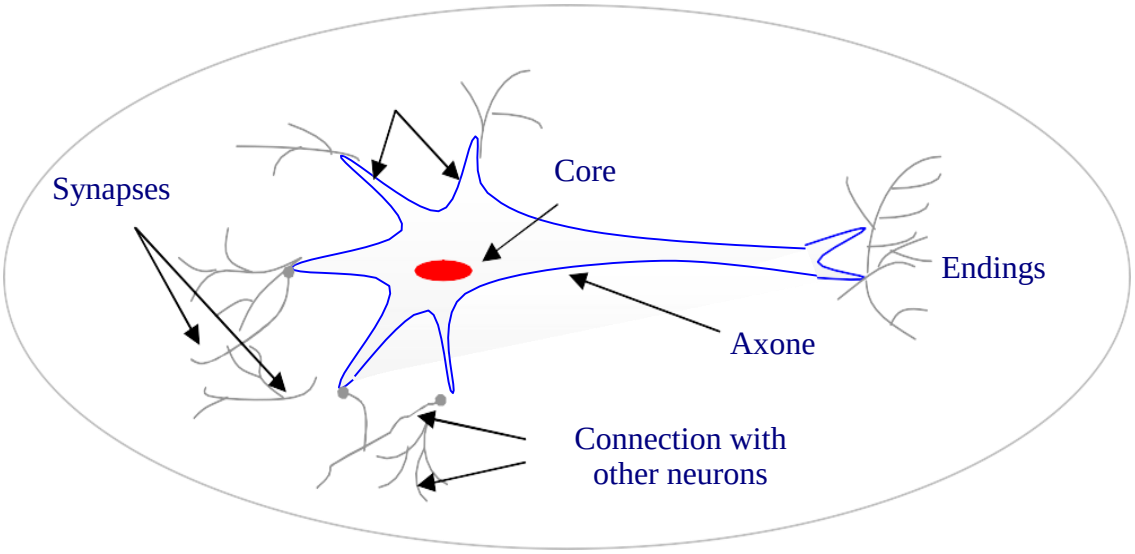

Figure 3.1 Simplified diagram of a human brain neuron.

The different elements that make up the biological neuron are as follows:

Cell body: it contains a nucleus surrounded by cytoplasm and organelles. Whose role is to combine the information received from other neurons.

Dendrites: Dendrites are short, slender, branching extensions of the cell body. They receive nerve stimuli and produce nerve impulse-generating potentials.

Axon: It is a long and unique extension of the cell body, along which the nerve impulse to a neuron.

Synapsis: The connectors between two neurons are known as synapses. they allow the transmission of an information from one to the other. The process of communication between neurons is done electrochemically at the synapses by neurotransmitters; these specific functions essentially depend on the properties of the outer membrane of the neuron, the latter fulfills five main functions:

-serves to propagate electrical impulses throughout the axon and dendrites;

-releases mediators outside the axon.

- reacts at the level of the cell body to the electrical impulses transmitted to it by the dendrites to generate or not a new impulse.

Finally, it allows the neuron to recognize other neurons so that it can locate itself in the anatomical architecture of the brain and find the cells to which it must be connected.

Generally, artificial neural networks are based on an electrical theory according to which the synaptic junction is where the neuron perceives a stimulus electrochemically. The synaptic membrane, when it does not receive excitation, is polarized at a voltage above a given threshold, the neuron then being activated and this triggers a process of depolarization; the neuron emits a positive voltage of approximately (+60 to +70mv) on the axon, behaving like a nonlinear system. It is this type of model that is mainly used to artificially simulate the neurons of the human brain.

3.6 Formal neuron

An artificial or formal neuron is a basic mathematical operator. A neuron has an output in addition to inputs that could be other neurons' outputs. The output's value is set by adding the inputs together and weighting them with coefficients (sometimes referred to as connection weights or synaptic weights), and then by computing a non-linear function (activation function) [86].

The weighted sum of a neuron's inputs is referred to as the neuron's state, often known as activity. Its operating diagram is given in Figure 3.2 The information is thus transmitted unidirectional. A neuron is characterized by three concepts: its state, its connections with other neurons and its activation function. Thus, neuron i receiving information from p neurons performs the following operation:

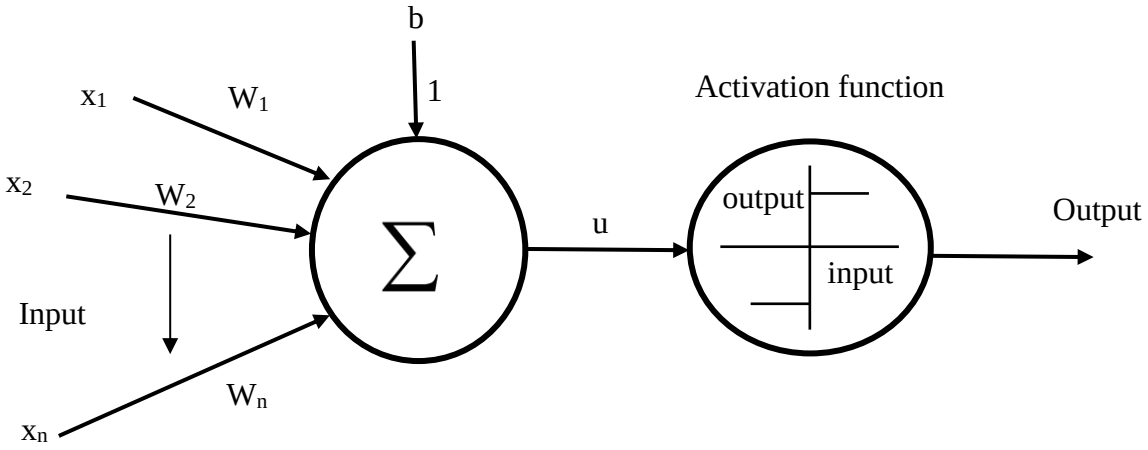

Figure 3.2 Diagram of the functioning of a formal neuron

$$y = f(u) = f\left(\sum_{i=1}^{n} w_i x_i + b\right) \qquad 3.1$$

• xi: the neuron inputs.

• y: the neuron output.

• f: the activation function associated with the neuron.

• Wi: The weight of the neural connections.

• b: the connection weight between the i neurons and the bias neuron (+1).

Activation Function	Equation	Function curve
Unit step	$y = \begin{cases} 0 & \text{if } x < 0 \\ 0.5 & \text{if } x = 0 \\ 1 & \text{if } x > 0 \end{cases}$	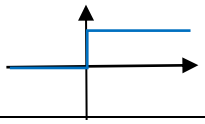
Linear	$y = x$	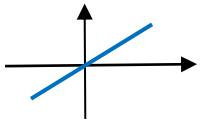
Sign(signum)	$y = \begin{cases} -1 & \text{if } x < 0 \\ 0 & \text{if } x = 0 \\ 1 & \text{if } x > 0 \end{cases}$	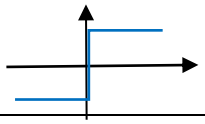
Sigmoid	$y = \frac{1}{1 + e^{x}}$	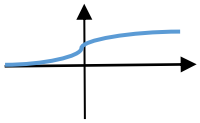
Hyperbolic tangent	$y = \frac{e^{x} - e^{-x}}{e^{x} + e^{-x}}$	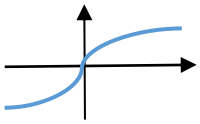

Table 3-1 Most used activation functions

3.7 Architectures of neural networks

A collection of processing units makes up a neural network., "processing elements", arranged in such a way that they form an architecture. These architectures are of various types.

There are several classifications of neural network architectures. The best known are based on the number of internal layers; simple or multi-layered or on the type of connection between network neurons; recurrent or non-recurrent, we can classify several models of neural networks.

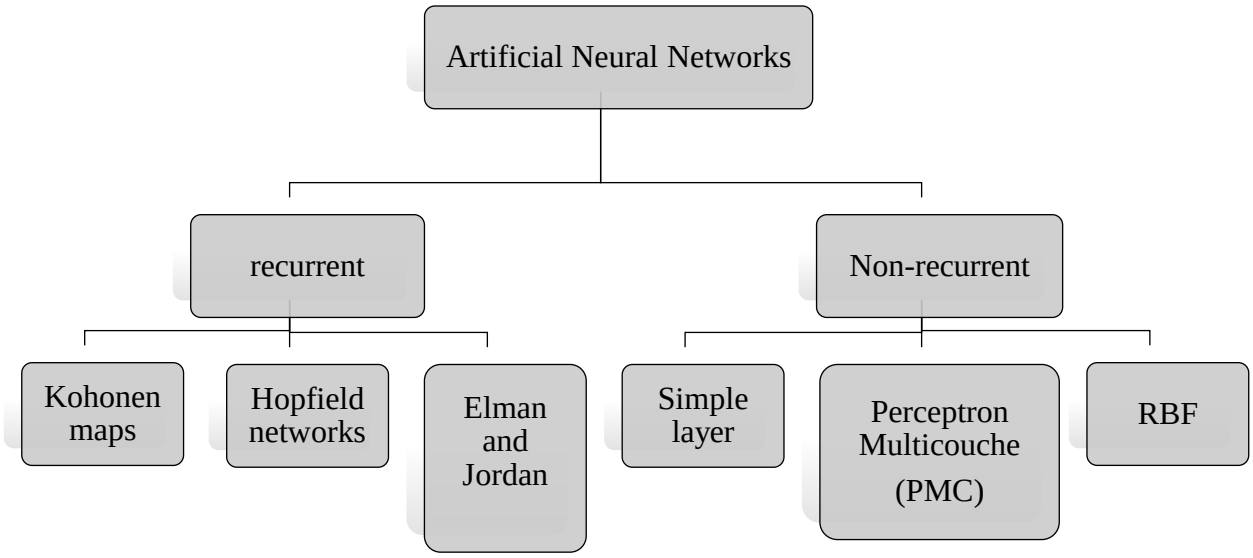

Figure 3.3 The different architects of neural networks

Single/multi-layer:

Neural networks can be grouped based on how many layers they have. multi-layer or single-layer:

a - Single layer: The single-layer neural network or perceptron is a formal neuron with a step-like activation function.

b – Multilayer: The most common type of neural network is one with multiple layers. There may be one or more hidden layers, which defines it. It covers a number of models, including Hopfield networks, radial basis function neural networks, multilayer perceptron, and Kohonen maps.

- Non-recurring/recurring:

Another way to categorize neural network architectures is according to whether information is flowing in a recurrent or non-recurrent fashion.

- Non-recurring:

a collection of interconnected neurons in such a way that data goes from inputs to outputs without feedback constitutes a non-recurrent neural network, also known as a non-looped, static, or "feedforward" neural network. There are several models of the non-recurring genre, mainly: multilayer neural networks (Perceptron Multilayer ‘PMC’) and radial basis function neural networks (RBF).

a - PMC neural networks

The multilayer perceptron (PMC) is a network of non-recurrent artificial neurons organized in several layers (figure 3.4) [87]. Gradient descent and back-propagation algorithms are used for learning.

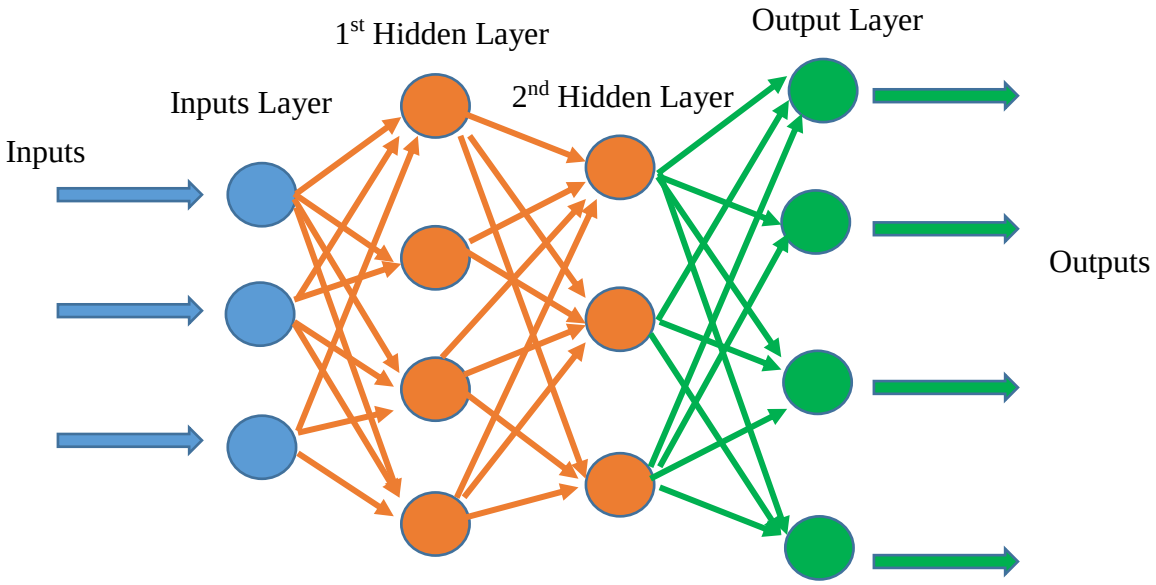

Figure 3.4 PMC neural network.

b - Radial basis function neural networks

Radial basis method neural networks (figure 3.5) are networks with a single hidden layer that typically have Gaussians as their activation functions (specified by their center and standard deviation) [88].

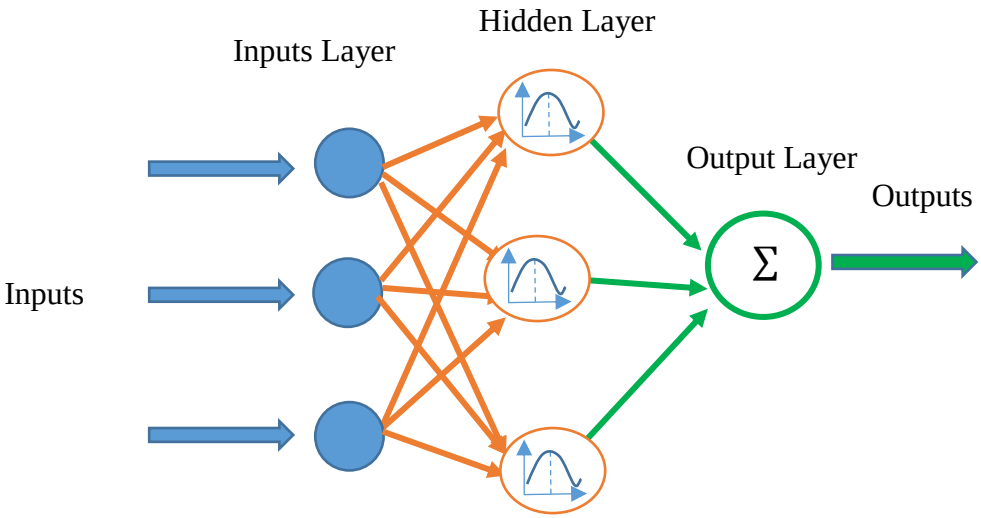

Figure 3.5 Radial basis function neural network.

- Recurring:

At the level of the neurons or between the layers, there is at least one feedback loop. as a result of taking the temporal component of the event into account, which is a characteristic of recurrent neural networks (Figure. 3.6). The challenges of applying these models is a serious flaw in them.

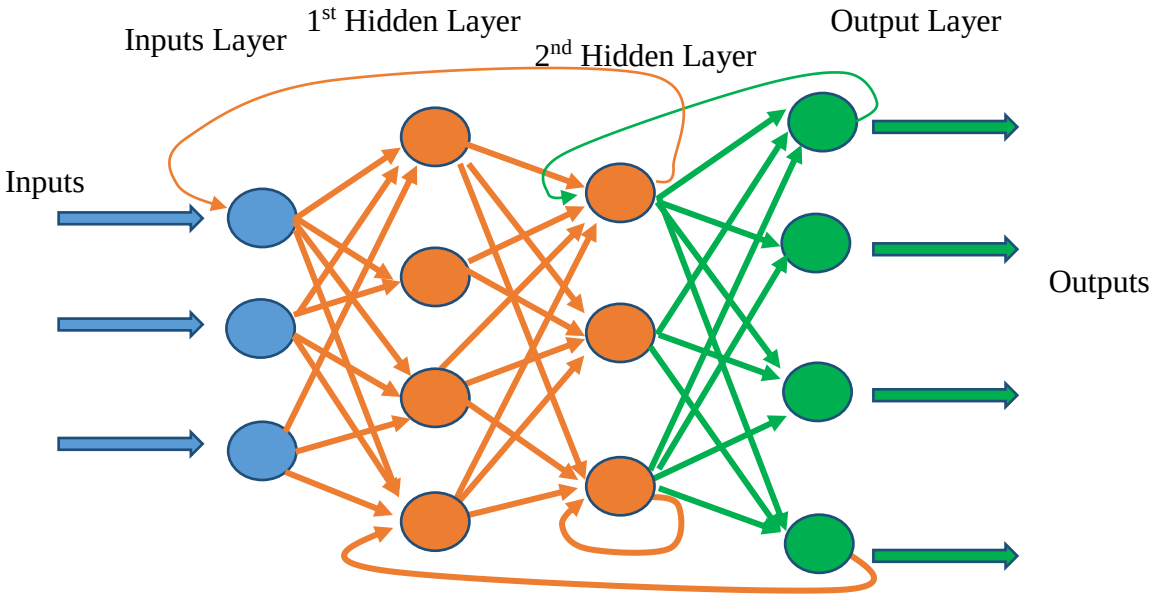

Figure 3.6 Recurrent neural network.

There are several models, the best known of which are the Kohonen maps and the Hopfield networks. Each neuron in a Hopfield network is connected to every other neuron, making them completely connected networks. In such networks, there is no differentiation between input and output neurons. Kohonen maps are unsupervised learning networks that build a discrete, topologically ordered map based on the input shapes.

3.7.1 Learning neural networks

In the learning phase of neural network development, the network's behavior varies until the desired behavior is achieved. The connection weights are the variables that are modified during learning.

Depending on whether learning is considered to be supervised or unsupervised, two main classes of learning algorithms have been established. This distinction is dependent on how the learning is constructed. in unsupervised learning, only the values (Input) are available; however, in the case of supervised learning, both (Input, Associated Output)pair are available [89].

3.7.2 Supervised and unsupervised learning

3.7.2.1 Supervised learning

Supervised learning's objective is to train network-reference behavior. We then assume that each input pattern is associated with a desired output that specifies the output values. Learning takes place as follows: Inputs are presented to the network and at the same time the outputs that one would like for this input. The network must then reconfigure itself. That is to say calculate its weights so that the output it gives corresponds to the desired output.

Learning is "supervised". This means that a "teacher" can provide the network with "examples" of what the network should do. This type of learning will be adopted by the optimization algorithm. Iteratively changing the weights that correspond with the gradient of the cost function is how this optimization is carried out: A technique particular to neural networks is used to estimate the gradient., then it is used by the optimization algorithm. The weights are initialized randomly before learning, then modified iteratively until a satisfactory compromise is obtained between the precision of the approximation on the set of apprentices.

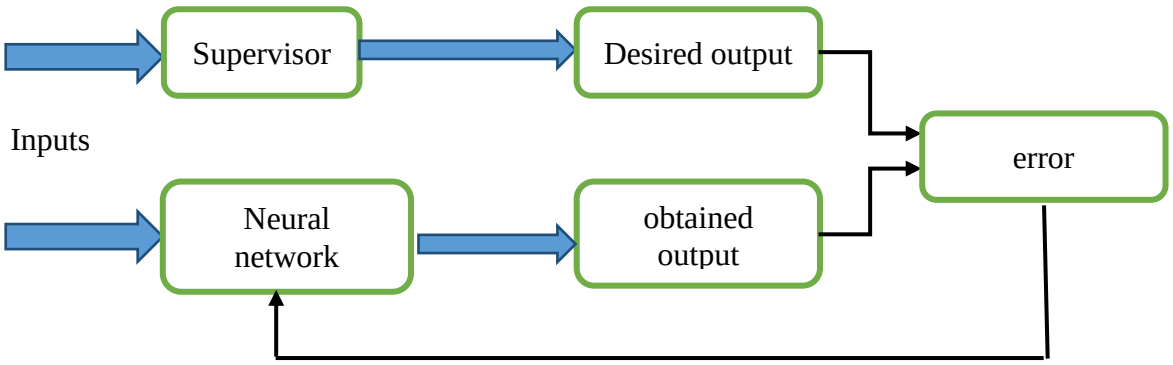

Figure 3.7 Supervised learning

3.7.2.2 Unsupervised learning

This sort of unsupervised learning, often known as "learning by competition," differs from supervised learning in that just input values are provided. In this case, the examples given at the input prompt the network to self-adapt and produce output values that are similar to input values in response. In general, in this category of learning, the training rule is not a function of the output behavior of the network, but rather of the local behavior of the neurons. There is no indication about the desired output in the input data. Rules that modify the network parameters in accordance with the input examples are used to carry out the learning. we may refer to Hebb's rule.

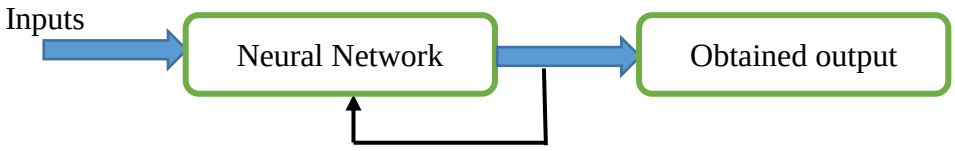

Figure 3.8 Non supervised learning

3.7.3 Learning methods

3.7.3.1 - Perceptron method

The perceptron's weights are set to random values upon initialization. The weights are changed each time a new example is shown to correspond with whether or not the perceptron correctly classified it. When all examples have been presented, the algorithm terminates without changing any weights.

The threshold linear perceptron learning procedure is an error correction procedure since the weights are not changed when the output computed by the present perceptron equals the expected output. Let's study the modifications on the weights when differs from:

If the calculated output=0 and expected output=1, this means that the perceptron has not sufficiently considered the active neurons of the input (i.e. the neurons having an input at 1) in this situation; the algorithm adds the retina value to the synaptic weights (reinforcement).

if computed output=1 and expected output=0; the algorithm subtracts the value of the retina from the synaptic weights (inhibition).

During the learning phase, knowing that the learning sample is a linearly separable set, all the examples are presented until convergence, i.e. until a complete presentation of the examples does not cause any modification of the weights.

3.7.3.2 - Hebb's method

Hebb's rule, from the neurophysiologist of the same name, the oldest (1949), stipulates that the efficiency of a synapse between a neuron A and a neuron B is increased if an action potential is emitted by B while it receives action potentials coming from A. This is a kind of reinforcement of causality, because if B is active at the same time as A while there is a synapse to connect them, it means that A participated in the triggering of B. The principle is to strengthen the connections

between two neurons when they are active simultaneously. This rule can be classified as unsupervised learning. This rule, observed on natural neural networks, is also applied in many artificial network learning techniques. It could be the basic mechanism allowing classification, or pattern recognition.

3.7.3.3 - Back-propagation method of the error gradient

The Least Mean Square LMS technique was created specifically for multilayer Perceptron, and the back propagation of the gradient BP (Back Propagation) is a generalization of this approach [90].The goal of this supervised approach is to modify the MLP network's weights in order to reduce a differentiable cost function, such as the quadratic error between the output of the network and the expected output:

$$E(n) = \left|\left|d(n) - x_{L(n)}\right|\right|^2 \qquad 3.2$$

Where d(n) is the desired output and xL(n) is the network output at time n.

The BP method makes sure that the gradient descends in order to minimize the error.

3.7.3.4 Reinforcement learning

Reinforcement learning is the process of discovering what to do and how to link behaviors to situations in order to maximize rewards numerically. The learner must experiment with different actions to decide which ones reward them the most. In the most intriguing scenario, decisions can influence future situations and longer-term rewards in addition to current advantages. (Reinforcement learning is different from supervised learning).

The latter requires a supervisor who dictates to the network what action is correct in such situation. In reinforcement learning, the network does not have a supervisor to its disposition, it interacts with the environment which gives it a quantitative feedback on the values of its actions.

3.7.3.5 - Levenberg-Marquardt method

Kenneth Levenberg first found the algorithm, which Donald Marquardt later made public. enables the numerical solution to a function problem's minimization., which is frequently nonlinear and dependent on a number of factors. The algorithm interpolates between the gradient algorithm and the Gauss-Newton algorithm. It finds a solution even if it deviates greatly from the minimum. since it is more stable than the Gauss Newton method [91]. Its main application is regression

through the method of least squares: given a number of data pairs (ti, yi), we seek the parameter of the function so that the sum of squares representing the deviations either at least:

$$s(a) = \sum_{i=1}^{m} \left[y_i - f(t_i/a) \right]^2 \qquad 3.3$$

3.8 Faults diagnosis of power transmission line by artificial neural networks (Application and simulation)

3.8.1 Implementation of ANN in test power system

As mentioned in chapter 2 the same power system is used in this part. The artificial neural networks were used for fault diagnosis of transmission lines [92]. figure 3.9 shows the implementation of ANN in this test power system. The measurements point was at the beginning of the transmission line to extract voltages and currents (V_{123}, I_{123}), these data are fed to the intelligent system which will shows the fault type (short circuit or open circuit), the fault zone (1, 2, 3, 4) and the faulty phase (1001 means phase A-Ground, 0101 phase B-Ground, 0011….) the fault classification will be represented later.

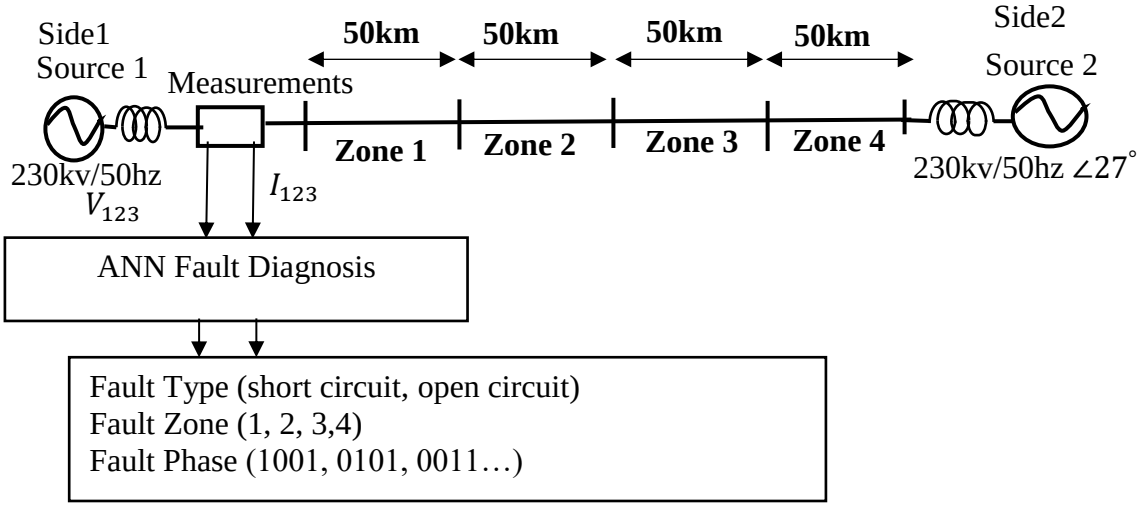

Figure 3.9 Diagram of the diagnostic system

3.8.2 Faults types

The electrical transmission line is vulnerable to several fault types. this thesis focuses on the most frequent ones, (Short circuits and Open circuits). The schematic representation of the faults is presented in Figure 3.10.

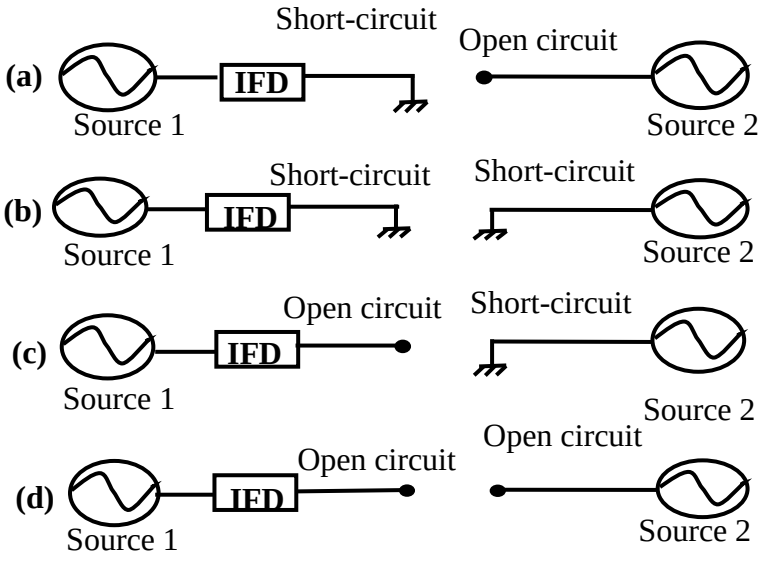

Figure 3.10 Faults types

(a) Short circuit to source 1 and open circuit to source 2, **(b)** Short circuit to both sides, **(c)** short circuit to source 2 and open circuit to source 1 and **(d)** open circuit. In all 4 cases the fault type can be a single phase to ground (L-G), two phases (L-L), two phases to ground (2L-G), three phases (3L-G).

To solve the difficulty of determining whether the fault is a short circuit or an open circuit in an interconnected system, two IFD systems are required, one on each side., as illustrated in figure3.11.

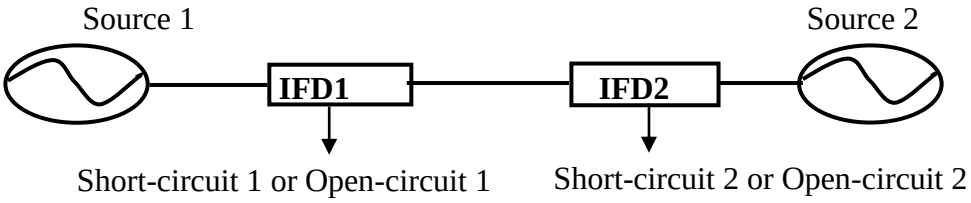

Figure 3.11 Two Surveillance systems

3.8.3 Diagnosis system output

The diagnosis system outputs are shown in Figure 3.12. The first output displays the fault type. A short circuit (SC), an open circuit (OC), and no fault are all indicated by the values [1 0], [0 1], and [0 0], respectively. The second output indicates which zone (1–4) the fault is located at. Which phase is faulty is indicated by the third output.

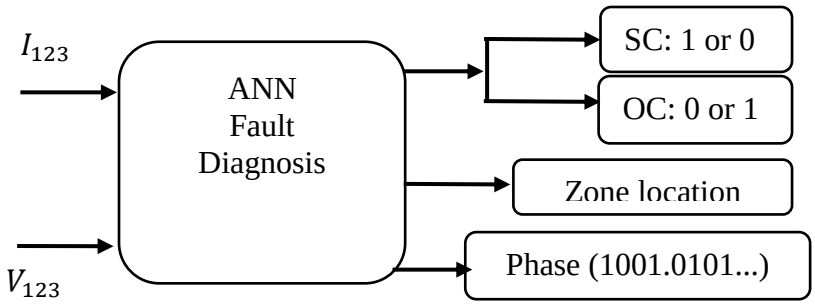

Figure 3.12 Diagnosis system output

Table 1 summarizes every case of the fault type short circuit (SC) or open circuit (OC) from the perspective of the intelligent system from each side.

Display	SC side1	SC side2	OC side1	OC side2
sc 1	1	0	0	1
sc 1 & sc2	1	1	0	0
sc 2	0	1	1	0
oc 1 & oc 2	0	0	1	1

Table 3-2 Sides point of view of the faults

3.8.4 Diagnostic by the artificial neural network ANN

The synoptic diagram of ANN diagnostics is displayed in Figure 3.14.

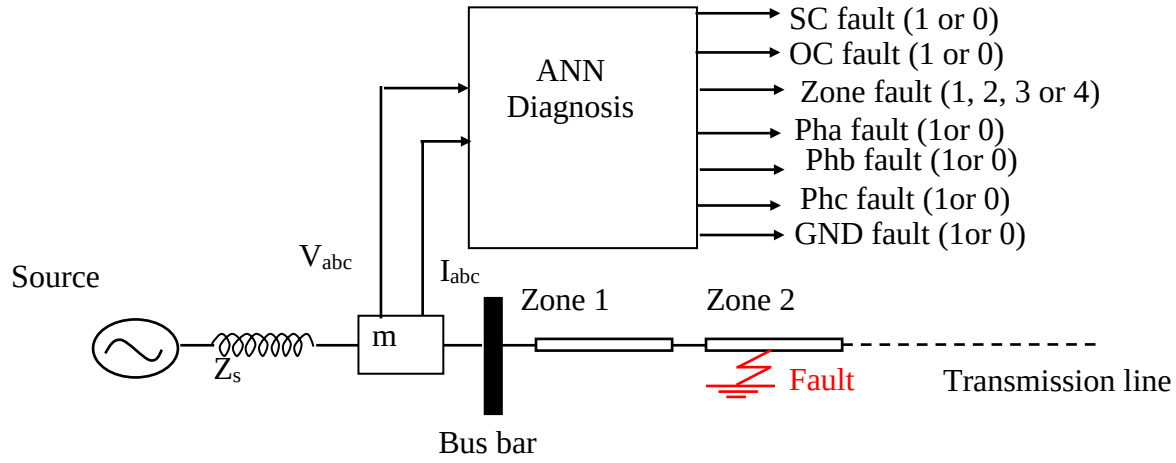

Figure 3.13 ANN Diagnosis system output

3.8.5 Neural network structure

Artificial neurons form the complex structure of a neural network, which can process many inputs and produce output, in this study, the input layer consists of six neurons for each of the six inputs, which are the magnitudes of I_1, I_2, I_3, and V_1, V_2, V_3. As we will demonstrate in the next section, the number of neurons in the hidden layer and the output layer changes as a result of outputs. Figure 3.14 depicts this network.

To produce the output, the value of V must be activated using the activation function. The output layer's activation function in this thesis was a linear activation function, while the hidden layer's activation function was the logistic sigmoid. The error is sent from the output layer to the hidden layer for the p iteration.

The Log Sigmoid Transfer Function, often known as the logistic sigmoid activation function:

$$y_j(p) = \frac{1}{1+e^{-V_j(p)}} \qquad 3.4$$

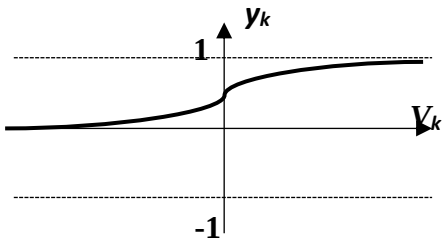

Figure 3.1 Transfer function of the log-Sigmoid

The linear activation function is:

$$y_k = 1.V_k \qquad 3.5$$

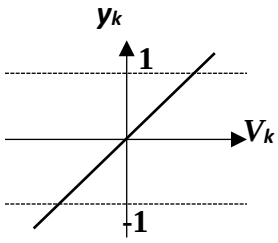

Figure 3.2 Linear transfer function

The MLP architecture employed in this investigation has been identified as (6, 40, 7). It denotes that the layers have a total of six (n=6) input variables, forty (m=40) hidden layer nodes, and seven neurons in the output (k=7).

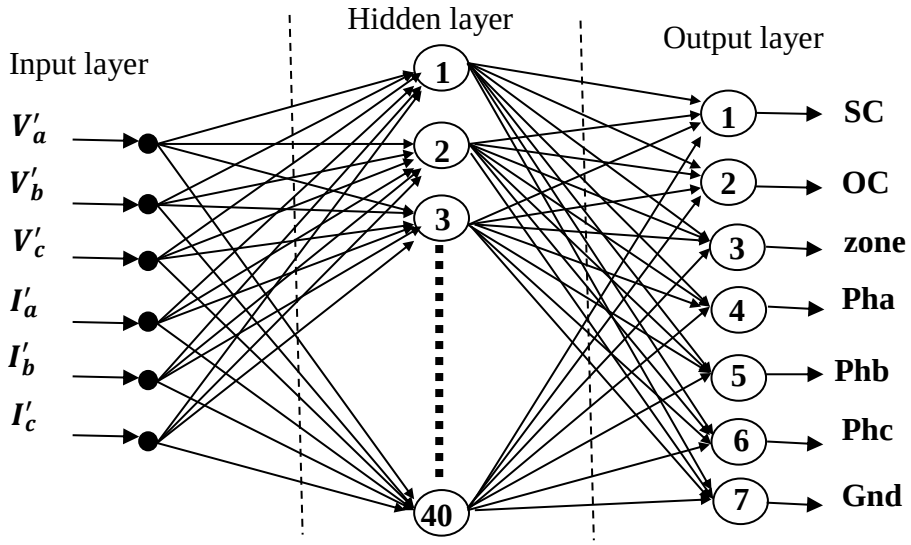

Figure 3.14 Artificial neurons network structure

3.8.6 Training algorithms (Levenberg-Marquardt method)

The Levenberg-Marquardt algorithm was used in attempt to reach the second-order training speed without the computing of the Hessian matrix. when the performance function (common in training feedforward networks) takes a form of a sum of squares. If weight value and threshold value make up p^{th} vector X_p, then X_{p+1} is derived from:

$$X_{p+1}=X_p+\Delta X \quad , \quad X_{p+1}=W_{p+1}+\Delta X \quad , \quad X_{p+1}=W_p \qquad 3.6$$

The Newton Algorithm states that ΔX is determined by:

$$\Delta X=-\left|\nabla^2 E(x)\right|^{-1}\nabla E(x) \qquad 3.7$$

Thus, the Hessian matrix can be roughly represented as:

$$H = J^T J \qquad 3.8$$

Where $\nabla^2 E(x)$ is the hessian matrix of error indicator function $E(x)$. $\nabla E(x)$ is the gradient.

E(x) is defined by the following equation:

$$E(x)=(1/2)\sum_{i=1}^{N} e_1^2(x) \qquad 3.9$$

e(x) stands for the training error.

Equations (3.9) and (3.10) are used to determine $\nabla E(x)$ and $\nabla^2 E(x)$, respectively.

$$\nabla E(x)=J^T(x)e(x) \qquad 3.10$$

$$\nabla^2 E(x)=J^T(x)e(x)+S(x) \qquad 3.11$$

Where $S(x)=\sum_{i=1}^{N} e_i(x)$ $\nabla^2 e_i(x)$. $J(x)$ is the jacobian matrix:

$$J(x)=\begin{bmatrix} \frac{\partial e_{1(x)}}{\partial x_1} & \frac{\partial e_{1(x)}}{\partial x_2} & \cdots & \frac{\partial e_{1(x)}}{\partial x_n} \\ \frac{\partial e_{2(x)}}{\partial x_1} & \frac{\partial e_{2(x)}}{\partial x_2} & \cdots & \frac{\partial e_{2(x)}}{\partial x_n} \\ \cdots & \cdots & \cdots & \cdots \\ \frac{\partial e_{n(x)}}{\partial x_1} & \frac{\partial e_{n(x)}}{\partial x_2} & \cdots & \frac{\partial e_{n(x)}}{\partial x_n} \end{bmatrix} \qquad 3.12$$

ΔX can be written as follows using the gauss-newton algorithm:

$$\Delta X=-[J^T(x)J(x)]^{-1}J(x)e(x) \qquad 3.13$$

ΔX presented as follows using the LM algorithm:

$$\Delta X=-[J^T(x)J(x)+\mu I]^{(-1)}J(x)e(x) \qquad 3.14$$

and the gradient can be calculated as follows:

$$g = J^T e \tag{3.15}$$

where J is the Jacobian matrix, which holds the network error's initial derivative with regard to weight and bias., and the network error vector is (e(x): Training error). It is much simpler to calculate the Jacobian matrix than the Hessian matrix using the standard backpropagation method. The following Newton-like updates employ this approximation to the Hessian matrix in the Levenberg-Marquardt technique.:

$$X_{p+1} = x_k - \left[H + \mu I\right]^{-1}.g \tag{3.16}$$

$$Xp+1 = xk - \left[JTJ + \mu I\right]-1.JTe \tag{3.17}$$

When the scalar μ is zero, this is merely Newton's approach, using an approximate Hessian matrix. This turns into a gradient descent with a lower step size as μ increases. The objective is to convert to Newton's approach as soon as possible because it is quicker and more accurate when it comes to errors that are close to zero. As a result, μ will decrease and increase only when the tentative step improves the performance function after each successful step (reduction of the performance function). In this method, the algorithm's performance function always decreases with each iteration.

3.8.7 Training base

3.8.7.1 Measurements adaptation with neural network input

The numbering of the various measurement intervals is utilized as inputs to minimize the complexity the neural network and process all potential values, like shown in table 2.(Ia is an example, all the currentsI_a ,I_b , I_c magnitudes and voltagesV_a,V_b,V_c magnitudes were employed) , the advantage of this strategy is that it covers the entire zone (1 km to 50 km), which prevents mixing between the zones when a fault occurs at a zone's borders and covers a various fault resistances.

Size measured	Variation intervals	Interval numbering (neural network inputs)
Ia (pu)	$I_a \leq 0.015$	1
	$\mathbf{0.015} < I_a \leq 0.03$	2
	$\mathbf{0.03} < I_a \leq 0.045$	3
	$\mathbf{0.045} < I_a \leq 0.1$	4
	$\mathbf{0.1} < I_a \leq 0.6$	5
	$\mathbf{0.6} < I_a \leq 1.27$	6
	$\mathbf{1.27} < I_a \leq 1.71$	7
	$\mathbf{1.71} < I_a \leq 2.61$	8
	$\mathbf{2.61} < I_a \leq 9$	9
Va (pu)	$V_a \leq 0.53$	1
	$\mathbf{0.53} < V_a \leq 0.7$	2
	$\mathbf{0.7} < V_a \leq 0.78$	3
	$\mathbf{0.78} < V_a \leq 0.85$	4
	$\mathbf{0.85} < V_a \leq 5$	5

Table 3-3 Variation intervals as ANN inputs

3.8.7.2 Training table

All of the training data for ANN is shown in the following table.

No	i_a	i_b	i_c	V_a	V_b	V_c	SC	OC	Zone	Ph_a	Ph_b	Ph_c	GND
1	5	5	5	5	5	5	0	0	0	0	0	0	0
2	9	5	5	1	5	5	1	0	1	1	0	0	1
3	5	9	5	5	1	5	1	0	1	0	1	0	1
4	5	5	9	5	5	1	1	0	1	0	0	1	1

5	9	9	5	1	1	5	1	0	1	1	1	0	1
6	9	9	5	2	1	5	1	0	1	1	1	0	0
7	5	9	9	5	1	1	1	0	1	0	1	1	1
8	5	9	9	5	2	1	1	0	1	0	1	1	0
9	9	5	9	1	5	1	1	0	1	1	0	1	1
10	9	5	9	1	5	2	1	0	1	1	0	1	0
11	9	9	9	1	1	1	1	0	1	1	1	1	1
12	1	5	5	5	5	5	0	1	1	1	0	0	0
13	5	1	5	5	5	5	0	1	1	0	1	0	0
14	5	5	1	5	5	5	0	1	1	0	0	1	0
15	1	1	5	5	5	5	0	1	1	1	1	0	0
16	5	1	1	5	5	5	0	1	1	0	1	1	0
17	1	5	1	5	5	5	0	1	1	1	0	1	0
18	1	1	1	5	5	5	0	1	1	1	1	1	0
19	8	5	5	2	5	5	1	0	2	1	0	0	1
20	5	8	5	5	2	5	1	0	2	0	1	0	1
21	5	5	8	5	5	2	1	0	2	0	0	1	1
22	8	8	5	2	2	5	1	0	2	1	1	0	1
23	7	8	5	4	2	5	1	0	2	1	1	0	0
24	5	8	8	5	2	2	1	0	2	0	1	1	1
25	5	7	8	5	4	2	1	0	2	0	1	1	0
26	8	5	8	2	5	2	1	0	2	1	0	1	1
27	8	5	7	2	5	4	1	0	2	1	0	1	0
28	8	8	8	2	2	2	1	0	2	1	1	1	1
29	2	5	5	5	5	5	0	1	2	1	0	0	0
30	5	2	5	5	5	5	0	1	2	0	1	0	0
31	5	5	2	5	5	5	0	1	2	0	0	1	0
32	2	2	5	5	5	5	0	1	2	1	1	0	0
33	5	2	2	5	5	5	0	1	2	0	1	1	0
34	2	5	2	5	5	5	0	1	2	1	0	1	0
35	2	2	2	5	5	5	0	1	2	1	1	1	0

36	7	5	5	3	5	5	1	0	3	1	0	0	1
37	5	7	5	5	3	5	1	0	3	0	1	0	1
38	5	5	7	5	5	3	1	0	3	0	0	1	1
39	7	7	5	3	3	5	1	0	3	1	1	0	1
40	6	7	5	5	3	5	1	0	3	1	1	0	0
41	5	7	7	5	3	3	1	0	3	0	1	1	1
42	5	6	7	5	5	3	1	0	3	0	1	1	0
43	7	5	7	3	5	3	1	0	3	1	0	1	1
44	7	5	6	3	5	5	1	0	3	1	0	1	0
45	7	7	7	3	3	3	1	0	3	1	1	1	1
46	3	5	5	5	5	5	0	1	3	1	0	0	0
47	5	3	5	5	5	5	0	1	3	0	1	0	0
48	5	5	3	5	5	5	0	1	3	0	0	1	0
49	3	3	5	5	5	5	0	1	3	1	1	0	0
50	5	3	3	5	5	5	0	1	3	0	1	1	0
51	3	5	3	5	5	5	0	1	3	1	0	1	0
52	3	3	3	5	5	5	0	1	3	1	1	1	0
53	6	5	5	4	5	5	1	0	4	1	0	0	1
54	5	6	5	5	4	5	1	0	4	0	1	0	1
55	5	5	6	5	5	4	1	0	4	0	0	1	1
56	6	6	5	4	4	5	1	0	4	1	1	0	1
57	6	6	5	5	4	5	1	0	4	1	1	0	0
58	5	6	6	5	4	4	1	0	4	0	1	1	1
59	5	6	6	5	5	4	1	0	4	0	1	1	0
60	6	5	6	4	5	4	1	0	4	1	0	1	1
61	6	5	6	4	5	5	1	0	4	1	0	1	0
62	6	6	6	4	4	4	1	0	4	1	1	1	1
63	4	5	5	5	5	5	0	1	4	1	0	0	0
64	5	4	5	5	5	5	0	1	4	0	1	0	0
65	5	5	4	5	5	5	0	1	4	0	0	1	0
66	4	4	5	5	5	5	0	1	4	1	1	0	0

67	5	4	4	5	5	5	0	1	4	0	1	1	0
68	4	5	4	5	5	5	0	1	4	1	0	1	0
69	4	4	4	5	5	5	0	1	4	1	1	1	0

Table 3-4 Training data for ANN

3.9 Simulation results

This section illustrates the results of tests conducted utilizing a variety of transmission line faults to evaluate the response time, reliability, and robustness of our IFD's systems. We found that our systems capable of identifying 138 different fault types (69 x 2). In less than 20 ms which is less than the response time of the protection system (200 ms).

3.10 Diagnostic performances

To show the efficiency of the ANN method of diagnosis, the following faults (SC: Short Circuit or OC: Open Circuit) have been presented, the variation of the three-phase currents and voltages have been presented for each case in the two sides of the transmission line, the identification of the fault type (SC or OC) on each of the two sides of the IFD, the location of the fault zone, and the fault phase (Ph A, B, C, GND). Every fault in every case happens at 0.1 seconds.

3.10.1 Faults detection in zone 1.

Four different single-phase fault categories are used in this situation:

- SC Phase A - GND (both sides),
- SC Phase A - GND (Side 1),
- SC Phase A - GND (Side 2),
- OC Phase A.

3.10.2 Short circuit fault in Ph_a-GND

The responses for each IFD are shown in Figures 3.17 through 3.26. while Figures 3.15 and 3.16 show the transient behavior of three-phase currents and voltages on both sides.

- A significant drop in voltage and a significant rise in current (of phase a) on side 1.
- A small drop in voltage and a significant rise in current (of phase a) on side 2.

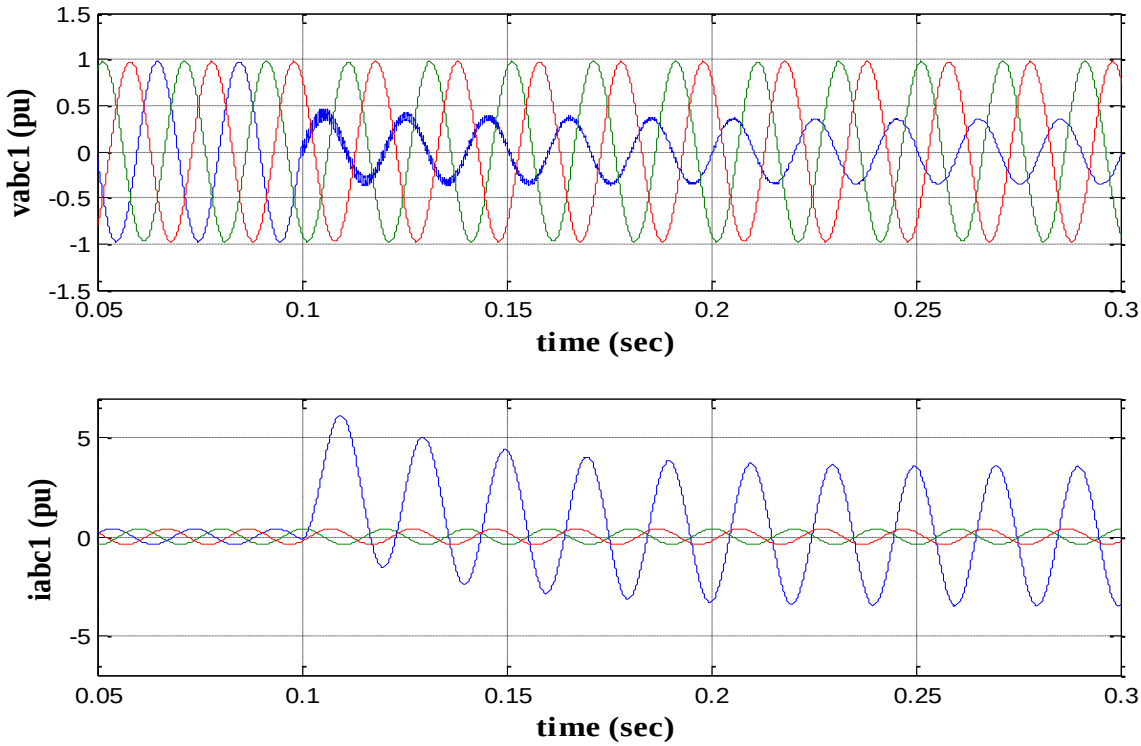

Figure 3.15 Voltages V_{abc1} and currents I_{abc1} of Ph_a-Gnd short-circuit

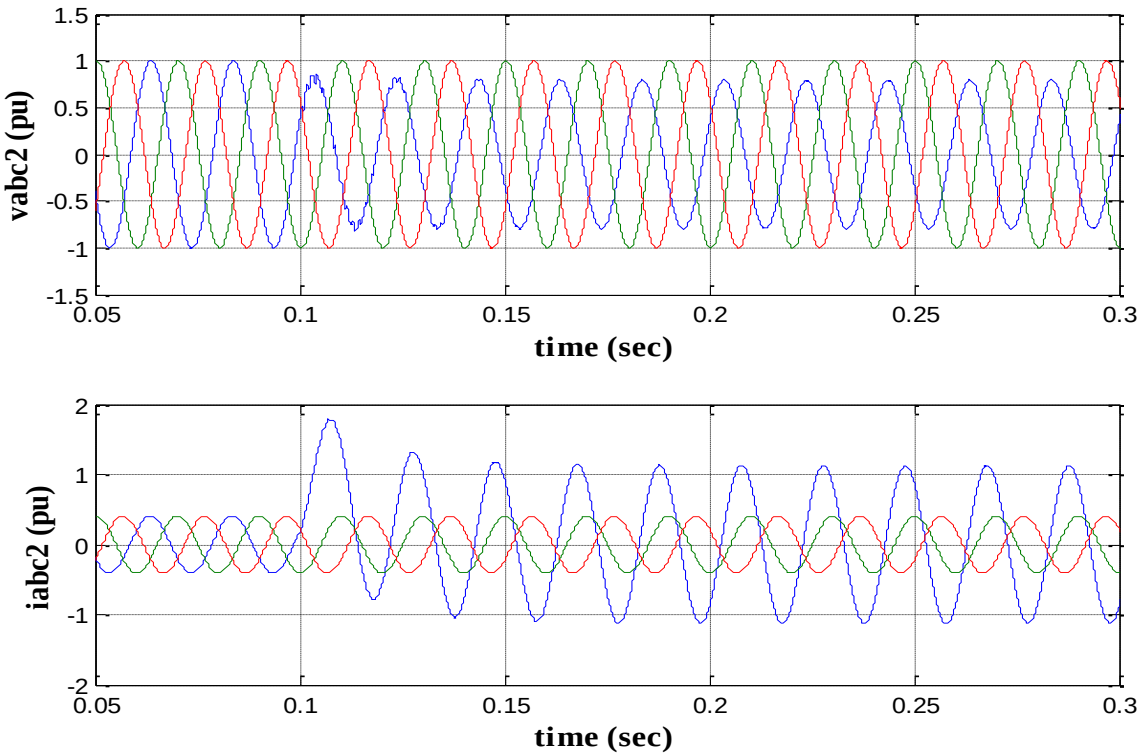

Figure 3.16 Voltages V_{abc2} and currents I_{abc2} of Ph_a-Gnd short-circuit

The effectiveness of ANN for fault signalization is displayed in Figures 3.17 through 3.19. We begin with the fault zone (location), then move on to the fault type short-circuit or open circuit for the two IFD systems, and finally the fault classification.

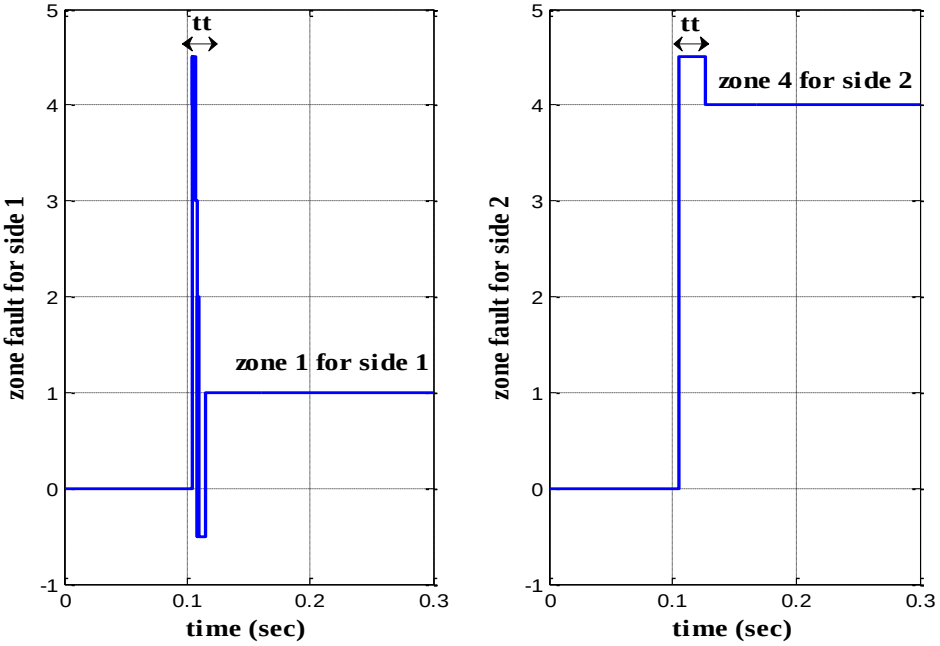

Figure 3.17 Pha-Gnd SC zone detection of the fault

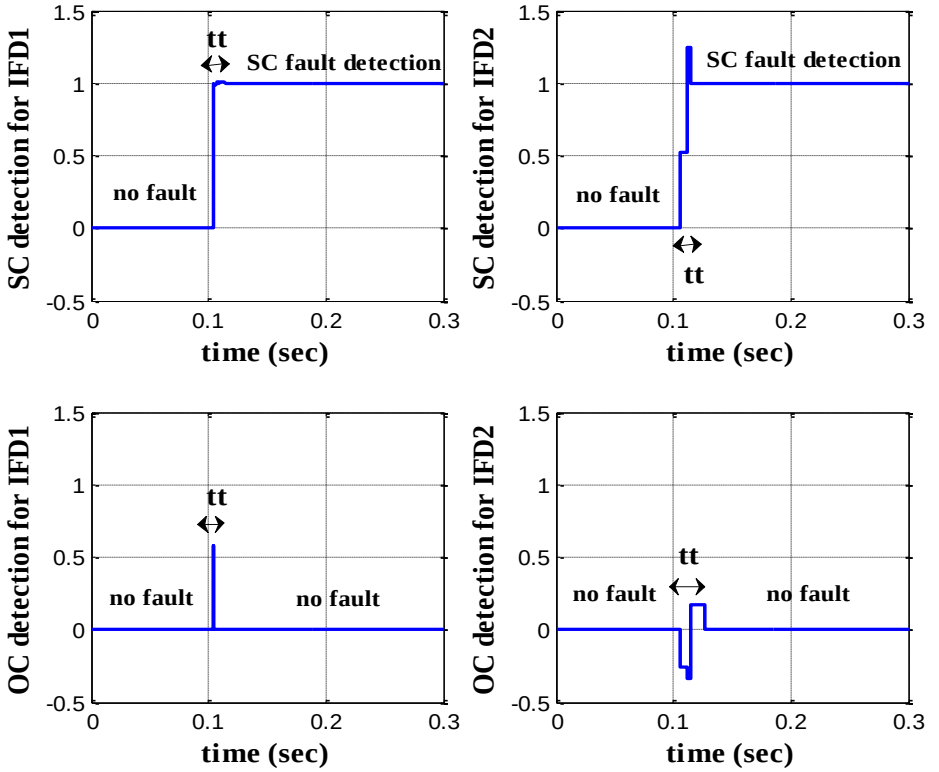

Figure 3.18 Identification of the fault type (SC-Side1 and SC-Side2)

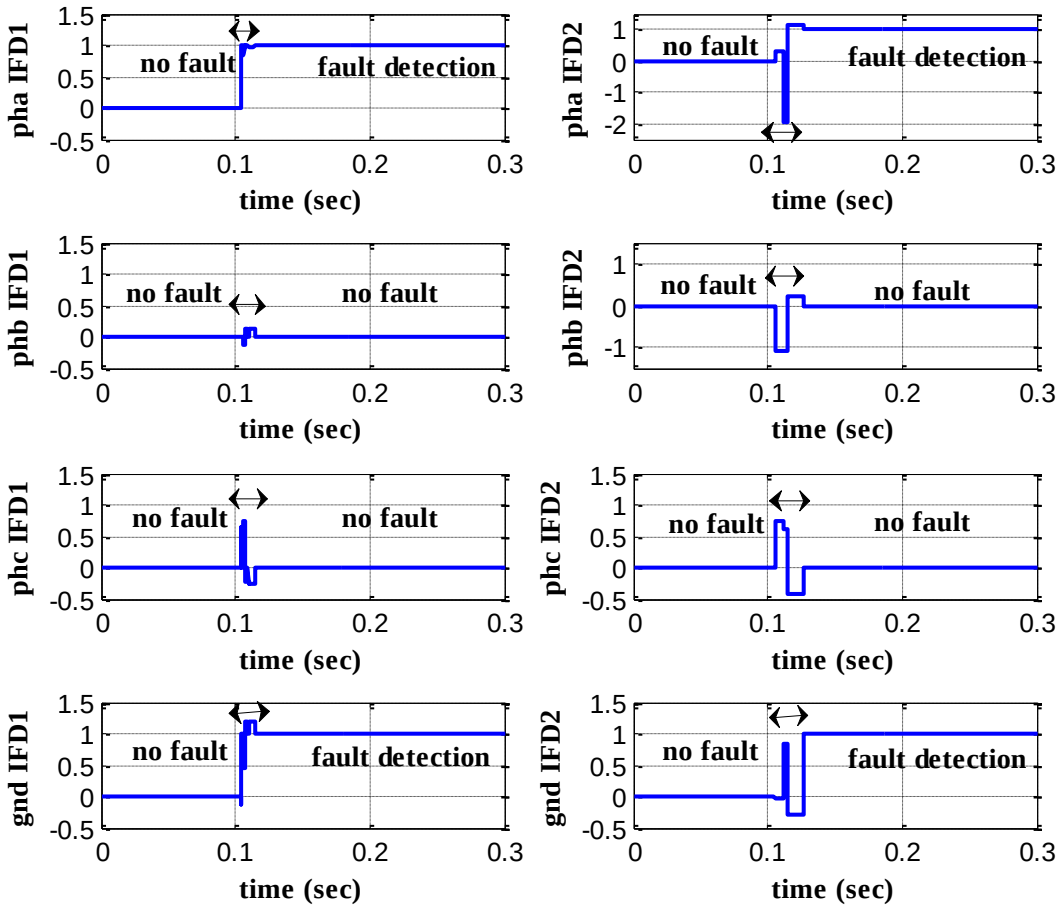

Figure 3.19 Faulty phase classification (Ph_a-GND)

Because of the random variation in voltages and currents on both sides of the line, fault signalization is accurate after small shifts and a significant transitional phase.

3.10.3 Short circuit fault in Pha-GND – Side 1

Observing in the figures 3.25 and 3.26:

- A large current and a drop in voltage in phase a (side 1) during the fault On side 2

-similarly observing a little transient voltage change and low current (both in phase a).

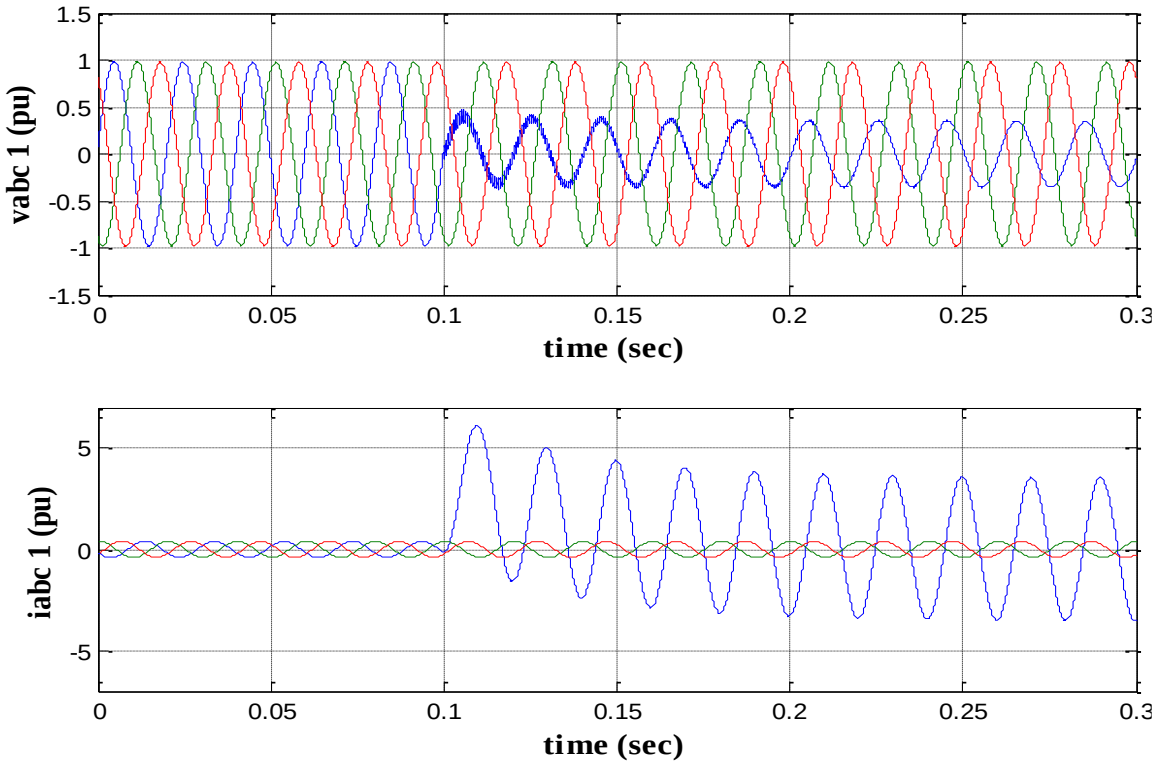

Figure 3.20 Voltages V_{abc1} and currents I_{abc1} of Ph_a-Gnd sc-side1

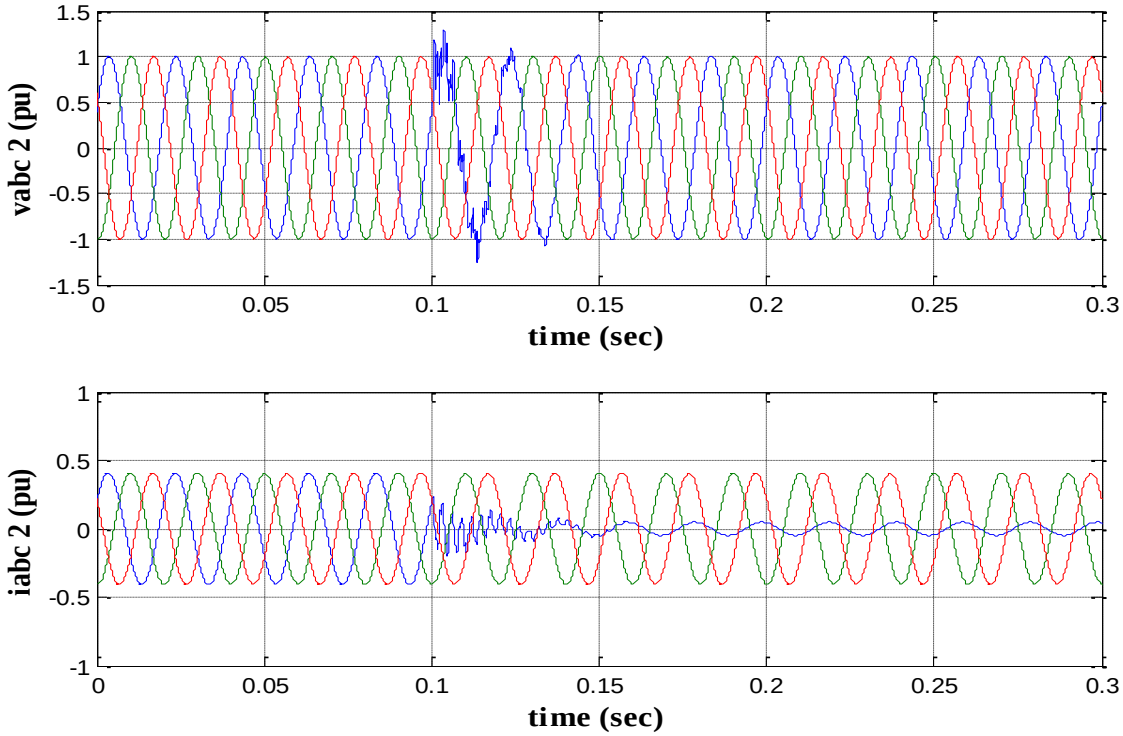

Figure 3.21 Voltages V_{abc2} and currents I_{abc2} of Ph_a-Gnd sc-side1

Identifying the right fault type, fault phase, and fault location by utilizing the neural network (Figs. 3.30, 3.31, and 3.32). Due to random changes in the current and voltage on both sides of the power line, always there is quick shifts or transients.

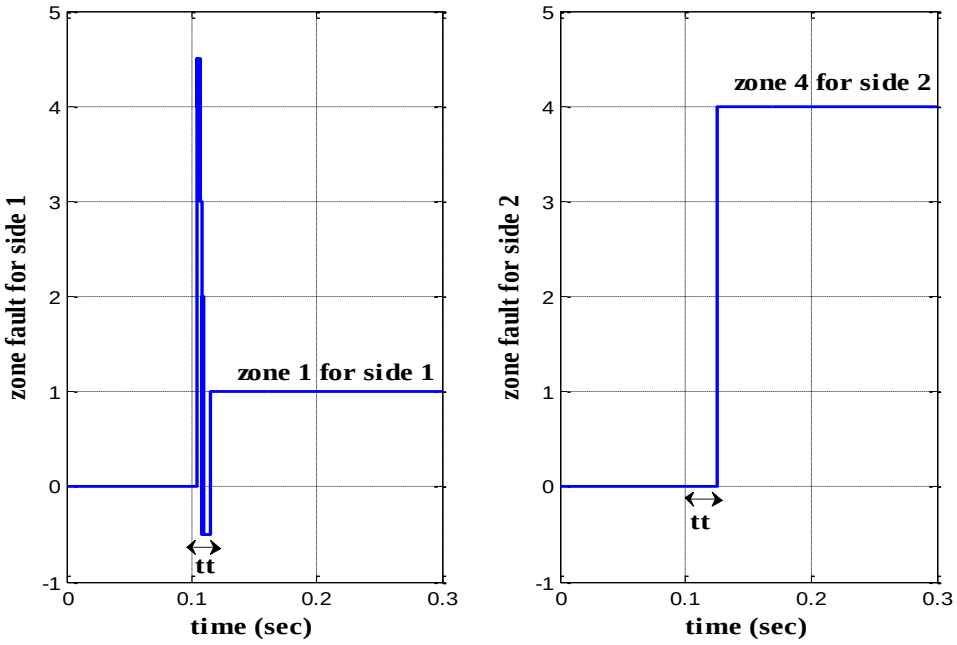

Figure 3.22 SC Ph_a-Gnd-Side1 fault zone detection

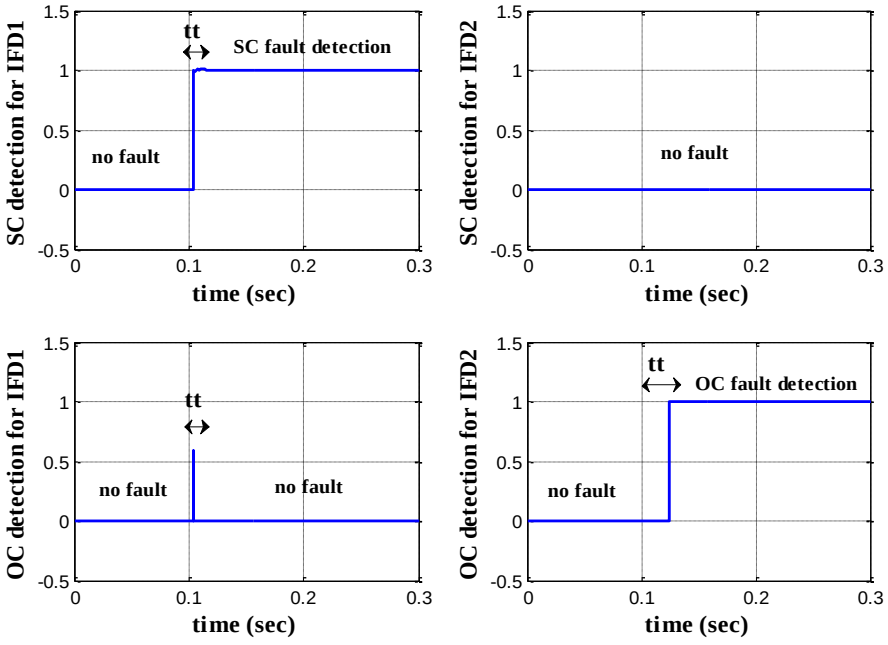

Figure 3.23 Identification of the fault type (SC-Side1 and OC-Side2)

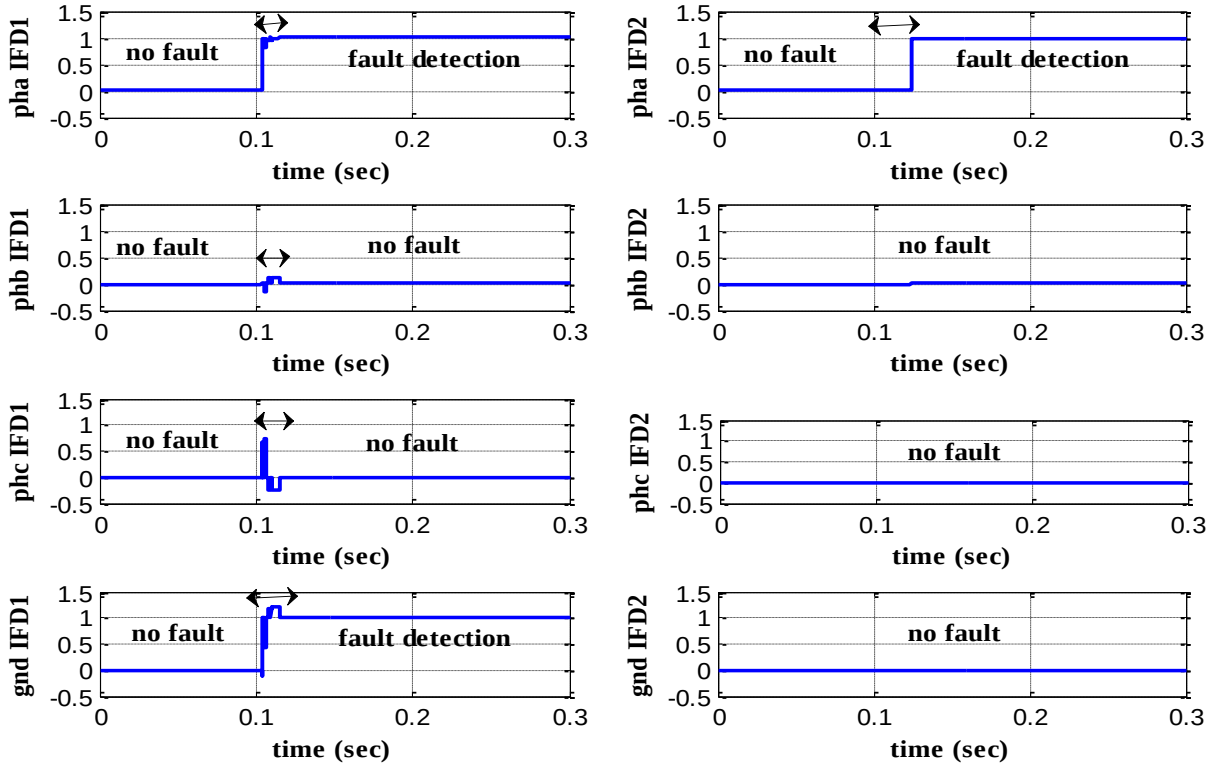

Figure 3.24 Identification of the fault phase (Ph_a-GND-Side1)

3.10.4 Short circuit fault in Pha-GND – Side 2

Now application of a short circuit in side 2 of the transmission line. The current on phase (a) at side 01 cancels out, and there is a brief transient voltage disturbance. Additionally, there was a notable rise in current and a small drop in voltage on Pha at side 02 (Figurs. 3.25 and 3.26).

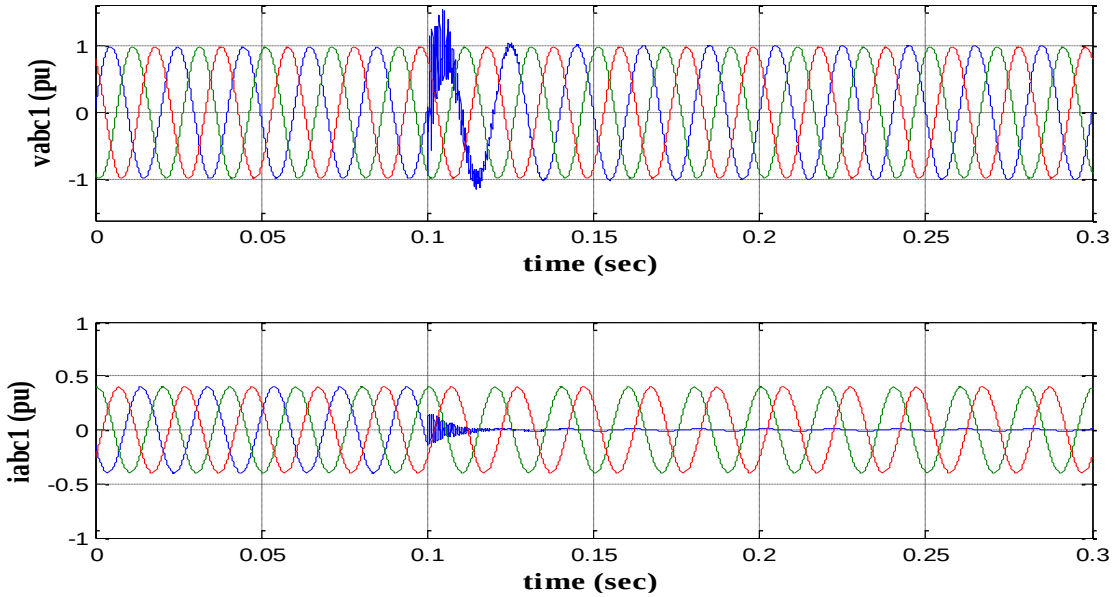

Figure 3.25 Voltages V_{abc1} and currents I_{abc1} of Ph_a-Gnd-Side2 during SC

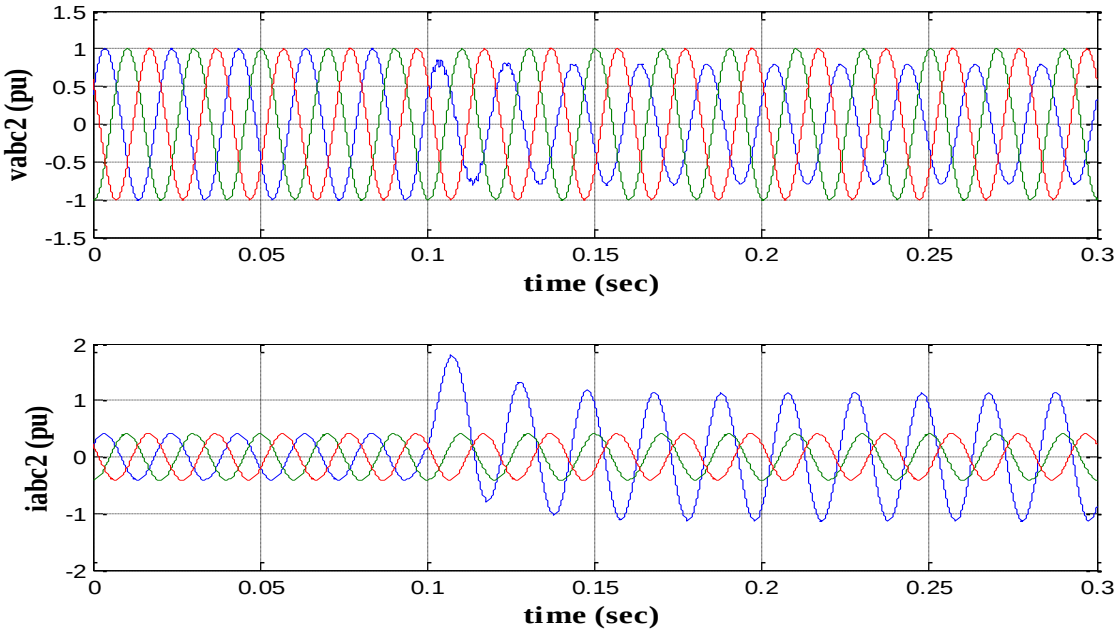

Figure 3.26 V_{abc2} and I_{abc2} of SC fault of Ph_a-Gnd-Side2

The implementation of ANN enables accurate fault location and identification with minor, transient variations: A short-circuit on phase (a) at side 2 is the cause of the fault in zone 1 when compared to IFD1 (Figs. 3.27, 28, 29, 30, 31 and 32).

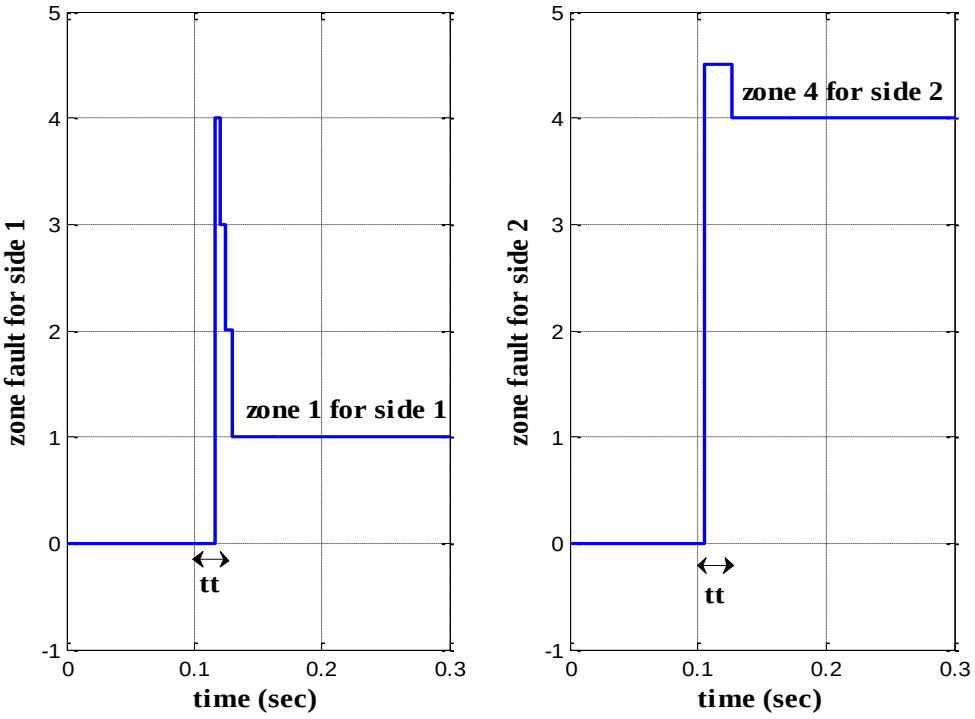

Figure 3.27 SC ph_a-Gnd-Side2 fault zone detection.

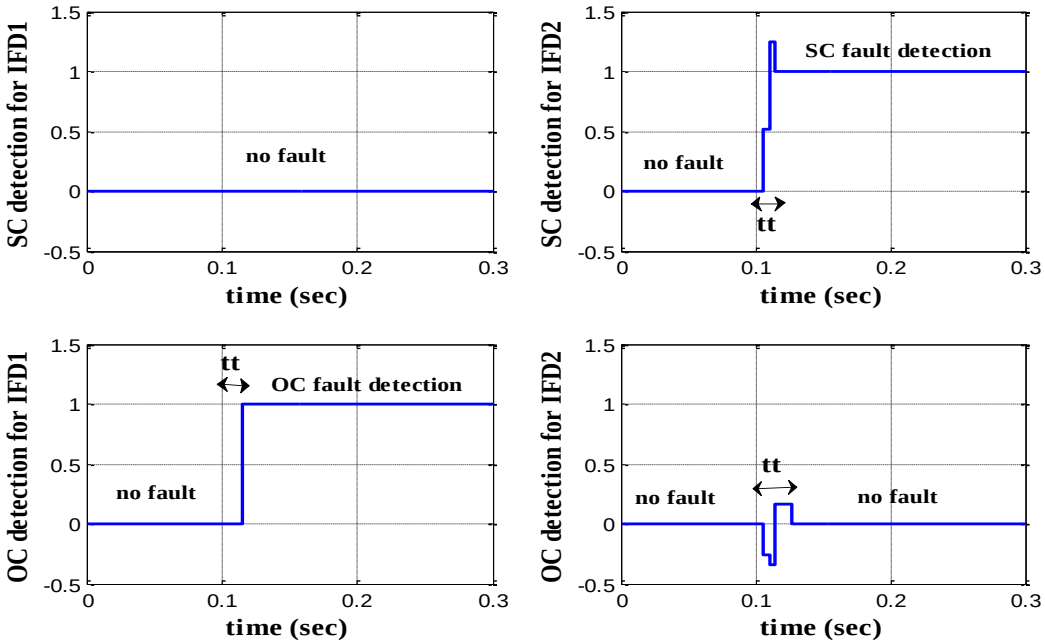

Figure 3.28 Identification of the fault type (OC to Side1 & SC to Side2).

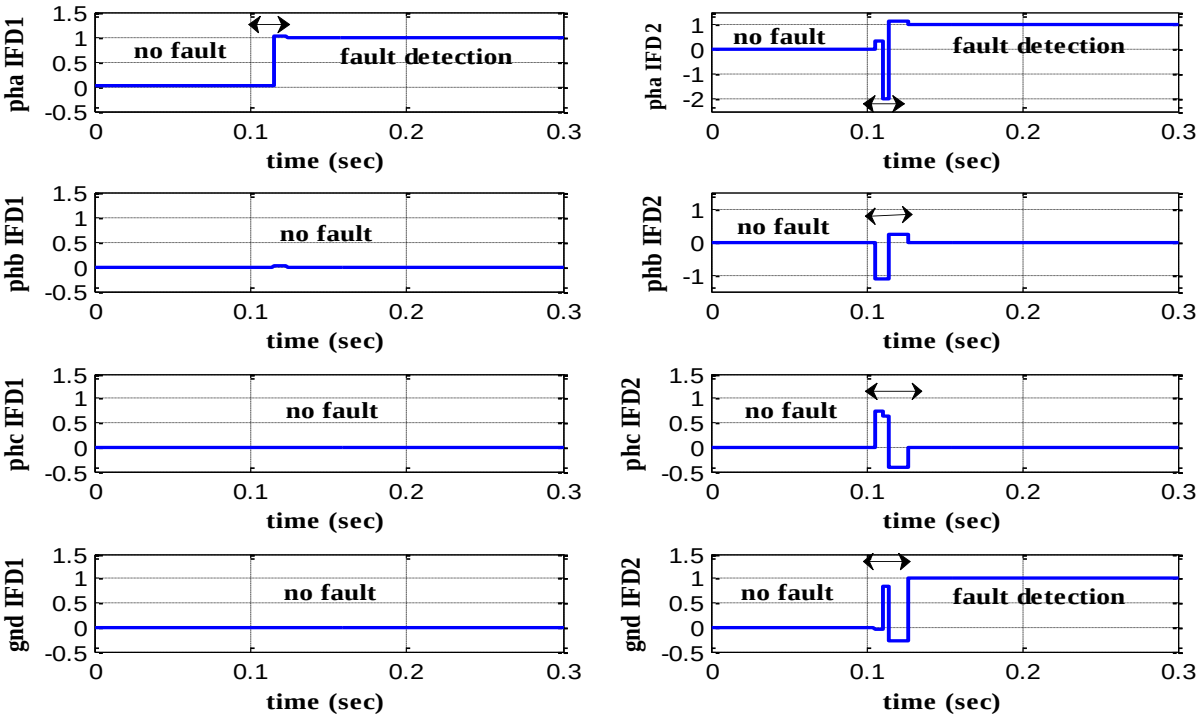

Figure 3.29 Identification of the fault phase (Ph_a-GND-Side2)

3.10.5 Open circuit fault in Pha

Figures 3.30 and 3.31 show simple voltage disturbances, then stability near the original values and a cancelling of the phase (a) currents on both sides as a result of the transmission line opening.

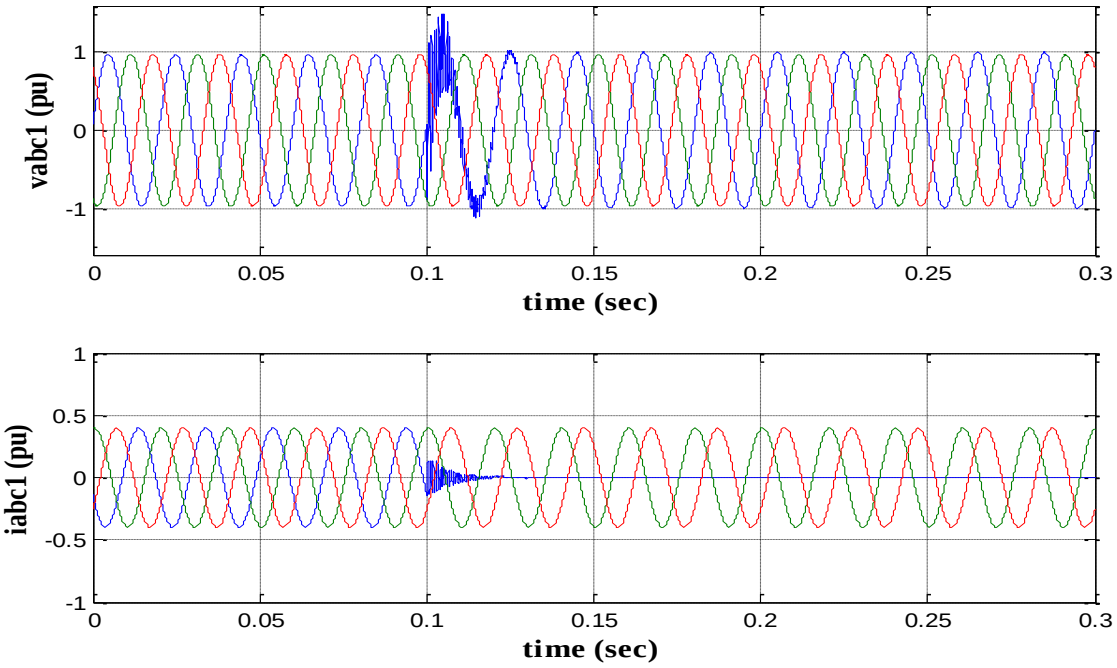

Figure 3.30 Voltages V_{abc1} and currents I_{abc1} of Pha during OC fault

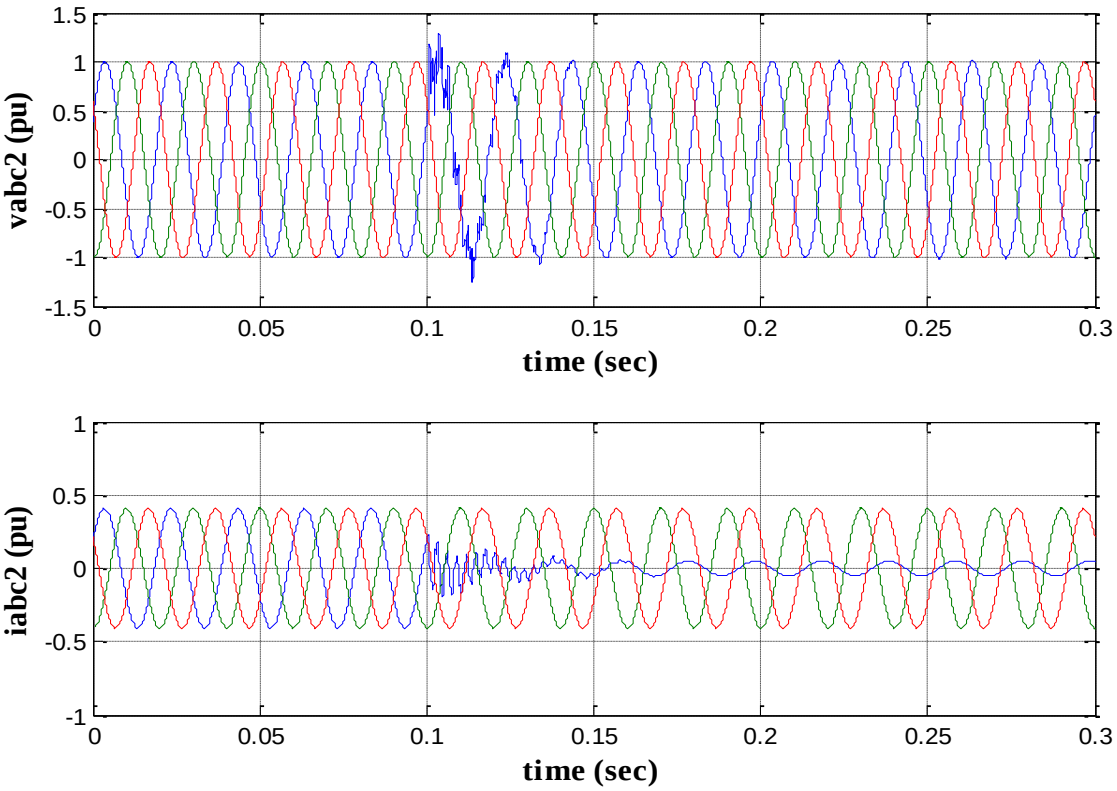

Figure 3.31 Voltages V_{abc1} and currents I_{abc1} of OC fault of Pha

As shown in (Figs 3.32, 3.33 and 3.34) the ANN was capable of identifying and signaling an open circuit fault in zone 1 phase (a).

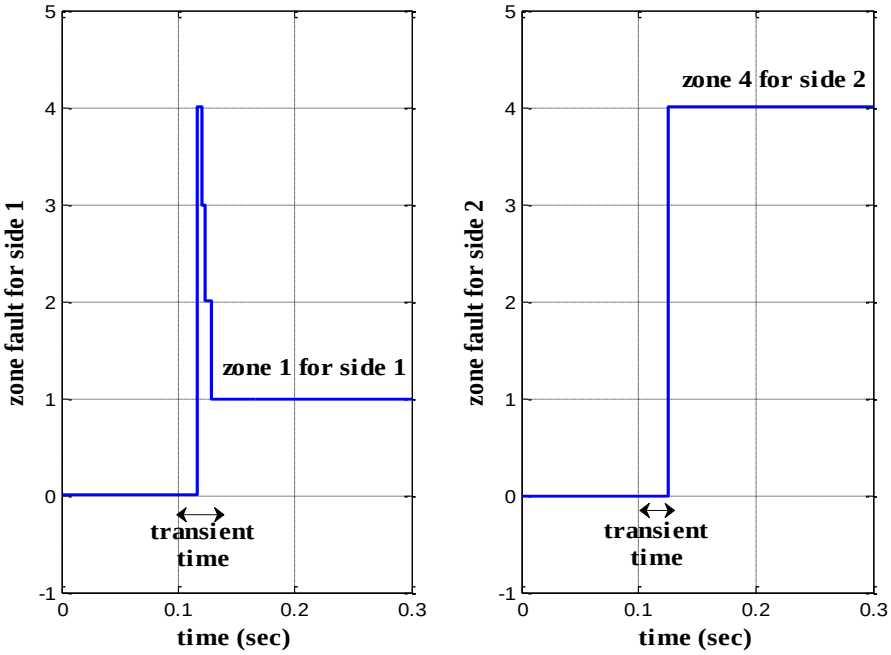

Figure 3.32 OC Pha fault zone detection

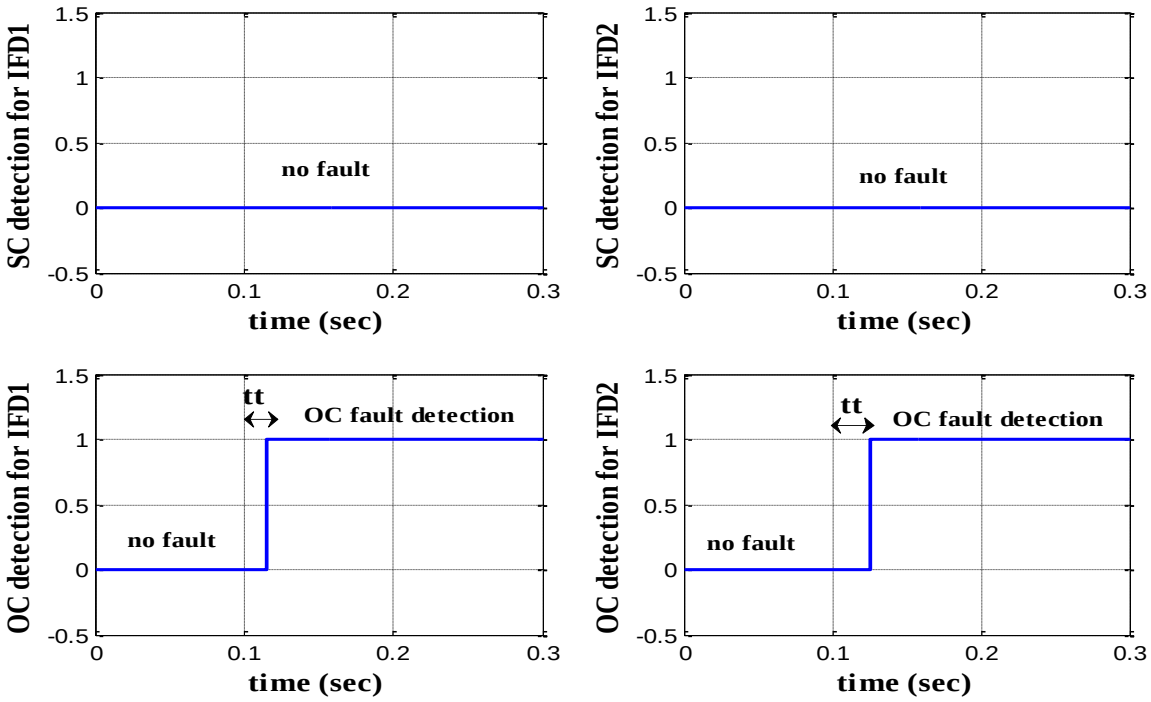

Figure 3.33 Identification of the fault type (OC-Side1 and OC-Side2)

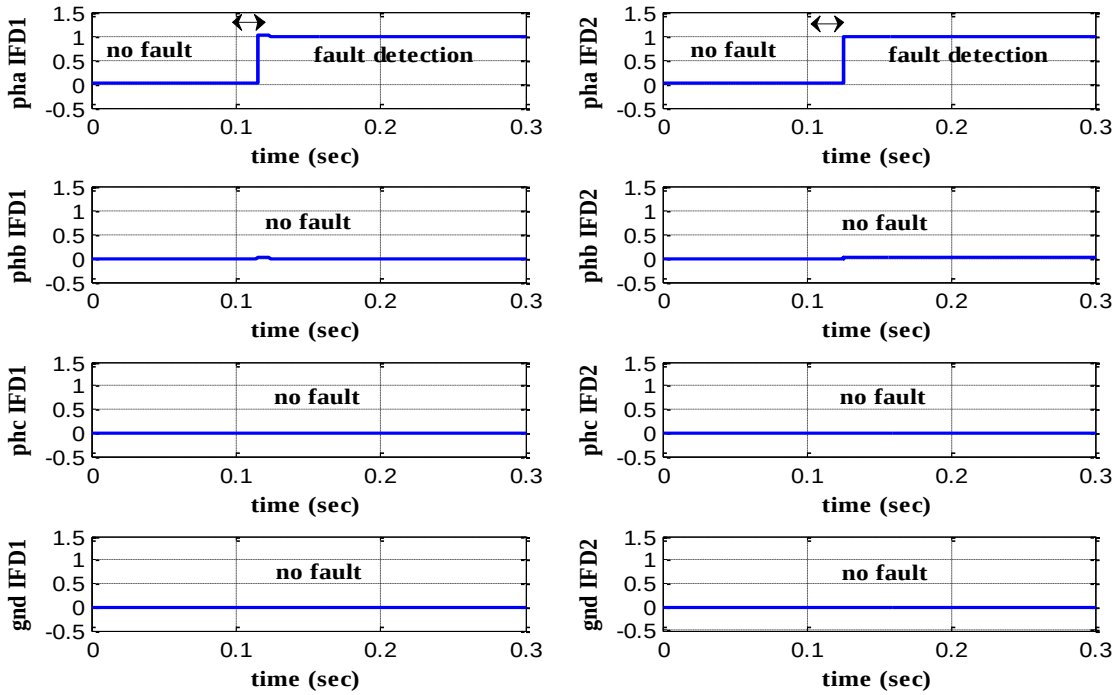

Figure 3.34 Identification of the fault phase (Pha)

3.10.6 Faults detection in zone 2

3.10.6.1 Short circuit fault in Pha-phb-GND

The ANN diagnosis method is put to the test using a variety of fault variations, a two-phase ground (LL-G) faults are used on both sides of transmission line. We can see in Figures 3.35 and 3.36 that the two sides of the transmission line have less voltage for two phases (a) and (b), and an rise in current for both phases (a) and (b) as a result of the short-circuit.

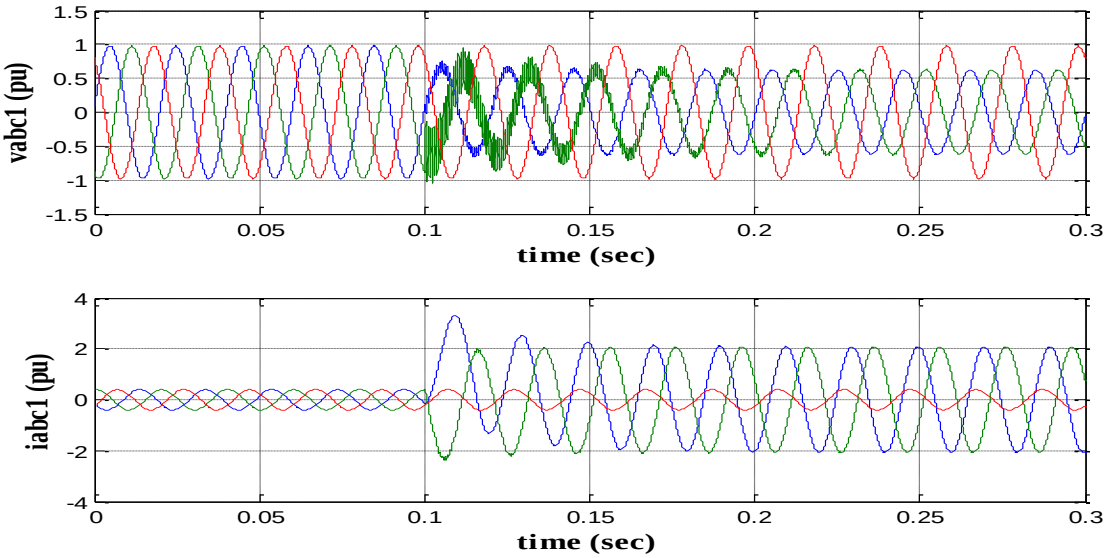

Figure 3.35 V_{abc1} and I_{abc1} of SC fault of Pha-Phb-Gnd

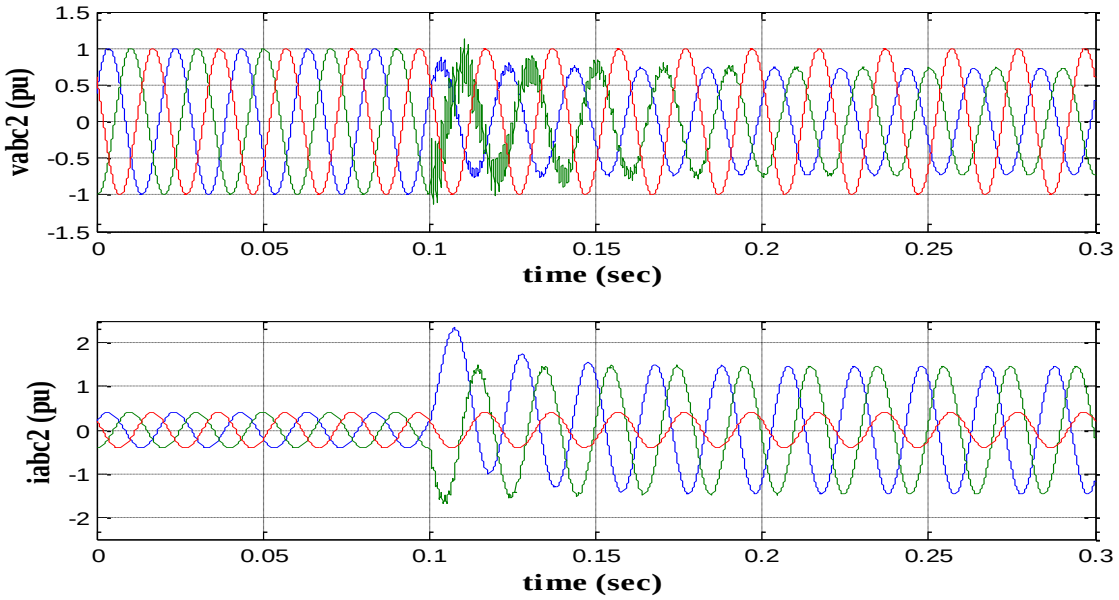

Figure 3.36 V_{abc2} and I_{abc2} with SC fault of Pha-Phb-Gnd

After applying the fault, the neural network was able to achieve roughly the same performance in terms of identification and localization, (significant transient regimes are observed).

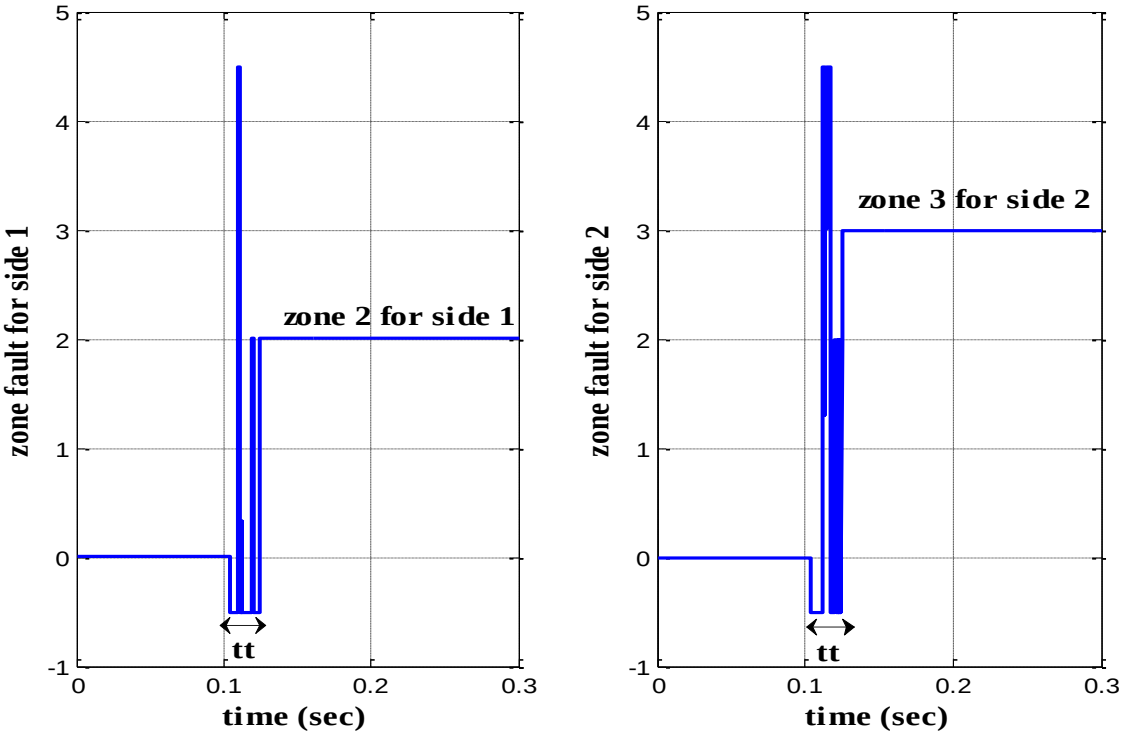

Figure 3.37 SC Pha-Phb-Gnd fault zone detection

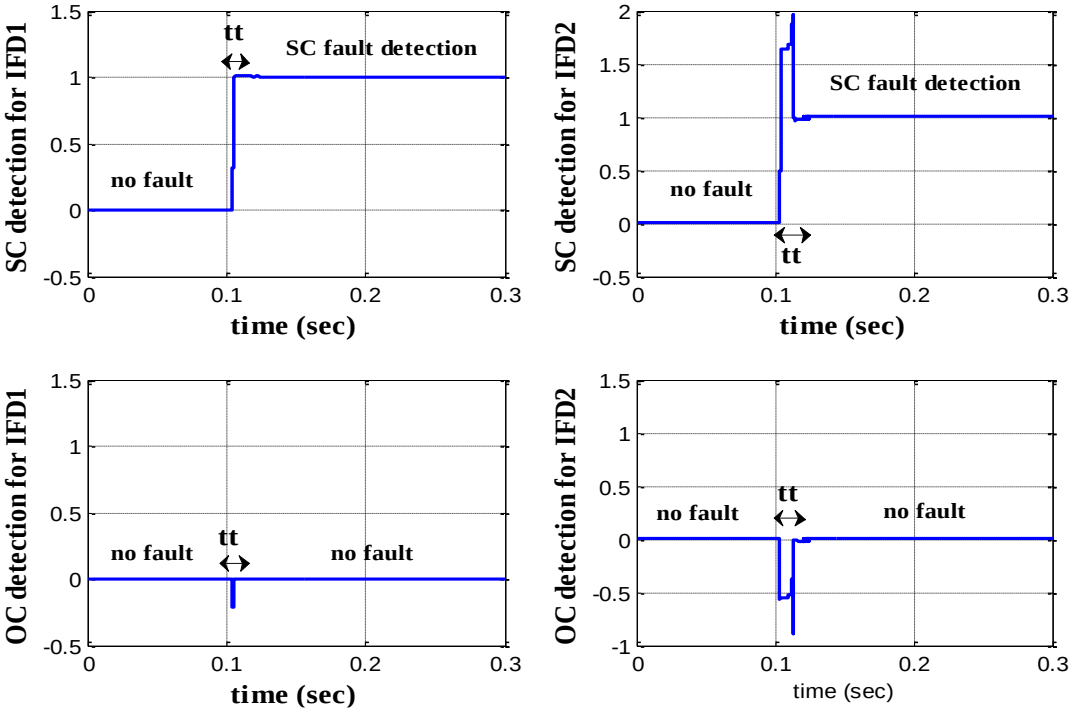

Figure 3.38 Identification of the fault type (SC-Side1 and SC-Side2)

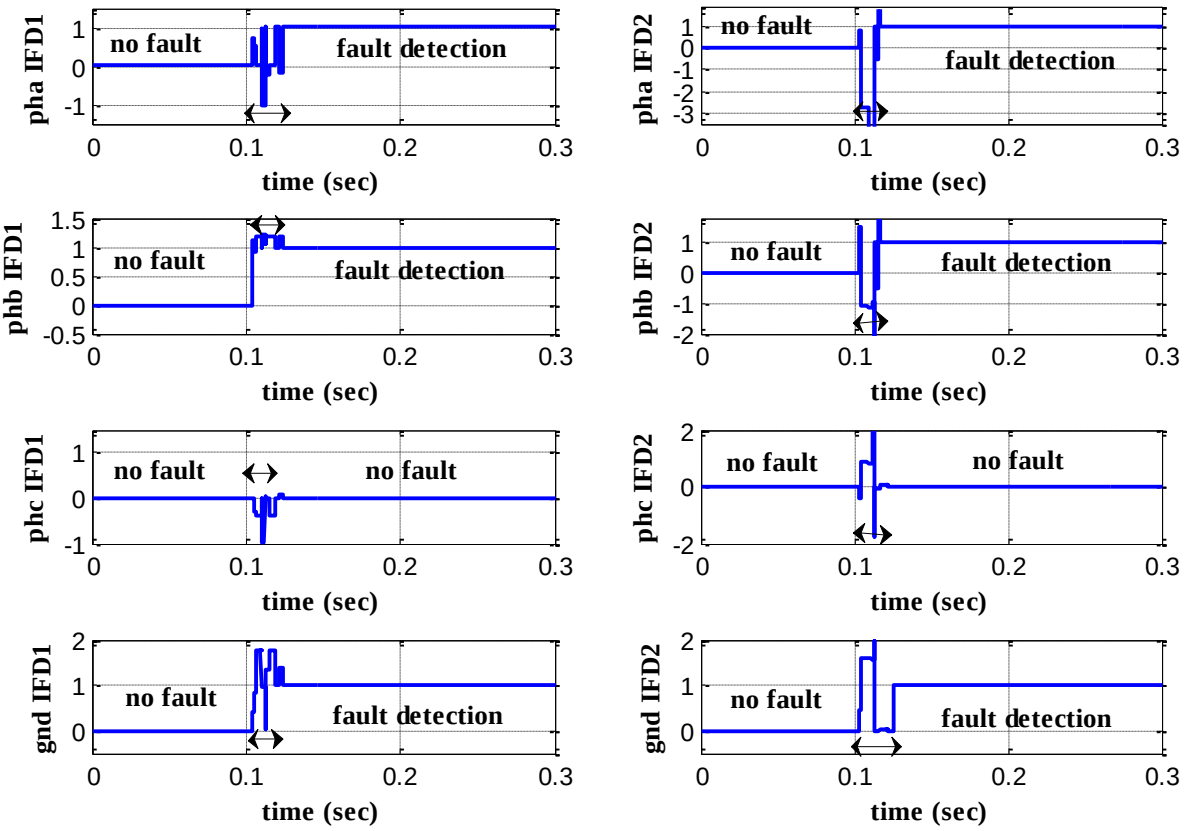

Figure 3.39 Identification of the fault phase (Pha-Phb-GND)

3.10.6.2 Short circuit fault Pha-phb-GND displacement at 15 km

As the same previous the identical fault type was used, but with a 15 km displacement towards side 2 (zone 2). We obtain practically the same variations of electrical characteristics with small drop in currents (in SC fault phases). The diagnostic method's neural network yields identical results to the earlier scenario in terms of detection, localization, and fault diagnosis performance (Figures 3.40 to 3.44).

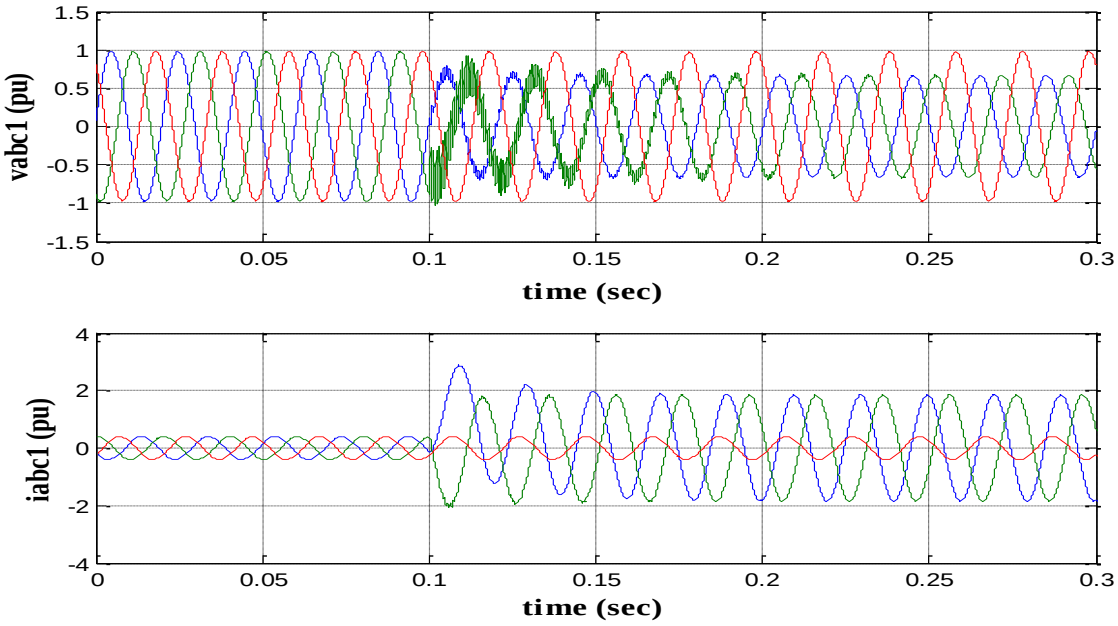

Figure 3.40 Voltages V_{abc1} and currents I_{abc1} of SC fault of Pha-Phb-Gnd (Fault at 15 km)

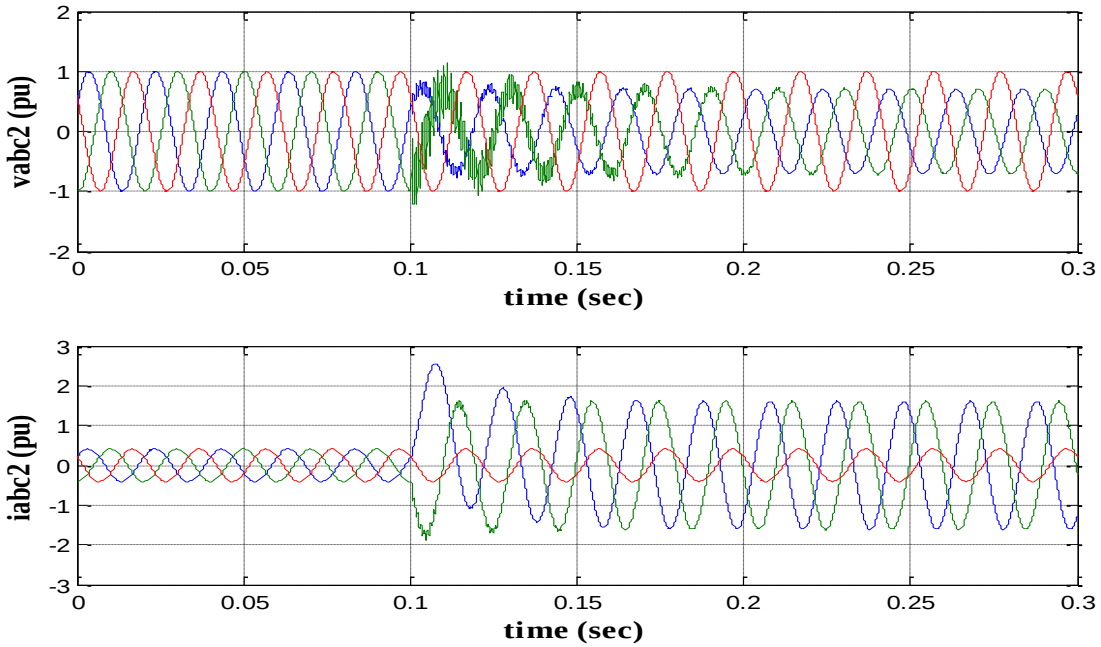

Figure 3.41 Voltages V_{abc2} and currents I_{abc2} of SC fault of Pha-Phb-GND (at 15 km).

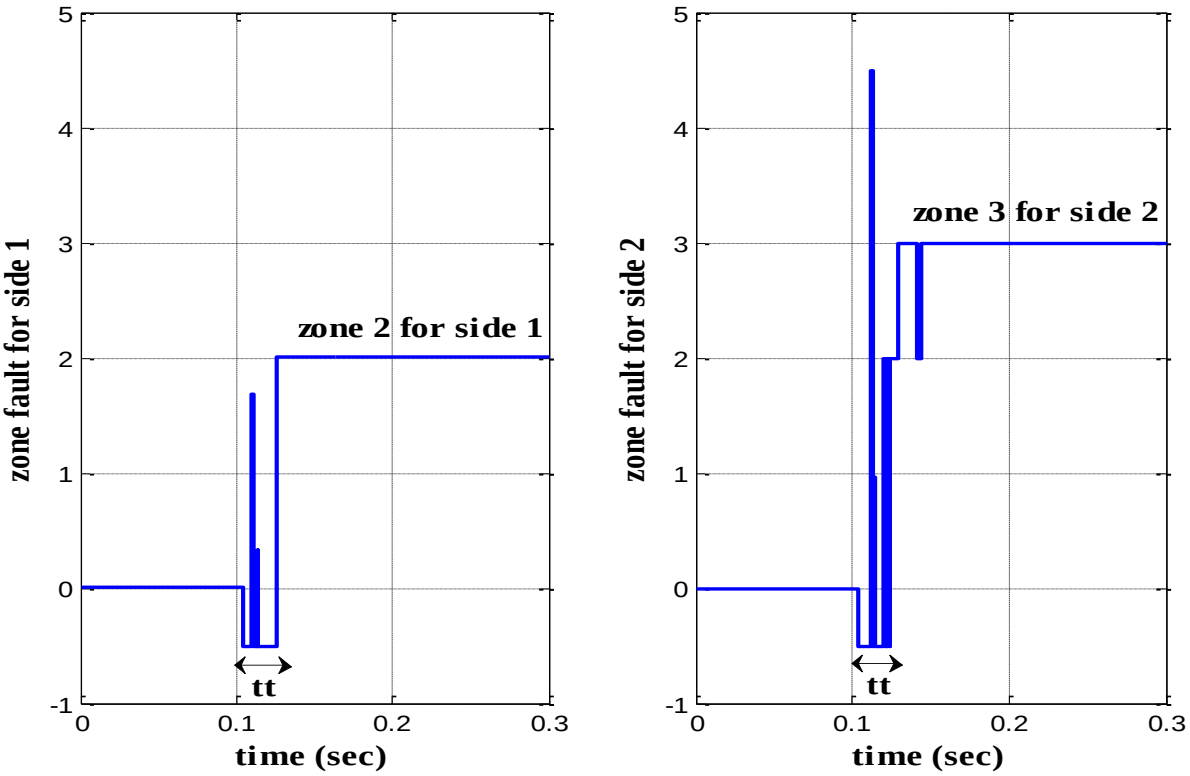

Figure 3.42 SC Pha-Phb-GND(Fault by15 km) fault zone detection.

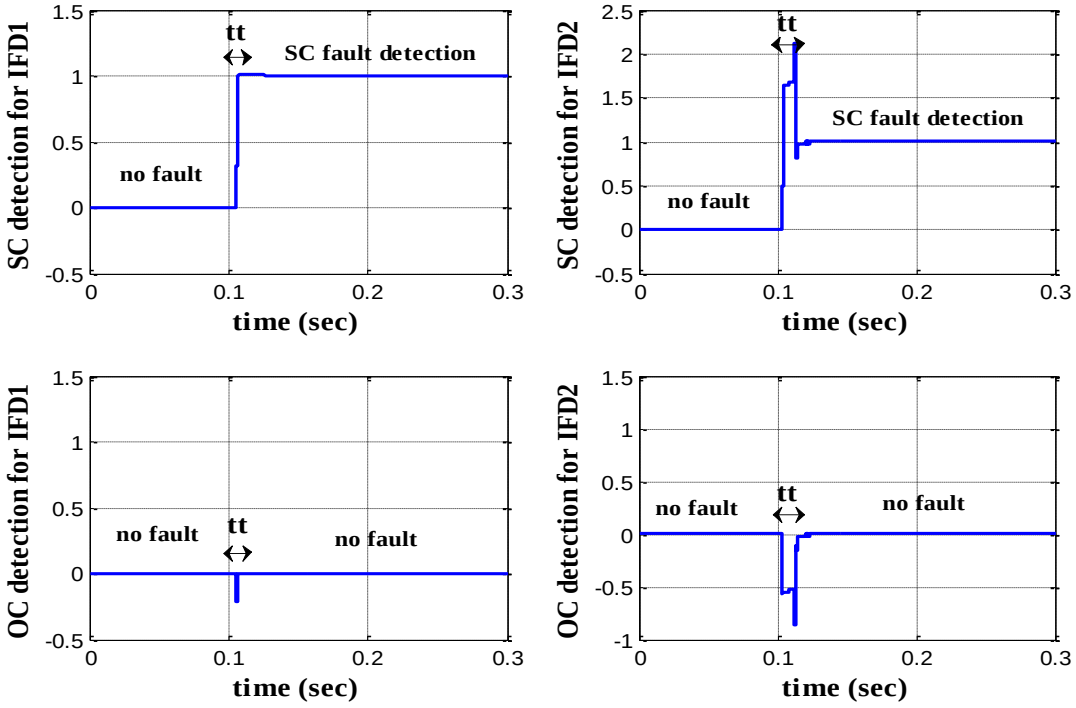

Figure 3.43 Faulty phase classification (SC-Side1 and SC-Side2): displacement by 15 km .

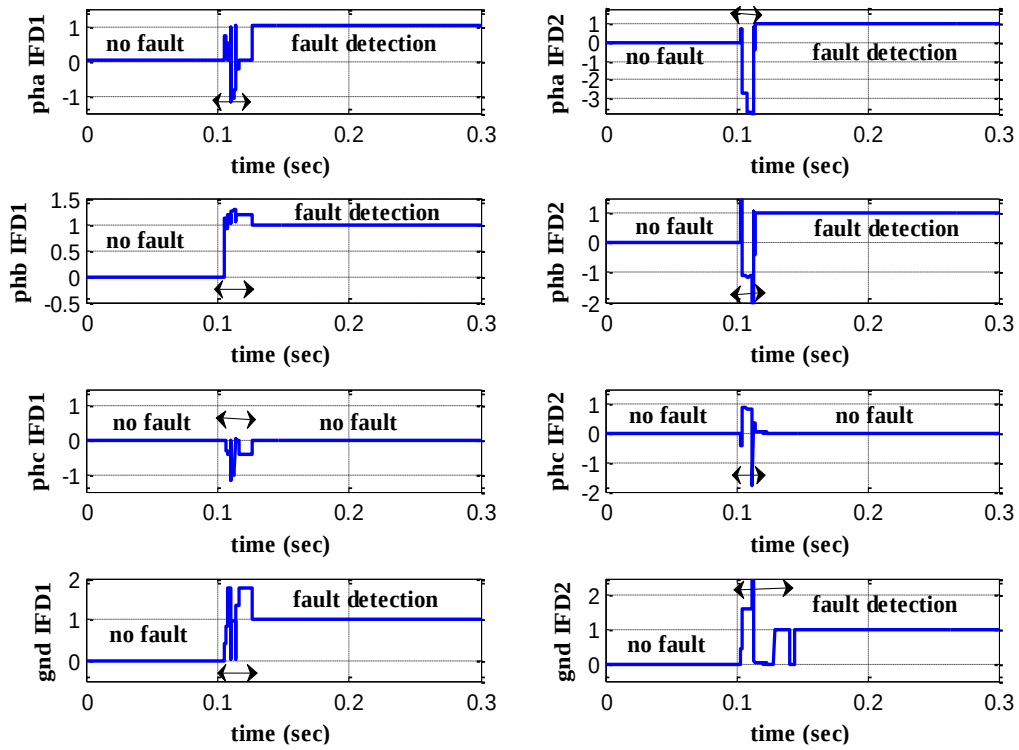

Figure 3.44 Identification of the fault phase (Pha-Phb-GND): displacement by 15 km.

3.10.7 Faults detection in zone 3

3.10.7.1 Short circuit fault in Pha-phb

The two phases (a) and (b) are now connected in a two-phase short circuit fault (drop of phase (a) on phase (b)), noticing an imbalance between the three voltage and current phases (Figs. 3.45 and 3.46).

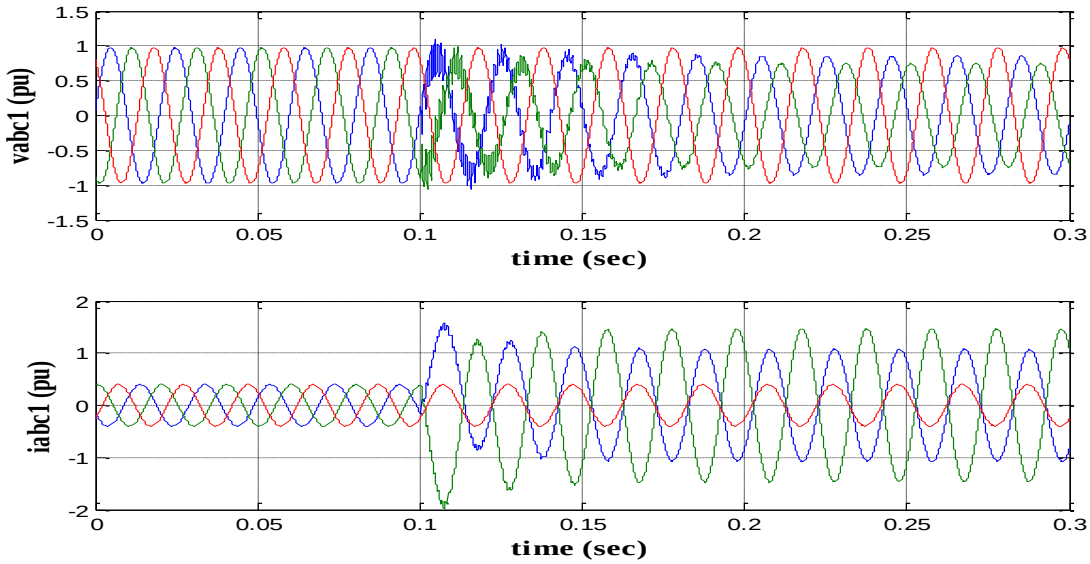

Figure 3.45 V_{abc1} and I_{abc1} of Pha-Phb during short-circuit

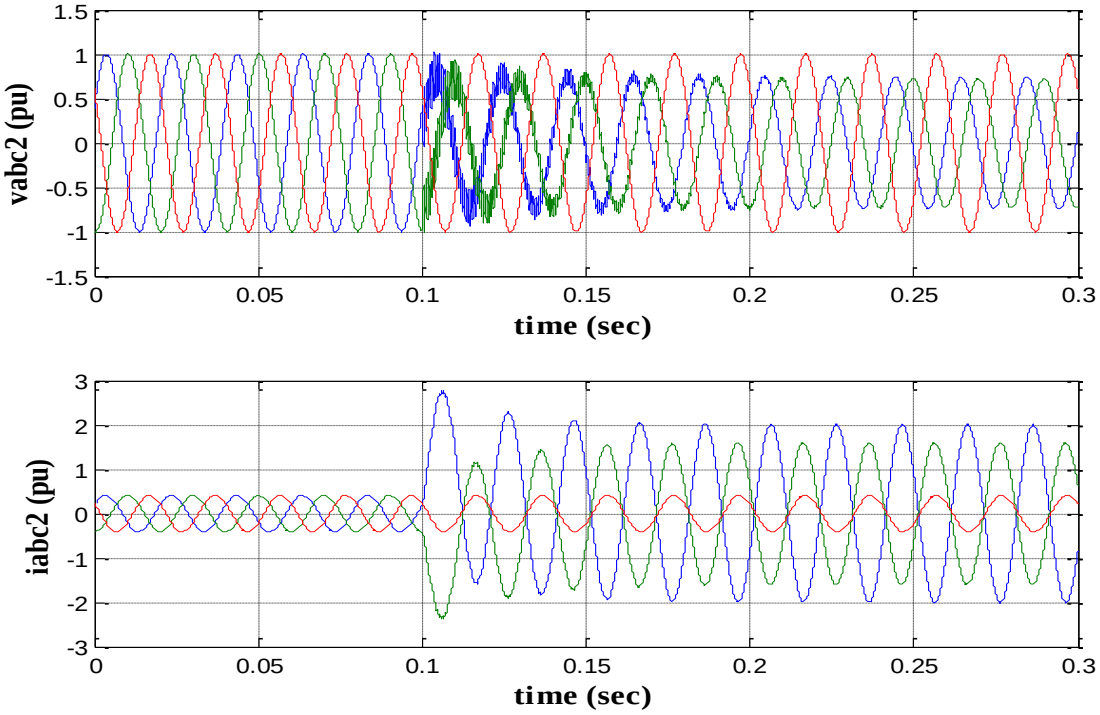

Figure 3.46 V_{abc2} and I_{abc2} of Pha-Phb during short-circuit

Noticing that, as indicated in figure 3.47, the neural network is able of identifying the short-circuit fault on phases (a) and (b) in zone 3 to side 1 point of view.

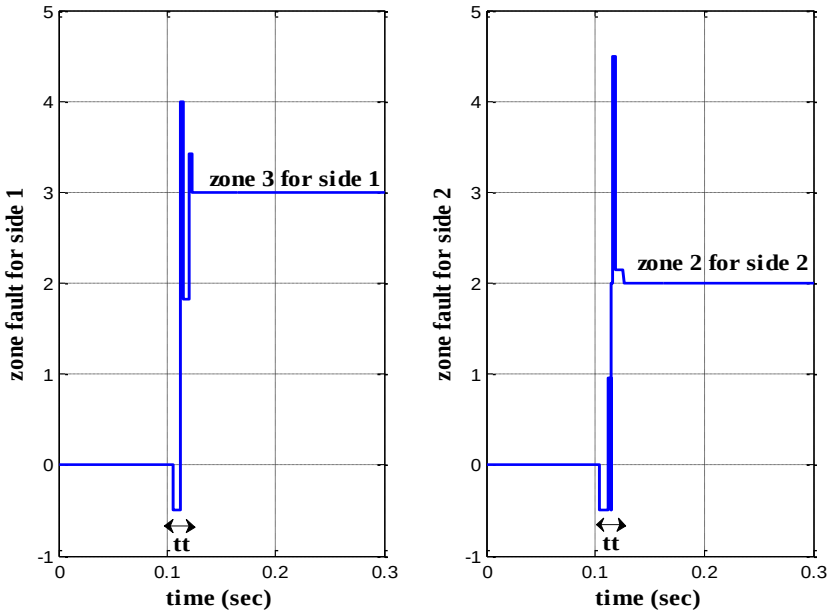

Figure 3.47 SC Pha-Phb fault zone detection

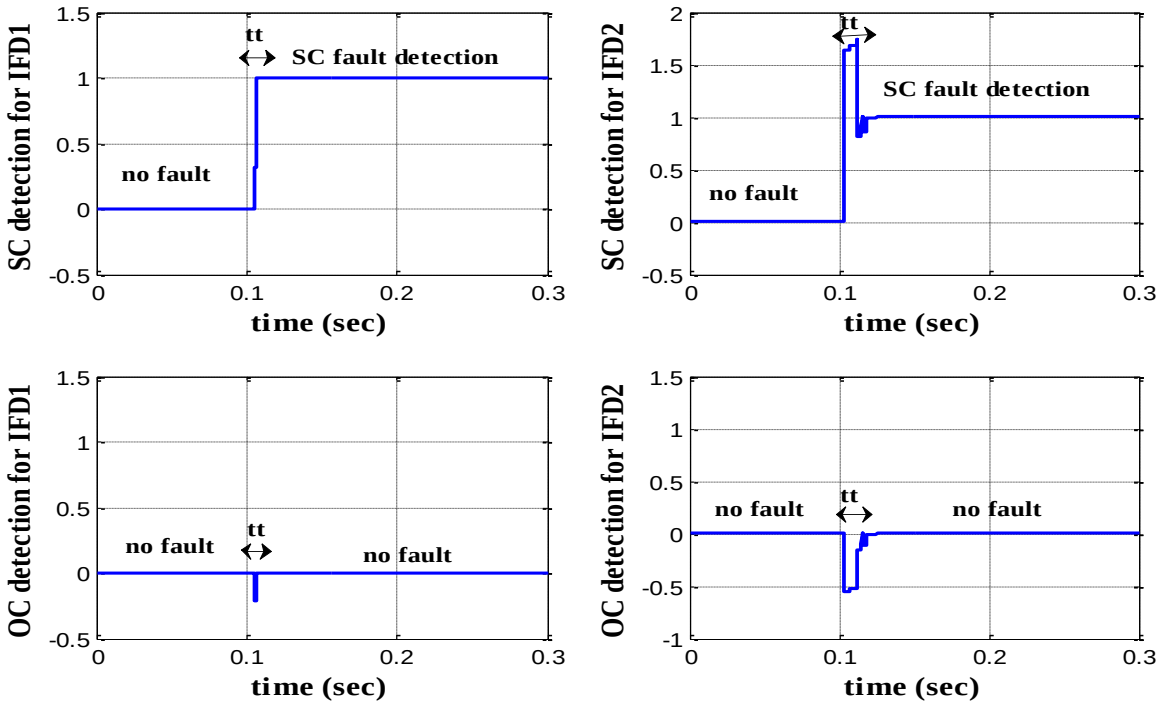

Figure 3.48 Identification of the fault type (SC-Side1 and SC-Side2)

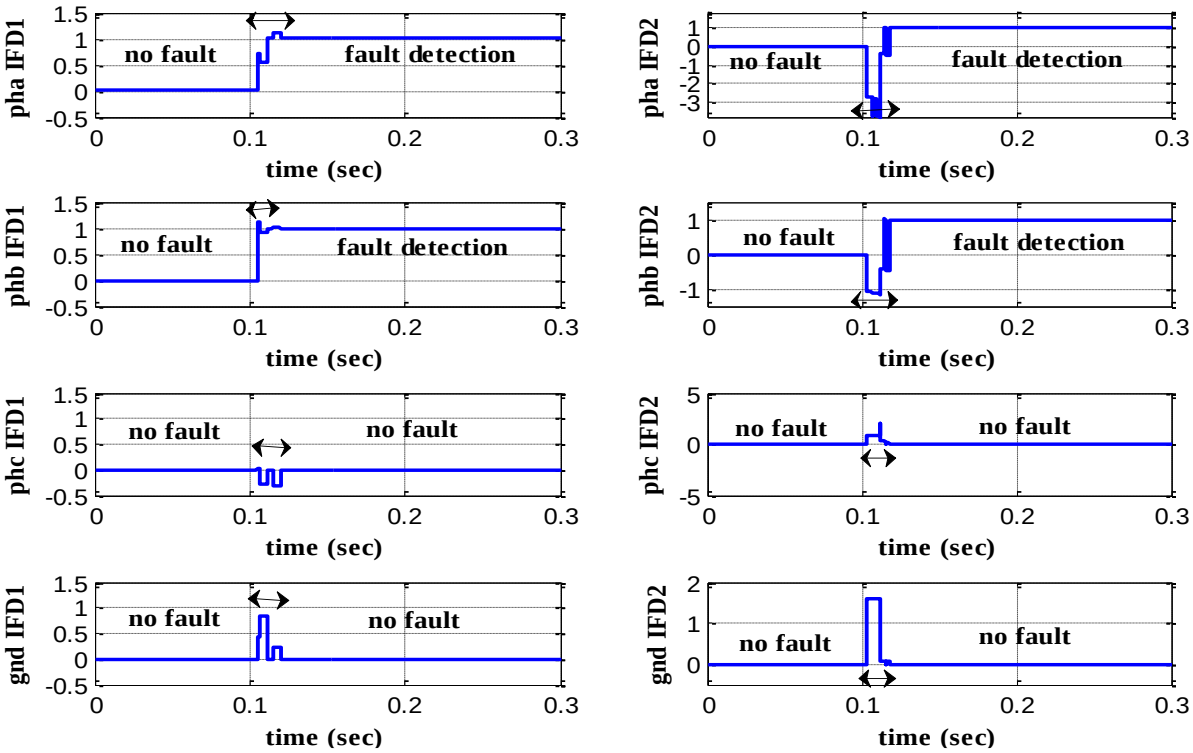

Figure 3.49 Identification of the fault phase (Pha-Phb)

3.10.8 Robustness test

Two tests are used to assess the robustness of the ANN method:

- Variations in source 2's voltage phase shift angle (from 27° to 10°)
- Variations in the fault resistance (from 0° to 15°).

3.10.8.1 Resistant short circuit fault (at 15 Ω) in zone2 (pha-GND-Side1)

The same fault type as in section "3.10.1" is applied in zone 2 on side 1 (single phase LG), but with a resistance of 15 Ω. The variation in the behavior of the voltages and currents is shown in Figures 3.50 and 3.51. the ANN method also was able to locate and identify the fault correctly as the same when the fault resistance was zero 0 Ω as shown in figs 3.52,3.53 and 3.54.

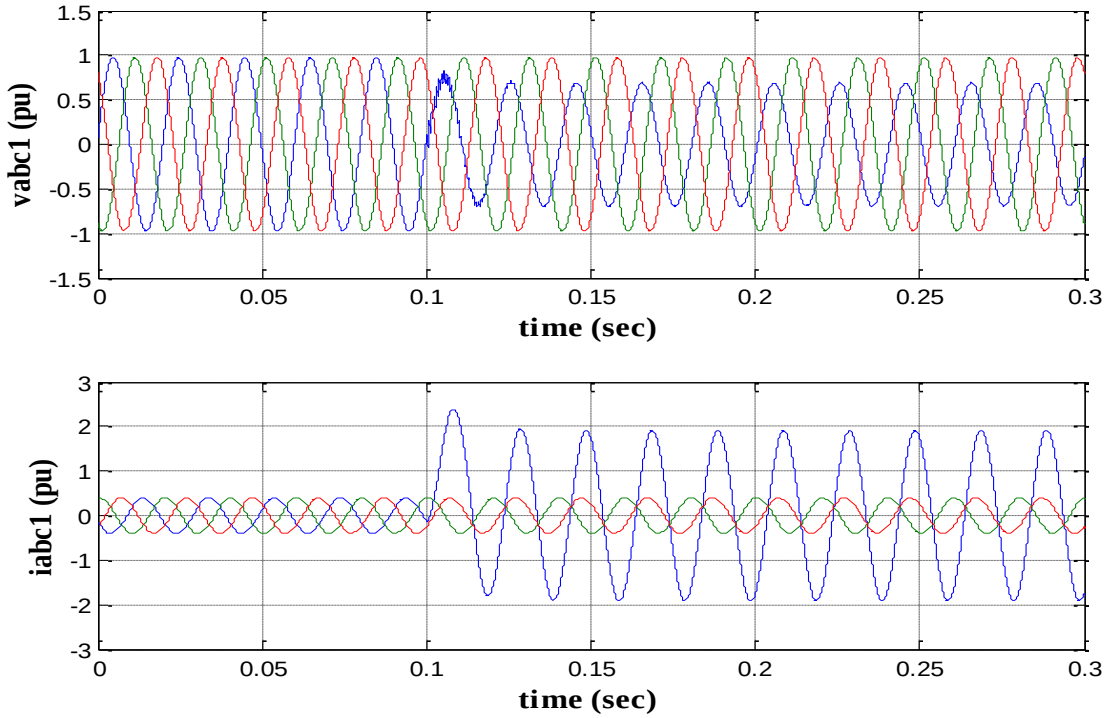

Figure 3.50 V_{abc1} and I_{abc1} of SC fault (at 15 Ω) of Ph_a-Gnd-Side1

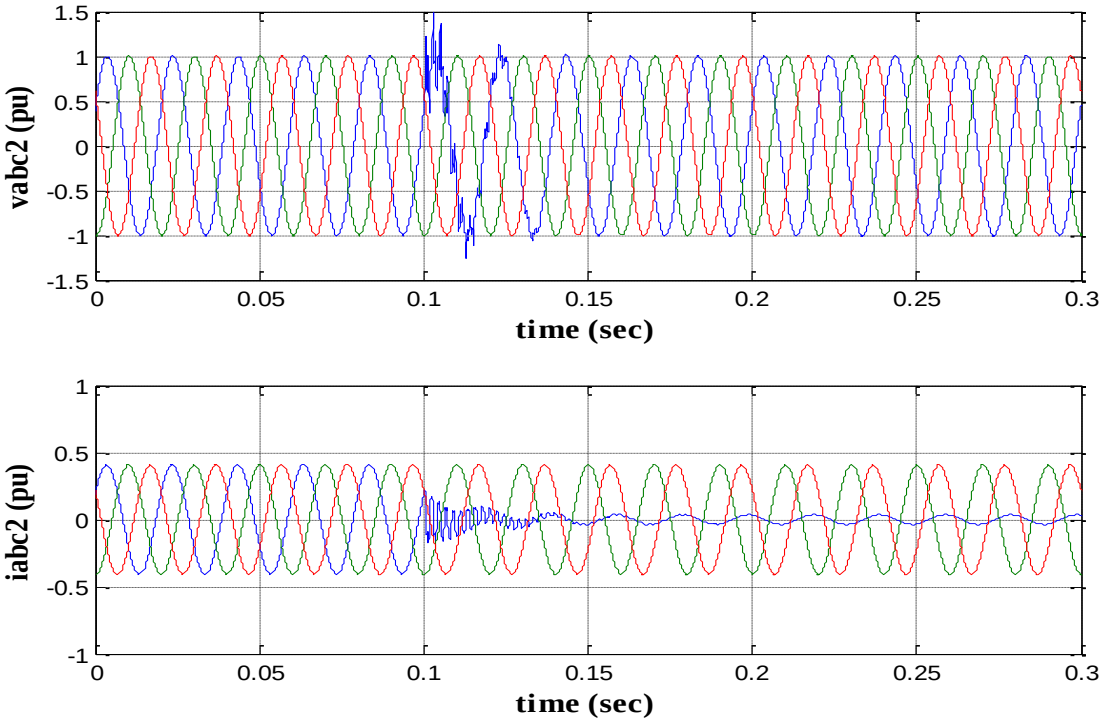

Figure 3.51 Voltages V_{abc2} and currents I_{abc2} of SC fault (at 15 Ω) of Pha-Gnd-Side1

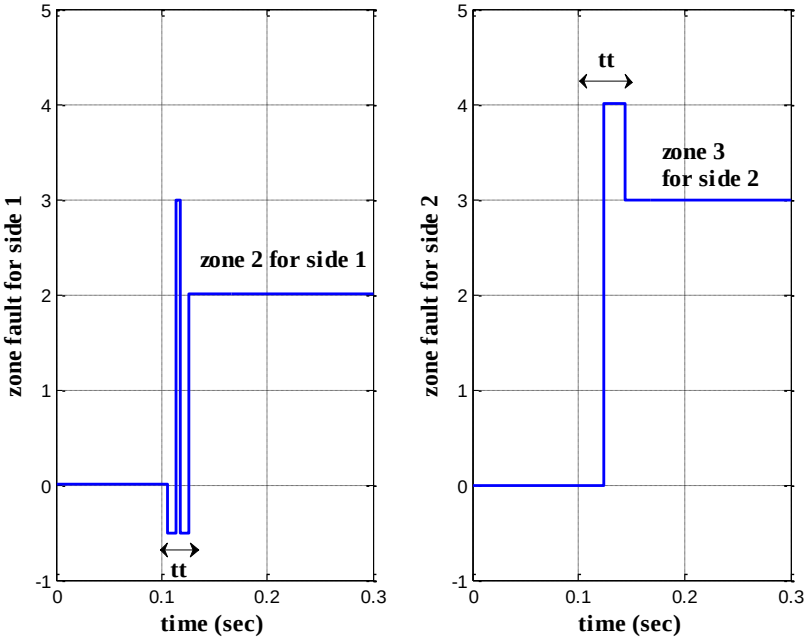

Figure 3.52 SC Pha-Gnd-Side1 (15 Ω) fault zone detection

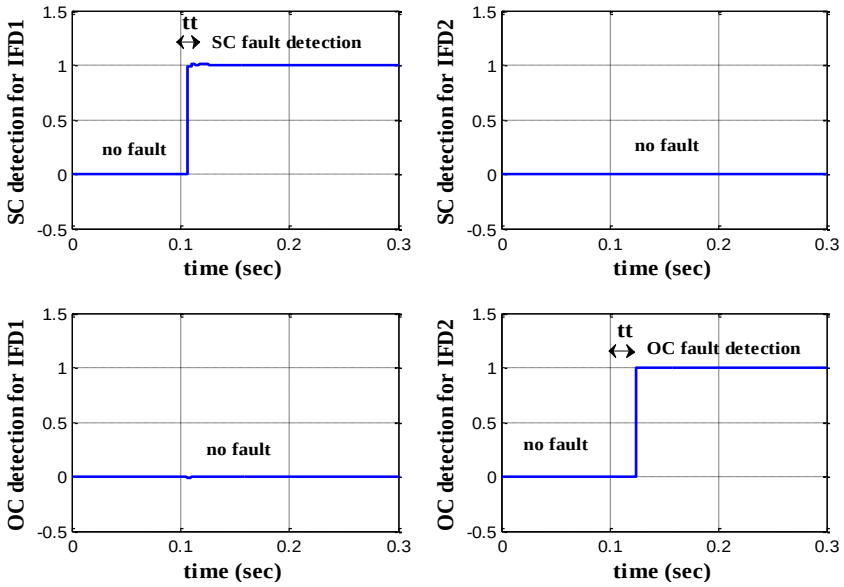

Figure 3.53 Fault type identification (SC-Side1 and OC-Side2): resistance variation by 15 Ω

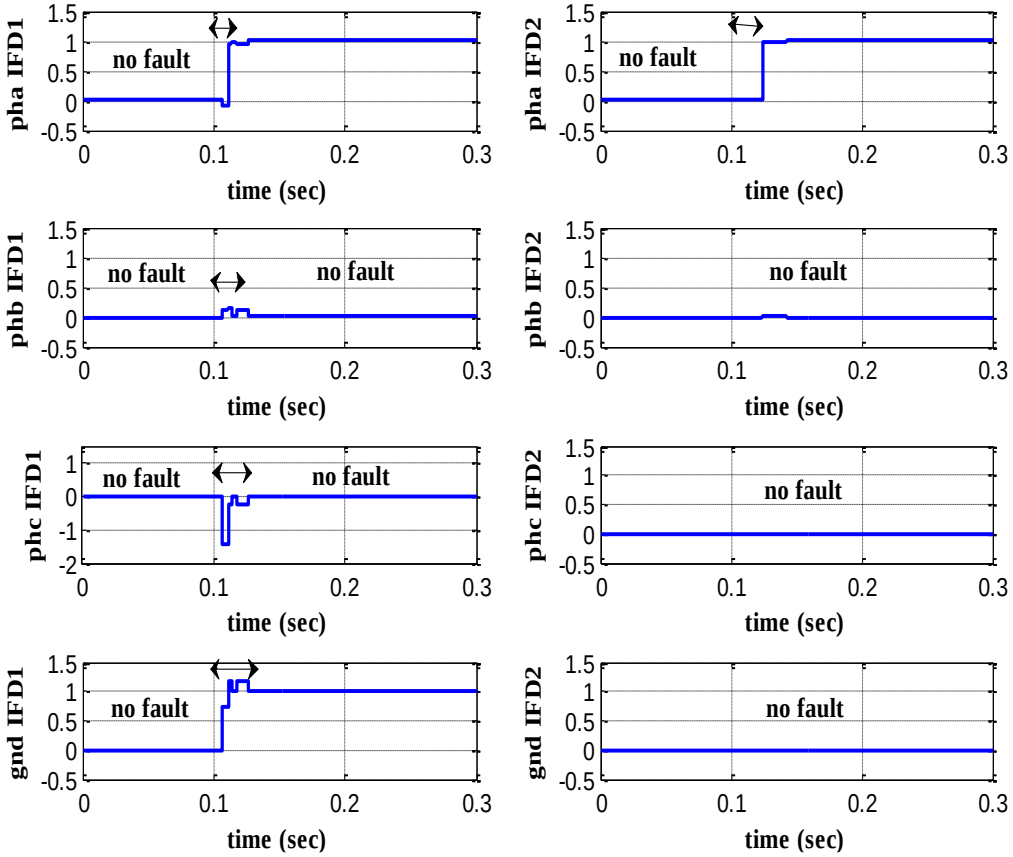

Figure 3.54 Faulty phase classification (Pha-GND-Side1): resistance variation by 15 Ω

3.10.8.2 Short circuit fault Pha–GND (zone 2) with load variation of power network (Angle variation from 27º to 10º)

By shifting source 2's voltage phase angle from 27º to 10º, further disturbance has been added in form of a change in the load or the amount of power being delivered by the transmission line. We see a rise in current and a drop in phase (a) voltage on side 1, as well as the cancellation of phase (a) current without a change in voltage as a result of the line opening at the fault location on side 2 (figures 3.59 and 3.60).

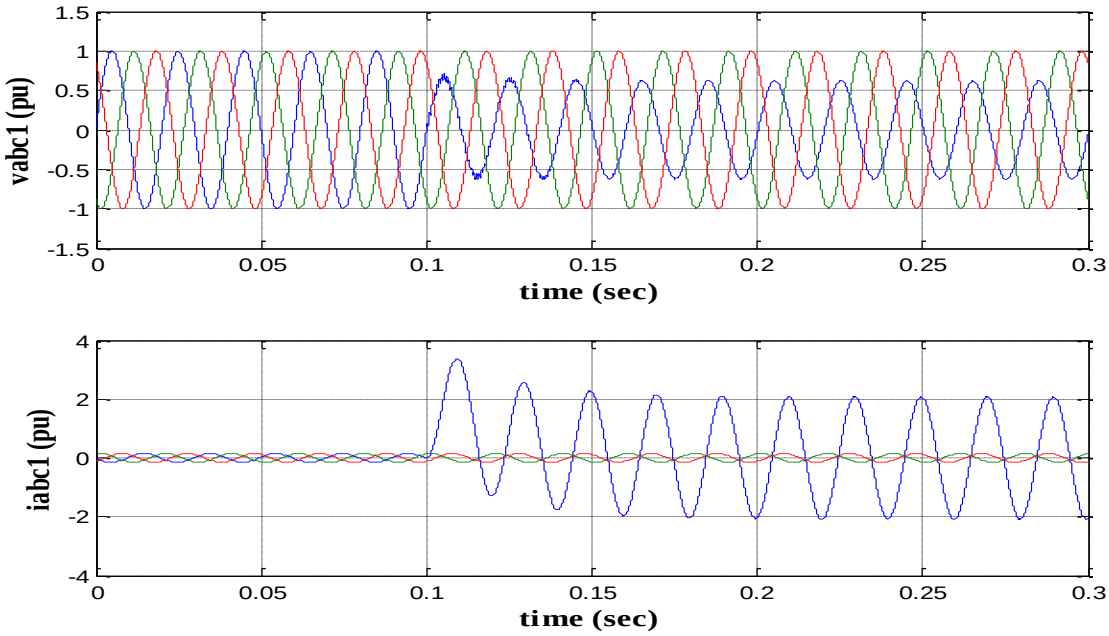

Figure 3.55 V_{abc1} and I_{abc1} of Pha during of short-circuit with load variation (side 1)

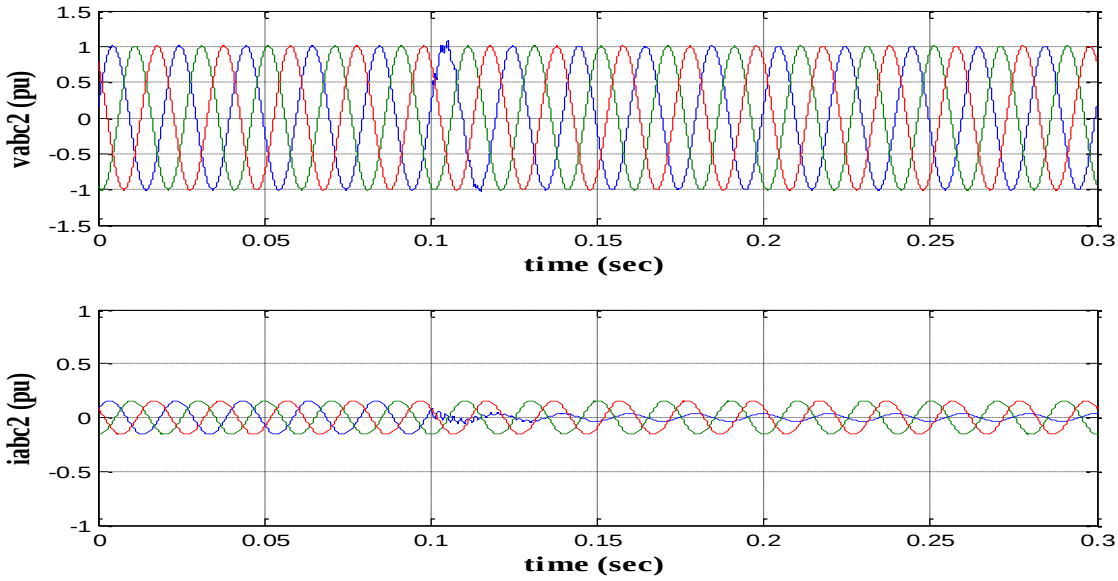

Figure 3.56 V_{abc1} and I_{abc1} of Pha during of short-circuit with load variation (side 2)

Similar performances are seen at the same transient durations for the neural network's signaling characteristics. (See figures 3.57, 3.58 and 3.59).

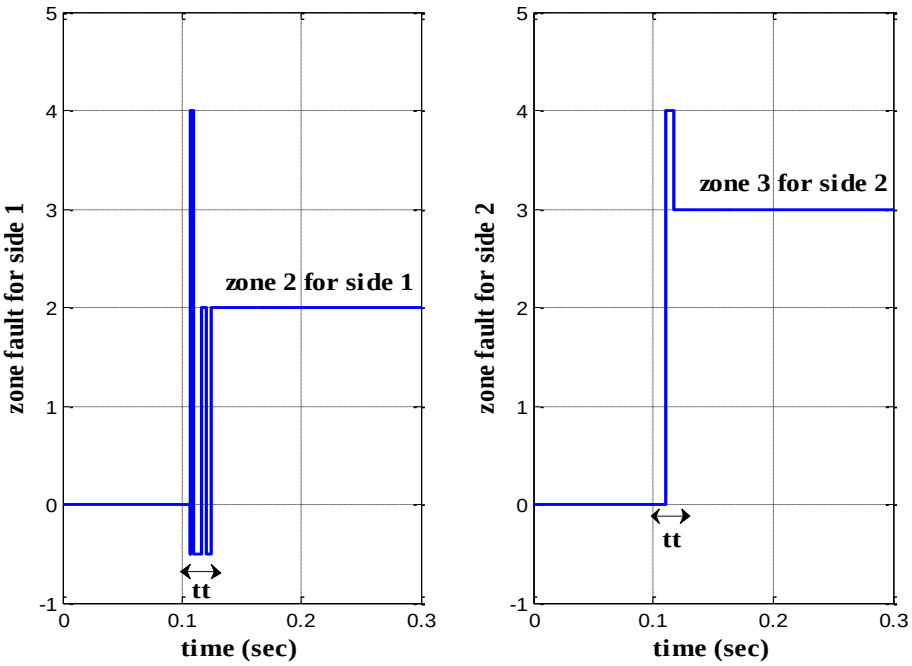

Figure 3.57 SC Ph_a-Gnd-Side1 (load variation) fault zone detection

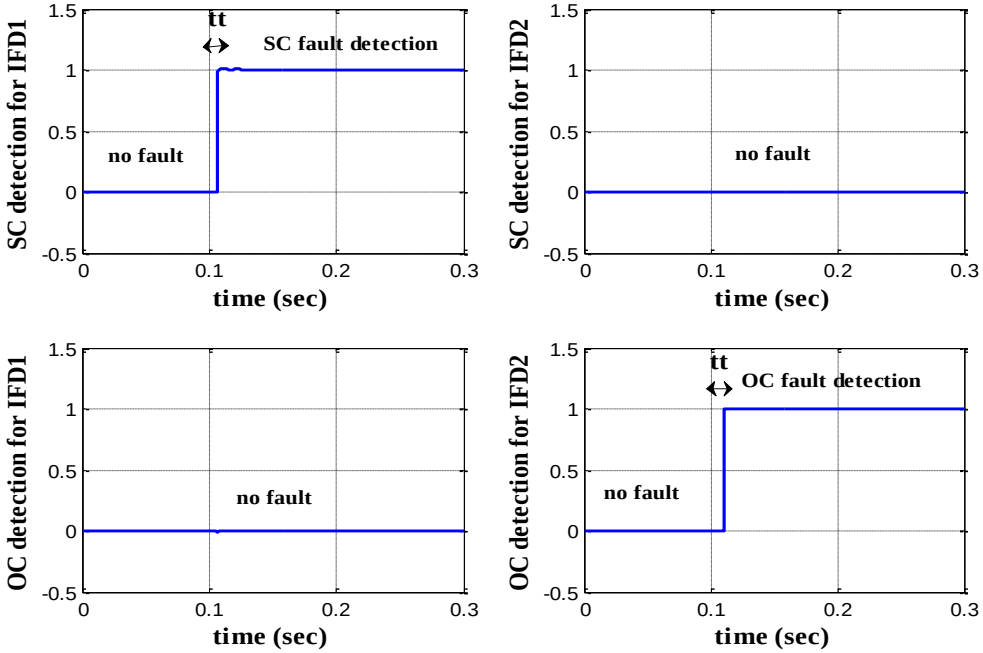

Figure 3.58 Identification of the fault type (SC-Side1 and OC-Side2) with load variation

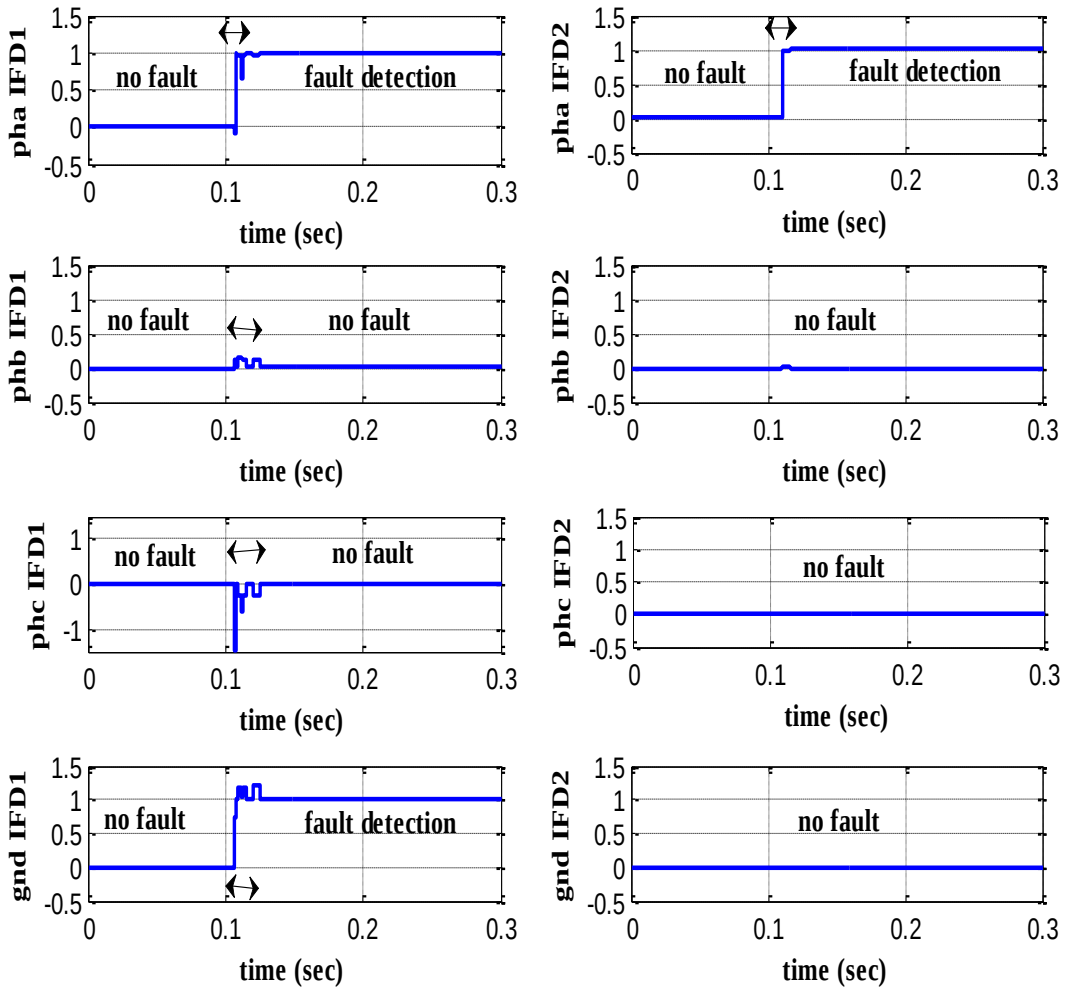

Figure 3.59 Identification of the fault phase (Pha-GND-Side1) with load variation

3.11 Conclusion

In this chapter, we've presented how to use artificial neural networks (ANNs) to locate, classify, and locate power transmission line faults. The measurement equipment at the transmission line's two ends produced three-phase voltage and current signals. The proposed method does not require complex feature extraction because it operates directly on the amplitudes of these signals., this method has the significant benefit of minimizing the computation time and optimizing the performance. Results indicate that this technique can complete the three tasks of fault localization, classification, and detection in less than 20ms after the fault occurs, and classifies faults accurately for all fault types. The accuracy was evaluated by simulating the same test system as chapter two. It was put through testing under various conditions, including various fault types, variations in fault resistance, and load phase angle. The results were very encouraging, showing that the system is accurate, fast (response time 20 ms, which is less than the protection

tripping time 200 ms), and reliable (the fault zone is well determined when the fault occurs on the zone's boundaries and covers a broad range of fault resistance). additionally, it has the benefit of high generalizability as it can be quickly implemented at any power grid.

Next chapter presents the implementation of another intelligent method where the fuzzy logic method was used in the same power system to compare its performance with the artificial neural networks ANN.

Chapter 4: Transmission Line Fault Diagnosis using Fuzzy Logic

4.1 Introduction

The applications of fuzzy logic are extremely numerous and varied [93]. Within the framework of monitoring and diagnosis, there are mainly expert systems. In these different contexts (in this case diagnostic), The human expert uses essentially imprecise natural language to communicate knowledge or data; therefore, fuzzy logic makes it possible to adjust for the data's inherent inaccuracies. and to account for the expression of the rules which allow for developing of a diagnostic [94] or to determine an action in the context of the monitoring of industrial systems [95].

This chapter begins by defining and explaining the terminology used in fuzzy logic [96], fuzzy set theory [97] and the mode of reasoning specific to fuzzy variables [98]. Finally, discussing the application the implementation of fuzzy logic in aim of fault diagnosis in power transmission line.

4.2 Fuzzy Logic

The premises of fuzzy logic appeared before the 1940s, with the first approaches, by American researchers, to the concept of uncertainty. He had to wait until 1965, for that the concept of fuzzy subset is proposed by L. Zadeh [57] , automation engineer of reputation international, professor at the University of Berkley in California, who contributed to the modeling of phenomena in fuzzy form, in order to overcome the limitations due to uncertainties of classical differential equation models.

In 1974 Mamdani [99]experimented with the theory set out by Zadeh on a steam boiler, a material whose complexity is well known, thus introducing fuzzy control into the regulation of an industrial process. This type of control was widely used in Japan in the late 80s and early 90s, on the subway (July 1987). Several applications then emerged in Europe, for sometimes very complex systems (such as the regulation of cement kilns).

Thanks to the Japanese researcher Sugeno [100], fuzzy logic was introduced in Japan as early as 1985. Japanese companies understood the technical and commercial advantage of fuzzy logic:

- Ease of implementation;
- Solution of complex multivariate problems;
- Possibility of integrating expert knowledge.

Japanese industry has developed consumer products based on fuzzy logic, namely:

-Home equipment, such as washing machines and vacuum cleaners.

-Audio-visual equipment (autofocus cameras, image-stabilized camcorders, photocopiers, etc.)

-Automobile on-board systems (such as ABS, suspension, and air conditioning);

-Transportation systems (train, metro, etc.); -Control/command systems used in the majority of industrial production, transformation, product treatment, etc. domains.

-Diagnostic or decision-making systems.

4.3 Fuzzy set theory

A membership function with denoted μA a value in the range [0, 1] characterizes a fuzzy set A of a discourse universe U. which assigns a degree of membership $\mu A\ (x)$ denoting the level of x's membership in A to each element x of $\mu A\ (x) = 1$ and $\mu A\ (x) = 0$ represent belonging and non-belonging, respectively. The range of actual values that the fuzzy variable x can take is known as the discourse universe or frame of reference [57] .

μA: U [0, 1]

As a result, an ordered set of pairs can be used to represent a fuzzy subset of U.

$$A = \{(x, \mu A(x)) | x\ U\} \qquad 4.1$$

The classical subset is actually a particular case of the fuzzy subset, which is the fuzzy subset whose membership function can only accept the values 0 or 1. The following notation, which shows for any element x of U its degree A(x) of membership in, is another common way to denote a fuzzy subset A of U.

$$A = \int_x \frac{\mu_A(x)}{xi} \text{ If U is continuous} \qquad 4.2$$

$$A = \sum_{xi} \frac{\mu_A(xi)}{xi} \text{ If U is discrete} \qquad 4.3$$

Definition 1.2 (Support): support of a fuzzy subset A is the subset (in the traditional meaning of the word) of the elements of a discourse universe X where the membership function has a strictly positive value. Each element of X is at least somewhat a part of A.$S(A) = \{x|\mu_A(x) > 0\}$

Definition 1.4 (Kernel): fuzzy subset's kernel A is the subset of the elements in a discourse

universe X for which the membership function is equal to 1. This set of points entirely belongs to A:

$$AN(A) = \{x|\mu_A(x) = 0.5\} \quad 4.4$$

Definition 1.5 (Height): The height of a fuzzy subset A in a universe of discourse X is the highest value that the membership function A on the set X can take. An element of X and A have the strongest degree of membership when it comes to:

$$H(A) = sup_x\, X\mu_A(x) \quad 4.5$$

Figure 4.1 illustrates the characteristics of a fuzzy set: support, height and kernel:

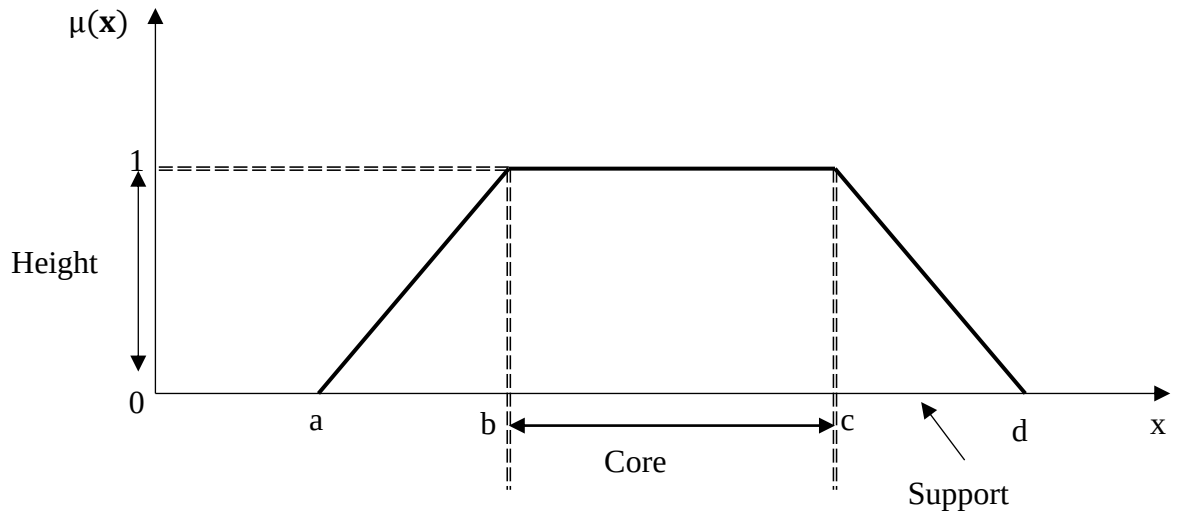

Figure 4.1 The characteristics of a fuzzy set

4.4 Linguistic variable

The notion of linguistic variable makes it possible to model imprecise knowledge or waves on a variable whose precise value is unknown. A linguistic variable, or fuzzy variable, is therefore a variable whose fuzzy values belong to sets blurs that can represent natural language words. Thus a fuzzy variable can take several linguistic values simultaneously. The universe of discourse is the domain in which these terms and these variables are defined [101].

The division of this universe of discourse by the fuzzy terms is called a fuzzy partition. When the universe of discourse is totally covered by fuzzy terms, and for all values, When the sum of the degrees of membership equals 1, that means a strong fuzzy partition.

A triple (x, T(x), U) can be used to represent the linguistic variable, with x serving as the linguistic variable's name, T(x) as its collection of linguistic values, and U serving as the universe of speech. Three terms for language small, medium, and large are used to provide an example of a linguistic variable called "speed" in Figure 4.2.

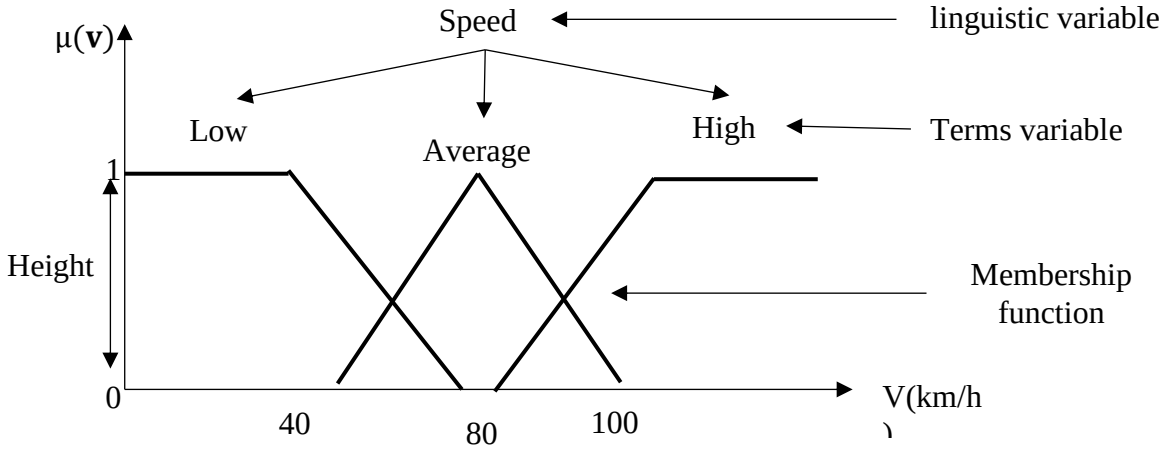

Figure 4.2 Example of the characteristics of a fuzzy set

4.5 Principle of fuzzy logic

4.5.1 Membership functions

Let x be an element of E that belongs to A (x A), and let E be a set and a subset of E (E A). We utilize the membership function A (x)between 0 and 1, which identifies the degree of x's membership in the fuzzy set A., to show this characteristic. The following functions are used more frequently to determine the membership function (Figure 4.3):

Triangle function

It is defined by three parameters [102], which determine the coordinates of the three vertices (figure 4.3).

$$\begin{array}{ll} \dfrac{x-a}{b-a} & \text{si } a \le x \le b \\ \dfrac{c-x}{c-b} & \text{si } b \le x \le c \\ 0 & \text{elsewhere} \end{array} \qquad 4.6$$

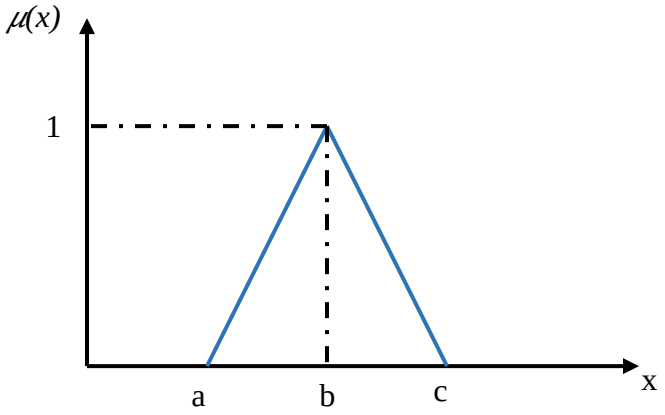

Figure 4.3 Form of function Triangular

b. Trapezoidal function

It is defined by four parameters [102] (figure 4.4):

$$\begin{cases} 0, & x < a \\ \frac{x-a}{b-a} & if\ a \le x < b \\ 1\ if & b \le x < c \\ \frac{d-x}{d-c} & if \quad c \le x \le d \\ 0, & x > d \end{cases} \qquad 4.7$$

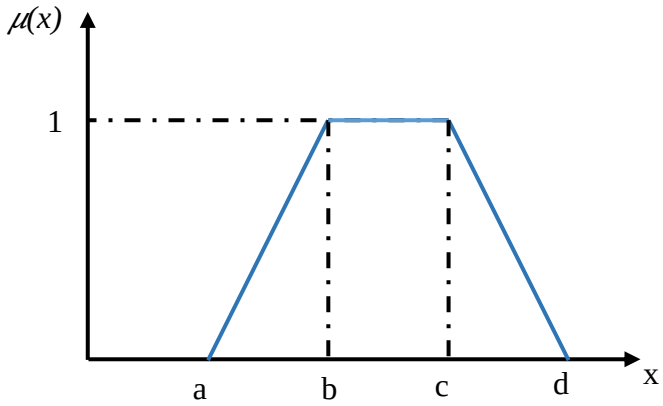

Figure 4.4 Form of trapezoidal function

Gaussian function

It is described by the two variables m, σ. (figure 4.5):

$$\mu A(x) = e^{(-\frac{(x-m)^2}{2\sigma^2})} \qquad 4.8$$

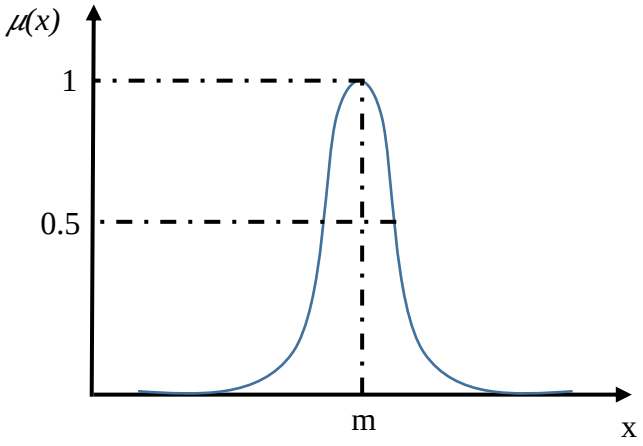

Figure 4.5 Form of Gaussian function

Choosing the form of the membership function is arbitrary and dependent on the designer's choices. The most popular geometric shapes in practice are: trapezoidal and triangular. The appearance of the trapezoidal shape is defined by four points A, B, C, D (figure 4.4). The triangle can be considered as a special case of the trapezium when two points coincide (B=C).

4.5.2 Operations on fuzzy sets

Let U contain two fuzzy sets A and B, with μA and μB serving as the corresponding membership functions. The membership function of fuzzy sets is used to define union, intersection, and complementation.

a. Equality

Two fuzzy subsets A and B are said to be equal if their membership functions are the same at all points of X. formally, A= B if and only if:$\forall x \in X$, μA(X) = μB(X).

b. Inclusion

Let X have two fuzzy subsets A and B. If any element x in X always belongs less to A than to B, then A is said to be included in B (A⊂B) for that element. Formally, $A \subset B$ if and only if: $\forall x \in X$, μA(X) ≤ μB(X).

c. Union

The fuzzy subset formed up of elements of X affected by the greater of the degrees with which they belong to A and B is known as the union of two fuzzy subsets A and B of X. formally, $A \cup B$ is expressed by: μA(X) $\cup B(x) = max$ (μA(X), μB(X))).

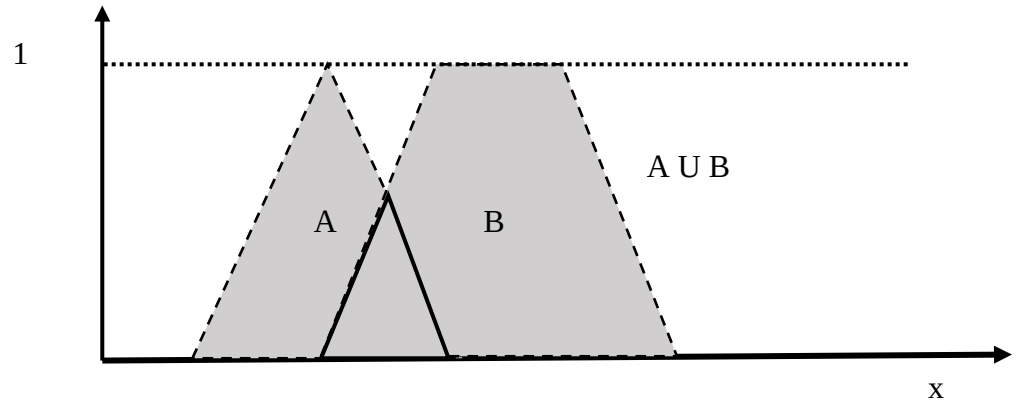

Figure 4.6 Two fuzzy subsets union

d. Intersection

The fuzzy subset of X is the intersection of the two fuzzy subsets A and B consisting of the elements of X assigned the smallest of the degrees with which they belong to A and B. formally, $A \cap B$ is expressed by: μA(X) $\cap B(x) = min$ (μA(X), μB(X))).

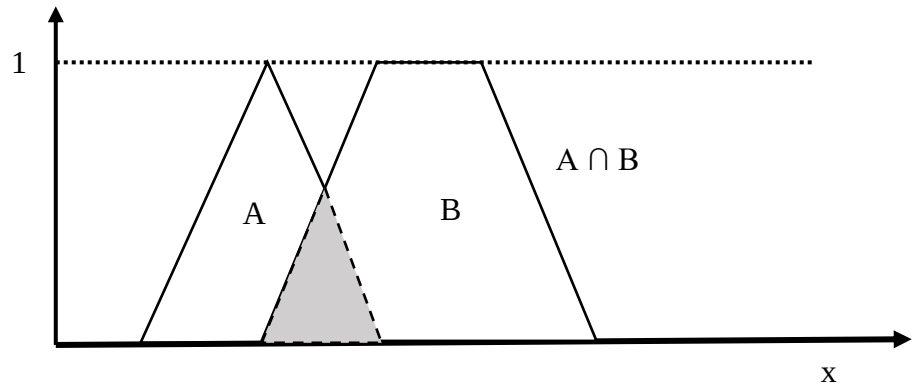

Figure 4.7 Two fuzzy subsets intersection

e. Complement

The symbol Ā represents the complement of a fuzzy subset of A. From the membership function of A, it is defined by: x ϵ X, $\mu\bar{A}(X) = 1 - \mu A(X)$

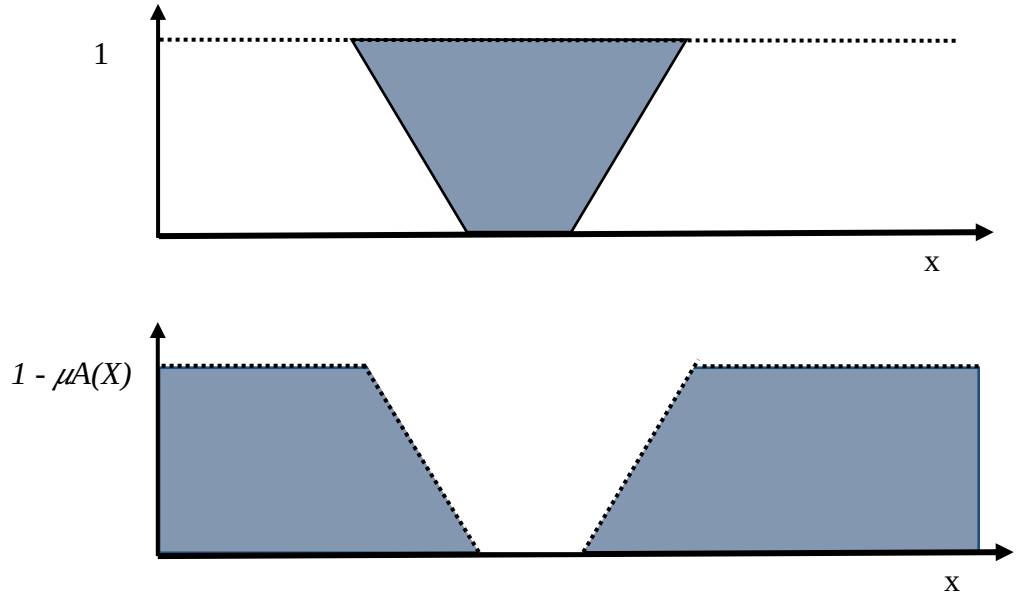

Figure 4.8 Fuzzy complement figure

4.6 Structure of a fuzzy process

A fuzzy logic model has a predefined structure. There are three main parts: fuzzification, fuzzy inference and defuzzification. You need to have a basic understanding of the global system and the operation of the fuzzy logic to be able to define each part. The model must be able to take different actions, which he will deal with to obtain values usable by the system [102].

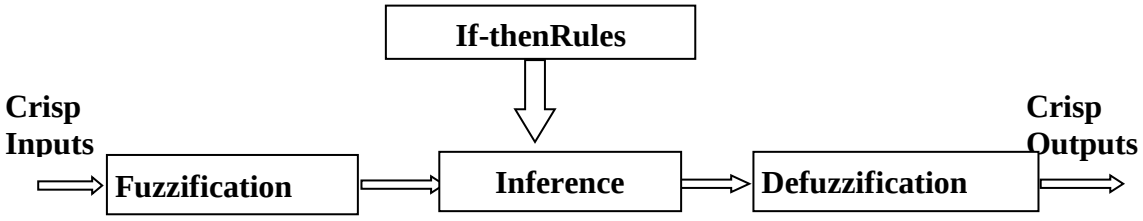

Figure 4.9 Fuzzy logic structure

4.6.1 Fuzzification

It consists in associating with each input value one or more fuzzy subsets as well as the associated degrees of membership. This step performs the transformation of values digital to fuzzy

symbolic information. The choice of how many fuzzy sets there are, the form of the membership functions, the recovery of these functions and their hard repair the universe of discourse is not obvious. However, there are factors that are more important than others [103].

4.6.2 Base of knowledge

The block of knowledge base containing information in the application domain and the expected command result. It is composed of a "database" and a "rule base linguistic (fuzzy) command". It contains:

• the database which contains the data required for fuzzy logic's normalization functions;

• The rule base is a collection of symbolic expressions that have been formalized using knowledge from experts. A rule states that if a condition is present in the functioning of the system then a decision is necessary to put the system in the desired operating state, and is of type: If ″ condition ″ Then ″ consequence″.

4.6.3 Mechanisms of inference

The inference block is the heart of fuzzy logic, it is called decision mechanism and allows to calculate the fuzzy set associated with the system using fuzzy logic's rules of implication and inference.

The fuzzy inference engine, also known as the decision-making logic, is the primary processing component (brain) of the fuzzy controller (systm).. Based on fuzzy reasoning and the collection of fuzzy rules creating the rule base, it can replicate human decision-making.

The operators "AND" and "OR" are used in the fuzzy rules. While the "OR" operator connects the various rules, the "AND" operator applies to the variables within a rule. There are numerous ways to interpret these operators.

R1: If x is A1 and y is B1 Then z is C1

Where

A2: If x is A2 and y is B2 Then z is C2

Typically, one of the following approaches is used for fuzzy logic tuning:

A- Max-Min inference method (Mamdani)

This approach implements the AND operator by the Min function, the THEN of each rule's conclusion by the Min function, and the OR operator (connection between all rules) by the Max

function. Due to how the THEN and OR operators of the inference are implemented, this technique is also known as the "Mamdani implication" or Max-Min approach [104].

B- Max-Product inference method (Larsan)

The difference from the previous method is in the way of performing the THEN conclusion. In this case, to define the partial membership function, we utilize the product of the membership degree of the condition produced by the operator AND between the input variables x, y by the formation of the minimum and the membership function of the set of the variable output.

C-Sugeno's method of inference

Sugeno's method of inference is a variant of the previous models, it also uses conditional rules, but the conclusion is of polynomial form, it is of form:

A1: If x is A1 and y is B1 Then z i = f i (x, y).

Similar to the earlier techniques, the minimum function realizes the operator AND. The polynomial function fi (x), which defines each rule, leads to the result THEN. The weighted average of each output's output results in the final output (OR operator).

$$z = \frac{G1z1 + G2z2}{G1 + G2} \qquad 4.9$$

D- Sum-Product inference method

In this case, the AND operator is realized by the product, as well as the THEN conclusion. However, the OR operator is realized by the average value of the membership degrees involved in the inference. Other methods have been developed, each with a specific variant. Nevertheless, the Mamdani method (Max-Min) and the Sugeno method are by far the most used.

4.6.4 Defuzzification

As we have seen, inference methods provide a resultant membership function μ res(z). But, the controller requires a precise (real) control signal at its input; therefore, it is necessary to provide for a transformation of this fuzzy set into a precise quantity. This transformation is called: defuzzification. There are various defuzzification techniques; the most popular ones are:

the average of the maximums method; the center of gravity method.

4.6.4.1 Defuzzification by center of gravity

The most used defuzzification method is that of identifying the membership function's center of gravity. The defuzzified output x* corresponds to the abscissa of the surface center of gravity of the membership function μ (x) is given by the following relation:

If the system output is discrete

$$x^* = \frac{\sum_{i=1}^{n} x_i \mu(x_i)}{\sum_{i=1}^{n} \mu(x_i)} \qquad 4.10$$

where n represents the sample's number of elements., μ denotes the membership function, and xi denotes the sample element. x* is defined as follows for the continuous membership function:

$$x^* = \frac{\int x \mu_A(x) dx}{\int \mu_A(x) dx} \qquad 4.11$$

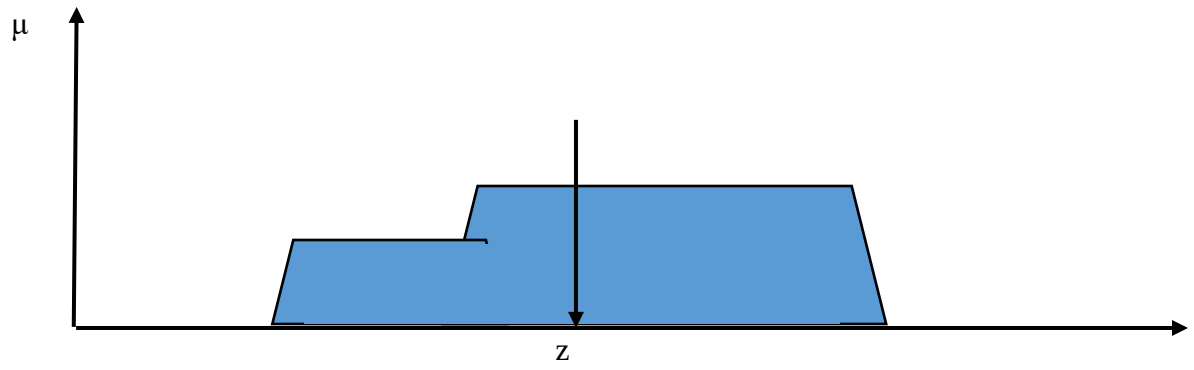

Figure 4.10 Defuzzification by center of gravity

4.6.4.2 Defuzzification by maximum value

The defuzzifier in this case shows the maximum value of the membership function that results from the inference. However, there are several values for which the resulting membership function is maximal, which makes this method challenging. This method only applies if the output set's membership function only has a single maximum. We choose as output the abscissa$y*$ corresponding to this maximum.

4.6.4.3 Maximum average method

The fuzzy set that contains the values for which the membership function is maximal is examined by the defuzzifier, and as a result, the average of these values is determined. In this

method, the output value is estimated by the abscissa of the point corresponding to the center of the interval M for which the membership function is maximum. This value is provided by the expression:

$$x^* = \left(\frac{\inf(M) + \sup(M)}{2}\right) \qquad 4.12$$

where inf (M) and et sup (M) serve as the interval's lower and upper limits, respectively.

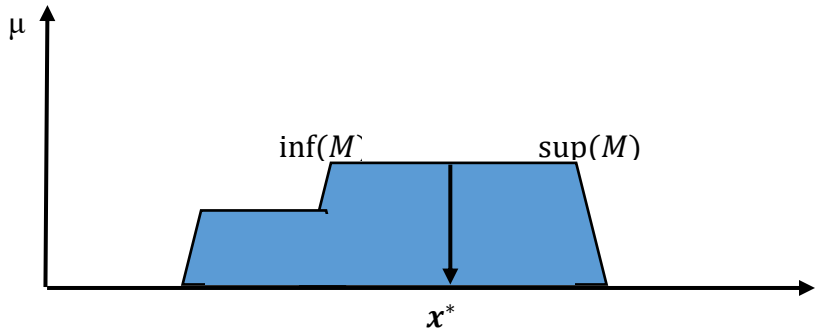

Figure 4.11 Defuzzification by the average of the maxima

4.7 Implementation of Fuzzy Logic in power system test

The implementation of the fuzzy logic diagnosis method at the transmission line's start is shown in Figure 4.11. One IFD isn't enough, as we previously demonstrated, another IFD must be added at the other end of the transmission line, as illustrated in Figure 4.12.

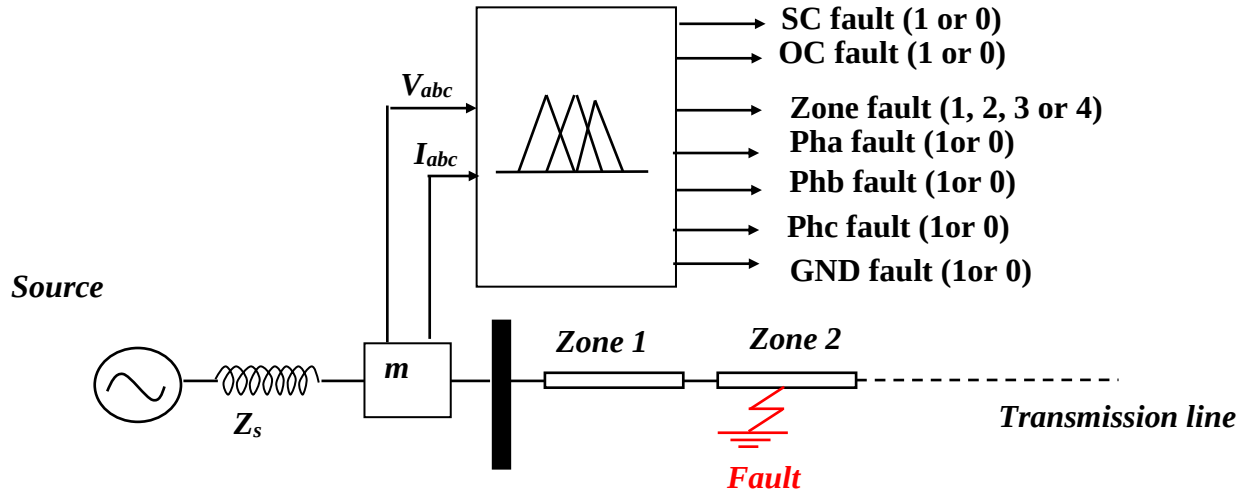

Figure 4.12 Fuzzy logic implantation

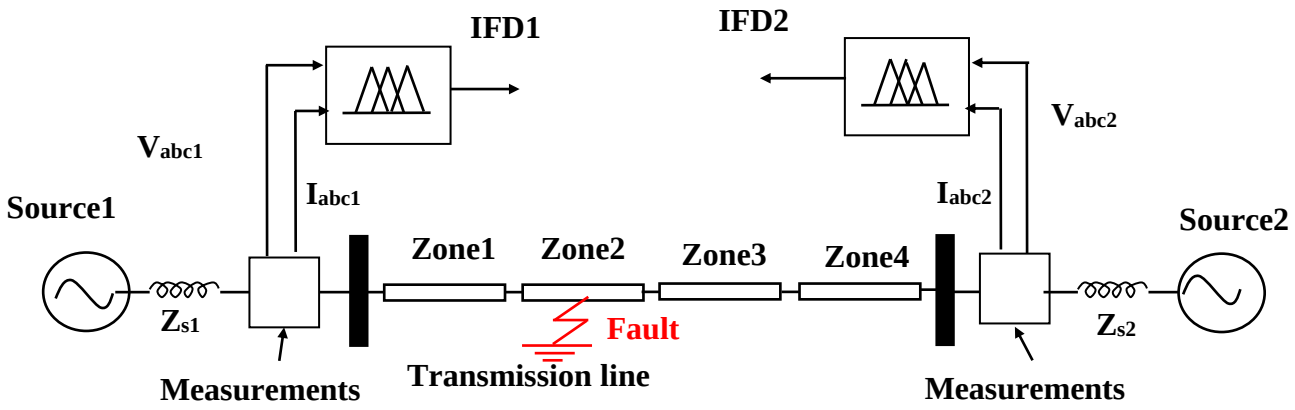

Figure 4.13 Implantation of Fuzzy logic in the transmission line ends.

In our case, the triangular form was chosen. Where the values of Ia, Ib, Ic, Va, Vb, and Vc were transformed into fuzzy values (very low, low, and high), as shown in figure 15. Additionally, figure 4.14 shows the outputs fuzzification

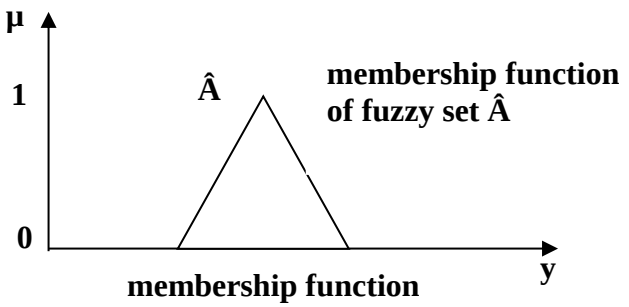

Figure 4.14 Membership function

4.7.1 Fuzzification and Rule base

The Rule base is defined as a limited set of rules. The rules that should be applied while making decisions are contained in the rule base.

These rules typically come from intuition and personal experience. An antecedent block (between the If and Then) and a consequent block (after Then) are the two basic components of a rule. Consequently, if (antecedent) Then (consequent). As in our situation, if *Ia*, *Ib*, and *Ic* are high and *Va*, *Vb*, and *Vc* are low, the system is clear and fault-free. Table 4.1 has a list of every rule.

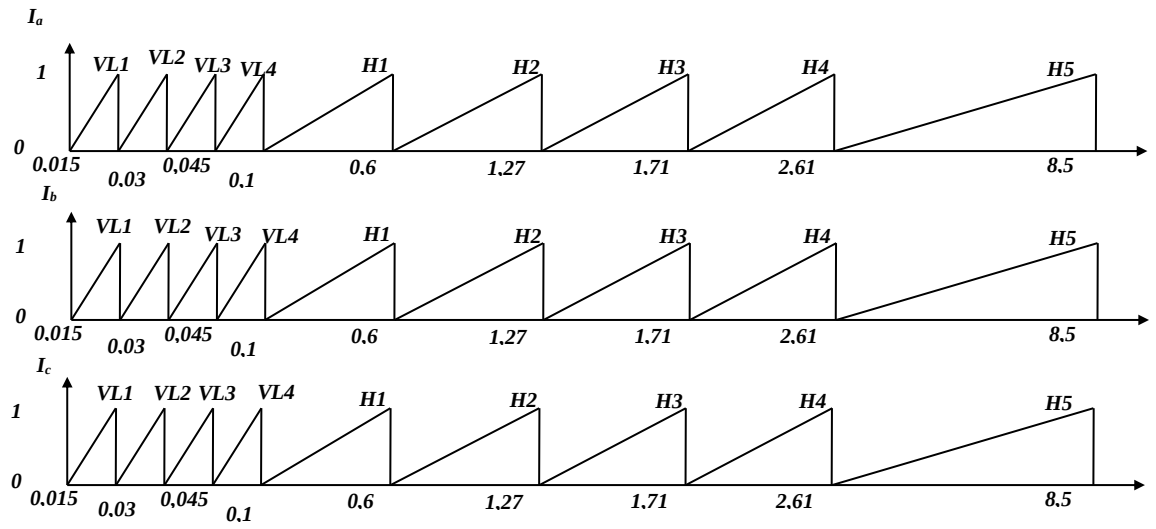

Figure 4.15 Current (I_a, I_b, and I_c) Fuzzification

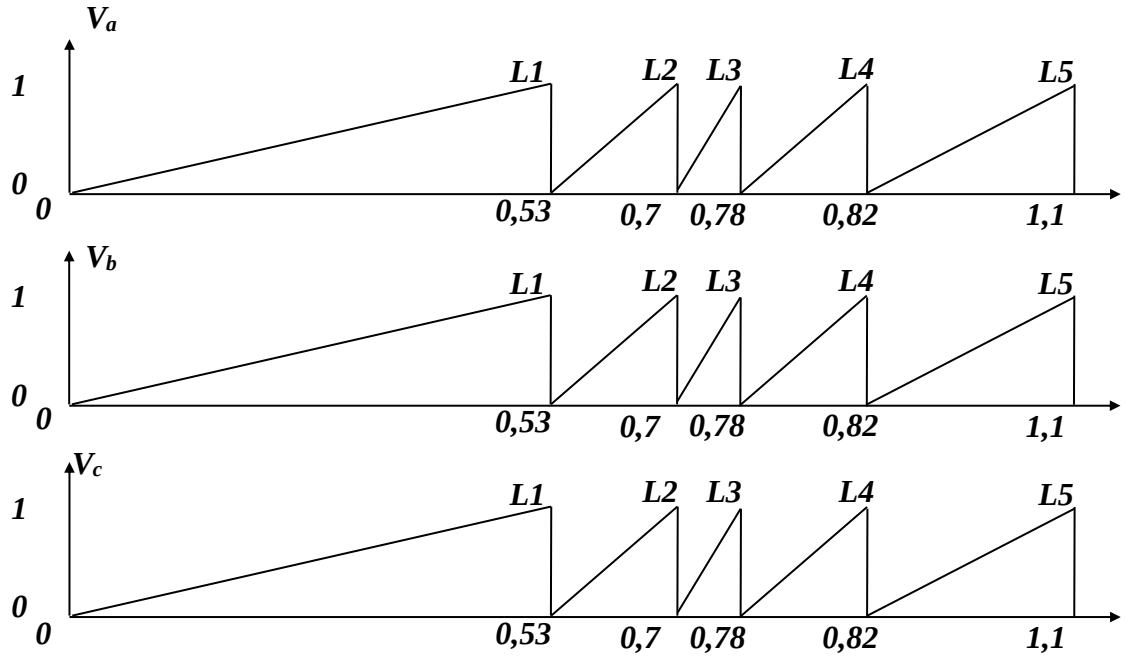

Figure 4.16 Fuzzification of the Voltage (V_a, V_b, and V_c)

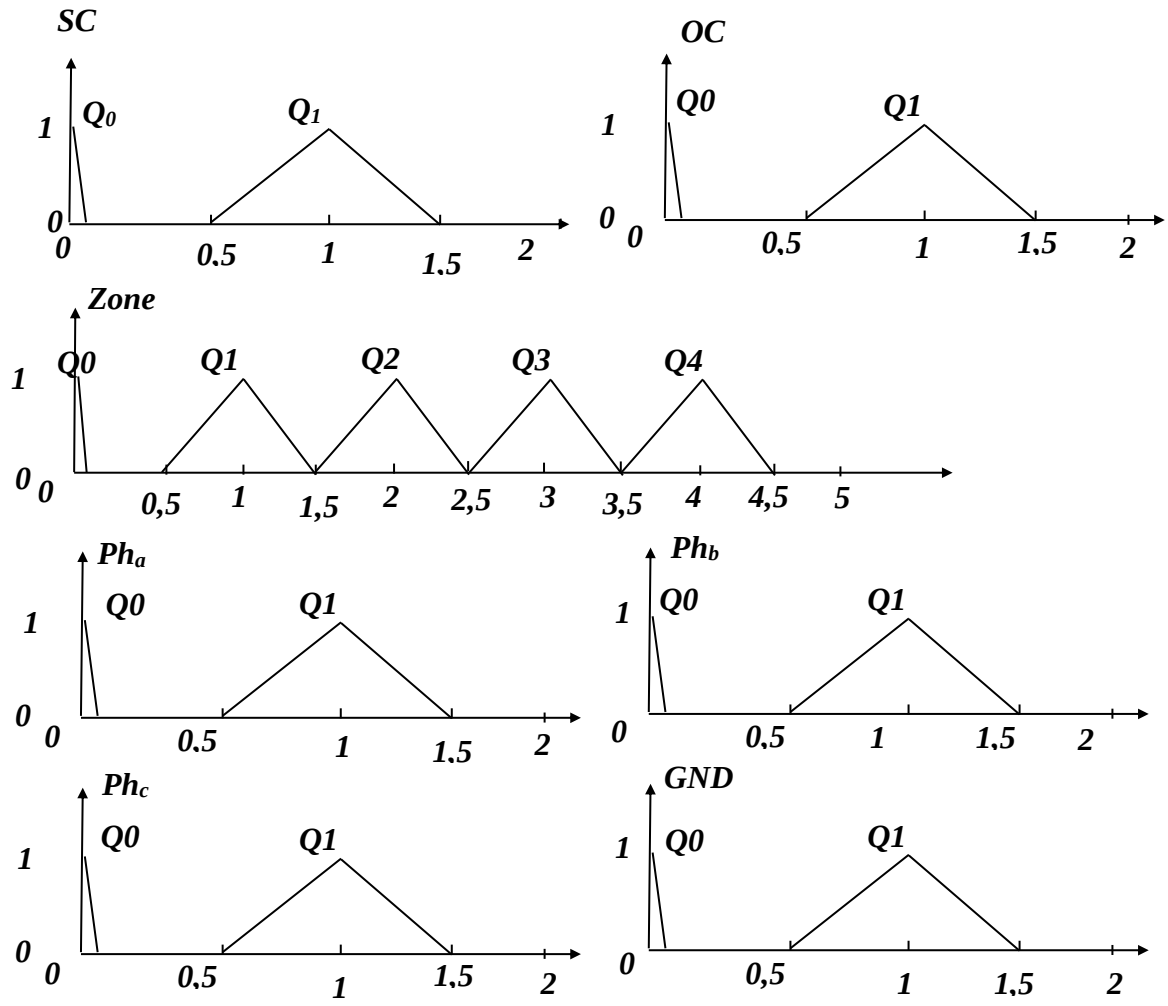

Figure 4.17 Fuzzification Outputs

Inferences Rules:

No	i_a	i_b	i_c	V_a	V_b	V_c	SC	OC	Zone	Ph_a	Ph_b	Ph_c	GND
1	H1	H1	H1	L5	L5	L5	Q0	Q0	Q0	Q0	Q0	Q0	Q0
2	H5	H1	H1	L1	L5	L5	Q1	Q0	Q1	Q1	Q0	Q0	Q1
3	H1	H5	H1	L5	L1	L5	Q1	Q0	Q1	Q0	Q1	Q0	Q1
4	H1	H1	H5	L5	L5	L1	Q1	Q0	Q1	Q0	Q0	Q1	Q1
5	H5	H5	H1	L1	L1	L5	Q1	Q0	Q1	Q1	Q1	Q0	Q1
6	H5	H5	H1	L2	L1	L5	Q1	Q0	Q1	Q1	Q1	Q0	Q0
7	H1	H5	H5	L5	L1	L1	Q1	Q0	Q1	Q0	Q1	Q1	Q1
8	H1	H5	H5	L5	L2	L1	Q1	Q0	Q1	Q0	Q1	Q1	Q0
9	H5	H1	H5	L1	L5	L1	Q1	Q0	Q1	Q1	Q0	Q1	Q1

10	H5	H1	H5	L1	L5	L2	Q1	Q0	Q1	Q1	Q0	Q1	Q0
11	H5	H5	H5	L1	L1	L1	Q1	Q0	Q1	Q1	Q1	Q1	Q1
12	VL1	H1	H1	L5	L5	L5	Q0	Q1	Q1	Q1	Q0	Q0	Q0
13	H1	VL1	H1	L5	L5	L5	Q0	Q1	Q1	Q0	Q1	Q0	Q0
14	H1	H1	VL1	L5	L5	L5	Q0	Q1	Q1	Q0	Q0	Q1	Q0
15	VL1	VL1	H1	L5	L5	L5	Q0	Q1	Q1	Q1	Q1	Q0	Q0
16	H1	VL1	VL1	L5	L5	L5	Q0	Q1	Q1	Q0	Q1	Q1	Q0
17	VL1	H1	VL1	L5	L5	L5	Q0	Q1	Q1	Q1	Q0	Q1	Q0
18	VL1	VL1	VL1	L5	L5	L5	Q0	Q1	Q1	Q1	Q1	Q1	Q0
19	H4	H1	H1	L2	L5	L5	Q1	Q0	Q2	Q1	Q0	Q0	Q1
20	H1	H4	H1	L5	L2	L5	Q1	Q0	Q2	Q0	Q1	Q0	Q1
21	H1	H1	H4	L5	L5	L2	Q1	Q0	Q2	Q0	Q0	Q1	Q1
22	H4	H4	H1	L2	L2	L5	Q1	Q0	Q2	Q1	Q1	Q0	Q1
23	H3	H4	H1	L4	L2	L5	Q1	Q0	Q2	Q1	Q1	Q0	Q0
24	H1	H4	H4	L5	L2	L2	Q1	Q0	Q2	Q0	Q1	Q1	Q1
25	H1	H3	H4	L5	L4	L2	Q1	Q0	Q2	Q0	Q1	Q1	Q0
26	H4	H1	H4	L2	L5	L2	Q1	Q0	Q2	Q1	Q0	Q1	Q1
27	H4	H1	H3	L2	L5	L4	Q1	Q0	Q2	Q1	Q0	Q1	Q0
28	H4	H4	H4	L2	L2	L2	Q1	Q0	Q2	Q1	Q1	Q1	Q1
29	VL2	H1	H1	L5	L5	L5	Q0	Q1	Q2	Q1	Q0	Q0	Q0
30	H1	VL2	H1	L5	L5	L5	Q0	Q1	Q2	Q0	Q1	Q0	Q0
31	H1	H1	VL2	L5	L5	L5	Q0	Q1	Q2	Q0	Q0	Q1	Q0
32	VL2	VL2	H1	L5	L5	L5	Q0	Q1	Q2	Q1	Q1	Q0	Q0
33	H1	VL2	VL2	L5	L5	L5	Q0	Q1	Q2	Q0	Q1	Q1	Q0
34	VL2	H1	VL2	L5	L5	L5	Q0	Q1	Q2	Q1	Q0	Q1	Q0
35	VL2	VL2	VL2	L5	L5	L5	Q0	Q1	Q2	Q1	Q1	Q1	Q0
36	H3	H1	H1	L3	L5	L5	Q1	Q0	Q3	Q1	Q0	Q0	Q1
37	H1	H3	H1	L5	L3	L5	Q1	Q0	Q3	Q0	Q1	Q0	Q1
38	H1	H1	H3	L5	L5	L3	Q1	Q0	Q3	Q0	Q0	Q1	Q1
39	H3	H3	H1	L3	L3	L5	Q1	Q0	Q3	Q1	Q1	Q0	Q1
40	H2	H3	H1	L5	L3	L5	Q1	Q0	Q3	Q1	Q1	Q0	Q0
41	H1	H3	H3	L5	L3	L3	Q1	Q0	Q3	Q0	Q1	Q1	Q1
42	H1	H2	H3	L5	L5	L3	Q1	Q0	Q3	Q0	Q1	Q1	Q0

43	H3	H1	H3	L3	L5	L3	Q1	Q0	Q3	Q1	Q0	Q1	Q1
44	H3	H1	H2	L3	L5	L5	Q1	Q0	Q3	Q1	Q0	Q1	Q0
45	H3	H3	H3	L3	L3	L3	Q1	Q0	Q3	Q1	Q1	Q1	Q1
46	VL3	H1	H1	L5	L5	L5	Q0	Q1	Q3	Q1	Q0	Q0	Q0
47	H1	VL3	H1	L5	L5	L5	Q0	Q1	Q3	Q0	Q1	Q0	Q0
48	H1	H1	VL3	L5	L5	L5	Q0	Q1	Q3	Q0	Q0	Q1	Q0
49	VL3	VL3	H1	L5	L5	L5	Q0	Q1	Q3	Q1	Q1	Q0	Q0
50	H1	VL3	VL3	L5	L5	L5	Q0	Q1	Q3	Q0	Q1	Q1	Q0
51	VL3	H1	VL3	L5	L5	L5	Q0	Q1	Q3	Q1	Q0	Q1	Q0
52	VL3	VL3	VL3	L5	L5	L5	Q0	Q1	Q3	Q1	Q1	Q1	Q0
53	H2	H1	H1	L4	L5	L5	Q1	Q0	Q4	Q1	Q0	Q0	Q1
54	H1	H2	H1	L5	L4	L5	Q1	Q0	Q4	Q0	Q1	Q0	Q1
55	H1	H1	H2	L5	L5	L4	Q1	Q0	Q4	Q0	Q0	Q1	Q1
56	H2	H2	H1	L4	L4	L5	Q1	Q0	Q4	Q1	Q1	Q0	Q1
57	H2	H2	H1	L5	L4	L5	Q1	Q0	Q4	Q1	Q1	Q0	Q0
58	H1	H2	H2	L5	L4	L4	Q1	Q0	Q4	Q0	Q1	Q1	Q1
59	H1	H2	H2	L5	L5	L4	Q1	Q0	Q4	Q0	Q1	Q1	Q0
60	H2	H1	H2	L4	L5	L4	Q1	Q0	Q4	Q1	Q0	Q1	Q1
61	H2	H1	H2	L4	L5	L5	Q1	Q0	Q4	Q1	Q0	Q1	Q0
62	H2	H2	H2	L4	L4	L4	Q1	Q0	Q4	Q1	Q1	Q1	Q1
63	VL4	H1	H1	L5	L5	L5	Q0	Q1	Q4	Q1	Q0	Q0	Q0
64	H1	VL4	H1	L5	L5	L5	Q0	Q1	Q4	Q0	Q1	Q0	Q0
65	H1	H1	VL4	L5	L5	L5	Q0	Q1	Q4	Q0	Q0	Q1	Q0
66	VL4	VL4	H1	L5	L5	L5	Q0	Q1	Q4	Q1	Q1	Q0	Q0
67	H1	VL4	VL4	L5	L5	L5	Q0	Q1	Q4	Q0	Q1	Q1	Q0
68	VL4	H1	VL4	L5	L5	L5	Q0	Q1	Q4	Q1	Q0	Q1	Q0
69	VL4	VL4	VL4	L5	L5	L5	Q0	Q1	Q4	Q1	Q1	Q1	Q0

Table 4-1 Inferences Rules

4.7.2 Inference

The rules in the base are exploited in this procedure to generate fuzzy decisions. Each rule is individually assessed during this process, and a choice is then chosen for each rule. The outcome is a set of fuzzy decisions. When combining fuzzy variables, logical operators like "AND," "OR," and "NOT" must be used.

4.7.3 Defuzzification

Defuzzification is an inverse transformation as compared to the fuzzification process because in this step, the fuzzy output is transformed into a crisp value and applied to the system. In our case, the centroid method is applied:

$$U_{out} = \frac{\sum_{i=1}^{n} h_i u_i}{\sum_{i=1}^{n} u_i} \qquad 4.13$$

u_i is the membership function and h_i is its center.

4.8 Simulation results

To analyze the performance of diagnosis by fuzzy logic, the same faults scenarios of chapter 03 are applied on the same electrical test network: We have presented the following faults (SC: Short Circuit or OC: Open Circuit). all fault occurs at 0,1sec.

4.8.1 Diagnostic performances

Similar to the previous part, we noted that our systems were capable of detecting 138 different fault types in significantly less time than the protection system's (200 ms) tripping time.

4.8.1.1 Faults detection in zone 1

In Zone 1, the following 4 types of single-phase faults are applied:

-SC Phase A - GND (both sides),

-SC Phase A - GND (Side 1),

-SC Phase A - GND (Side 2),

-OC Phase A.

4.8.1.1.1 Short circuit fault in Ph_a-GND

Figures 4.18 and 4.19 demonstrate the two sides' three-phase current and voltage transient behavior.

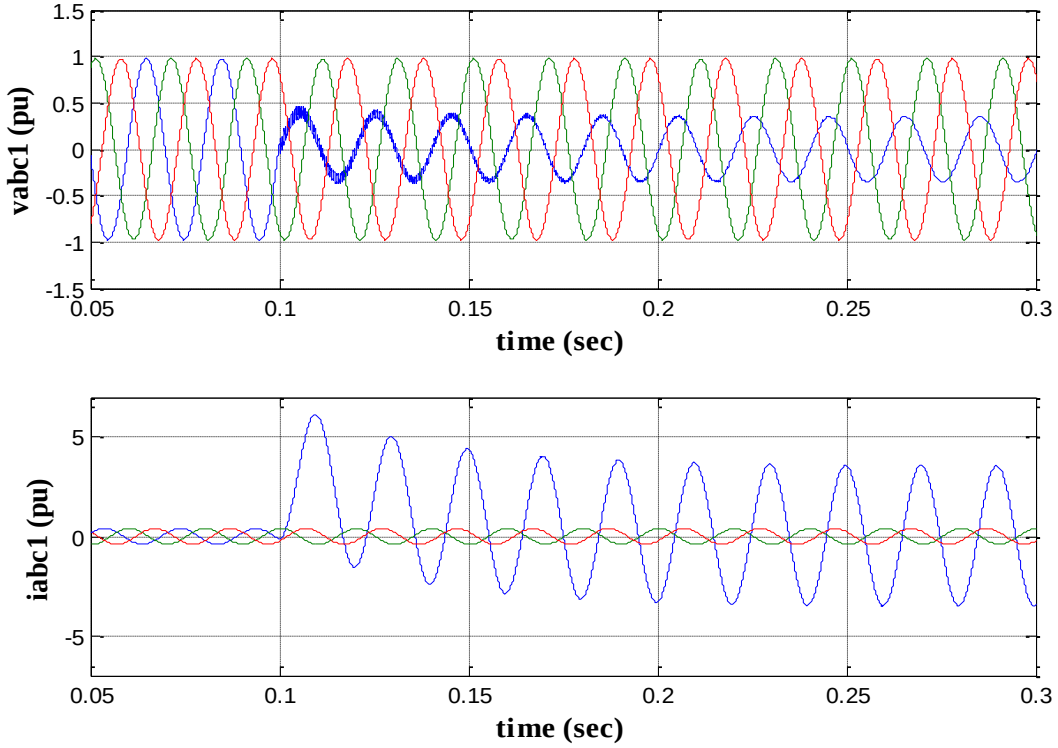

Figure 4.18 Voltages V_{abc1} & currents I_{abc1} of Pha during short-circuit

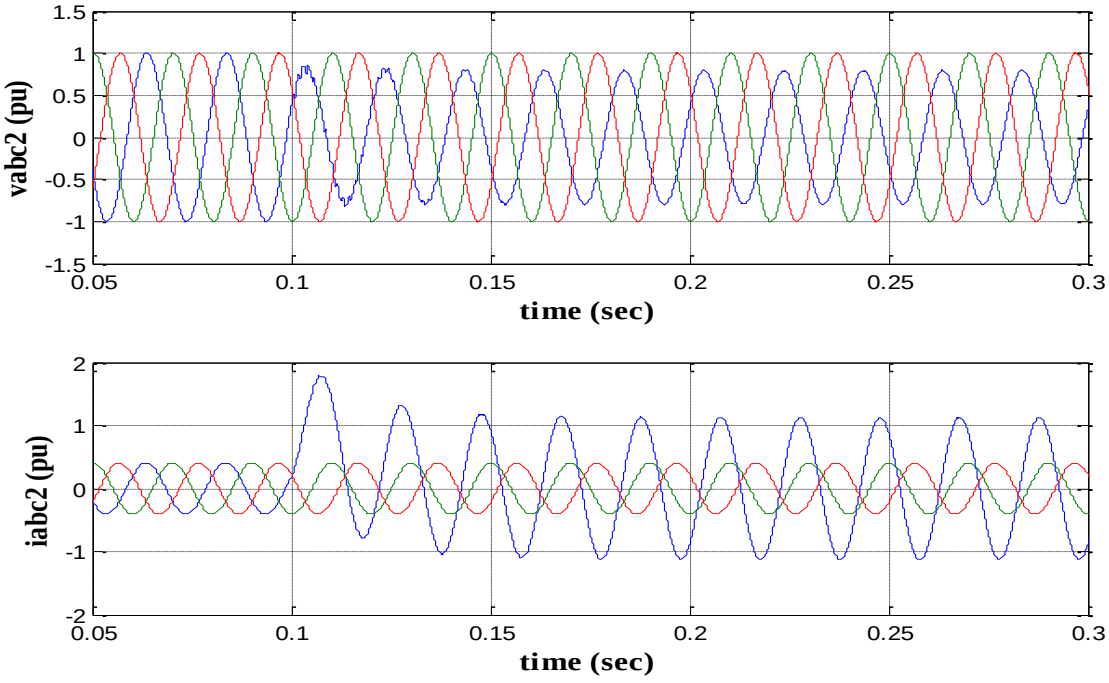

Figure 4.19 Voltages V_{abc2} & currents I_{abc2} of Pha during short-circuit

According to IFD1's point of view, the fault location is zone 1, whereas according to IFD2's, it is zone 4. (See Fig. 4.20) and the diagnostic system signaled the short-circuit SC (See Fig. 4.21) in the Phase Pha-GND (see Fig. 4.22).

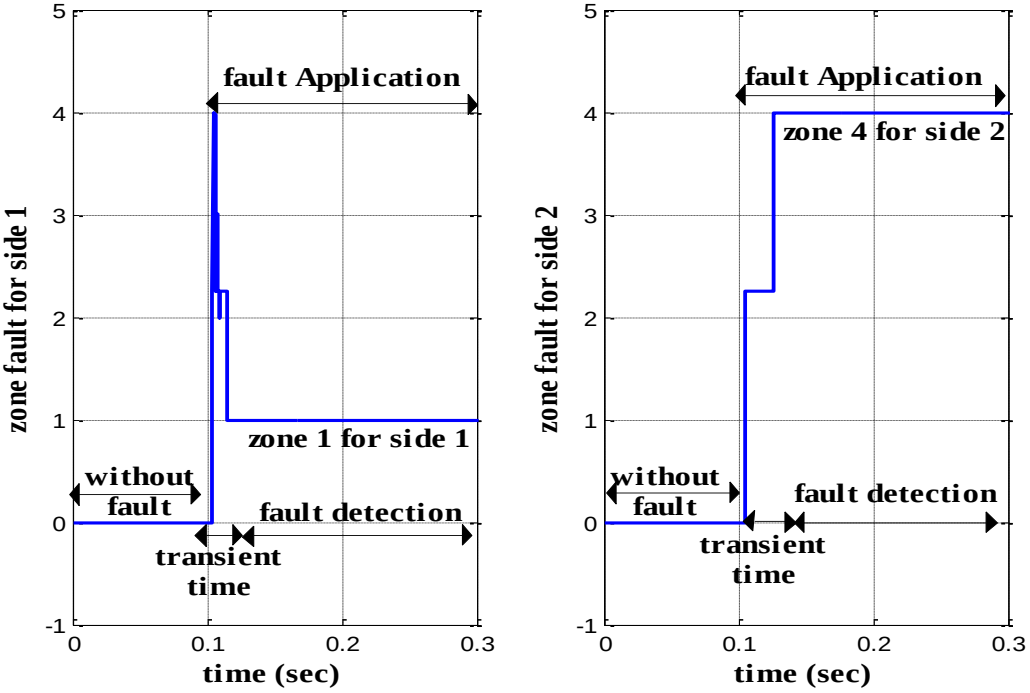

Figure 4.20 SC ph_a-GND fault zone detection

According to Figure 4.21, this fault is a short-circuit (SC) for both IFD systems.

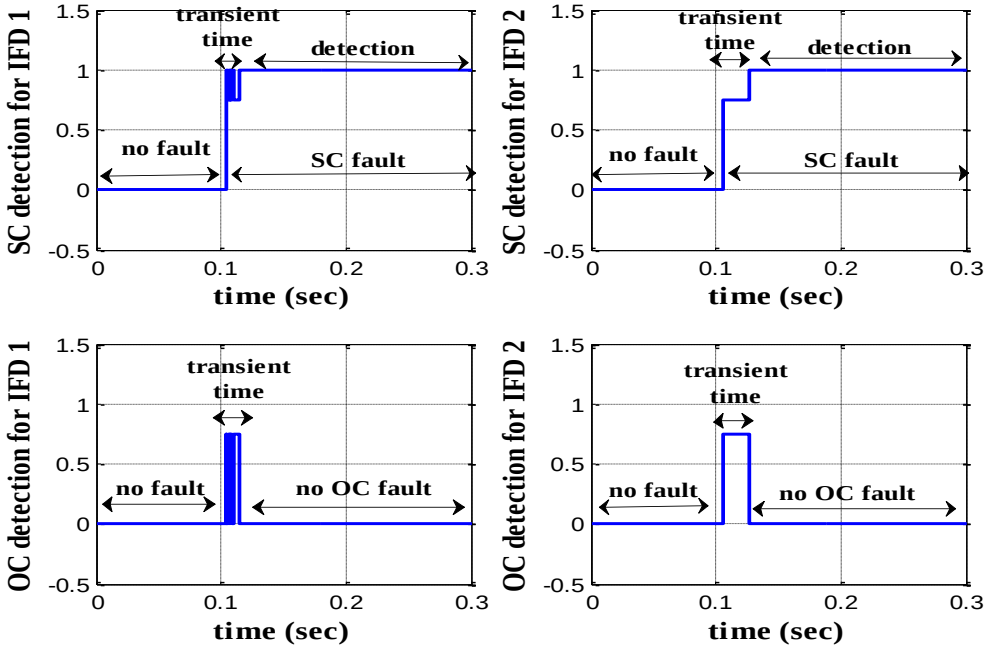

Figure 4.21 Identification of the fault type (SC-Side1 and SC-Side2)

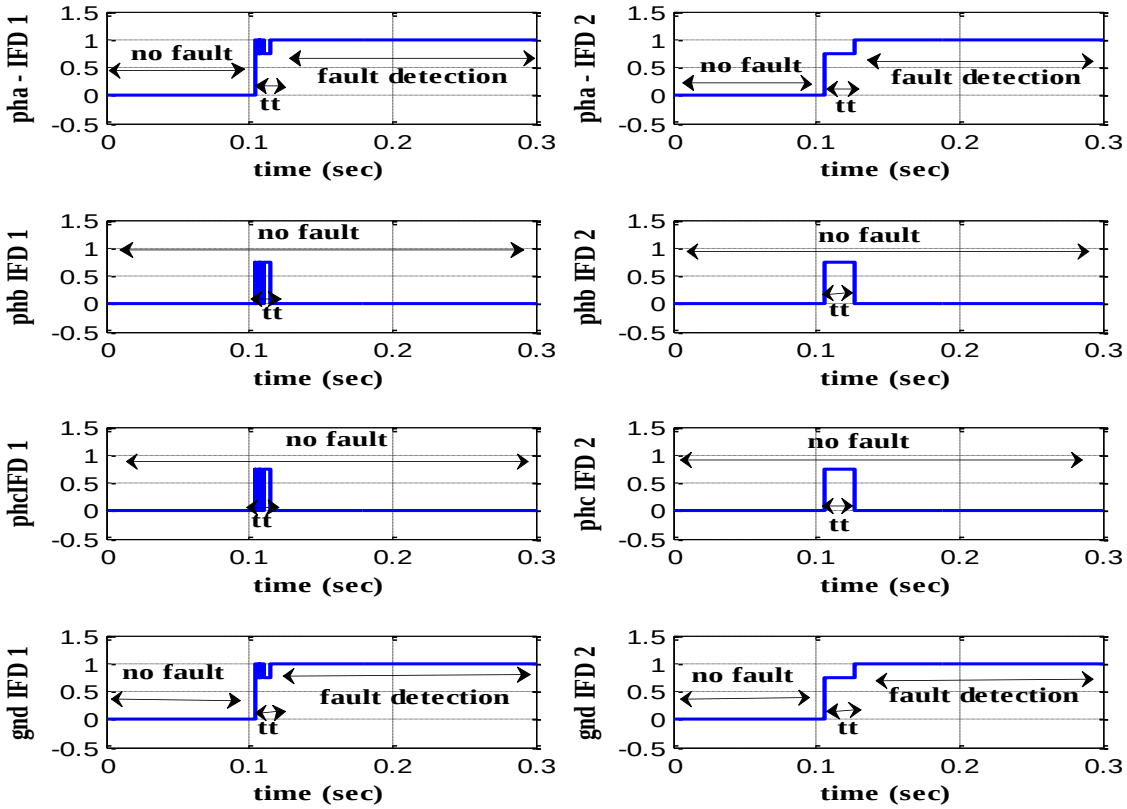

Figure 4.22 Identification of the fault phase (Ph_a-GND)

4.8.1.1.2 Short circuit fault in Ph_a-GND – Side 1

Figures 4.23 and 4.24 depict a rise in current and a drop in voltage of phase Pha (side 1) during the fault, respectively. We also observe a low current and a small transient voltage variation (in phase a) on side 2.

Using the fuzzy logic, we obtain a correct signaling identical to the variation of the current and voltage in the two zones: The SC fault in zone 01 (side 1) with a small delay at IFD2 (side 2) and a small transient regime at IFD1 (side 1) and the opening circuit with IFD2 (Side 2), like shown in figures 4.25, 4.26 and 4.27.

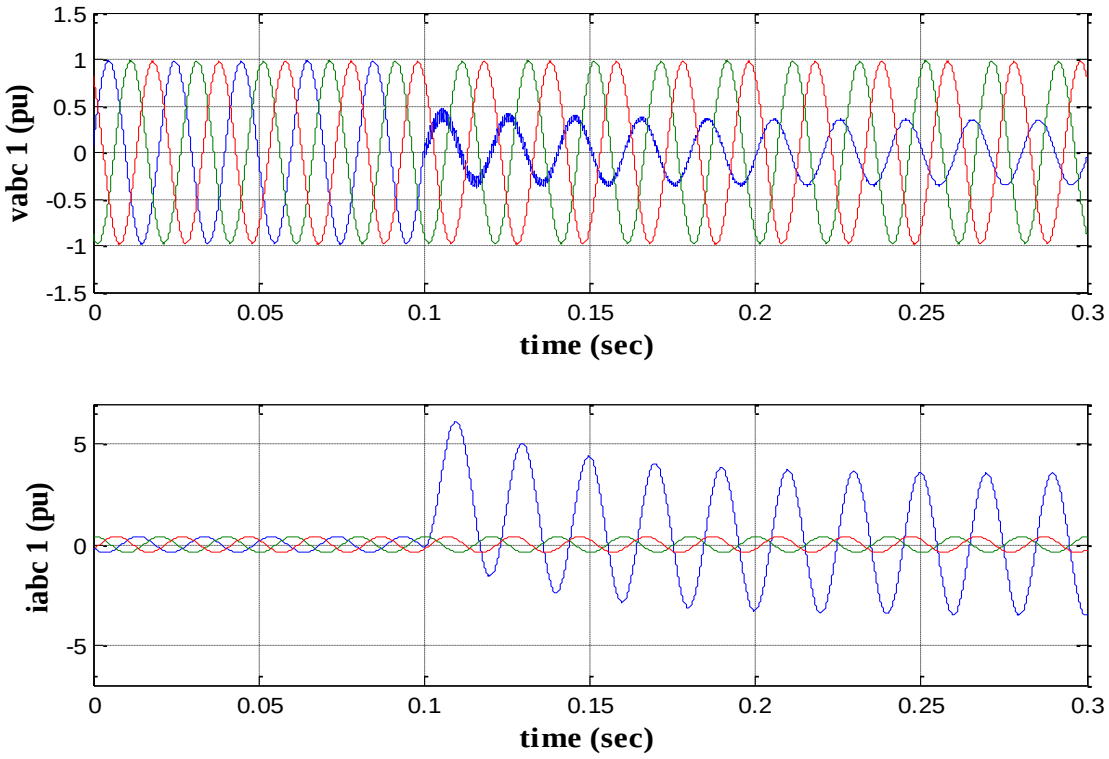

Figure 4.23 Voltages V_{abc1} and currents I_{abc1} of Pha during short-circuit to side1

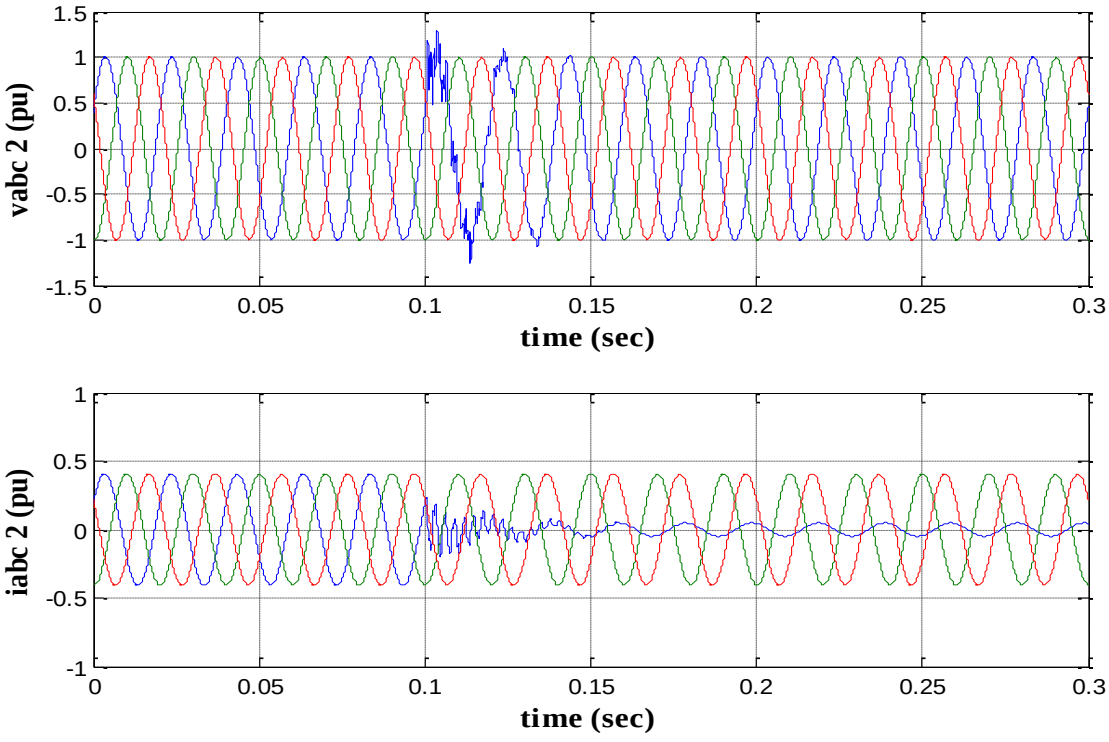

Figure 4.24 V_{abc2} & I_{abc2} of Pha during short-circuit to side2

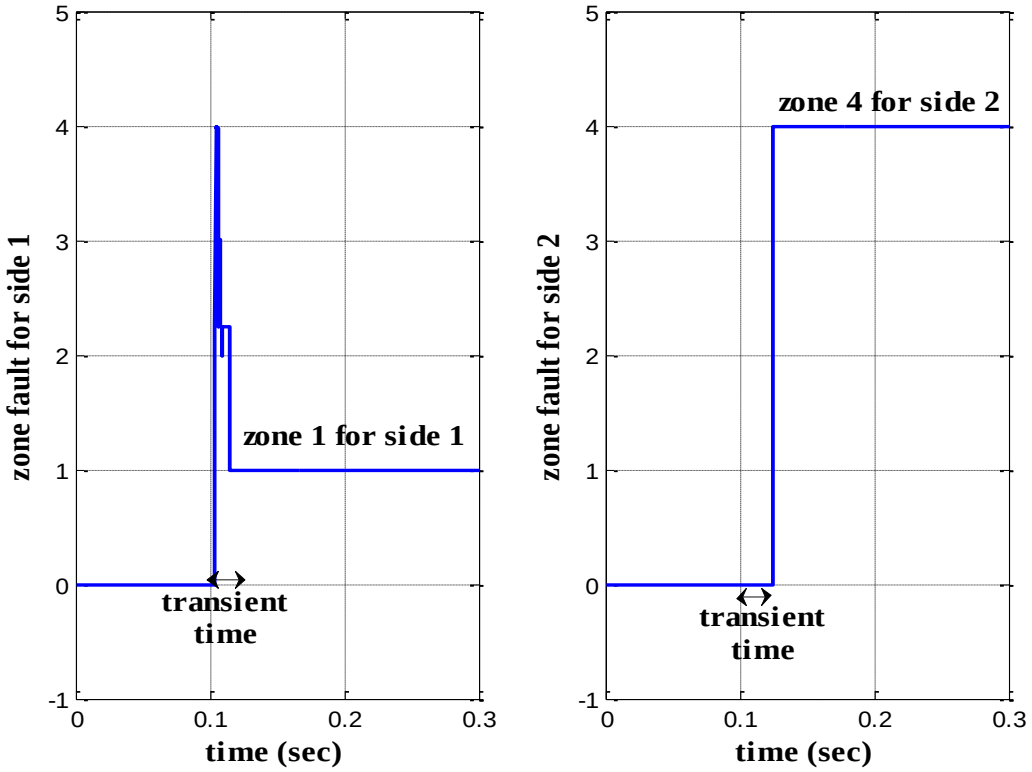

Figure 4.25 SC pha-GND-Side1 fault zone detection

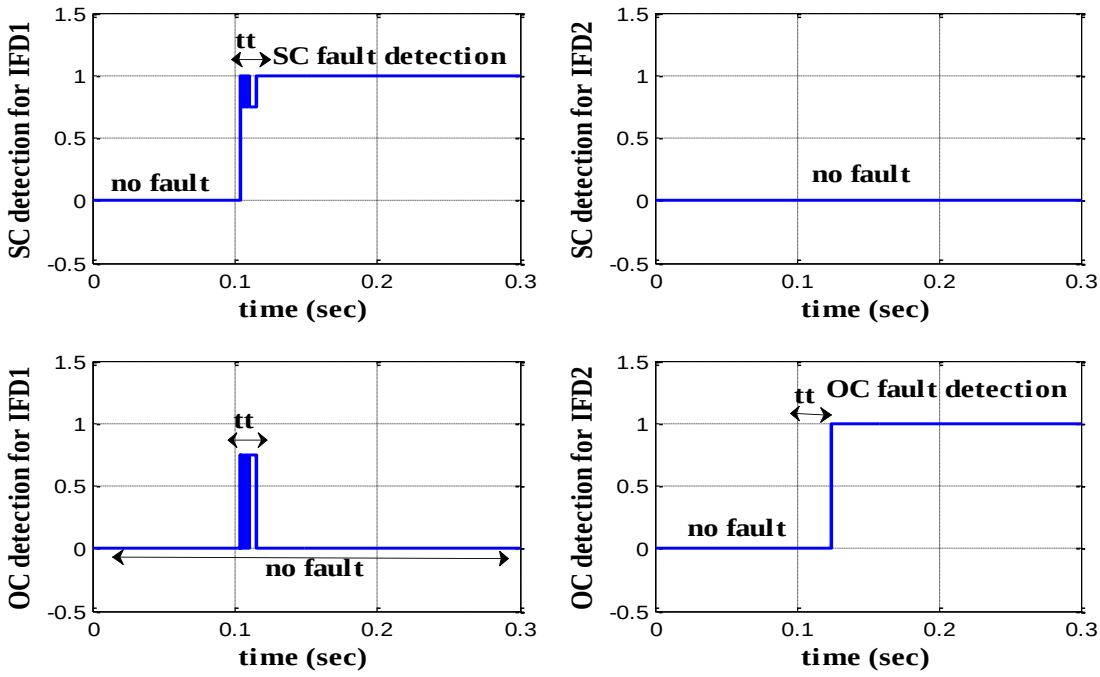

Figure 4.26 Identification of the fault type (SC-Side1 & OC-Side2)

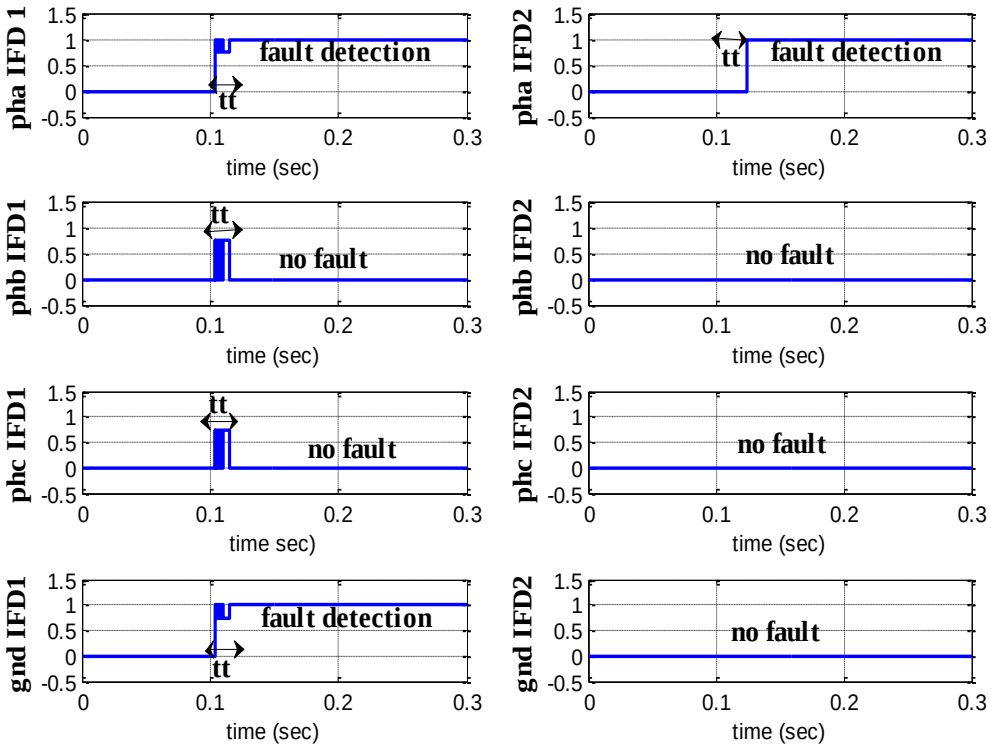

Figure 4.27 Identification of the fault phase (Ph_a-GND-Side1)

4.8.1.1.3 Short circuit fault in Ph_a-GND – Side 2

A short circuit fault is applied to side 2 of the transmission line (Figs. 4.33 and 4.34). When compared to IFD1, the fault is in zone 1 and is a short-circuit on phase (a) at side 2. (Figs. 4.28, 4.29, 4.30, 4.31 and 4.32). fuzzy logic diagnostic approach was capable of identifying and diagnose the fault accurately with small fast transient fluctuations.

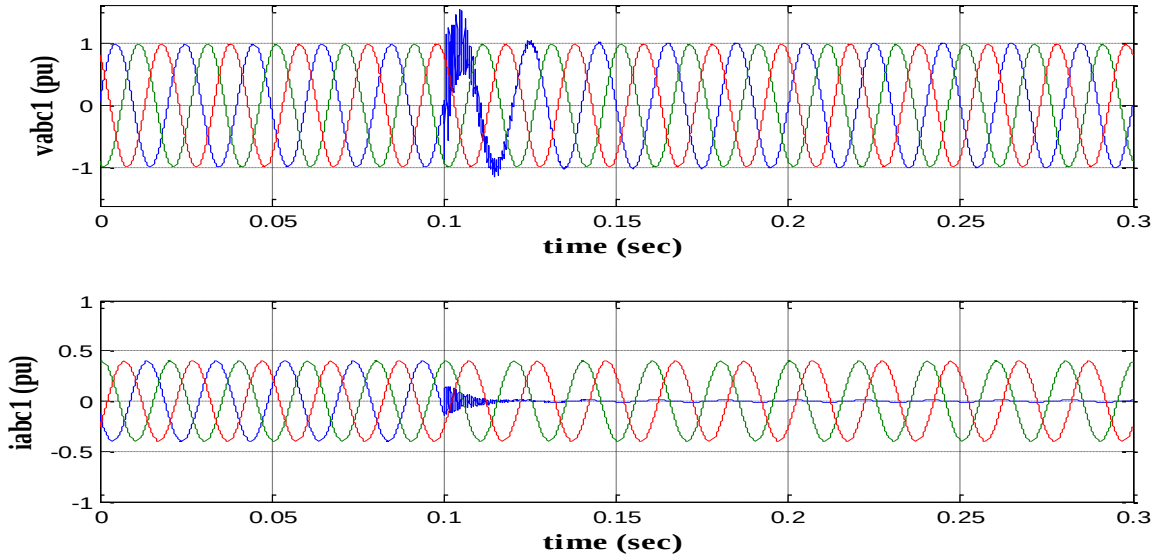

Figure 4.28 Voltages V_{abc1} and currents I_{abc1} of Pha during short-circuit side 1

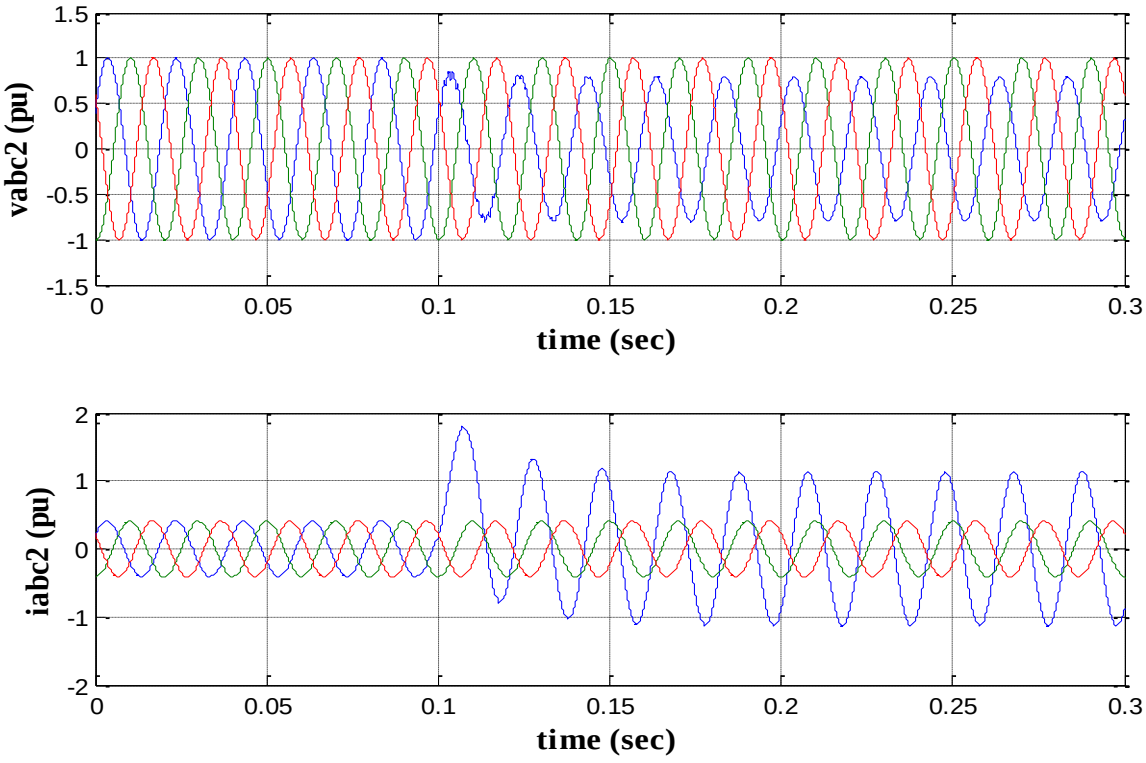

Figure 4.29 V_{abc2} & I_{abc2} of Pha during short-circuit side 2

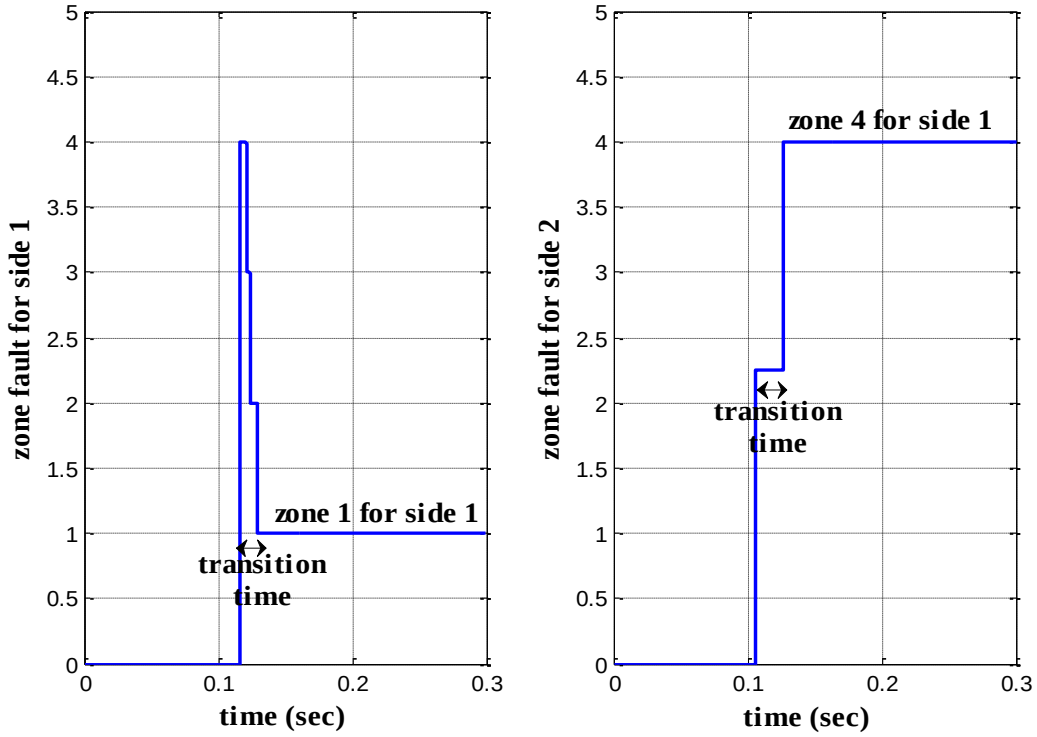

Figure 4.30 SC ph_a-GND-Side2 fault zone detection

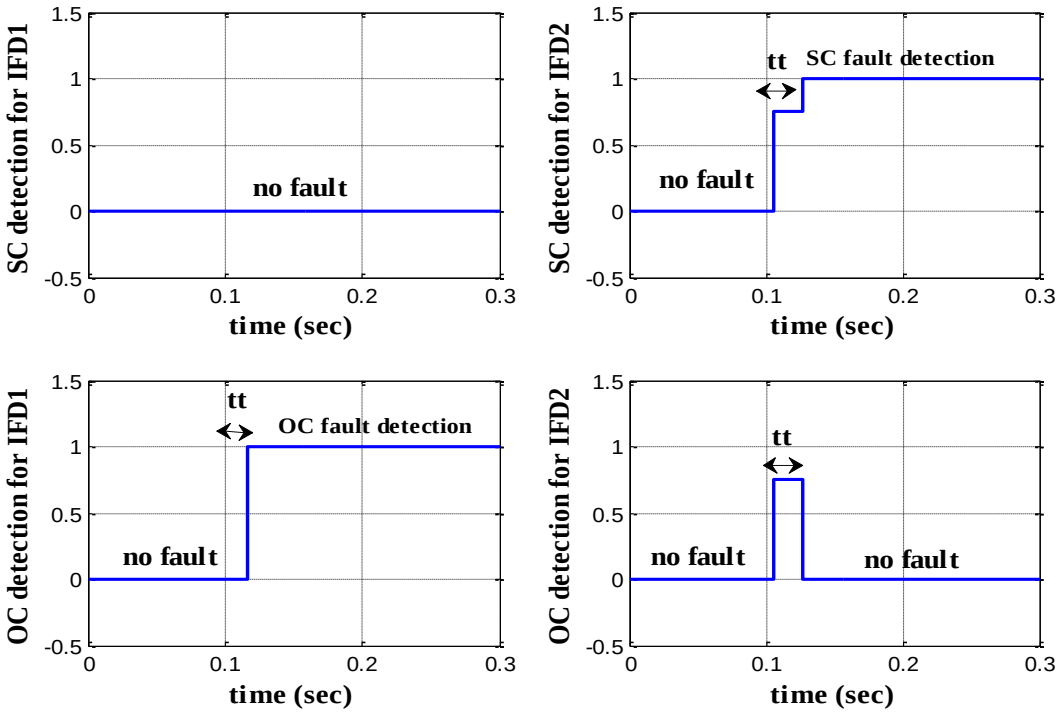

Figure 4.31 Identification of the fault type (OC-Side1 and SC-Side2)

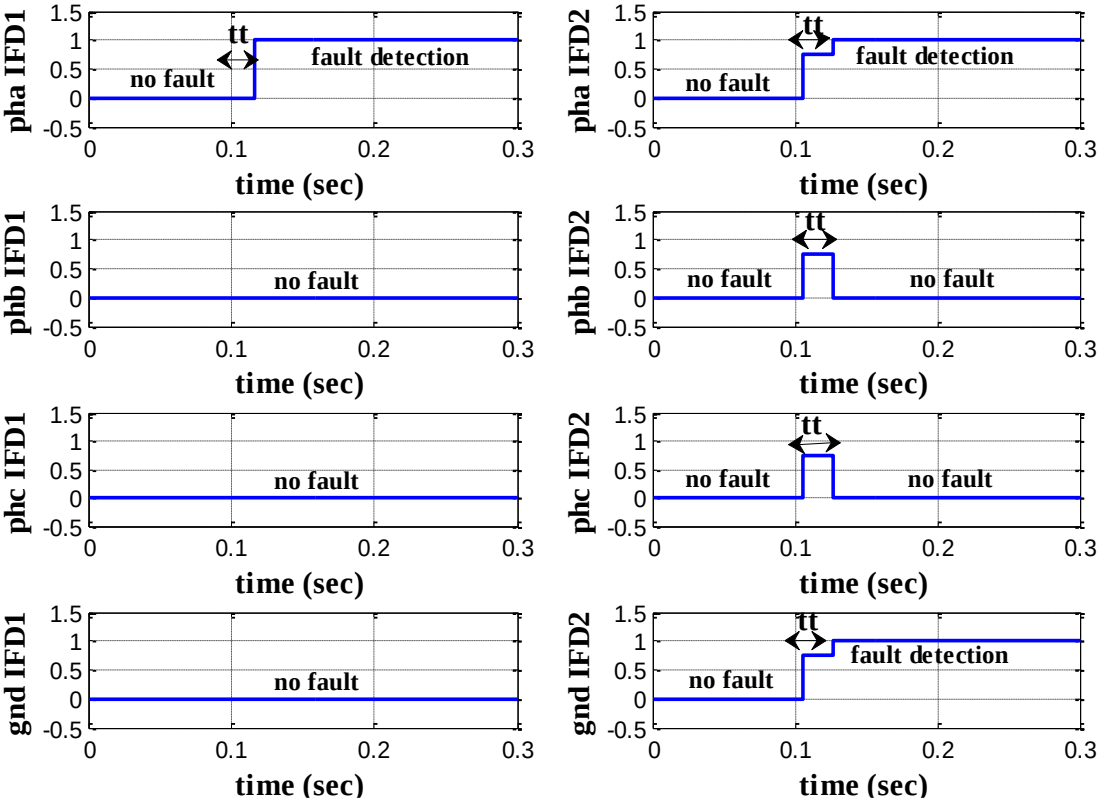

Figure 4.32 Identification of the fault phase (Ph_a-GND-Side2)

4.8.1.1.4 Open circuit fault in Pha

Noticing that the power transmission line's opening caused simple voltage fluctuations and the cancellation of phase (a) currents on both sides in figures 4.33 and 4.34. According to Figures 4.35 and 4.36, fuzzy logic was capable of recognizing the opening of phase (a) and to indicate a fault in zone 1 according to side 1.

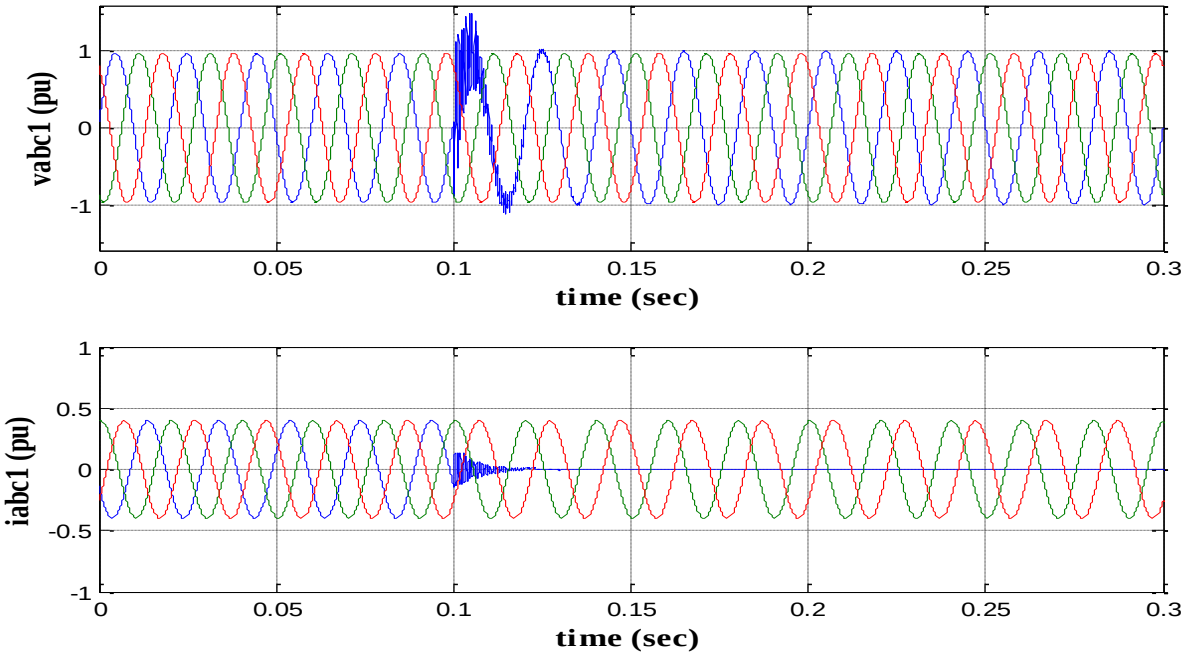

Figure 4.33 V_{abc1} and I_{abc1} of Ph_a during open circuit side1

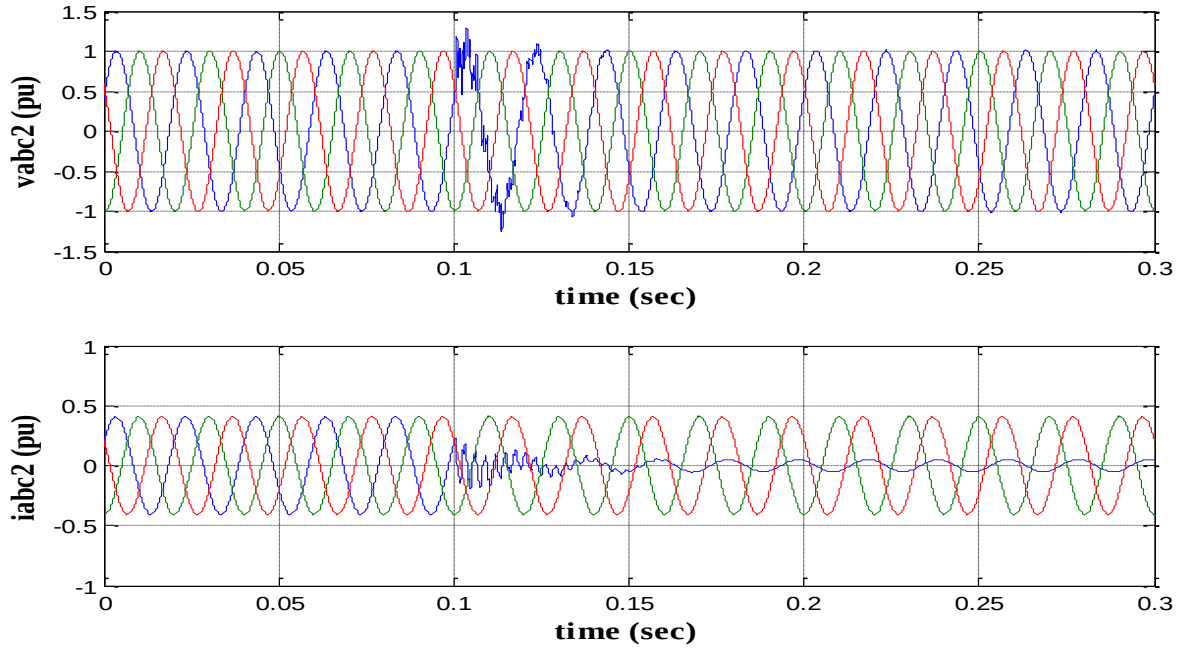

Figure 4.34 Voltages V_{abc2} and currents I_{abc2} of Ph_a during open circuit side 2

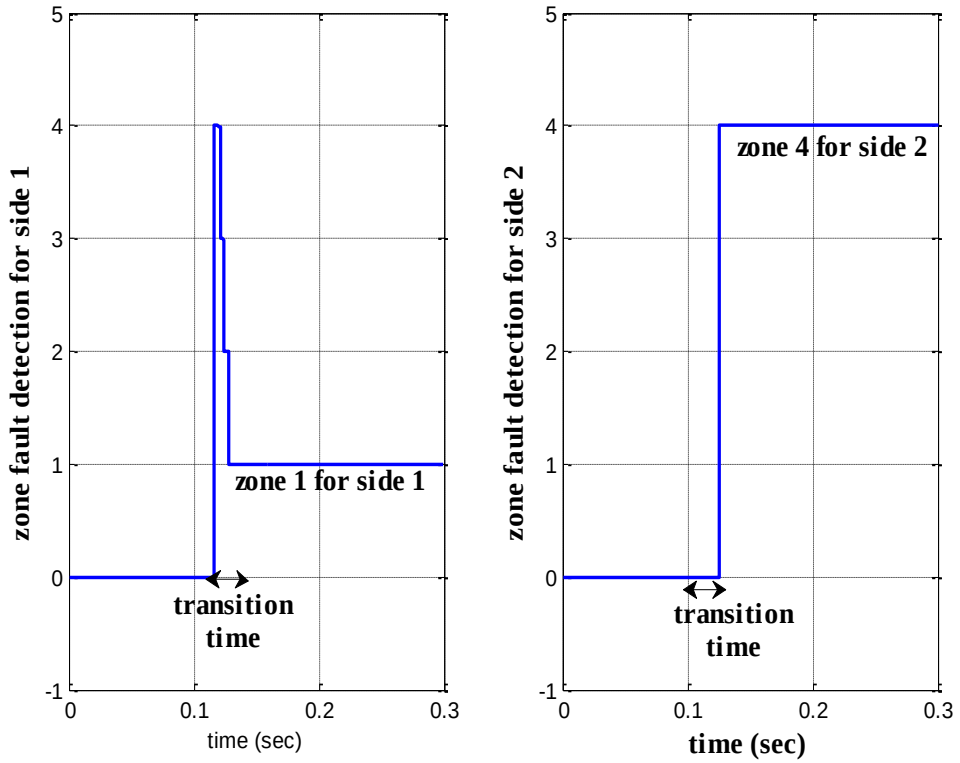

Figure 4.35 OC ph_a fault zone detection

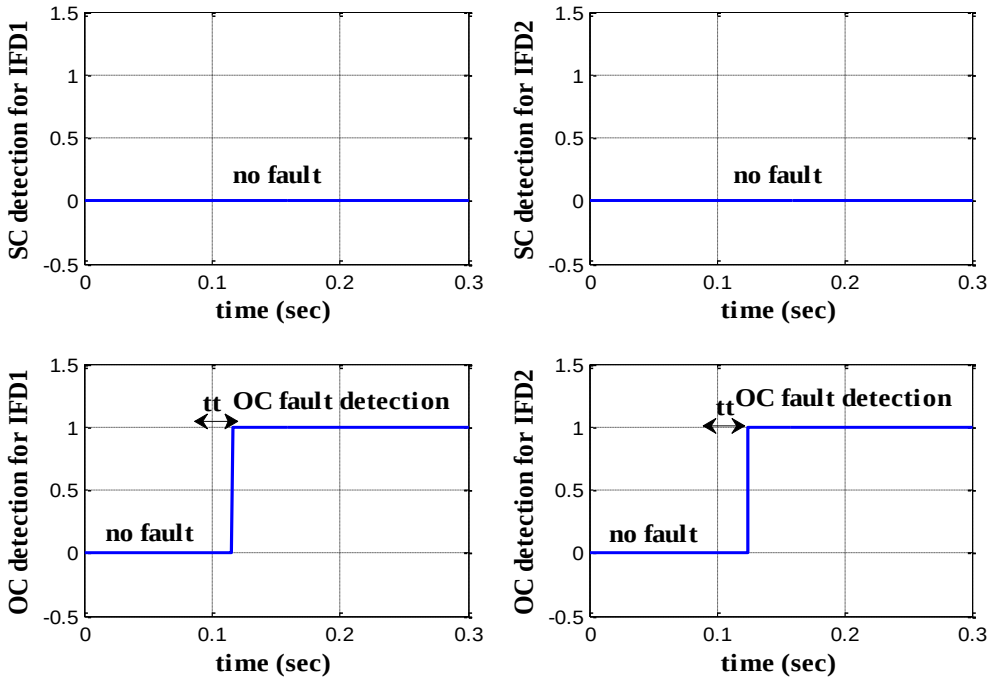

Figure 4.36 Identification of the fault type (OC to both sides)

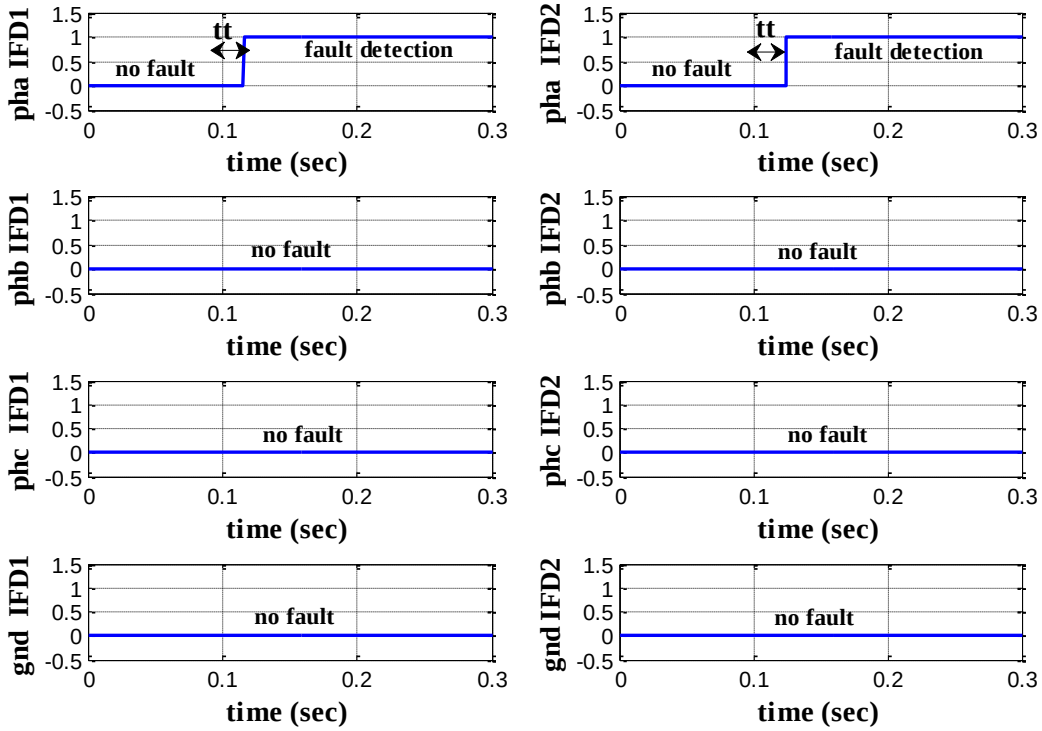

Figure 4.37 Identification of the fault phase (Ph_a)

4.8.1.2 Faults detection in zone 2

4.8.1.2.1 Short circuit fault in Pha-phb-GND

Figures 4.38 and 4.39 show the system behavior in the presence of an LL-G short circuit. The fault zone was identified correctly using fuzzy logic: Zone 2 with IFD 1 and zone 3 with IFD 2. A short circuit on Pha and Phb. And, very short detection times of 20 ms (Figs. 4.40, 4.41 and 4.42).

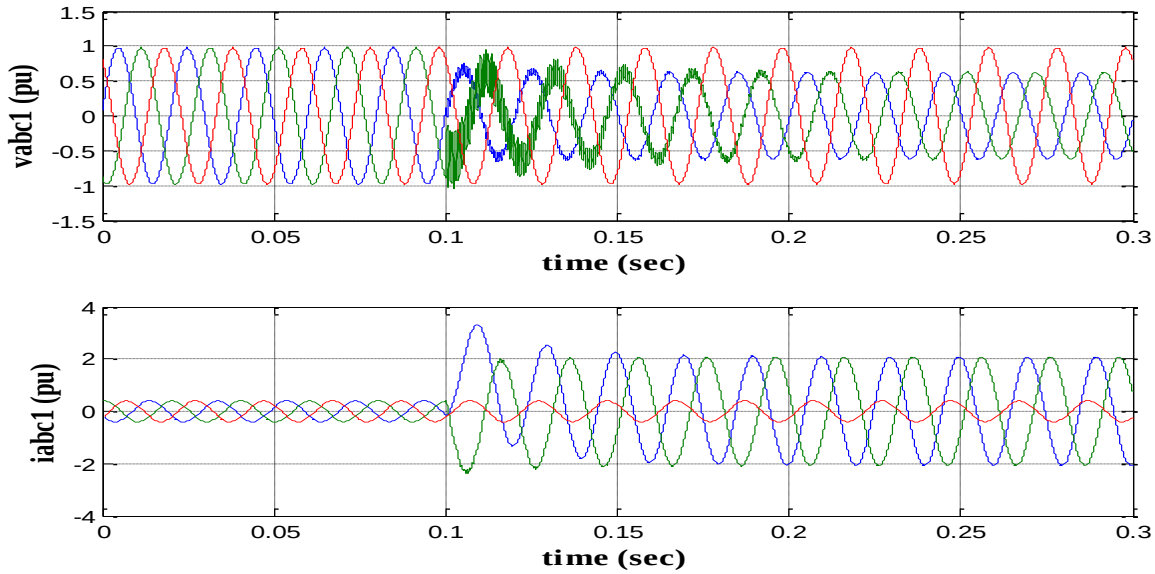

Figure 4.38 V_{abc1} and I_{abc1} of Pha-Phb-Gnd during short-circuit

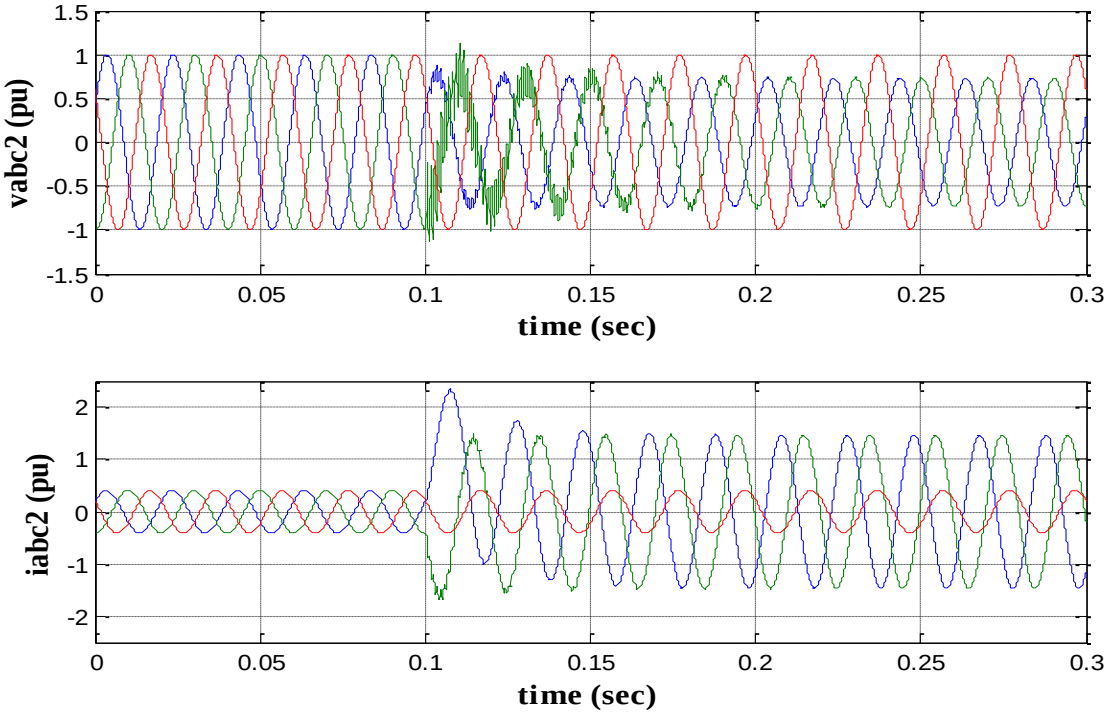

Figure 4.39 Voltages V_{abc2} and currents I_{abc2} of Pha-Phb-Gnd during short-circuit

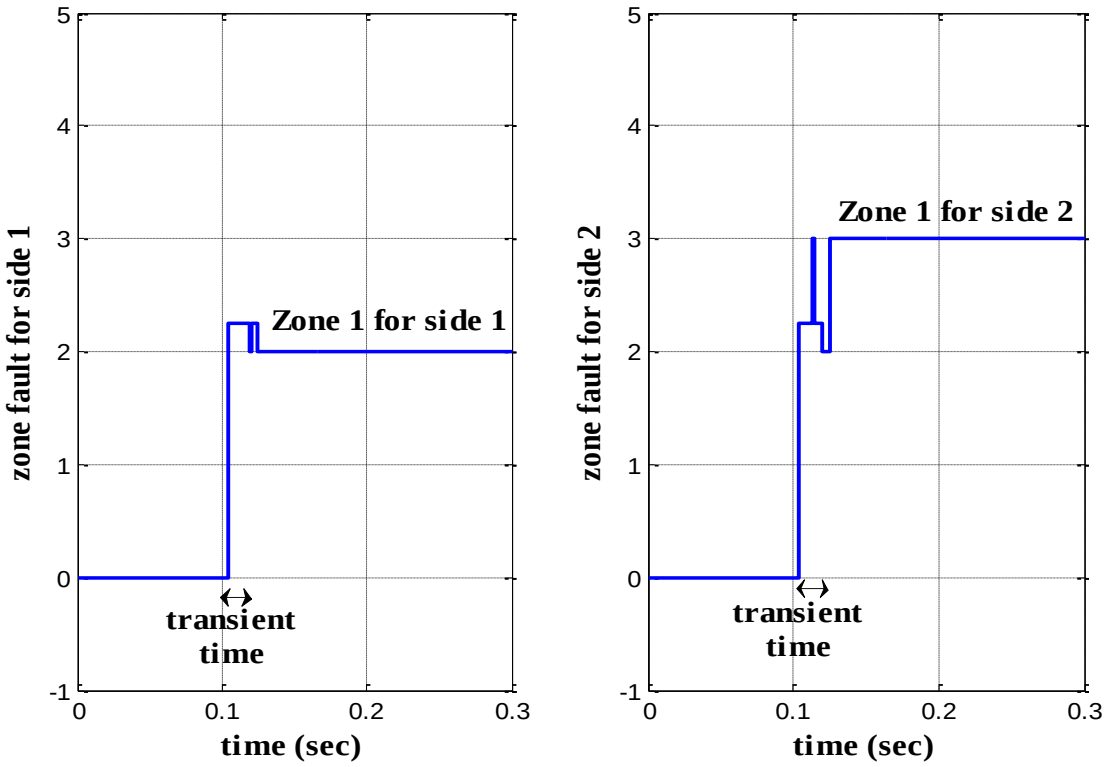

Figure 4.40 SC Pha-Phb-Gnd fault zone detection

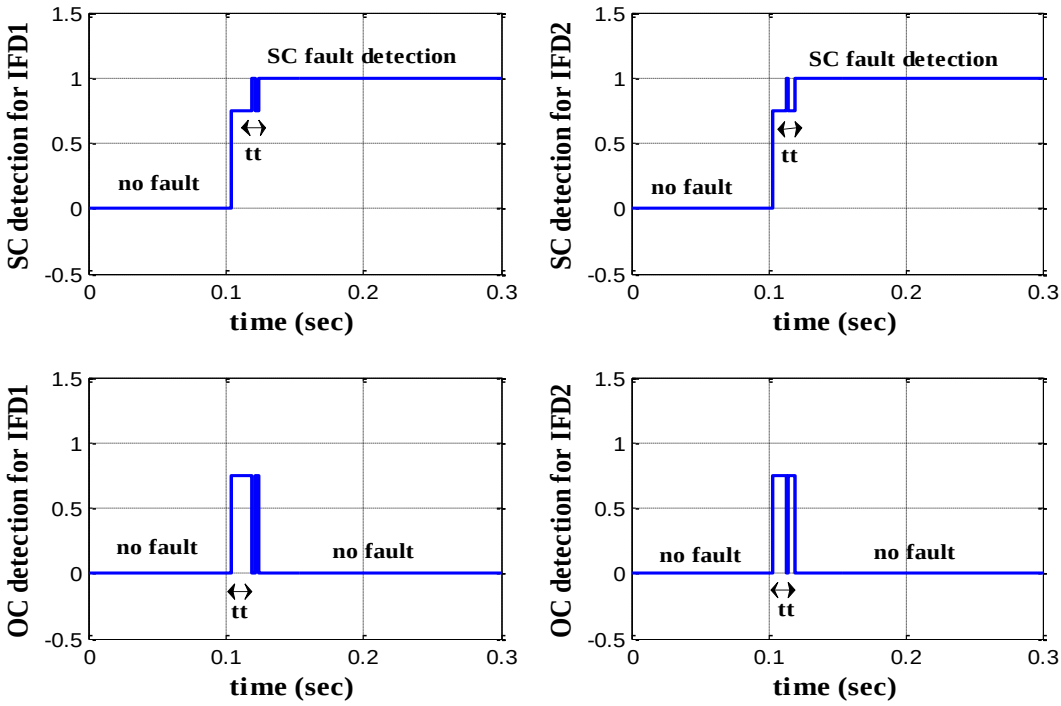

Figure 4.41 Identification of the fault type (SC to sides)

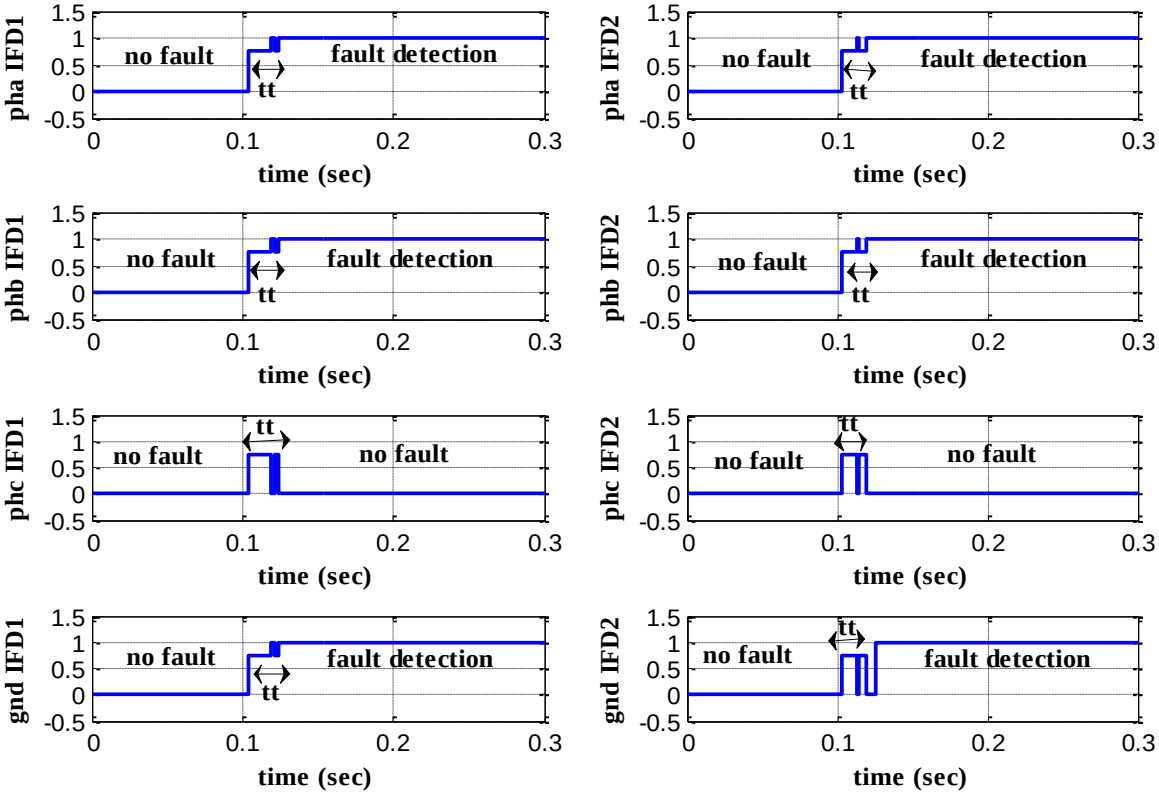

Figure 4.42 Identification of faulty phase (Pha-Phb-GND)

4.8.1.2.2 Short circuit fault displacement by 15 km (Ph_a-ph_b-Gnd)

A similar fault type is applied but with a 15 km displacement toward side 2 (zone 2). We obtain practically the same variations of electrical characteristics (Figs 4.43 and 4.44) and the same signatures (Figs 4.45, 4.46 and 4.47).

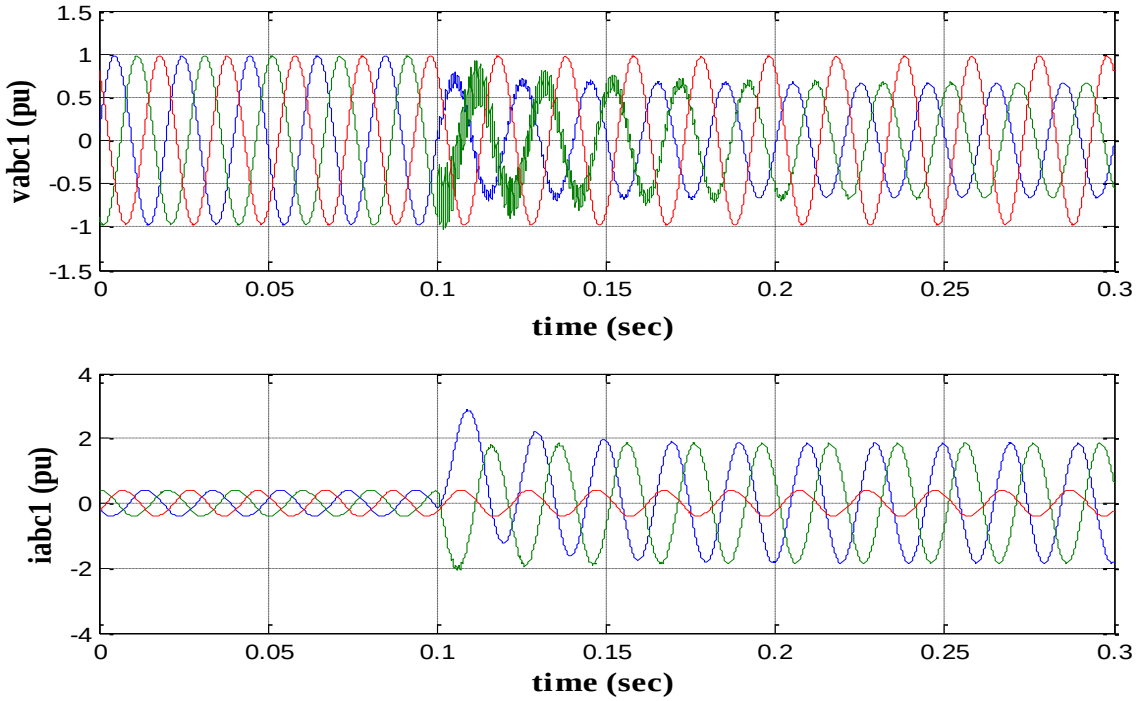

Figure 4.43 V_{abc1} and I_{abc1} of Phag-Phbg during short-circuit (by 15 km)

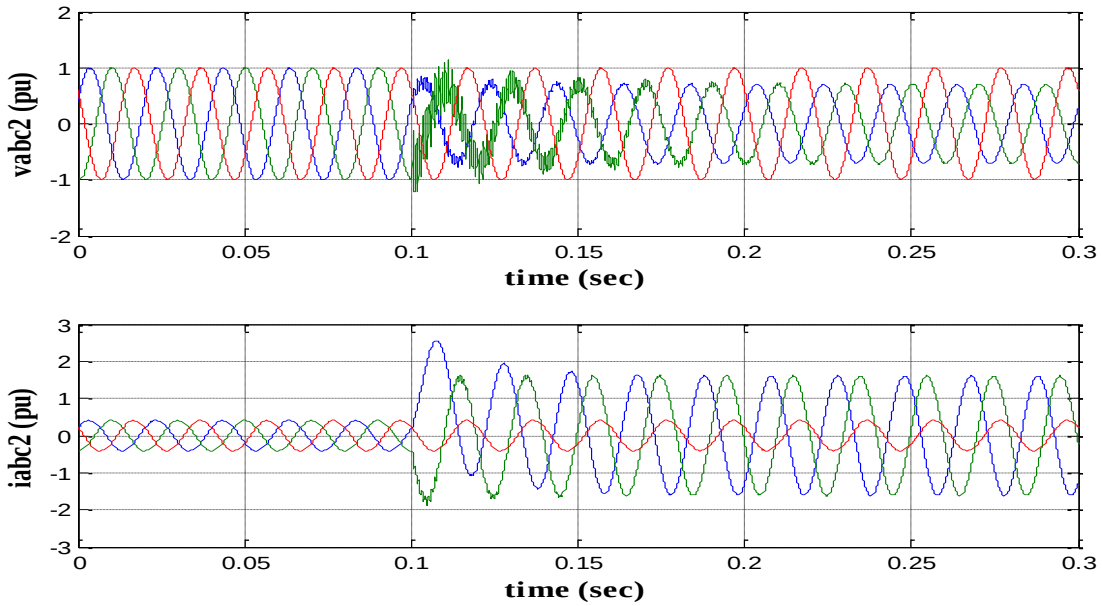

Figure 4.44 V_{abc2} and I_{abc2} of Phag-Phbg during short-circuit (by 15 km)

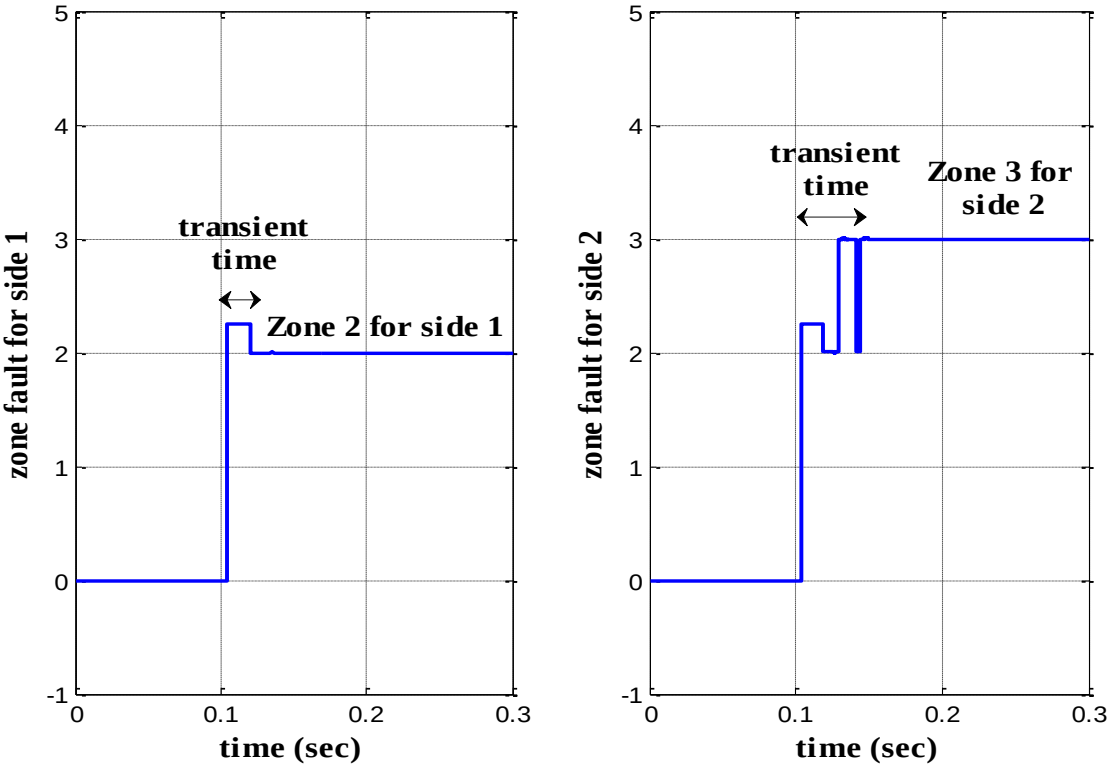

Figure 4.45 Zone detection of Phag-Phbg SC (by 15 km)

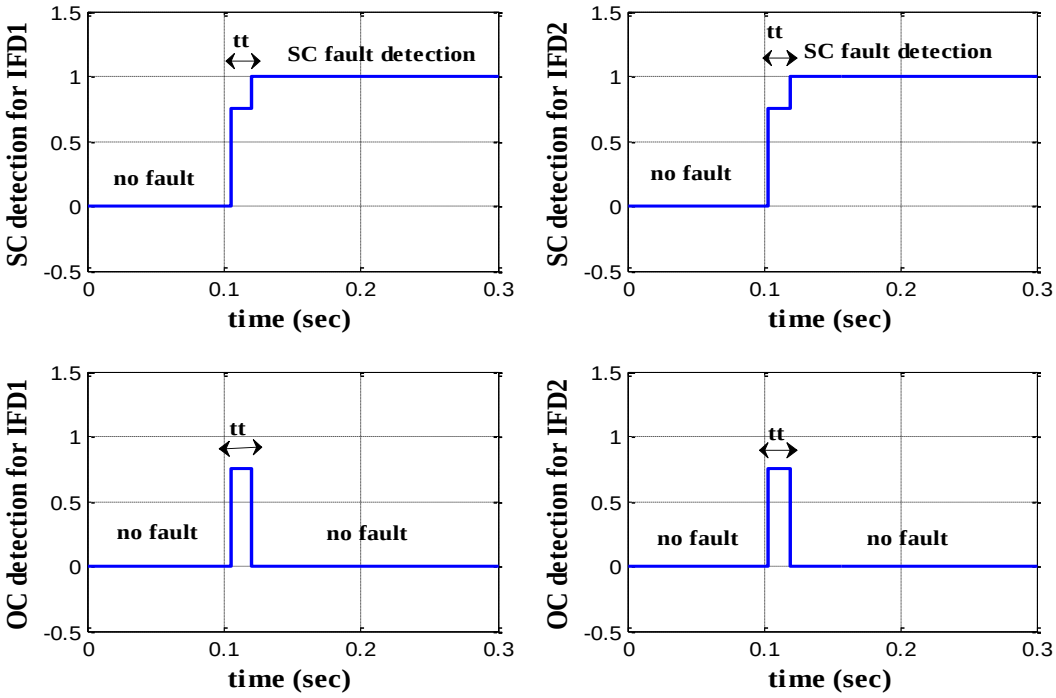

Figure 4.46 Identification of the fault type short-circuit to both sides (by 15 km)

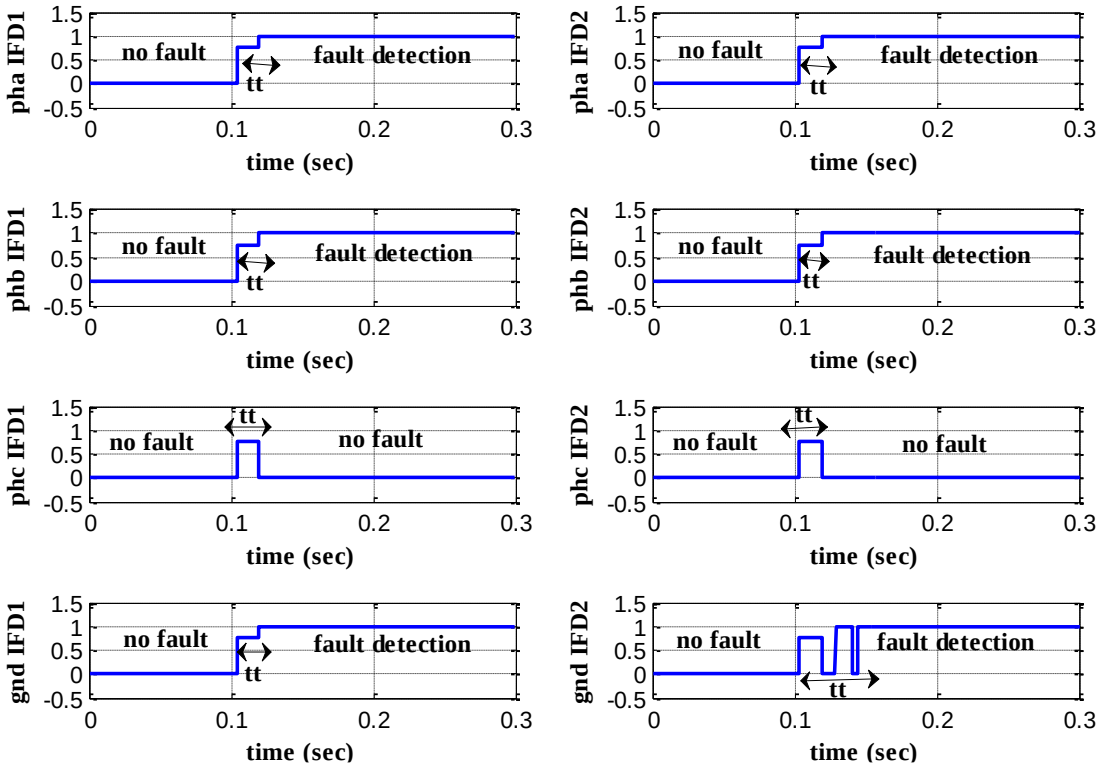

Figure 4.47 Identification of the faulty phase Phag-Phbg short-circuit (by 15 km).

4.8.1.3 Faults detection in zone 3

4.8.1.3.1 Short circuit fault of Pha-phb

Applying a two-phase short circuit fault of phase (a) and phase (b), as shown in figures 4.48 and 4.49: The fuzzy logic detects an SC fault in zone 3, on phases (a) and (b), see figures 4.50, 4.51 and 4.52.

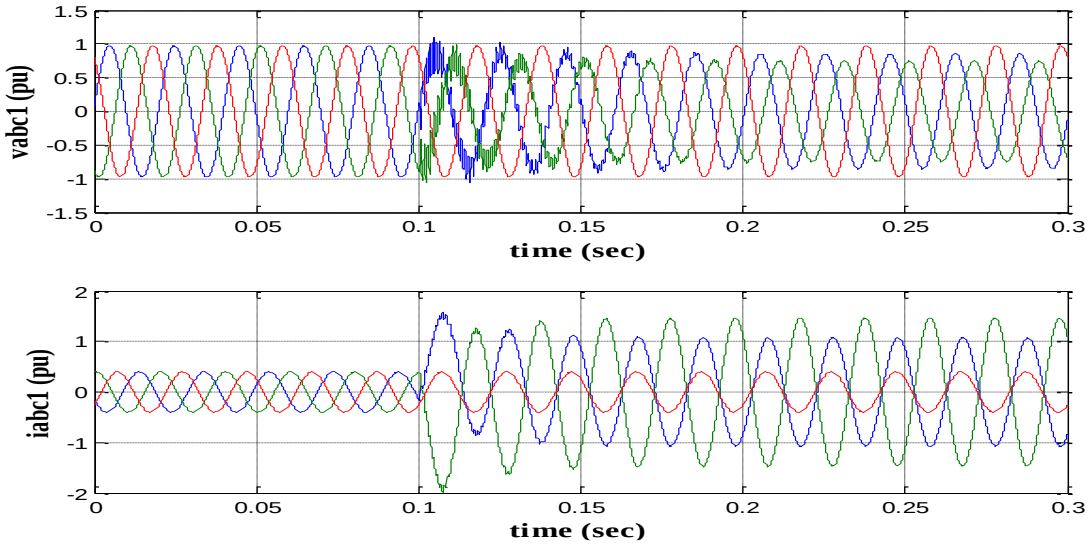

Figure 4.48 Voltages V_{abc1} and currents I_{abc1} of Pha-Phb during short-circuit

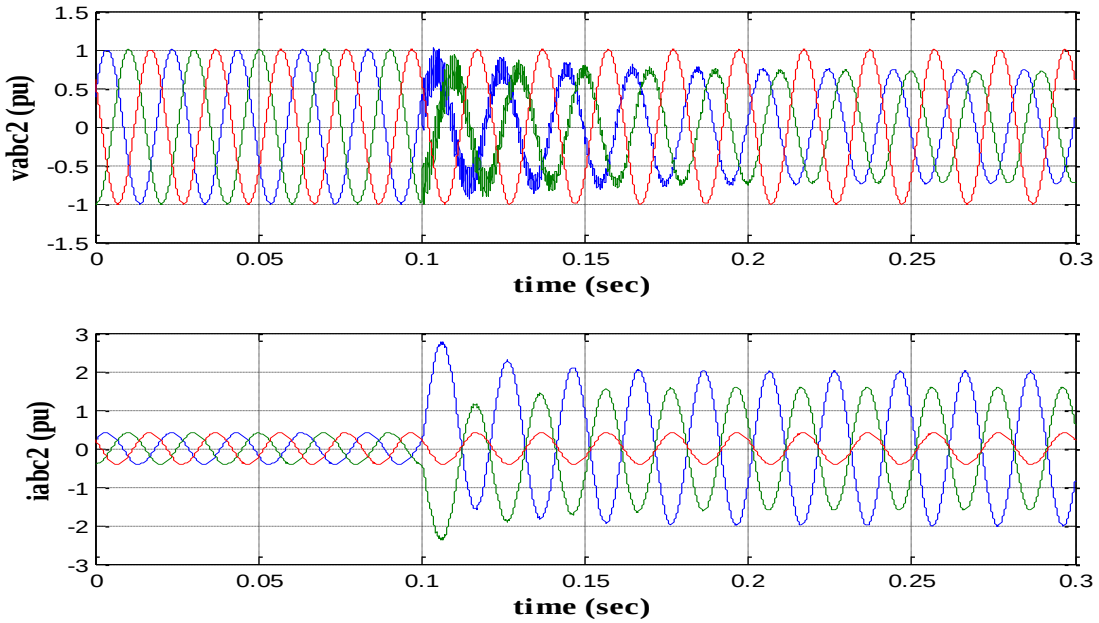

Figure 4.49 V_{abc2} and I_{abc2} of Pha-Phb during short-circuit

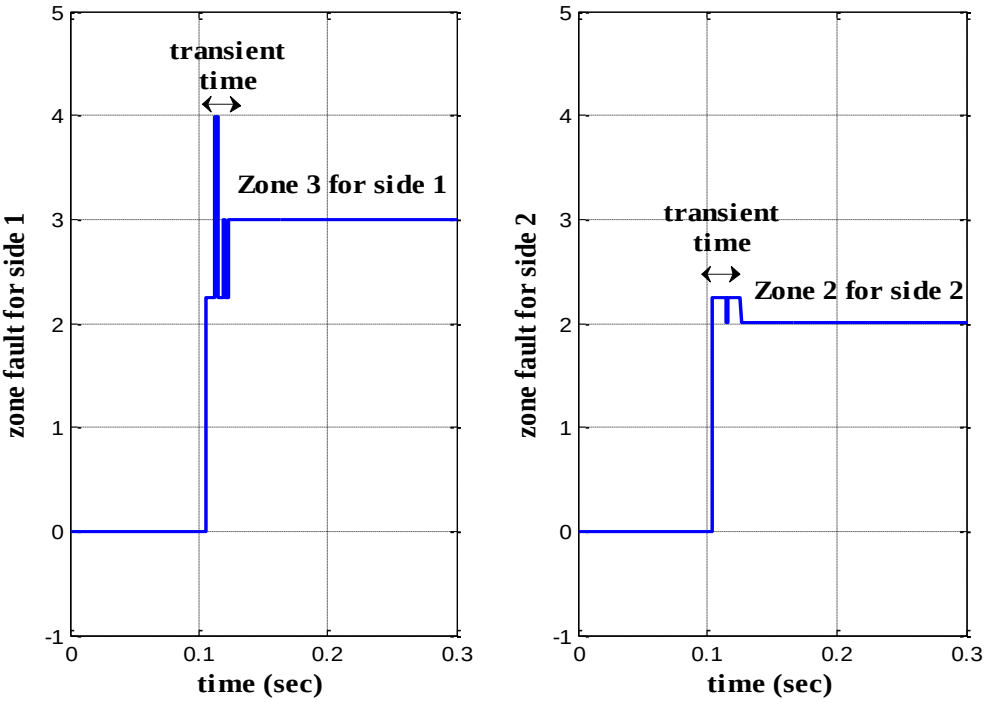

Figure 4.50 SC Ph_a-Ph_b fault zone detection

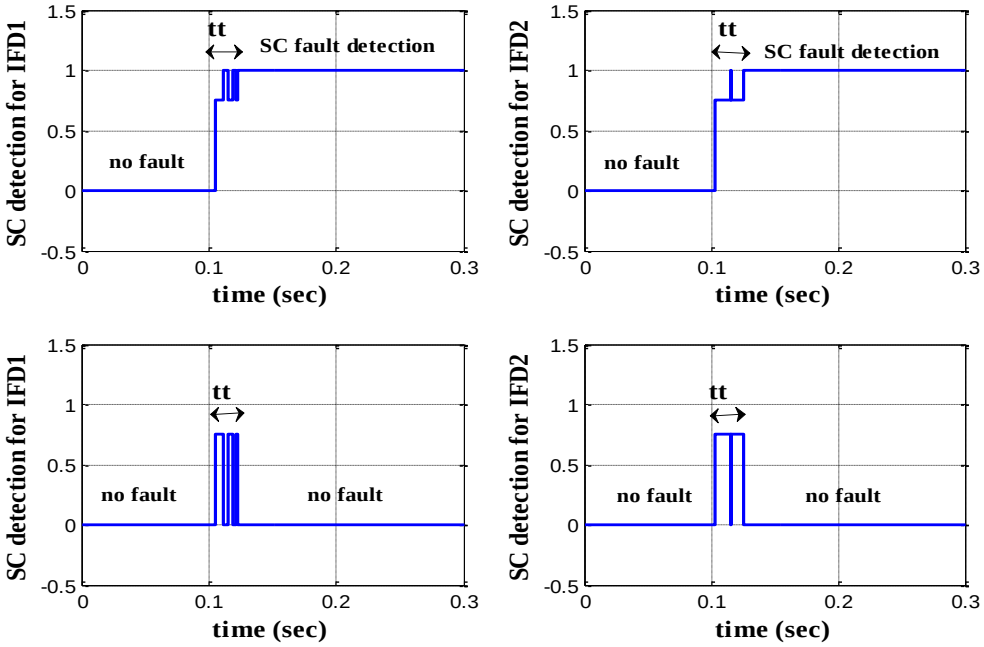

Figure 4.51 Identification of the fault type (short-circuit to both Sides)

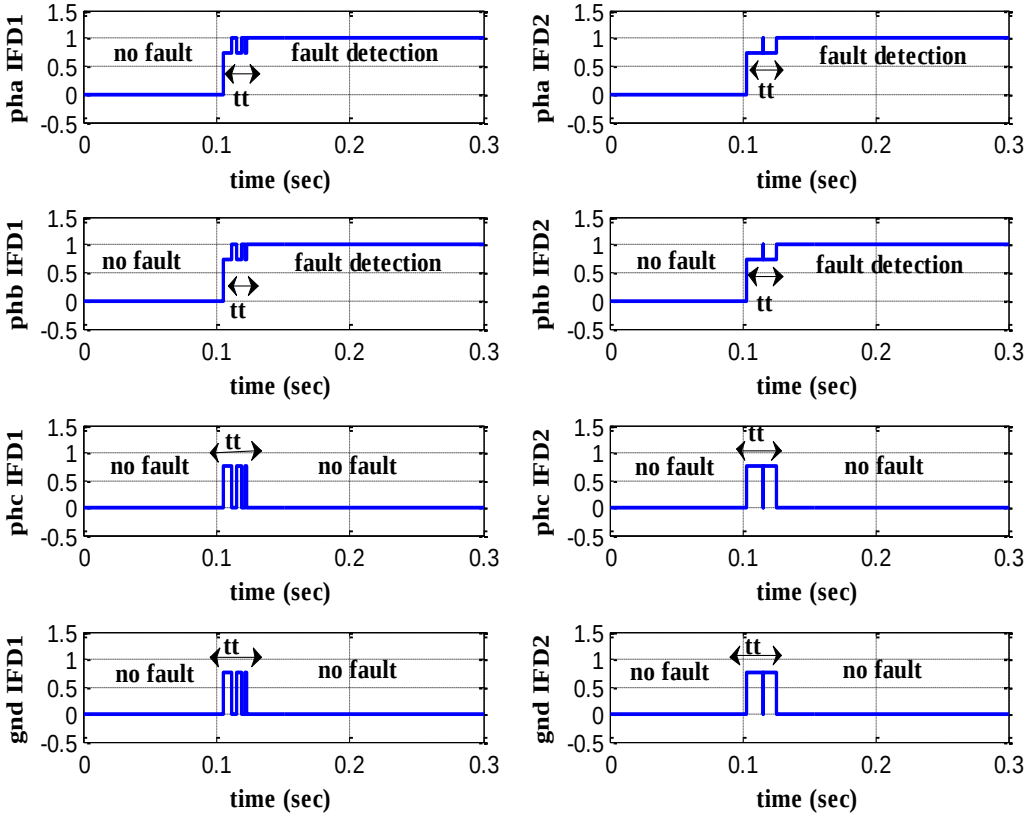

Figure 4.52 Identification of the fault phase (Ph_a-Ph_b)

4.8.2 Robustness test

Under the same conditions as in Chapter 03, two tests fault resistance variation and load variation are used to evaluate the robustness of fuzzy logic.

4.8.2.1 Resistant short circuit fault (at 15 Ω) in zone2 (pha-GND-Side1)

In zone 2 on side 1, a single phase (LG) resistive short-circuit fault (15 Ω) is applied.: Fault signaling remains correct (Figs 4.55, 4.56 and 4.57) despite variations in fault current and voltage (Figs 4.53 and 4.54).

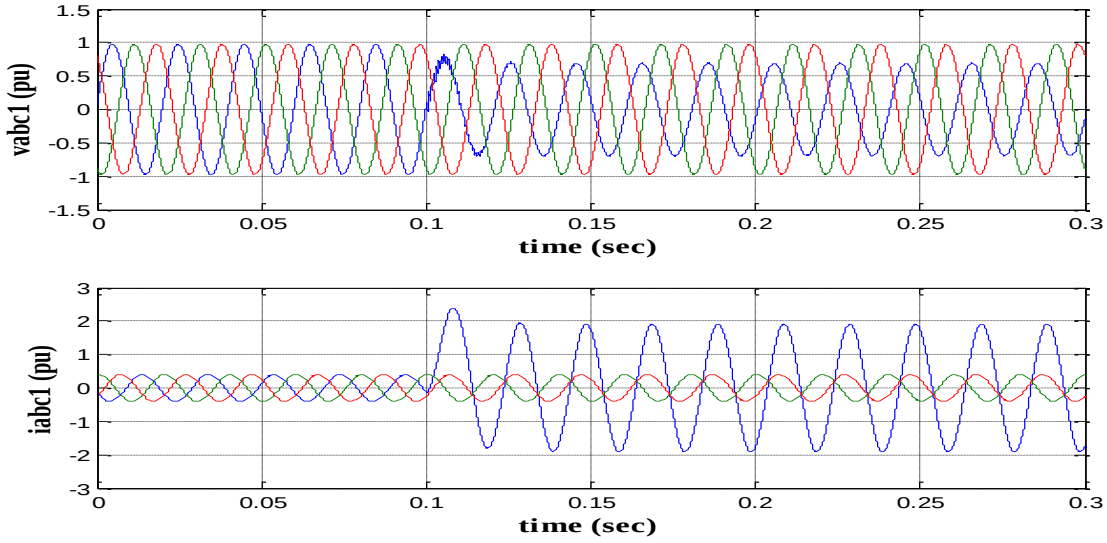

Figure 4.53 V_{abc1} and I_{abc1} of SC fault (at 15 Ω).

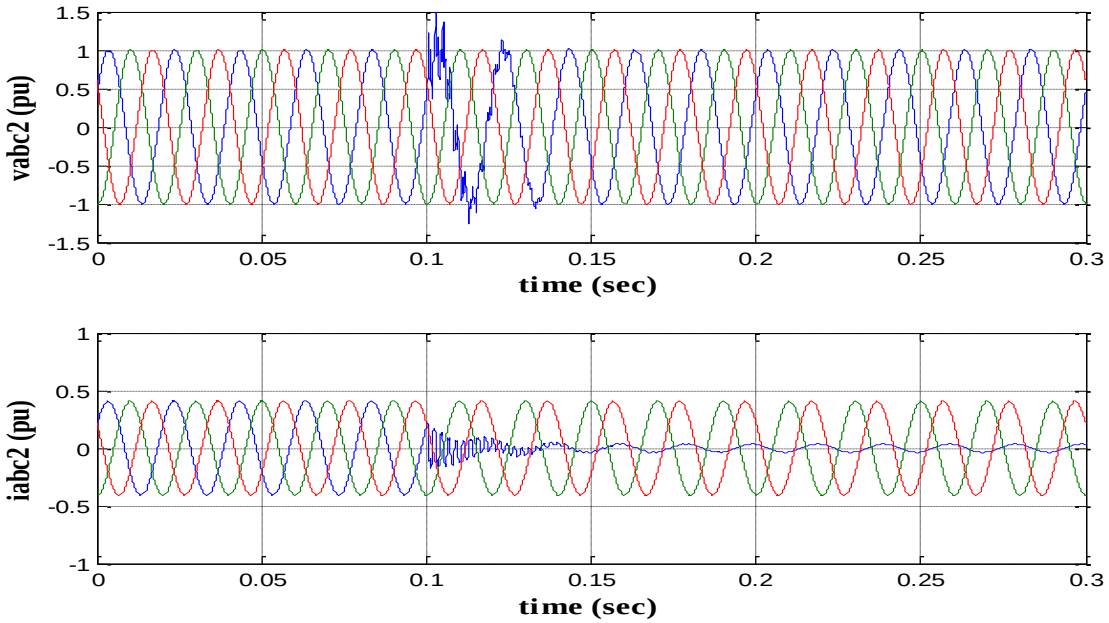

Figure 4.54 Voltages V_{abc1} and currents I_{abc1} of SC fault (at 15 Ω) of Pha-GND-Side1

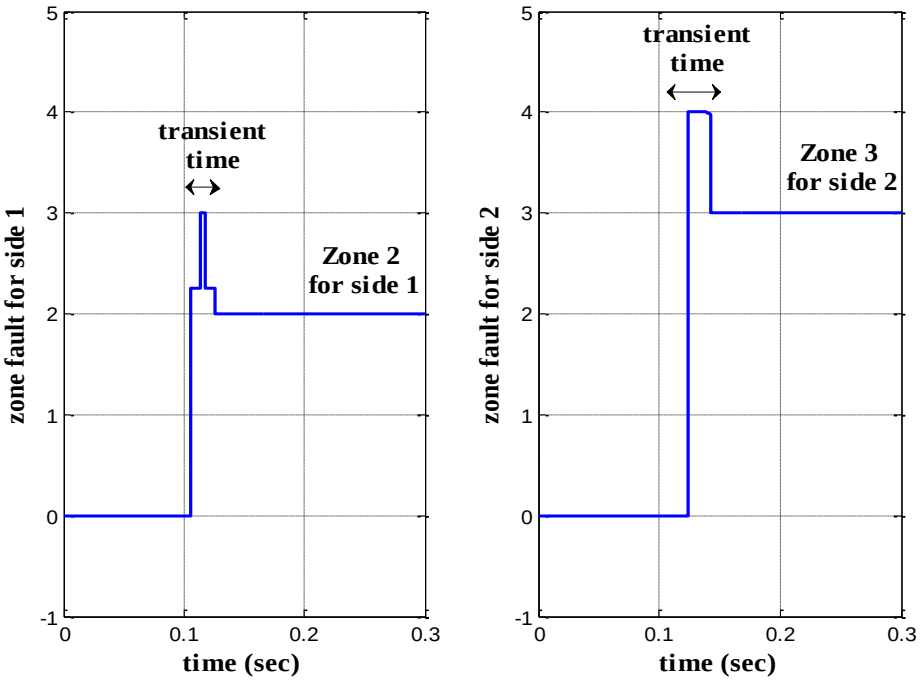

Figure 4.55 Zone detection of short-circuit to side1 (at 15 Ω)

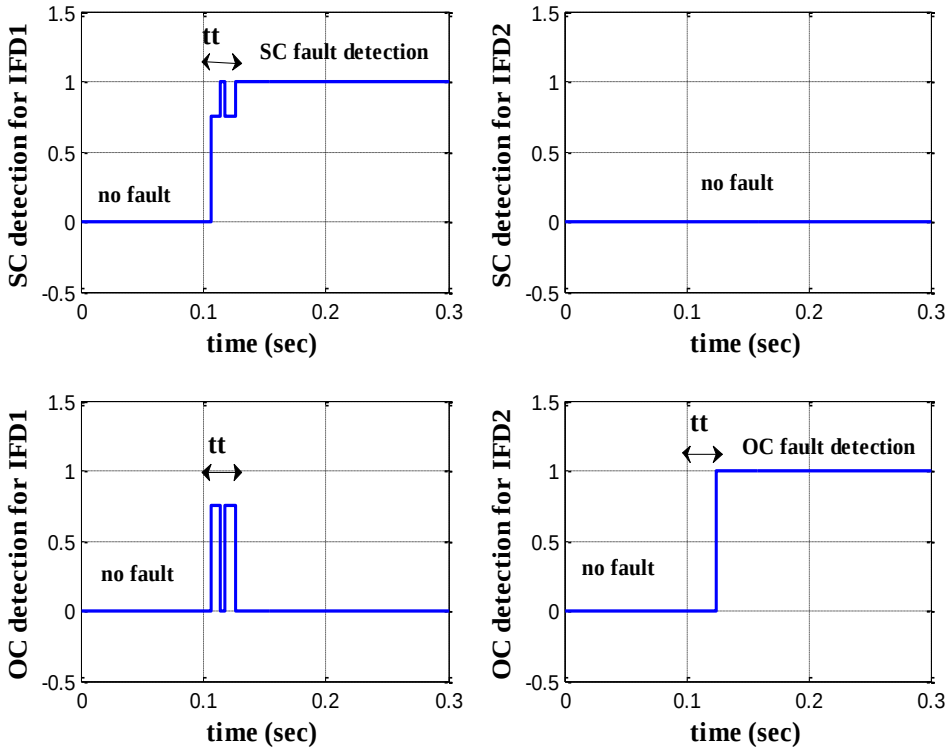

Figure 4.56 Identification of the fault type (SC to Side1 and OC to Side2): at 15 Ω

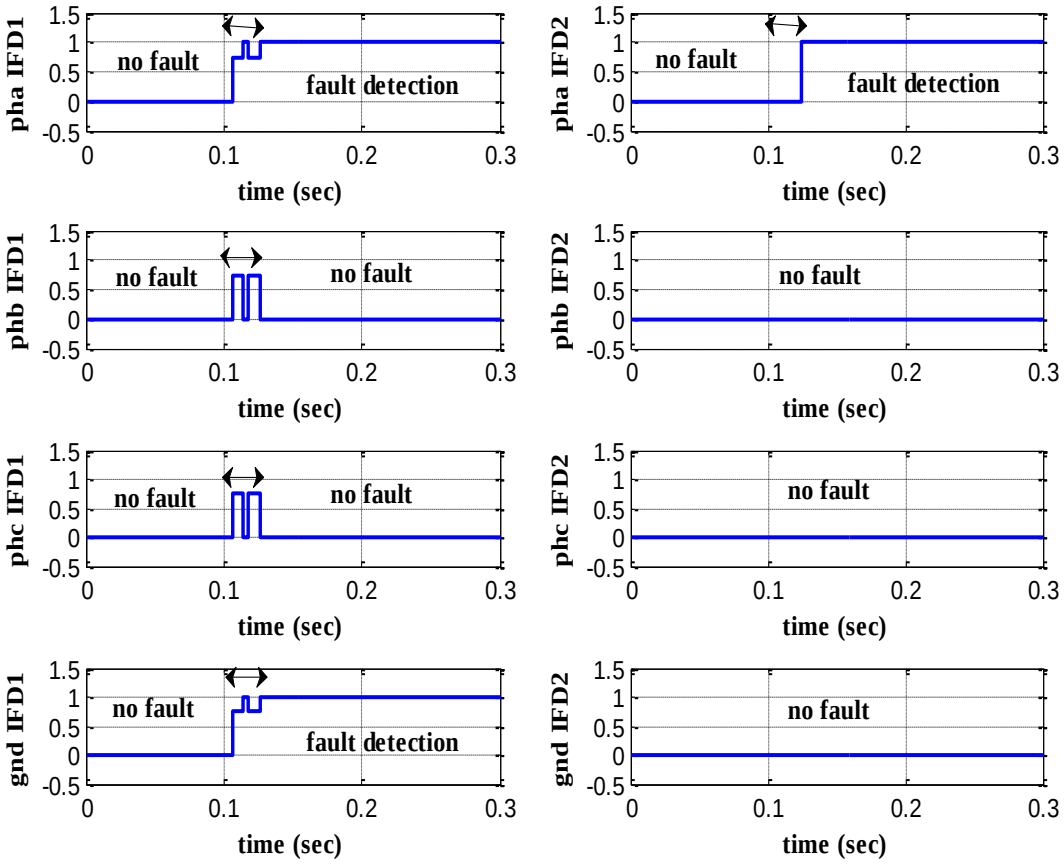

Figure 4.57 Identification of faulty phase (Ph_{ag}): of 15 Ω resistance

4.8.2.2 Short circuit fault Ph_a–GND (zone 2) with load variation of power network (Angle variation from 27º to 10º)

By shifting source 2's voltage phase angle from 27º to 10º, further disturbance has been added in form of a change in the load or the amount of power being delivered by the transmission line. The same current and voltage variations are observed in both sides of the networks (Figs 4.58 and 4.59). And a correct signalling of fault on figures 4.60, 4.61 and 4.62 because of the robustness of diagnosis by the fuzzy logic.

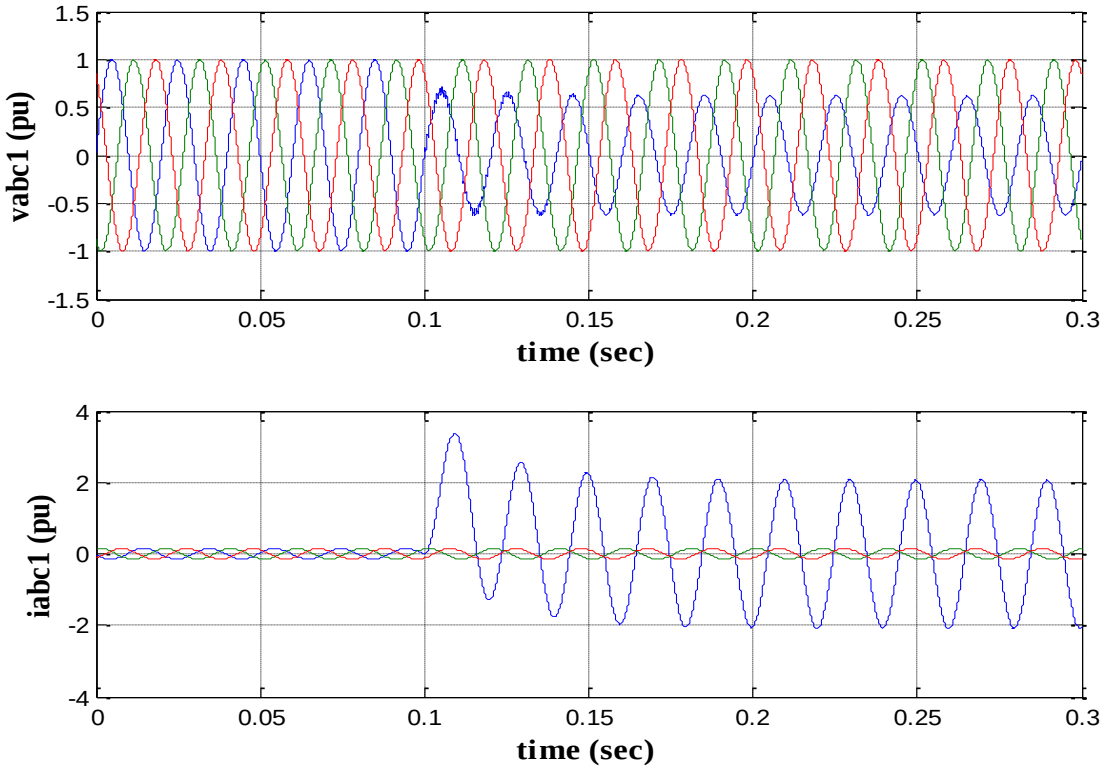

Figure 4.58 Voltages V_{abc1} and currents I_{abc1} of Phag short-circuit to side1(load variation)

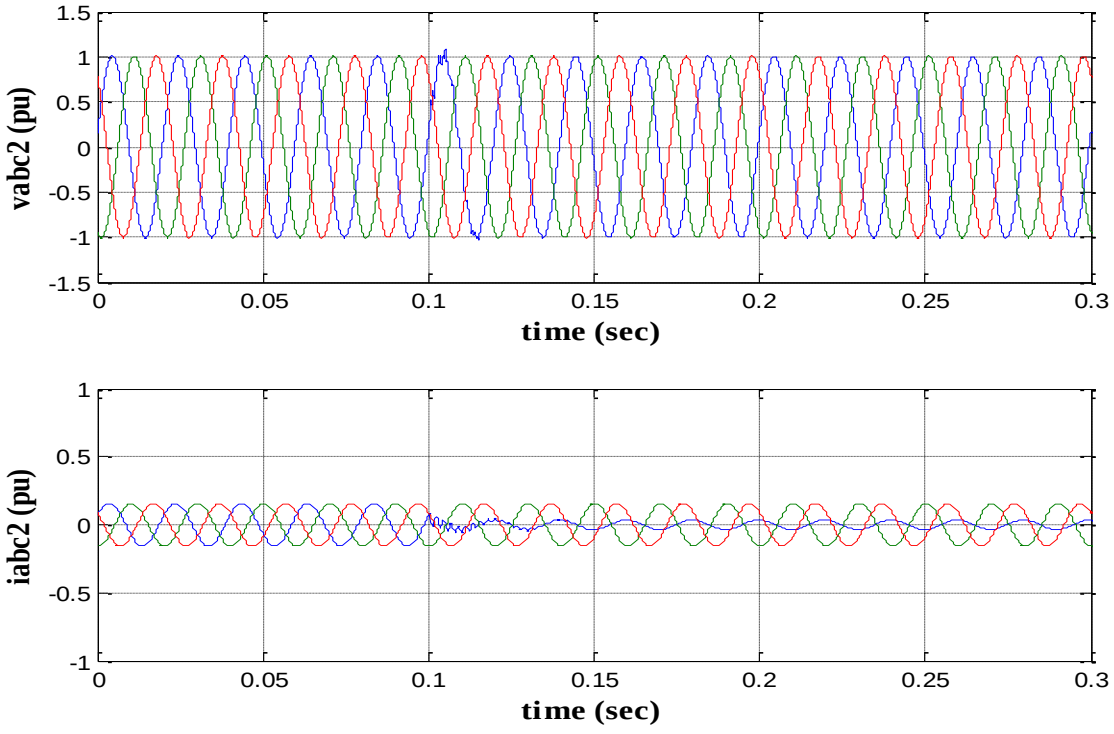

Figure 4.59 Voltages V_{abc2} and currents I_{abc2} of Phag short-circuit to side2(load variation)

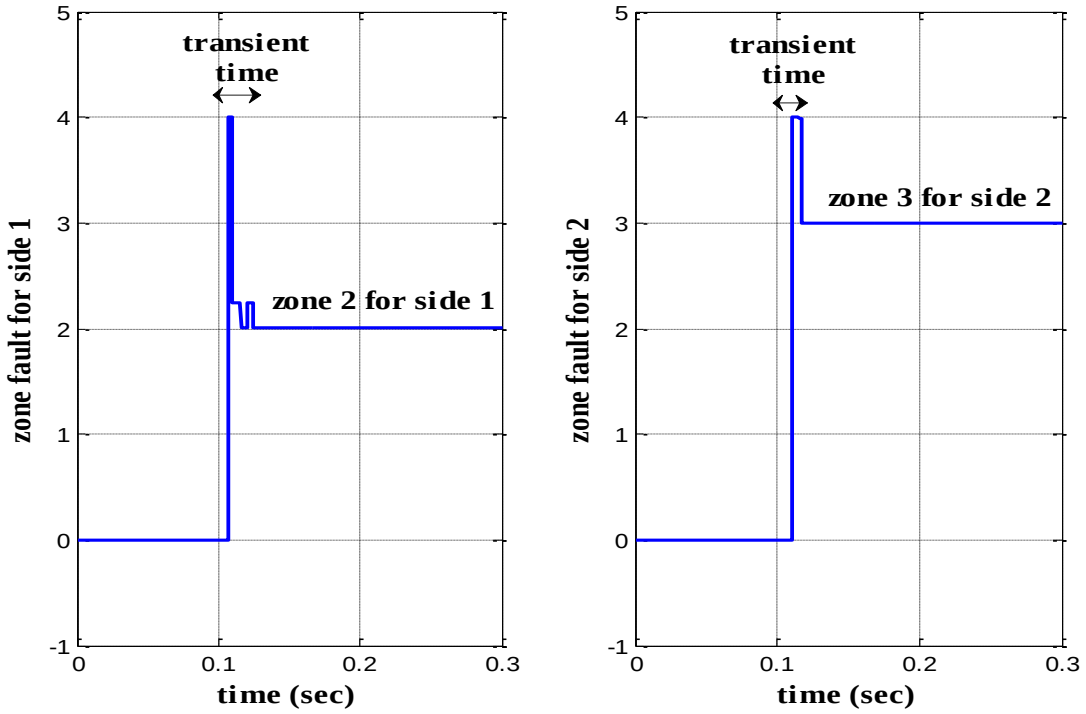

Figure 4.60 SC Ph_a-GND-Side1 fault zone detection (For load variation)

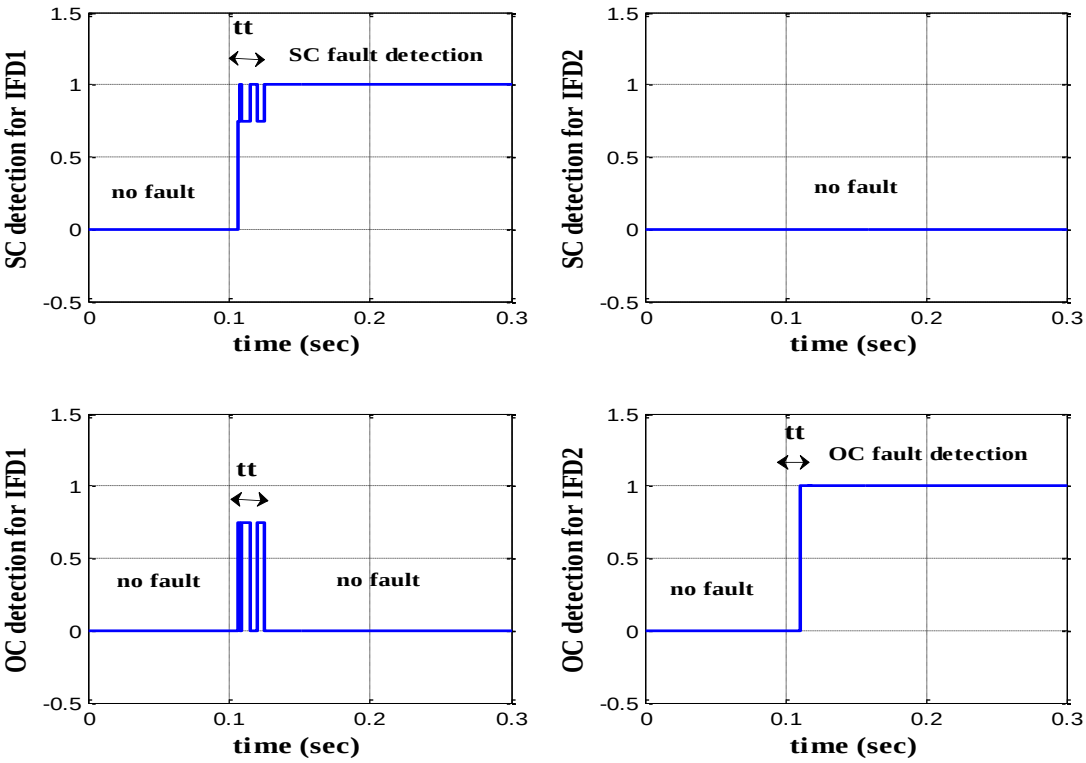

Figure 4.61 Identification of the fault type (SC-Side1 and OC-Side2): For load variation

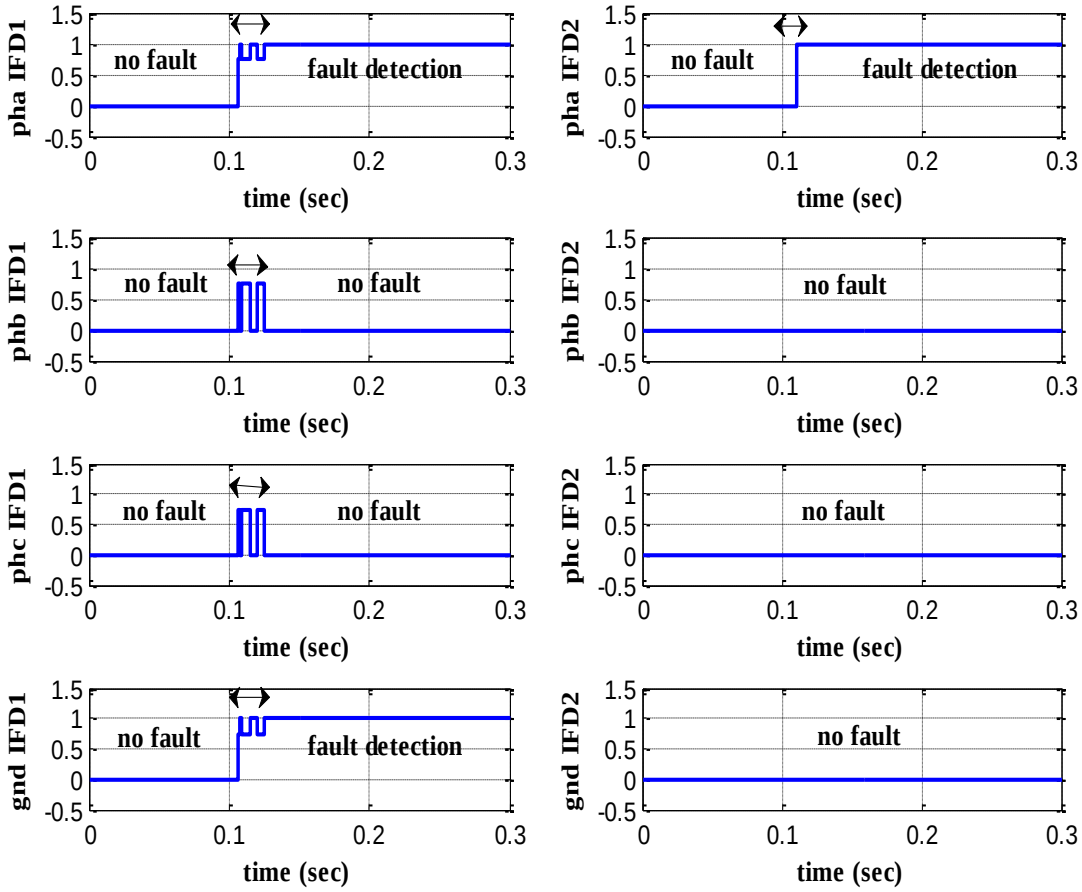

Figure 4.62 Identification of the fault phase (Pha-GND-Side1): For load variation

4.9 Conclusion

This chapter presents fuzzy logic method for detection, classification and faults location in power transmission line. Similarly, with the artificial neural network in chapter 03, The fuzzy logic technique offers the significant benefit of minimizing computation time and enhancing performance. The analysis of the results shows the advantage of diagnostic robustness by fuzzy logic.

General Conclusion

In this thesis a several methods have been proposed in objective of fault detection, type classification and fault zone location in power system transmission lines, a test power system is used in Matlab environment and analyzed under different fault conditions to compare between the different diagnosis methods and analyze their performances as two signal based diagnosis method are used (Park's vectors and Wavelet transform) in addition to two artificial intelligent methods(artificial neural network ANN method and fuzzy logic FL method).

In the first part, we have showed the stat of the art of diagnosis the fault in industrial systems starting with some terminologies and concepts. then we have presented the most used diagnosis methods in general.

The detection, classification, and location of transmission line short-circuit faults by Park's vectors is presented in chapter two. different transmission line conditions have been investigated, with the ideal condition having a particular Park circle shape and each form of a fault in the transmission line having a unique circumferential thickness and circle shape. For the same objective discrete wavelet transform DWT is used, the detail coefficients are obtained by decomposition the current signals at one end, these coefficients are calculated to six levels of DWT and used as a fault indicator when the detail coefficient is greater than a well determined threshold, in both methods, we found difficulties for the instantaneous and fast signaling of faults, for this the artificial intelligence algorithms are introduced in chapters three and four.

Chapters three and four present two methods for detection, classification and faults location in power transmission line, the first method is ANN in chapter three and the second is the FL in chapter four. The proposed methods directly work on the amplitudes of the three-phase voltages and currents rather than relying on complex feature extraction processes. This technique, combined with a novel training strategy that only uses a small number of training samples, has the significant advantage of speeding up computation and enhancing performance.

The results demonstrate that both techniques accurately classify faults for all fault types and complete the fault detection, classification, and localization in less than 20 ms after the fault occurs. Both approaches were put to the test under various conditions, including various load angle variations, various fault types, as well as varied fault resistances. The results indicate that both of these modern techniques present a robust performance and reliable to implement in smart grids.in

addition both are fast (response time 20 ms), economical as they do not require a complex computational costs. And precise (The fault zone is correctly located when the fault occurs on the boundaries of the zone and include a wide variety of fault resistance). Additionally, both have the benefit of high generalizability as they are both simple to implement on any power grid.

In perspective, this work can be continued and completed to improve the speed and the diagnostic systems:

- Experimental implementation of these diagnostic systems in a real electrical micro grid and Integration of high-performance real-time controllers (dSPACE, FPGA, DSP ...).
- Introduction of new strategies and new algorithms such as the neuro-fuzzy and SVM for the diagnosis of faults.
- Investigation to diagnose another types of faults and disturbances in power system.
- Investigation to use the artificial intelligence to diagnose the HVDC transmission lines.
- Introduction of redundant diagnosis systems for faults in the transmission lines.

Bibliography

1. Prasad, A., J. Belwin Edward, and K. Ravi, *A review on fault classification methodologies in power transmission systems: Part—I.* Journal of Electrical Systems and Information Technology, 2018. **5**(1): p. 48-60.
2. Das, A.M.P.K.K.A., *Transmission Line Faults in Power System and the Different Algorithms for Identification, Classification and Localization: A Brief Review of Methods.* 2020.
3. Samantaray, S.R., *A systematic fuzzy rule based approach for fault classification in transmission lines.* Applied Soft Computing, 2013. **13**(2): p. 928-938.
4. Taheri, R., M. Eslami, and Y. Damchi, *A current-based algorithm for one-end fault location in series capacitor compensated double-circuit transmission lines.* Computers and Electrical Engineering, 2023. **106**: p. 108618.
5. Ghorbani, A., M. Sanaye-Pasand, and H. Mehrjerdi, *Accelerated distance protection for transmission lines based on accurate fault location.* Electric Power Systems Research, 2021. **193**: p. 107021.
6. Lu, D., et al., *Unsynchronized fault location on untransposed transmission lines with fully distributed parameter model considering line parameter uncertainties.* Electric Power Systems Research, 2022. **202**: p. 107622.
7. Mitra, S., R. Mukhopadhyay, and P. Chattopadhyay, *PSO driven designing of robust and computation efficient 1D-CNN architecture for transmission line fault detection.* Expert Systems with Applications, 2022. **210**: p. 118178.
8. Biswas, S., et al., *An intelligent fault detection and classification technique based on variational mode decomposition-CNN for transmission lines installed with UPFC and wind farm.* Electric Power Systems Research, 2023. **223**: p. 109526.
9. Ayambire, P.N., et al., *An Improved Fault Detection Method for Overhead Transmission Lines Based on Differential Tunnel Magnetoresistive Sensor Array Approach.* IEEE Canadian Journal of Electrical and Computer Engineering, 2022. **45**(4): p. 409-417.
10. Di Santo, S.G. and C.E.d.M. Pereira, *Fault location method applied to transmission lines of general configuration.* International Journal of Electrical Power & Energy Systems, 2015. **69**: p. 287-294.

11. Ghorbani, A., M. Sanaye-Pasand, and H. Mehrjerdi, *Accelerated distance protection for transmission lines based on accurate fault location.* Electric Power Systems Research, 2021. **193**.
12. Moravej, Z., M. Pazoki, and M. Khederzadeh, *New smart fault locator in compensated line with UPFC.* International Journal of Electrical Power & Energy Systems, 2017. **92**: p. 125-135.
13. Taheri, R., M. Eslami, and Y. Damchi, *Single-end current-based algorithm for fault location in series capacitor compensated transmission lines.* International Journal of Electrical Power & Energy Systems, 2020. **123**.
14. Alencar, G.T.d., R.C.d. Santos, and A. Neves, *A new robust approach for fault location in transmission lines using single channel independent component analysis.* Electric Power Systems Research, 2023. **220**: p. 109281.
15. Mousaviyan, I., S.G. Seifossadat, and M. Saniei, *An Ultra-High-Speed Algorithm for Fault Classification in Double Circuit Transmission Lines Using Only the First Group of Received Current Traveling Waves.* Electric Power Systems Research, 2022. **206**: p. 107841.
16. Lopes, F.V., et al., *Accurate Two-Terminal Transmission Line Fault Location Using Traveling Waves.* IEEE Transactions on Power Delivery, 2018. **33**(2): p. 873-880.
17. Parsi, M., et al., *Wavelet based fault location on power transmission lines using real-world travelling wave data.* Electric Power Systems Research, 2020. **186**.
18. Gonzalez-Sanchez, V.H., V. Torres-García, and D. Guillen, *Fault location on transmission lines based on travelling waves using correlation and MODWT.* Electric Power Systems Research, 2021. **197**.
19. Mamiş, M.S., M. Arkan, and C. Keleş, *Transmission lines fault location using transient signal spectrum.* International Journal of Electrical Power & Energy Systems, 2013. **53**: p. 714-718.
20. Abd el-Ghany, H.A., A.M. Azmy, and A.M. Abeid, *A General Travelling-Wave-Based Scheme for Locating Simultaneous Faults in Transmission Lines.* IEEE Transactions on Power Delivery, 2020. **35**(1): p. 130-139.
21. Ding, J., et al., *Distributed Traveling-Wave-Based Fault-Location Algorithm Embedded in Multiterminal Transmission Lines.* IEEE Transactions on Power Delivery, 2018. **33**(6): p. 3045-3054.

22. Akmaz, D., et al., *Transmission line fault location using traveling wave frequencies and extreme learning machine.* Electric power systems research, 2018. **155**: p. 1-7.
23. Naidu, O.D. and A.K. Pradhan, *A Traveling Wave-Based Fault Location Method Using Unsynchronized Current Measurements.* IEEE Transactions on Power Delivery, 2019. **34**(2): p. 505-513.
24. Ghazizadeh-Ahsaee, M., *Time-domain based fault location for series compensated transmission lines without requiring fault type.* Electric Power Systems Research, 2020. **181**.
25. Saber, A., et al., *Time-Domain Fault Location Algorithm for Double-Circuit Transmission Lines Connected to Large Scale Wind Farms.* IEEE Access, 2021. **9**: p. 11393-11404.
26. Kumar, B.R., et al., *Phase angle-based fault detection and classification for protection of transmission lines.* International Journal of Electrical Power & Energy Systems, 2021. **133**.
27. Ji, L., et al., *A New Single Ended Fault Location Method for Transmission Line Based on Positive Sequence Superimposed Network during Auto Reclosing.* IEEE Transactions on Power Delivery, 2019: p. 1-1.
28. Fan, R., et al., *Precise Fault Location on Transmission Lines Using Ensemble Kalman Filter.* IEEE Transactions on Power Delivery, 2018. **33**(6): p. 3252-3255.
29. Shaik, A.G. and R.R.V. Pulipaka, *A new wavelet based fault detection, classification and location in transmission lines.* International Journal of Electrical Power & Energy Systems, 2015. **64**: p. 35-40.
30. Krishnanand, K.R., P.K. Dash, and M.H. Naeem, *Detection, classification, and location of faults in power transmission lines.* International Journal of Electrical Power & Energy Systems, 2015. **67**: p. 76-86.
31. Naidu, O.D., A.K. Pradhan, and N. George, *A Hybrid Time-Domain Protection Scheme for Series Compensated Transmission Lines.* IEEE Transactions on Power Delivery, 2022. **37**(3): p. 1823-1833.
32. Liang, Y., et al., *Transmission line frequency-domain fault location method based on the phasor-time space curve characteristics that considers decaying DC deviation.* International Journal of Electrical Power & Energy Systems, 2022. **142**: p. 108308.
33. Kumar, B.R., et al., *Phase angle-based fault detection and classification for protection of transmission lines.* International Journal of Electrical Power & Energy Systems, 2021. **133**: p. 107258.

34. Han, J., et al., *Faulted-Phase classification for transmission lines using gradient similarity visualization and cross-domain adaption-based convolutional neural network.* Electric Power Systems Research, 2021. **191**.
35. Moradzadeh, A., et al., *Hybrid CNN-LSTM approaches for identification of type and locations of transmission line faults.* International Journal of Electrical Power & Energy Systems, 2022. **135**: p. 107563.
36. Bhuyan, A., et al. *Convolutional Neural Network Based Fault Detection for Transmission Line*. in *2022 International Conference on Intelligent Controller and Computing for Smart Power (ICICCSP)*. 2022.
37. Harish, A., A. Prince, and M.V. Jayan, *Fault Detection and Classification for Wide Area Backup Protection of Power Transmission Lines Using Weighted Extreme Learning Machine.* IEEE Access, 2022. **10**: p. 82407-82417.
38. Goni, M.O.F., et al., *Fast and Accurate Fault Detection and Classification in Transmission Lines using Extreme Learning Machine.* e-Prime - Advances in Electrical Engineering, Electronics and Energy, 2023. **3**: p. 100107.
39. Ogar, V.N., S. Hussain, and K.A.A. Gamage, *The use of artificial neural network for low latency of fault detection and localisation in transmission line.* Heliyon, 2023. **9**(2): p. e13376.
40. Rafique, F., L. Fu, and R. Mai, *End to end machine learning for fault detection and classification in power transmission lines.* Electric Power Systems Research, 2021. **199**.
41. Chen, K., J. Hu, and J. He, *Detection and Classification of Transmission Line Faults Based on Unsupervised Feature Learning and Convolutional Sparse Autoencoder.* IEEE Transactions on Smart Grid, 2016: p. 1-1.
42. Fathabadi, H., *Novel filter based ANN approach for short-circuit faults detection, classification and location in power transmission lines.* International Journal of Electrical Power & Energy Systems, 2016. **74**: p. 374-383.
43. Jiao, Z. and R. Wu, *A New Method to Improve Fault Location Accuracy in Transmission Line Based on Fuzzy Multi-Sensor Data Fusion.* IEEE Transactions on Smart Grid, 2019. **10**(4): p. 4211-4220.
44. T. Wang, G.Z., J. Zhao, Z. He, J. Wang and M. J. Pérez-Jiménez, *Fault Diagnosis of Electric Power Systems Based on Fuzzy Reasoning Spiking Neural P Systems.* IEEE Transactions on Power Systems, 2015. **30**.

45. Farshad, M. and J. Sadeh, *Accurate Single-Phase Fault-Location Method for Transmission Lines Based on K-Nearest Neighbor Algorithm Using One-End Voltage.* IEEE Transactions on Power Delivery, 2012. **27**(4): p. 2360-2367.
46. Chiang, L., E. Russell, and R. Braatz, *Fault Detection and Diagnosis in Industrial Systems*. 2001.
47. Isermann, R. and P. Ballé, *Trends in the application of model-based fault detection and diagnosis of technical processes.* Control Engineering Practice, 1997. **5**(5): p. 709-719.
48. Thomas, P., *Fault detection and diagnosis in engineering systems: Janos J. Gertler; Marcel Dekker Inc., New York, 1998, ISBN 0-8247-9427-3.* Control Engineering Practice, 2002. **10**(9): p. 1037-1038.
49. Gertler, J., *Analytical Redundancy Methods in Fault Detection and Isolation - Survey and Synthesis.* IFAC Proceedings Volumes, 1991. **24**(6): p. 9-21.
50. Samy, I. and D.-W. Gu, *Fault Detection and Isolation (FDI),* in *Fault Detection and Flight Data Measurement: Demonstrated on Unmanned Air Vehicles Using Neural Networks*, I. Samy and D.-W. Gu, Editors. 2011, Springer Berlin Heidelberg: Berlin, Heidelberg. p. 5-17.
51. Cardoso, A.J.M. and E. Saraiva, *The Use of Park's Vector in the Detection of Electrical Failures on Three-Phase Induction Motors*. 1987.
52. Boudiaf, M., L. Cherroun, and M. Benbrika, *Real-time diagnosis of three-phase induction machine using Arduino-Uno card based on park's circle method.* Diagnostyka, 2018. **19**(3): p. 63-71.
53. Heckbert, P.S. *Fourier Transforms and the Fast Fourier Transform (FFT) Algorithm*. 1998.
54. Graps, A., *"An Introduction to Wavelets".* IEEE Comp. Sci. Engi., 1995. **2**: p. 50-61.
55. Mendel, J.M., *Fuzzy logic systems for engineering: a tutorial.* Proceedings of the IEEE, 1995. **83**(3): p. 345-377.
56. Moraga, C., *Introduction to Fuzzy Logic*. Facta universitatis. Series electronics and energetics, 2005. **18**: p. 319-328.
57. Zadeh, L.A., *Fuzzy sets.* Information and Control, 1965. **8**(3): p. 338-353.
58. Uhrig, R.E. *Introduction to artificial neural networks*. in *Proceedings of IECON '95 - 21st Annual Conference on IEEE Industrial Electronics*. 1995.

59. *Artificial Neural Networks (ANNs)*, in *Condition Monitoring with Vibration Signals*. 2019. p. 239-258.
60. Khelifi, A., et al. *Artificial Neural Network-based Fault Detection*. in *2018 5th International Conference on Control, Decision and Information Technologies (CoDIT)*. 2018.
61. Tzafestas and Dalianis. *Fault diagnosis in complex systems using artificial neural networks*. in *1994 Proceedings of IEEE International Conference on Control and Applications*. 1994.
62. Ayoubi, M. and R. Isermann, *Neuro-fuzzy systems for diagnosis.* Fuzzy Sets and Systems, 1997. **89**(3): p. 289-307.
63. Frank, P.M., *Principles of Model-Based Fault Detection.* IFAC Proceedings Volumes, 1992. **25**(10): p. 213-220.
64. Patton, R.J. and J. Chen, *Observer-based fault detection and isolation: Robustness and applications.* Control Engineering Practice, 1997. **5**(5): p. 671-682.
65. Martínez-Sibaja, A., et al., *Dedicated Observer Scheme for Fault Diagnosis and Isolation in Instruments of an Anaerobic Reactor.* Procedia Technology, 2013. **7**: p. 173-180.
66. Frank, P.M., *Enhancement of Robustness in Observer-Based Fault Detection.* IFAC Proceedings Volumes, 1991. **24**(6): p. 99-111.
67. Duan, G.R., G.P. Liu, and S. Thompson, *Disturbance Attenuation in Luenberger Function Observer Designs — A Parametric Approach.* IFAC Proceedings Volumes, 2000. **33**(14): p. 41-46.
68. Besanöon, G., Q. Zhang, and H. Hammouri, *High-gain observer based state and parameter estimation in nonlinear systems.* IFAC Proceedings Volumes, 2004. **37**(13): p. 327-332.
69. Jiang, B., V. Cocquempot, and C. Christophe, *FAULT DIAGNOSIS USING SLIDING MODE OBSERVER FOR NONLINEAR SYSTEMS.* IFAC Proceedings Volumes, 2002. **35**(1): p. 71-76.
70. Isermann, R., *Fault diagnosis of machines via parameter estimation and knowledge processing—Tutorial paper.* Automatica, 1993. **29**(4): p. 815-835.
71. Weber, P., et al., *Multiple Fault Detection And Isolation.* IFAC Proceedings Volumes, 1999. **32**(2): p. 7903-7908.
72. Basseville, M., *Information criteria for residual generation and fault detection and isolation.* Automatica, 1997. **33**(5): p. 783-803.

73. Andanapalli, K. and B.R.K. Varma. *Park's transformation based symmetrical fault detection during power swing*. in *2014 Eighteenth National Power Systems Conference (NPSC)*. 2014.
74. Sm, S. and D.P.S. Raju, *Stator winding fault diagnosis of three-phase induction motor by Park's Vector Approach.* International Journal of Advanced Research in Electrical, Electronics and Instrumentation Engineering, 2013. **2**: p. 2901-2906.
75. Burriel-Valencia, J., et al. *Multilayer Park's vector approach, a method for fault detection on induction motors*. in *2015 IEEE International Conference on Industrial Technology (ICIT)*. 2015.
76. Touati, K.O.M., M. Boudiaf, and L. Cherroun. *Fault Diagnosis of Power Transmission Line usingPark's Method*. in *2022 19th International Multi-Conference on Systems, Signals & Devices (SSD)*. 2022.
77. Antonino-Daviu, J., et al., *Application and optimization of the discrete wavelet transform for the detection of broken rotor bars in induction machines.* Applied and Computational Harmonic Analysis, 2006. **21**(2): p. 268-279.
78. Sheikh, H., C. Prins, and E. Schrijvers, *Artificial Intelligence: Definition and Background*, in *Mission AI: The New System Technology*, H. Sheikh, C. Prins, and E. Schrijvers, Editors. 2023, Springer International Publishing: Cham. p. 15-41.
79. Walczak, S. and N. Cerpa, *Artificial Neural Networks*, in *Encyclopedia of Physical Science and Technology (Third Edition)*, R.A. Meyers, Editor. 2003, Academic Press: New York. p. 631-645.
80. Hopfield, J.J., *Artificial neural networks.* IEEE Circuits and Devices Magazine, 1988. **4**(5): p. 3-10.
81. Sadeeq, M.A.M. and A.M. Abdulazeez. *Neural Networks Architectures Design, and Applications: A Review*. in *2020 International Conference on Advanced Science and Engineering (ICOASE)*. 2020.
82. Schmidhuber, J., *Deep learning in neural networks: An overview.* Neural Networks, 2015. **61**: p. 85-117.
83. Venkatasubramanian, V., R. Vaidyanathan, and Y. Yamamoto, *Process fault detection and diagnosis using neural networks—I. steady-state processes.* Computers & Chemical Engineering, 1990. **14**(7): p. 699-712.
84. Haykin, S., *Neural Networks: A Comprehensive Foundation*. 1998: Prentice Hall PTR.

85. Grossberg, S., *Nonlinear neural networks: Principles, mechanisms, and architectures.* Neural Networks, 1988. **1**(1): p. 17-61.
86. Basheer, I.A. and M. Hajmeer, *Artificial neural networks: fundamentals, computing, design, and application.* Journal of Microbiological Methods, 2000. **43**(1): p. 3-31.
87. Popescu, M.-C., et al., *Multilayer perceptron and neural networks.* WSEAS Transactions on Circuits and Systems, 2009. **8**.
88. Ghosh, J. and A. Nag, *An Overview of Radial Basis Function Networks*, in *Radial Basis Function Networks 2: New Advances in Design*, R.J. Howlett and L.C. Jain, Editors. 2001, Physica-Verlag HD: Heidelberg. p. 1-36.
89. Shanthamallu, U.S. and A. Spanias, *Neural Networks and Deep Learning*, in *Machine and Deep Learning Algorithms and Applications*, U.S. Shanthamallu and A. Spanias, Editors. 2022, Springer International Publishing: Cham. p. 43-57.
90. Teuwen, J. and N. Moriakov, *Chapter 20 - Convolutional neural networks*, in *Handbook of Medical Image Computing and Computer Assisted Intervention*, S.K. Zhou, D. Rueckert, and G. Fichtinger, Editors. 2020, Academic Press. p. 481-501.
91. Wilamowski, B.M. and H. Yu, *Improved Computation for Levenberg–Marquardt Training.* IEEE Transactions on Neural Networks, 2010. **21**: p. 930-937.
92. Touati, K.O.M., et al., *Intelligent fault diagnosis of power transmission line using fuzzy logic and artificial neural network.* Diagnostyka, 2022. **23**(4): p. 1-21.
93. Tamir, D., N. Rishe, and A. Kandel, *Fifty Years of Fuzzy Logic and its Applications*. Vol. 326. 2015.
94. Maciej Kościelny, J. and M. Syfert, *Fuzzy Logic Application to Diagnostics of Industrial Processes.* IFAC Proceedings Volumes, 2003. **36**(5): p. 711-716.
95. Frank, P.M. and B. Köppen-Seliger, *Fuzzy logic and neural network applications to fault diagnosis.* International Journal of Approximate Reasoning, 1997. **16**(1): p. 67-88.
96. Zadeh, L.A., *Fuzzy logic = computing with words.* IEEE Transactions on Fuzzy Systems, 1996. **4**(2): p. 103-111.
97. Zadeh, L.A., G.J. Klir, and B. Yuan, *Fuzzy Sets, Fuzzy Logic, and Fuzzy Systems: Selected Papers*. 1996: World Scientific.
98. Zadeh, L.A., *The concept of a linguistic variable and its application to approximate reasoning—I.* Information Sciences, 1975. **8**(3): p. 199-249.

99. Mamdani, E.H., *Advances in the linguistic synthesis of fuzzy controllers.* International Journal of Man-Machine Studies, 1976. **8**(6): p. 669-678.
100. Sugeno, M., *An introductory survey of fuzzy control.* Information Sciences, 1985. **36**(1): p. 59-83.
101. Guo, Z.X. and W.K. Wong, *2 - Fundamentals of artificial intelligence techniques for apparel management applications*, in *Optimizing Decision Making in the Apparel Supply Chain Using Artificial Intelligence (AI)*, W.K. Wong, Z.X. Guo, and S.Y.S. Leung, Editors. 2013, Woodhead Publishing. p. 13-40.
102. Thaker, S. and V. Nagori, *Analysis of Fuzzification Process in Fuzzy Expert System.* Procedia Computer Science, 2018. **132**: p. 1308-1316.
103. Zimmermann, H.J., *Fuzzy Analysis*, in *Fuzzy Set Theory—and Its Applications*, H.J. Zimmermann, Editor. 2001, Springer Netherlands: Dordrecht. p. 93-109.
104. Mamdani, E.H. and S. Assilian, *An experiment in linguistic synthesis with a fuzzy logic controller.* International Journal of Man-Machine Studies, 1975. **7**(1): p. 1-13.

ملخص:

في أنظمة الطاقة، تعد خطوط النقل جزءًا مهمًا من الشبكة الكهربائية. لذلك من المهم حمايتها من كافة الأعطال المختلفة التي قد تحدث بأسرع وقت ممكن لتزويد الطاقة الكهربائية بشكل مستمر. تقدم هذه الرسالة حلولاً حديثة ودراسة مقارنة لاكتشاف الأخطاء وتصنيفها وتحديد موقعها في خطوط نقل الطاقة باستخدام الشبكة العصبية الاصطناعية (ANN) مقارنة بالمنطق الضبابي بالإضافة إلى طريقتين تعتمدان على الإشارة باستخدام طريقة تحويلات بارك والتحويل الموجي.

تم إنشاء أنواع مختلفة من الأعطال في خط النقل باستخدام نموذج محاكاة. في الأساليب القائمة على معالجة الإشارة، يتم جمع البيانات المستخدمة في طرف واحد فقط من خط النقل، بالنسبة لطرق الشبكة العصبية الاصطناعية والمنطق الضبابي، تم استخدام نظام مراقبة ذكي (IFD) تشخيص خطأ ذكي عند كلا طرفي خط نقل. تم العثور على أن كلا الطريقتين قويتان ودقيقتان وموثوق بهما لاكتشاف الخطأ عند حدوثه، وتحديد نوع الخلل إذا كان دائرة قصيرة أو دائرة مفتوحة، وتحديد موقع الخطأ، وتحديد في أي طور وقع الخطأ.

الكلمات المفتاحية: تشخيص نظام الطاقة، كشف الأعطال، خط النقل الكهربائي، الشبكة العصبية الاصطناعية، المنطق الضبابي. تحويلات بارك والتحويل الموجي.

Abstract

In power systems, transmission lines are an important part of the electrical grid. Thus it is important to protect it from all the different faults that may occur as soon as possible to supply electric power continuously. This thesis presents modern solutions and a comparative study of fault detection, classification and location in power system transmission lines using artificial neural network (ANN) compare to the fuzzy logic in addition to two signal-based methods using Park's vectors method and the Wavelet Transform. Faults in the transmission line of various types have been created using a simulation model. in signal based methods the data used is collected at only one end of the transmission line, however, for the ANN and FL methods, an intelligent monitoring system (IFD: Intelligent Fault Diagnosis) was used at both ends of overhead transmission line, both approaches were found to be robust, accurate, and reliable to detect the fault when it occurs, determining the fault type short circuit or opening of a power line (open circuit), locating the fault, and determining which phase was faulted.

Keywords: Power system diagnosis, Fault detection, Electrical transmission line, Artificial neural network, Fuzzy logic. Park's vectors. Wavelet transform.

Résumé

Dans les systèmes électriques, les lignes de transmission constituent une partie importante du réseau électrique. Il est important de le protéger contre tous les différents défauts qui peuvent survenir le plus tôt possible pour fournir de l'énergie électrique vers les utilisateurs. Cette thèse présente des solutions modernes et une étude comparative de la détection, de la classification et de la localisation des défauts dans les lignes de transmission du système électrique utilisant un réseau de neurones artificiels (ANN) en comparaison avec la logique floue en plus de deux méthodes basées sur le traitement de signal utilisant la méthode de Park et la transformée en ondelettes. Des défauts dans la ligne de transmission de différents types ont été créés à l'aide d'un modèle de simulation. Dans les méthodes basées sur l'analyse de signal, les données utilisées sont collectées dans une seule extrémité de la ligne de transmission, cependant, pour les méthodes ANN et FL, un système de surveillance intelligent (IFD : Intelligent Fault Diagnosis) a été utilisé dans les deux extrémités de la ligne électrique. Les deux approches se sont avérées robustes, précises et fiables pour détecter, de localiser et d'identifier les différents types de défauts lorsqu'il se produit.

Mots-clés : Diagnostic de système électrique, Détection de défauts, Ligne de transmission électrique, Réseau de neurones artificiels, Logique floue. Transformation de Park. Transformée en ondelettes.